EFFECT OF CRACK-REDUCING TECHNOLOGIES AND SUPPLEMENTARY CEMENTITIOUS MATERIALS ON SETTLEMENT CRACKING OF PLASTIC CONCRETE AND DURABILITY PERFORMANCE OF HARDENED CONCRETE

By
Eman Ibrahim
David Darwin
Matthew O'Reilly

A Report on Research Sponsored by

THE ACI FOUNDATION

Structural Engineering and Engineering Materials
SM Report No. 134
September 2019

THE UNIVERSITY OF KANSAS CENTER FOR RESEARCH, INC.
2385 Irving Hill Road, Lawrence, Kansas 66045-7563

EFFECT OF CRACK-REDUCING TECHNOLOGIES AND SUPPLEMENTARY CEMENTITIOUS MATERIALS ON SETTLEMENT CRACKING OF PLASTIC CONCRETE AND DURABILITY PERFORMANCE OF HARDENED CONCRETE

By

Eman Ibrahim
David Darwin
Matthew O'Reilly

A Report on Research Sponsored by

THE ACI FOUNDATION

Structural Engineering and Engineering Materials
SM Report No. 134

THE UNIVERSITY OF KANSAS CENTER FOR RESEARCH, INC.
LAWRENCE, KANSAS
September 2019

ABSTRACT

The effects of crack-reducing technologies and supplementary cementitious materials on plastic settlement cracking and the durability of concrete subjected to freezing and thawing were evaluated. The study of settlement cracking included 86 concrete mixtures containing internal curing (IC), a shrinkage-reducing admixture (SRA), optimized and non-optimized aggregate gradations, or the supplementary cementitious materials (SCMs) slag cement and silica fume. Some concrete mixtures contained combinations of these technologies, such as supplementary cementitious materials and internal curing. Both crack length and width were measured. The study of durability included 28 concrete mixtures, divided into three programs. Program 1 involved concrete containing different dosage rates of one of two shrinkage-reducing admixtures. Program 2 involved concrete containing different volume replacements of Class F and Class C fly ash and different combinations of a rheology-modifying admixture (RMA) with and without Class C fly. Program 3 involved concrete containing different dosage rates of one of two shrinkage compensating admixtures, one based on MgO that also incorporated a shrinkage-reducing admixture and one based on CaO. The study evaluated the effect of the technologies and materials on freeze-thaw durability, based on ASTM C666 Procedure B, scaling resistance, based on a modified version of Canadian Test BNQ NQ 2621-900 Annex B, and characteristics of the air-void system, obtained following ASTM C457. The research also examined the correlation between air-void characteristics, compressive strength, freeze-thaw durability, and scaling resistance for the mixtures.

All mixtures experienced increased settlement cracking as slump increased; the increase, however, was very low for the concrete containing both slag cement and silica fume, with or without internal curing. All crack reducing technologies and supplementary cementitious materials tested resulted in a reduction in settlement cracking at all slumps compared to mixtures without these technologies and materials. The use of a non-optimized aggregate gradation increased settlement cracking compared to mixtures with an optimized gradation. The combination of slag cement and silica fume in concrete provided a greater reduction in settlement cracking than slag cement alone. In terms of durability, mixtures with an average air-void spacing factor of 0.007 in. (0.18 mm) or less performed well in the freeze-thaw test. Mixtures with an average air-void

spacing factor of 0.007 in. (0.18 mm) or less and a compressive strength greater than 4000 psi (27.6 MPa) performed well in the scaling test. In terms of specific performance, one SRA had no effect on freeze-thaw durability, while the other caused reduced durability. Concrete with either SRA exhibited a reduction in scaling resistance. Mixtures containing Class F fly ash, RMA, or Class C fly ash in conjunction with RMA at all dosages studied performed well in the freeze-thaw test if the air-void spacing factor was 0.007 in. (0.18 mm) or less. Class F or Class C fly ash alone had no effect on scaling resistance when the concrete had an air-void spacing factor of 0.0071 in. (0.18 mm) or less. The RMA without and with Class C fly ash resulted in reduced scaling resistance. This reduction was in all cases associated with a concrete compressive strength below 4000 psi (27.6 MPa). An SCA based on CaO had no effect on the freeze-thaw durability at the dosage used in this study. The SCA based on MgO resulted in lower freeze-thaw durability, but only in mixtures that had increased air-void spacing; the increased air-void spacing may have been due to the shrinkage-reducing admixture incorporated in the admixture, which can reduce the stability of the air-void system. With the exception of one mixture with high air-void spacing factor [0.0096 in. (0.24 mm)], the two SCAs had no effect on scaling resistance at all dosages used in this study. All mixtures exhibited a lower air content in the hardened concrete than in the plastic concrete. This reduction in air content was significantly greater for mixtures containing high dosages of SRAs or the RMA.

Keywords: air-void characteristics, bridge deck cracking, fly ash, freeze-thaw durability, internal curing, lightweight aggregate, mass loss, scaling resistance, settlement cracking, silica fume, shrinkage-compensating admixture, shrinkage-reducing admixture, slag cement, spacing factor.

ACKNOWLEDGEMENTS

This report is based on a thesis presented by Eman Ibrahim in partial fulfillment of the requirements for the Ph.D. degree from the University of Kansas. Support was provided by the ACI Foundation and sponsoring organizations: ABC Polymers, the ACI Foundation's Strategic Development Council (SDC), Active Minerals International, the American Society of Concrete Contractors, Baker Concrete Construction, BASF Corporation, FORTA Corporation, the Expanded Shale, Clay and Slate Institute, the Euclid Chemical Company, GCP Applied Technologies, the University of Kansas Transportation Research Institute, PNA Construction Technologies, Inc., Premier Construction Products, Sika Corporation, and Structural Group, Inc. Financial support the first author’s academic studies were provided by the Ministry of Higher Education and Scientific Research in Iraq MOHESR. Additional support was provided by the Kansas Department of Transportation, Ash Grove Cement Company, and Midwest Concrete Materials.

TABLE OF CONTENTS

LIST OF TABLES

LIST OF FIGURES

CHAPTER 1: INTRODUCTION

1.1 GENERAL

Bridge deck cracking significantly reduces the service life of bridges, resulting in significant costs to owners. Cracks provide paths for water, oxygen, and deicing chemicals to penetrate through the bridge deck, resulting in accelerated corrosion of reinforcement and freeze-thaw damage to the concrete. Transportation agencies have worked to limit degredation of reinforcing steel by using corrosion-resistant reinforcement, increased cover to the reinforcement, and low permeability concrete (Russell 2004, Darwin et al. 2011). However, research has shown that cracks in bridge decks can accelerate the initiation and propagation of corrosion of reinforcement (Yoon et al. 2000, Marcotte and Hansson 2003, Transportation Research Board 2006).

Bridge deck cracking occurs due to the interaction of several factors that affect concrete performance, including settlement of plastic concrete, plastic and drying shrinkage, temperature changes, and external loading. These factors can produce tensile stresses in concrete. When the tensile stresses exceed the tensile strength of the concrete, cracks occur. Bridge deck cracking followed by reinforcement corrosion is considered the main cause of bridge deck deterioration (Russell 2004). Reducing cracking therefore has the potential to greatly extend the service life of structures.

The purpose of this study is to evaluate the effects of crack reduction technologies and supplementary cementitious materials on plastic settlement cracking and the durability of concrete subjected to freezing and thawing. Mixtures assessed for settlement cracking contained internal curing using pre-wetted lightweight aggregate (LWA), supplementary cementitious materials (SCMs) consisting of slag cement and silica fume, and shrinkage-reducing admixtures (SRA). Concrete evaluated for freeze-thaw durability, scaling resistance, and air-void characteristics contained varied combinations of SRAs, fly ash, a rheology modifying admixture (RMA), and shrinkage compensating admixtures (SCA). The study also investigates the correlation between air-void characteristics, freeze-thaw durability, and scaling resistance of these mixtures. This chapter summarizes the types of bridge deck cracking, describes previous studies, and presents the objective of this research.

1.2 SIGNIFICANCE OF BRIDGE DECK CRACKING

The primary cause of structural deficiencies of bridges is concrete distress and reinforcing steel corrosion caused by bridge deck cracking (Russell 2004). According to the National Bridge Inventory (NBI 2016), bridge conditions have improved over the last ten years. The percentage of structurally deficient bridge area declined from 9 to 7 percent over the period from 2006 to 2015 (U.S. Government Accountability Office 2016). This may be the result of increased expenditures, as the Federal Highway Administration (FHWA) reported that the total estimated spending on bridges increased from $11.5 billion in 2006 to nearly $17.5 billion in 2012 (FHWA 2016). Furthermore, the FHWA estimates that the total annual spending to update existing bridges will increase up to nearly $20.5 billion over the next 16 years (Kirk and Mallett 2013). Because of its impact on bridge deck durability and corrosion of reinforcing steel, there continues to be significant interest in crack reduction technologies.

1.3 BRIDGE DECK CRACKING

This section describes the mechanisms of bridge deck cracking, the types of cracks, and the factors that have the greatest impact on bridge deck cracking.

1.3.1 Mechanisms of Cracking

Bridge deck cracks are classified based on whether the concrete is plastic or hardened when the cracking occurs. Cracks in plastic concrete occur within the first few hours of concrete placement and include plastic settlement and plastic shrinkage cracking. Cracks in hardened concrete include drying shrinkage and thermal cracking.

Plastic settlement cracks or subsidence cracks occur in fresh concrete. Once concrete is consolidated, bleed water rises and solid particles settle. When this vertical displacement is resisted by a rigid inclusion, such as a reinforcing bar near the concrete surface, a difference in settlement develops. This differential settlement creates a weakened concrete zone above the reinforcement and produces tensile stresses that develop directly above the reinforcement, resulting in settlement cracks above and parallel to the bar (Powers 1968). Settlement may also create a void under the reinforcing bar and influence the local bond. Since these cracks form above and parallel to the bar,

they provide a direct path for water and deicing chemicals to reach the bar and increase the risk of corrosion (Mindess et al. 2003). Settlement cracks can be differentiated from plastic shrinkage cracks (discussed next) by their pattern, which follows the line of the restraining elements, which for bridge decks is the reinforcement. Even if these cracks are not immediately visible on the concrete surface, the weakened concrete zone can provide a location for cracks to form after the concrete has hardened (Babaei and Purvis 1995).

This study addresses this type of cracking, discusses the potential of reducing settlement in plastic concrete, and evaluates crack reduction technologies that can be used to limit this type of cracking. Section 1.4 discusses settlement cracking in detail.

Plastic shrinkage cracks occur in fresh concrete when the rate of evaporation of water at the concrete surface exceeds the rate of rise of bleed water to the surface. Due to evaporation, moisture is lost resulting in the formation of menisci between particles, producing negative capillary forces (Mindess et al. 2003). Developing capillary forces compresses the particles and brings water to the concrete surface. This process tends to rearrange the particles and reduces the volume of the concrete, causing shrinkage. Differential shrinkage between the surface and the concrete just below the surface results in cracks at the surface. Increasing the evaporation rate or decreasing the amount of bleed water leads to increased plastic shrinkage cracking. The evaporation rate will increase as the concrete temperature, ambient air temperature, wind speed increase and the relative humidity decreases. Figure 1.1 shows the relationship between the rate of evaporation and the concrete and air temperatures, wind speed, and relative humidity (ACI Committee 305 2010). The amount of bleed water will be reduced if silica fume or finely-ground cement is used, because of the high surface area of these materials. These finely ground materials retain water, decreasing bleed and raising the risk of plastic shrinkage cracking. The use of air-entraining admixtures, high-range water reducing admixtures (HRWRAs), and reducing the water content of the concrete mixture will also reduce bleed water, increasing the potential for plastic shrinkage cracking (Krauss and Rogalla 1996, Pendergrass and Darwin 2014).

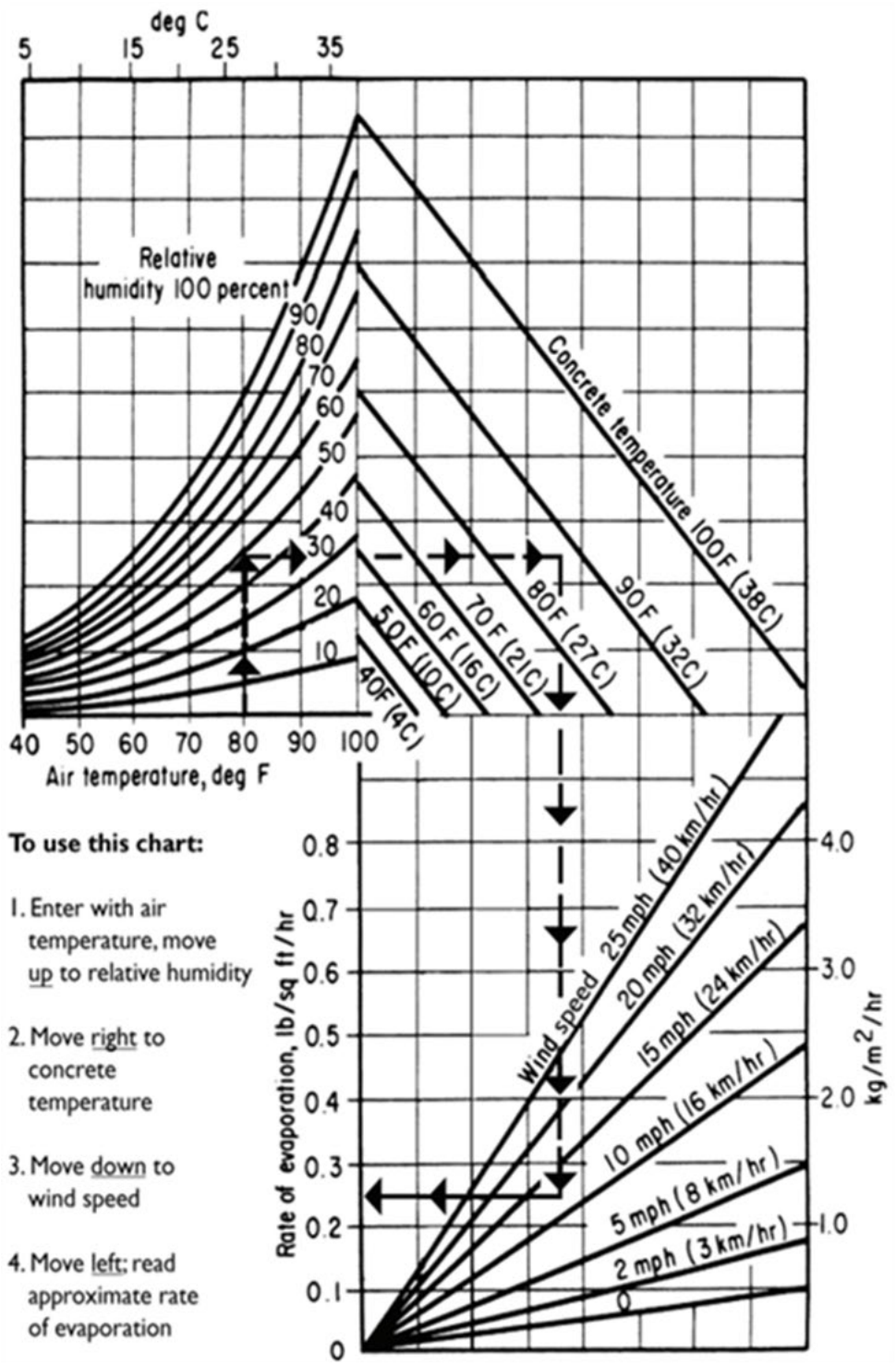

Figure 1.1 – ACI nomograph for estimating surface water evaporation rate of concrete i. e. the "ACI Hot Weather Concreting Evaporation Nomograph," (ACI Committee 305 2010)

Autogenous shrinkage occurs in hardened concrete during the hydration process and does not involve moisture loss to the environment. The process involves self-desiccation that takes place if water is not available in the cement paste for continued hydration. As hydration continues, water is drawn out of capillary pores between the cement particles, leading to the development of capillary stresses, causing a reduction in the concrete volume called autogenous shrinkage (Holt 2001). This type of shrinkage is most often observed in concretes with water-cementitious material ratios (*w/cm*) below 0.42.

Drying shrinkage cracks result from volume changes in hardened concrete due to the loss of moisture from cement paste to the environment. As water contained in capillary pores, hardened calcium silicate hydrate (C-S-H) gel, and solid surfaces is lost during evaporation, internal stresses increase from three phenomena: capillary stresses, disjoining pressure, and surface free energy.

Capillary stresses develop when the relative humidity (RH) drops due to evaporation of pore water near the concrete surface. The stress increases as the pore radius decreases.

Disjoining pressure is due to the water absorbed on the surface of C-S-H at all RHs. Disjoining pressure increases with an increase of the thickness of absorbed water between particles. This pressure and capillary stresses are only significant factors down to a RH of 45 percent.

Surface free energy significantly increases when RH is lower than 45 percent, and increases due to the removal of absorbed water from the C-S-H surfaces.

Stresses that are caused by volume changes increase with an increase of the specific surface area of the particles (Mindess at al. 2003). Volume changes induce tensile stresses in restrained concrete. Concrete bridge decks are restrained by many structural components, including reinforcement, shear studs, girders, and abutments. Due to this restraint, tensile stresses can develop in the bridge deck when the concrete shrinks, resulting in drying shrinkage cracking in bridge decks (Schmitt and Darwin 1995). Drying shrinkage occurs over a long time, but nearly 80 percent of shrinkage occurs within the first three months (Holt 2001). Drying shrinkage is affected most by concrete material properties, especially cement paste and aggregate content. Reducing cement paste and increasing the aggregate contents can achieve a reduction in shrinkage since the aggregate in concrete resists the shrinkage of the paste. Other factors that also impact drying

shrinkage include cement type, aggregate type, particle fineness, and admixtures (Schmitt and Darwin 1995, Mindess et al. 2003).

Thermal cracks in bridge decks are caused by tensile stresses resulting from the restraint of volume changes due to temperature effects. Temperature changes in bridge decks are caused by the decrease in temperature as newly placed concrete cools and by changes in weather conditions. During early hydration, concrete temperature rises, causing expansion, which induces no significant residual stresses since concrete is in a plastic state and has low stiffness. As the concrete gains stiffness, the concrete temperature reaches a peak. After that, the rate of hydration slows, the concrete begins to cool to the ambient temperature, and its volume decreases. This reduction in volume is restrained by girders, reinforcement, shear studs, and abutments, causing tensile stresses that increase the potential for cracking in bridge decks (Babaei and Fouladgar 1997). Thermal cracking increases with an increase in difference in the temperature between the concrete deck and girders. Babaei and Purvis (1996) and Babaei and Fouladgar (1997) suggested that the maximum difference in temperature between the deck and girders should be 22º F (12º C) to avoid thermal cracking.

The difference in the coefficients of thermal expansion between concrete and steel can cause thermal cracking since the materials do not expand at the same rate (Krauss and Rogalla 1996). Previous studies have indicated that reducing the potential of thermal cracking is achieved by lowering the concrete temperature at placement (Pendergrass and Darwin 2014, Khajehdehi and Darwin 2018), increasing the air content (Breitenbucher and Mangold 1994), and slowing the cooling rates (Chui and Dilger 1993). McLeod, Darwin, and Browning (2009) recommended that the temperature of concrete at the time of placement be between 55º and 70º F (13º to 21º C) to limit the potential for thermal cracking.

Structural cracks, such as flexural cracks that may form on the upper surface of bridge decks in negative moment regions due to the self-weight of the deck or traffic loads, are caused by loads applied to a bridge. The sequence of placing concrete during construction may also induce tensile stresses in bridge decks. Overall, flexural stresses play a smaller role in bridge deck cracking than volume changes and enviromental conditions (Krauss and Rogalla 1996) and will not be addressed further in this study.

1.3.2 Patterns of Bridge Deck Cracking

Bridge deck cracks can be classified into five groups according to their orientation relative to the span of bridges. These groups are transverse, longitudinal, diagonal, pattern, and random cracks (Durability 1970, Schmitt and Darwin 1995). The orientation of cracks is useful to determine the reinforcement exposure to the environment. For example, cracks that are above and parallel to the reinforcement expose a large area of steel to the environment and accelerate general steel corrosion, whereas cracks perpendicular to a bar expose a limited area of steel to the environment causing local steel corrosion (Krauss and Rogalla 1996). Figure 1.2 shows examples of transverse, longitudinal, diagonal, and pattern or map cracks.

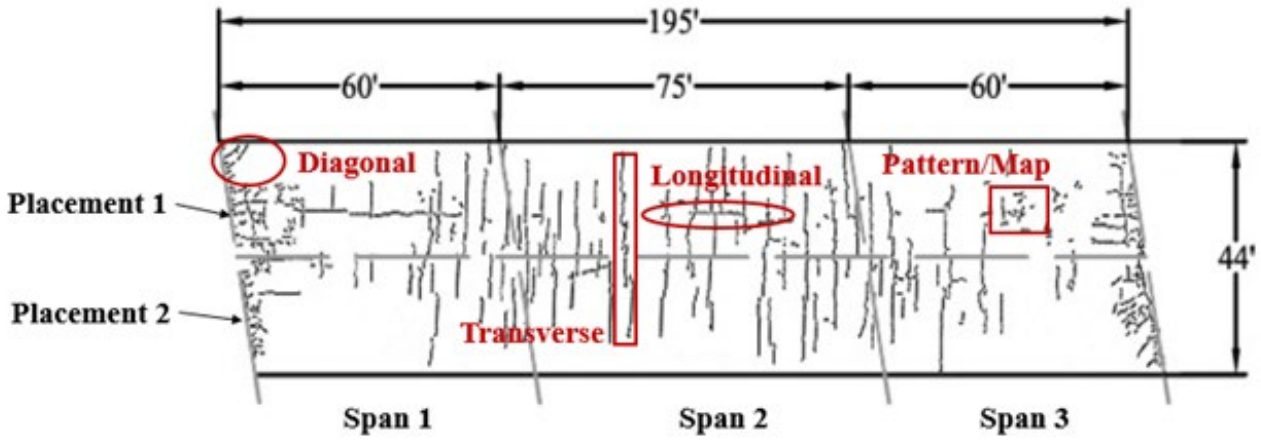

Figure 1.2 – Bridge deck cracking patterns as shown on a crack map: Transverse, Longitudinal, Diagonal, and Pattern/Map (Darwin et al. 2004)

Transverse cracks are oriented perpendicular to the longitudinal axis of a bridge deck. Transverse cracks are the most common type found in bridge decks and are often observed soon after a deck is placed. They tend to form above the top layer of the transverse bars (Durability 1970, Schmitt and Darwin 1995), providing a direct path for water and deicing salts to reach the steel and accelerate the initiation of corrosion (Krauss and Rogalla 1996).

Longitudinal cracks are oriented parallel to the longitudinal axis of a bridge deck. They may form in any type of deck, but tend to occur above the top longitudinal bars in solid-slab bridges

and above void tubes in the hollow-slab bridges. These cracks may occur before the bridge is loaded and can extend through the deck (Durability 1970). Longitudinal cracks can occur due to the resistance of the reinforcement and void tubes to the sedimentation of plastic concrete. These cracks are also common at the end of bridge decks if the deck is integral with the abutment (Schmitt and Darwin 1995, Miller and Darwin 2000, Lindquist et al. 2005).

Diagonal cracks occur at the end of skewed bridges, over single column piers, and near integral abutments. These cracks do not follow any pattern and are caused by both external loading and drying shrinkage.

Pattern or map cracks are observed in all types of bridges and can occur at any location on a bridge deck. Because these cracks are shallow in depth and fine in width, they do not necessarily cause durability problems. They occur due to improper curing at early ages, which allows rapid evaporation of the surface moisture (Durability 1970, Schmitt and Darwin 1995). They also result from overfinishing of the deck surface, which can bring excess cement particles to the surface, increasing shrinkage of the surface concrete, which is restrained by the material below (Pendergrass and Darwin 2014).

Random cracks are classified as any cracks that do not fit into any of the other categories. These cracks can have a variety of orientations and form due to many factors (Pendergrass and Darwin 2014).

1.3.3 Factors Affecting Bridge Deck Cracking

Cracking in bridge decks is caused by the combined effects of a number of factors. The main factors are discussed in this section and involve concrete material properties, environmental conditions, construction procedures, and structural design.

1.3.3.1 Concrete Material Properties

Many studies have investigated the effect of variation of concrete mixture proportions and concrete composition on the potential for cracking.

Water to Cementitious Material (*w/cm*) Ratio

Reducing the water-cementitious material (*w/cm*) ratio in concrete slightly increases cracking in bridge decks (Schmitt and Darwin 1999, Brown et al. 2001, Darwin et al. 2004). A

reduction in the *w/cm* ratio in concrete can minimize concrete permeability, which improves the durability of concrete. However, this reduction also increases compressive strength, which reduces concrete creep that can relieve tensile stresses in concrete caused by restrained shrinkage. A *w/cm* ratio less than 0.42 also increases autogenous shrinkage in concrete (Krauss and Rogalla 1996). Schmitt and Darwin (1995) found that crack density in bridge decks is more influenced by cement paste volume (water and cement volume) than the *w/cm* ratio.

Cement

The quantity and particle size of the cement in concrete have an effect on cracking. An increase in cement content results in greater concrete shrinkage and a higher potential rate of cracking (Krauss and Rogalla 1996, Schmitt and Darwin 1999). In addition, high cement content induces more heat due to hydration causing thermal stresses (ACI Committee 231 2010). This effect is more pronounced in concrete with a low *w/cm* ratio due to the possibility of autogenous shrinkage (Krauss and Rogalla 1996, Mindess et al. 2003, Darwin et al. 2004). McLeod et al. (2009) suggested using a cement content between 500 and 540 lb/yd^3 (297 and 320 kg/m^3) to minimize the potential of cracking in bridge decks. In addition, cement particle size also has an impact on the concrete behavior. Fine cement particles increase the heat of hydration and reduce the size of the pores in the hardened cement paste, resulting in, respectively, higher thermal stresses and higher capillary stresses, which, in turn, cause drying shrinkage (Chariton and Weiss 2001).

Cement Paste Volume

The volume of cement paste (water and cement) in concrete has a significant effect on bridge deck cracking. Increasing the cement paste volume (by increasing water content, cementitious material content, or both) results in greater shrinkage (Schmitt and Darwin 1999, Brown et al. 2001, Lindquist et al. 2008, ACI Committee 231 2010). Schmitt and Darwin (1999) observed that a concrete with cement paste volume greater than 27 percent exhibited higher cracking. In addition, increasing cement paste volume increases bleed water and settlement cracking in plastic concrete (Al-Qassag et al. 2015). Based on a statistical analysis of bridge decks supported by steel girders, Khajehdehi and Darwin (2018) found that increased cement paste content was the most important factor in predicting increased cracking.

Aggregate

Aggregate content, type, and size can affect shrinkage. Increasing aggregate content reduces shrinkage since aggregate has a restraining effect on the volume changes that occur in the paste (Mindess et al. 2003). Increasing aggregate content also results in a reduction in cement paste volume, which reduces cracking. The use of a larger maximum aggregate size is also helpful because it allows a reduction in aggregate surface area, which lowers the volume of paste required to lubricate the plastic concrete. Aggregates with a low coefficient of thermal expansion, such as limestone, can also reduce cracking (French et al. 1999). The gradation of aggregate also affects the properties of plastic and hardened concrete. Concrete containing a well-graded combined aggregate exhibits less bleeding, increased cohesiveness, and improved workability and finshibility, compared with concrete containing poorly-graded aggregate (Obla and Lobo 2007, Lindquist et al. 2008). The use of well-graded aggregate allows an increase in the volume of aggregate without segregation, leading to less shrinkage and cracking by reducing the paste content. Futhermore, well-graded aggregate requires approximetaly 15 percent less water for the same cement content to maintain a constant slump (Cramer et al. 1995).

Air-Entraining Admixtures

Air-entraining admixtures (AEAs) are added to the concrete to provide voids within the cement paste for water to freeze without causing damage (Mindess et al. 2003, Schmeckpeper and Lecoultre 2008). AEAs reduce the surface tension of water within plastic concrete to promote the formation of air voids during mixing. The entrained air improves concrete workability by reducing friction between aggregates particles. It also reduces bleeding and segregation during the handling and transportation of concrete. American Concrete Institute (ACI) Committee 201 recommends an air volume within the range of 5 to 6 percent to help ensure sufficient frost resistance for concrete with a maximum size aggregate of 1 in. (25.4 mm). The construction specification for a low-cracking high-performance concrete (LC-HPC) bridge deck in Kansas, however, requires an air volume within the range of 6.5 to 9.5 percent based on early analyses indicating reduced cracking for decks cast with concretes with increased air contents (Schmitt and Darwin 1995, Miller and Darwin 2000, Lindquist et al. 2005, Kansas Department of Transportation 2014).

High-Range Water-Reducing Admixtures

High-range water-reducing admixtures (HRWRAs) are used to achieve the desired slump for a given cement paste content. HRWRAs place like charges on cement particles that then repel each other (Mindess et al. 2003), releasing water that is trapped when the particles floc. Adding HRWRAs to the concrete increases the potential for settlement cracking (Kayir and Weiss 2002) and plastic shrinkage cracking (Sayahi 2016). HRWRAs may reduce the adhesion between cement particles and the surface of entrained air, leading to a reduction in the stability of the air-void system (Ramachandran 1995, Ley et al. 2010). Freeman (2009) observed that adding HRWRAs may contribute to a coarser air-void system, causing an increase in the space between air voids for a given air volume and a reduction in freeze-thaw durability.

Shrinkage-Reducing Admixtures

Shrinkage-reducing admixtures (SRAs) improve fresh and hardened concrete shrinkage performance. The presence of an SRA in concrete reduces the surface tension of the pore solution, decreasing capillary pressure and plastic and drying shrinkage. Lura et al. (2007) and Mora et al. (2009) found that the use of an SRA also reduces plastic shrinkage cracking by reducing the surface tension of water in the pores of plastic concrete and delaying development of capillary pressure in concrete. This reduction in capillary pressure results in less consolidation of the particles and less bleed water, thus minimizing evaporation, leading to less plastic shrinkage cracking and settlement. In addition, adding SRAs to the concrete increases the viscosity of plastic concrete, resulting in less settlement (Bentz 2006, Sant et al. 2010). The use of SRAs in air-entrained concrete may cause a reduction in the stability of the air-void system in plastic concrete and a reduction in the air content of hardened concrete, increasing the spacing factor and reducing freeze-thaw durability (Schemmel et al. 1999, Pendergrass et al. 2017) and scaling resistance (Cope and Ramey 2001).

Shrinkage-Compensating Admixtures

Shrinkage-compensating admixtures (SCAs) contribute to reducing the effects of drying shrinkage. Magnesium oxide (MgO) expands when it reacts with mixing water, forming magnesium hydroxide, $Mg(OH)_2$, causing expansion. The version of this SCA that is on the market also contains an SRA that reduces the drying shrinkage of concrete. The second SCA,

calcium oxide (CaO), expands when it reacts with mixing water, forming calcium hydroxide Ca $(OH)_2$, also causing expansion in concrete mixtures. CaO induces a greater percentage of the expansion during the first day of casting than MgO, which expands gradually during the curing period. The CaO exhibits additional expansion when used in concrete containing supplementary cementitious materials (SCMs), both without and with internal curing (IC) (Khajehdehi et al. 2018).

Rheology-Modifying Admixtures

Rheology-modifying admixtures (RMAs), which include viscosity modifying admixtures (VMAs), are water-soluble polymers that increase the viscosity of mixing water and improve cohesiveness of concrete (Khayat and Yahia 1994). RMAs decrease bleed water and increase concrete stability and the degree of aggregate suspension within plastic concrete, resulting in a reduction in settlement cracking (Brettmann et al. 2015, Al-Qassag et al. 2016).

Supplementary Cementitious Materials (SCMs)

Supplementary cementitious materials (SCMs), including silica fume, slag cement, and fly ash, are used in concrete as a partial replacement for portland cement, most often to improve durability.

Silica fume is used to improve durability and minimize permeability of concrete. It is a by-product of the production of silicon metal and alloys and consists of particles with diameters approximately one-one hundreth the size of cement particles. Silica fume particles have a high surface area and require more water for a given workabilty than portland cement, which can be offset by using a water-reducing admixture (ACI Committee 234 2006). The high silica content and extreme fineness of silica fume make it a very reactive pozzolan. During cement hydration, silica fume comes in contact with water and a silica-rich gel forms and coats the cement particles. A pozzolanic reaction between silica gel and calcium hydroxide (Ca $(OH)_2$), formed during the hydration of portland cement along with calcium-silicate hydrate (C-S-H), creates additional calcium-silicate hydrate (C-S-H) that forms in the voids within hardened cement paste, producing a very dense structure (Grutzeck et al. 1982). Wang et al. (1986) found that a small addition (2 to 5 percent) of silica fume can produce a denser structure within the interfacial transition zone at the boundary of aggregate particles. Silica fume minimizes the number of large pores, producing a

discontinuous pore structure and increasing the density of the transition zone (Mindess et al. 2003). Mindess (1987) concluded that silica fume increases the strength of concrete by increasing the strength of the bond between the cement paste and the aggregate, while Cong et al. (1992) and Darwin and Slate (1970) found that the increase in strength is due to the increase in cement paste strength. Because silica fume reduces the permeability of concrete, it provides improved protection against the corrosion of reinforcing steel (Maage and Sellevold 1987).

Silica fume significantly reduces bleeding in plastic concrete, increasing the potential of plastic shrinkage cracking (McDonald 1991).Concrete with a low *w*/*cm* ratio containing silica fume exhibits increased autogenous shrinkage (Paillere et al. 1989).

Fly ash is used to improve concrete properties. It is a by-product of burning coal. There are two classes available, F and C, based on the chemical composition of the fly ash. Class F fly ashes are produced from bituminous and anthracite coals. Class C fly ashes are produced from lignitic coals and contain a high level of calcium oxide, which provides some cementitious properties without the presence of $Ca(OH)_2$ (Mindess et al. 2003). Fly ash is a pozzolan and reacts with the $Ca(OH)_2$ produced from cement hydration to generate C-S-H. Because fly ash particles have a smaller specific surface area and a lower silica content than silica fume, the pozzolanic reaction of this material is much slower than that of silica fume, leading to less early heat evolution and a slower rate of strength gain. Fly ash improves the properties of both plastic and hardened concrete. For plastic concrete, the spherical shape of the particles can increase workability and pumpability with no addition of water (Mindess et al. 2003), increase cohesiveness, reduce bleeding, and improve finishability (Russell 2004). For hardened concrete, fly ash can reduce permeability and chloride diffusivity, and increase resistivity and resistance to sulfate attack (Russell 2004).

Slag cement is a by-product of the blast-furnace production of pig iron and is rich in lime, silica, and alumina. When it is cooled rapidly by quenching with water and ground, calcium aluminosilicate glass is generated, which has cementitious properties (Mindess et al. 2003). The process of quenching is called granulation, and the final material is ground granulated blast furnace slag, known as slag cement (Ramachandran 1995). During the hydration process, slag cement reacts very slowly with water because of impervious coatings that form around the particles early

in hydration. Alkalis and sulfate produced by the hydration of portland cement can break down these coatings and activate slag cement. Since this material has a lower lime content than portland cement, the composition of C-S-H resulting from the hydration of slag cement has a lower C/S ratio than obtained with portland cement, which leads to some pozzolanic behavior as $Ca(OH)_2$ reacts with excess silica (Bakker 1980, Roy and Idron 1983, Mindess et al. 2003). Slag cement in concrete increases workability due to smooth slip planes created in the cement paste and reduces water demand (Meusel and Rose 1983). Concrete containing slag cement has a lower permeability than concrete containing only portland cement, and this reduction increases with the increase in slag content increase (Rose 1987).

Slump

Slump also has a considerable effect on early age cracking. Many studies have indicated that increasing slump can increase the settlement of plastic concrete and induce plastic settlement cracking above fixed objects, such as reinforcing bars, near the upper surface of a concrete placement (Dakhil et al. 1975, Schmitt and Darwin 1999, Lindquist et al. 2005, McLeod et al. 2009, Yuan et al. 2011, Al-Qassag et al. 2015).

1.3.3.2 Environmental Conditions

Environmental conditions include ambient temperature, relative humidity, and wind speed. These factors affect the evaporation rates, bleeding and settlement, initial hydration temperature, and thermal stresses; therefore, they have an impact on bridge deck cracking (Schmeckpeper and Lecoultre 2008).

Ambient Temperature

An increase in ambient temperature decreases the workability, because higher temperature increases the rate of evaporation and the rate of hydration (Mindess et al. 2003). Increasing the rate of evaporation can cause plastic shrinkage cracking. An increase in the ambient temperature range on the date of concrete placement can induce more cracking due to thermal effects (French et al. 1999, Lindquist et al. 2005, Khajehdehi and Darwin 2018). Krauss and Rogalla (1996) suggested placing concrete at night to reduce temperature effects.

Relative Humidity

Low relative humidity can contribute to an increase in early age cracking (Cheng and Johnston 1985) by increasing the rate of evaporation of water from the surface of plastic concrete and thereby causing high plastic shrinkage. Schmitt and Darwin (1995), however, observed no relationship between relative humidity and deck cracking if curing is applied immediately after finishing to protect fresh concrete from the surrounding environment.

Wind Speed

Wind speed also effects the rate of evaporation, and thus the amount of plastic shrinkage cracking (ACI Committee 308 2016). Increasing the rate of evaporation causes the development of capillary forces, which compress the particles and draw more bleed water to the surface, accelerating the rate of bleeding and settlement (Klieger 1955, Powers 1968, Lura et al. 2007, Henkensiefken et al. 2010). Researchers suggest that windbreaks and water fogging be provided when the evaporation rate exceeds 0.2 lb/ft^2 (1.0 kg/m^2) in normal concrete, and 0.1 lb/ft^2 (0.5 kg/m^2) in concrete with a low *w/c* ratio, silica fume, or HRWRA (Krauss and Rogalla 1996, Mindess et al. 2003). (See Figure 1.1).

1.3.3.3 Construction Procedures

Construction procedures represent another factor that can affect cracking in bridge decks. These include the sequence of placement, consolidation, finishing procedures, and curing (Krauss and Rogalla 1996). Earlier studies found that the placing sequence does not seem to influence cracking (Cheng and Johnston 1985). Later studies reported that the placing sequence is important, but it is not a primary cause of deck cracking (Krauss and Rogalla 1996). Effective consolidation can reduce bridge deck cracking, while insufficient consolidation can lead to more cracking (Khajehdehi and Darwin 2018). Insufficient vibration of concrete with a low concrete cover increases plastic settlement cracking (Issa 1999). Finishing procedures also affect bridge deck cracking; early finishing reduces the number and width of cracks (Horn et al. 1975, Stewart et al. 1969). Overfinishing and the addition of water to facilitate finishing can reduce scaling resistance (Klieger 1955, Malisch et al. 1966).

Proper curing immediately after finishing can limit plastic shrinkage cracking. The construction specifications for LC-HPC bridge decks in Kansas require placing two layers of wet burlap on bridge decks. The first layer must be placed within ten minutes of finishing concrete and the second layer is placed within five minutes of the first. This procedure, *when followed*, effectively eliminated plastic shrinkage cracking on LC-HPC decks (Lindquist et al. 2008, McLeod et al. 2009, Yuan et al. 2011, Pendergrass et al. 2011). The curing period also impacts cracking; Lindquist et al. (2008) and Reynolds et al. (2009) observed that increasing the curing period from 7 to 14 days will reduce shrinkage of concrete.

1.3.3.4 Structural Design Factors

Structural design factors may interact with material properties to contribute to cracking in bridge decks. These can include girder type and degree of restraint, span length, top concrete cover, deck thickness, and reinforcing bar size and spacing. This section summarizes the impact of these factors.

Girder Type and Degree of Restraint

The main cause of bridge deck cracking is the restraint to volume change provided by the supporting girders. Cracks increase with an increase in the degree of restraint between the deck and girders. A composite bridge deck does not allow any shrinkage or expansion to occur in concrete without the development of stresses; however, a non-composite bridge deck can reduce restraint of the deck and stresses developed to a small degree (Krauss and Rogalla 1996). Several studies indicate that decks supported by steel girders exhibit more cracking than decks supported by concrete girders (Cheng and Johnston 1985, Frosch et al. 2003). Since steel is more thermally conductive and has a higher coefficient of thermal expansion than concrete, larger temperature variations and thermal stresses can occur when steel girders are used. Moreover, steel girders do not shrink, while concrete girders do, providing less restraint than steel (Krauss and Rogalla 1996).

Span Length

Research on the effect of span length on cracking has shown mixed results. Some studies indicate that decks on longer spans exhibit more cracks than short spans. In theory, longer spans are typically supported by larger girders that provide more restraint, resulting in higher tensile

stresses and more cracking (Krauss and Rogalla 1996). Other studies have shown that the span length has no effect on cracking (Schmitt and Darwin 1995, Miller and Darwin 2000, Lindquist et al. 2005).

Top Cover

Increased top cover reduces the tendency for settlement cracking (Dakhil et al. 1975, Weyers et al. 1982). Schmitt and Darwin (1995) suggested that a range of top cover of 2 to 3 in. (50 to 75 mm) to reduce the risk of settlement cracking on monolithic bridge decks. Krauss and Rogalla (1996) also recommended a minimum top cover of 2 in. (50 mm) to reduce settlement cracking and provide corrosion protection. AASHTO LRFD Bridge Design Specifications (2013) require a top cover of at least 2.5 in. (65 mm).

Deck Thickness

Some studies have indicated that increased deck thickness reduces cracking (Ramey et al. 1997, French et al. 1999), although increased thickness may lead to non-uniform shrinkage and thermal stresses (Krauss and Rogalla 1996). Horn et al. (1972) found that increasing deck thickness from 6.4 to 8.6 in. (165 to 220 mm) can reduce deck cracking.

Reinforcing Bar Size and Spacing

Reducing bar size and decreasing bar spacing can distribute stresses and reduce crack widths (Schmitt and Darwin 1995, Krauss and Rogalla 1996). Dakhil et al. (1975) found that increased bar size increases settlement cracking. Schmitt and Darwin (1995) recommended limiting the top transverse bars to No. 4 or No. 5 (No. 13 or No. 16) and spacing to less than 6 in. (150 mm). Other researchers also recommended reducing the maximum bar size to No. 5 (No. 16) (Ramey et al. 1997, Babaei and Fouladgar 1997) or to No. 4 (No. 13) bars with a maximum spacing of 6 in. (150 mm) (Krauss and Rogalla 1996).

1.4 PLASTIC CONCRETE SETTLEMENT

This section addresses plastic settlement cracking, including the mechanism of settlement cracking, and the forces that drive concrete settlement.

The mechanism behind settlement cracking was summarized in Section 1.3.1 and is illustrated in Figure 1.3. Settlement in plastic concrete can occur due to two driving forces: settlement of particles and evaporation (Powers 1968).

1.4.1 Settlement Due to Self-Weight

Once concrete is cast and consolidated, the heavier particles settle due to gravity as bleed water rises to the surface. This displacement occurs within the first few hours, up to final set of the concrete, causing a reduction in concrete depth. The amount of settlement is proportional to the concrete depth. It is also influenced by the concrete properties. Concrete with fine materials or low water content can reduce bleed water, leading to less settlement.

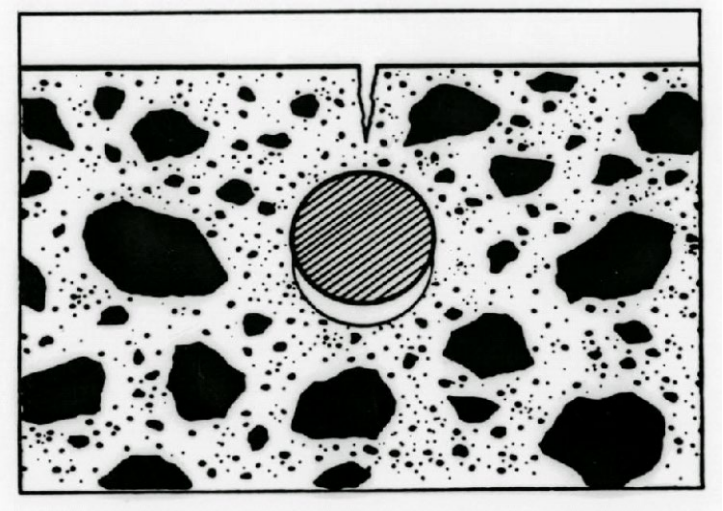

Figure 1.3 – Settlement crack formed due to obstructed settlement of plastic concrete (Price 1982)

1.4.2 Settlement Due to Evaporation

At early ages, bleed water rises to the concrete surface. When the rate of rising bleed water exceeds the rate of evaporation, the surface remains wet. Once the bleed water evaporates, menisci form and result in capillary pressure. This capillary pressure causes the solid particles to rearrange and draws more bleed water to the surface. Developing capillary pressure causes more consolidation of the particles and leads to further settlement (Klieger 1955, Powers 1968, Lura et al. 2007, Henkensiefken et al. 2010). The evaporation rate is influenced by the curing method and

the environment. To limit evaporation, concrete should be covered immediately after consolidation and kept wet.

1.5 PREVIOUS STUDIES OF SETTLEMENT CRACKING

This section describes previous work evaluating the differential settlement of fresh mortar or concrete resulting in settlement cracks. The studies include different approaches to measure settlement and assess the factors that impact settlement. The studies also examined various crack reduction technologies that are used to reduce plastic settlement cracking, including fibers, lightweight aggregate (LWA), shrinkage-reducing admixtures (SRAs), and silica fume.

1.5.1 Assessment of Settlement Cracking in Fresh Concrete

Dakhil, Cady, and Carrier (1975)

Dakhil, Cady, and Carrier (1975) studied settlement cracking as a function of concrete slump [2, 3, and 4 in. (50, 75, and 100 mm)], reinforcing bar size [No. 4, No. 5, and No. 6 (No. 13, No. 16, and No.19)], and concrete cover depth [0.75, 1, 1.5, and 2 in. (20, 25, 40, and 50 mm)]. Three specimens were tested for each set of variables resulting in 108 specimens. Concrete was placed in 12 × 12 × 8 in. (305 × 305 × 205 mm) forms with a single reinforcing bar supported in each form with the desired cover. The concrete was consolidated using a 1-in. (25-mm) electric spud vibrator, screeded in a direction parallel to the reinforcing bar, and cured with wet burlap. After 4 hours, the specimens were photographed and inspected visually for cracks. Only visible cracks above the reinforcing bar were counted as settlement cracks.

The results show that the probability of settlement cracking increases with increasing slump, increasing bar size, and decreasing concrete cover, with concrete cover serving as the primary factor that affects cracking, as shown in Figure 1.4.

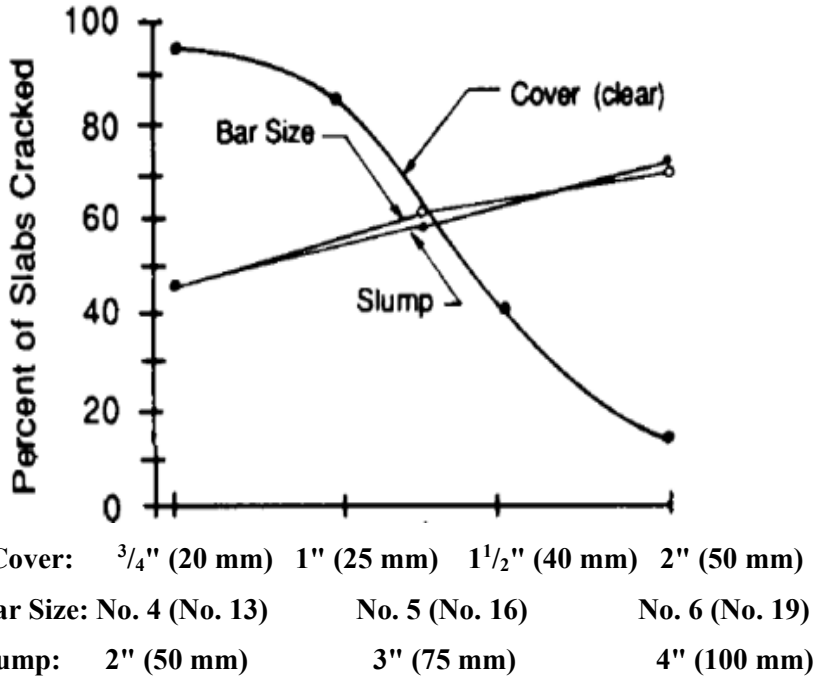

Figure 1.4 – Settlement cracking as a function of slump, bar size, and cover (Dakhil et al. 1975)

Weyers, Conway, and Cady (1982)

Weyers, Conway, and Cady (1982) used photoelastic analysis to evaluate the effect of the spacing between adjacent reinforcing bars on settlement and stress distribution above the reinforcing bars. Gelatin was used in place of concrete. The study examined the spacings of 3, 4, 5, and 6 in. (75, 100, 125, and 150 mm) between No. 5 (No. 16) reinforcing bars for settlement cracking. The gelatin mixture used in this study consisted of 8 percent plain unflavored gelatin, 16 percent glycerin, and 76 percent water by weight. The mixture was cast in 22 × 1 × 8.5 in. (560 × 25 × 215 mm) wood molds that were sealed with Plexiglas sheets. A 1-in. (25-mm) gelatin cover was used for all bar spacings. For 6-in. (150-mm) spacing, cover depths of 1.5, 2, and 2.5 in. (40, 50, and 65 mm) were also evaluated.

The researchers found that the maximum tensile stress in the gelatin decreased with increasing cover depth. The effect of the reinforcing bar spacing was less pronounced on tensile stress distribution than the cover depth.

Qi, Weiss, and Olek (2004)

Qi, Weiss, and Olek (2004) used a non-contact laser measurement device to measure the settlement of fresh mortar. They investigated the effect of cover thickness and fibers on settlement. The study included two groups of mortar mixtures with different cover depths. Each group contained two specimens, with fiber volumes of 0.0 and 0.2 percent. Specimens had a No. 5 (No. 16) steel reinforcing bar attached to 20 × 11 × 6 in. (510 × 280 × 150 mm) plywood molds with a cover depth of 0.5 in. (13 mm) for one group of specimens and 1.5 in. (40 mm) for the other. Mixture proportions of the mortar of 1:0.5:2:2 (cement: water: sand: pea aggregate by weight) were used. The laser was attached to an automated traveling table to measure the differential settlement over a large area of the surface. Settlement was measured 10 and 240 minutes after concrete placement up to 3 in. (75 mm) away from the center of the reinforcing bar in the longitudinal direction and 1 in. (25 mm) along the reinforcing bar in the transverse direction.

The results show that settlement increases proportionally to the distance away from the reinforcement. The specimens with high differential settlement exhibited more cracking over the bar. The study indicated that settlement was more uniform and cracking decreased as cover increased. The specimens with mortar containing 0.2 percent fiber by volume exhibited less differential settlement, and thus less settlement cracking, than specimens without fibers.

Combrinck and Boshoff (2013)

Combrinck and Boshoff (2013) studied plastic settlement cracking in concrete and the effect of both reinforcement spacing and concrete cover on the development of settlement cracks. Concrete was cast in two 24 × 8 × 8 in. (610 × 205 × 205 mm) molds, which had transparent side panels to monitor the formation of settlement cracks below the surface, as shown in Figure 1.5a. No. 3 (No. 10) reinforcing bars were attached to the molds at two different spacings: 6 and 8 in. (150 and 205 mm). Three concrete covers, 0.6, 1.2, and 1.8 in. (15, 30, and 45 mm), were investigated for both spacings. The *w/c* ratio for the concrete was 0.62, and the slump was 3.5 in. (90 mm). After the concrete was cast and consolidated, the specimens were cured at 73° F (23° C), 65 percent relative humidity, and no wind. An LVDT was used to measure settlement, and settlement crack formation was monitored visually with the unaided eye and high-resolution images.

Combrinck and Boshoff observed that differential settlement of plastic concrete caused different defects as shown in Figure 1.5b, and 1.5c: (1) Tensile cracks that formed due to the development of tensile stresses above the bar, which started at the surface and extended vertically toward the bar. (2) Shear cracks that started at the bottom from the points close to the bar and extended to the surface at an angle. Although shear cracks may not be visible on the surface, they can form weak spots in concrete that extend after loading and shrinkage. (3) Voids formed beneath the reinforcing bar due to differential settlement in the concrete. These voids reduced the concrete strength and the mechanical bond between the concrete and the bar. The study, which used a single bar size, indicated that low concrete cover and reinforcement spacing resulted in greater settlement cracking.

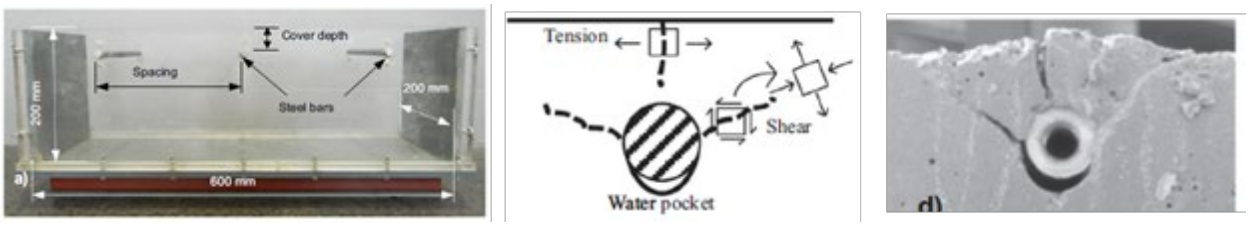

(a) **(b)** **(c)**

Figure 1.5 – (a) Steel bar mold. (b) and (c) Tensile crack, shear crack, and water pocket formation below the reinforcing bar. (Combrinck and Boshoff 2013)

Brettmann, Darwin, and O'Reilly (2015)

Brettmann, Darwin, and O'Reilly (2015) developed a test procedure to evaluate settlement cracking in concrete. They investigated the influence of slump and the addition of either a rheology-modifying admixture (RMA) or polypropylene fibers on settlement cracking. For each mixture, concrete was cast in three 12 × 12 × 8 in. (305 × 305 × 205 mm) wood molds with a nominal clear cover of $1^1/_8$ in. (28.5 mm) [1.5 in. (38 mm) cover to the center of the bar] over a No. 6 (No. 19) reinforcing bar attached to the mold. Brettmann et al. cured the specimens using a sloped hard plastic enclosed in a layer of plastic sheet to cover the specimens.

The results show that settlement cracking increases as slump increases. The addition of the RMA or fibers to the concrete improved the cohesiveness of the concrete and reduced settlement cracking.

1.5.2 Effect of Fibers on Plastic Settlement Cracking

Qi, Weiss, and Olek (2003)

Qi, Weiss, and Olek (2003) evaluated the effect of fiber reinforcement on the settlement of plastic concrete in a drying environment. The study involved concrete mixtures with a *w/c* ratio of 0.5 and an aggregate volume of 65 percent. Synthetic fine fibrillated polypropylene and coarse polypropylene fibers were used at dosages by volume of 0.05, 0.1, 0.2, and 0.3 percent for the fine fibers, and 0.1, 0.2, 0.3, 0.5, and 0.7 percent for the coarse fibers. The concrete was cast in 5 × 3 in. (125 × 75 mm) cylinders and cured in a chamber at 100° F (38º C), 50 ± 2 percent relative humidity, with a wind speed of 15 mph (24 km/h) for six hours. After six hours, the specimens were stored at room temperature and no wind for eight more hours. A non-contact laser beam was used to measure differences in the height of the concrete surface.

The results indicate that adding fibers to the concrete mixtures significantly reduces settlement displacement, 60 percent for 0.3 percent by volume of fine fibers. At the same dosage rate, fine fibers can achieve a reduction in settlement about twice that achieved by coarse fibers. The higher efficiency is attributed to the greater surface area of the fine fibers, enhancing the consistency of the mixture, leading to less settlement.

Al-Qassag, Darwin, and O'Reilly (2015)

Al-Qassag, Darwin, and O'Reilly (2015) continued the work of Brettmann et al. (2015) and investigated the effect of different types of fibers and a mineral rheology-modifying admixture (RMA) on settlement cracking. The study examined concrete with *w/c* ratios of 0.45 or 0.5 and cement paste contents of 24.3 or 27 percent by volume. The mixtures included control mixtures without fibers or a RMA, mixtures containing different types of synthetic fibers with dosages between 1.5 and 7.5 lb/yd^3 (0.89 and 4.45 kg/m^3), and a mixture containing a RMA at a dosage of 0.05 percent of total weight of dry material. Concrete was cast in 12 × 12 × 8 in. (305 × 305 × 205 mm) wood molds with a No. 6 (No. 19) reinforcing bar attached to the mold providing a nominal clear cover of $1\frac{1}{8}$ in. (28.5 mm). Specimens were covered using a sloped, hard plastic top enclosed in a plastic sheet to eliminate evaporation and reduce the effect of plastic shrinkage, and cured at 73º F (23º C) and a relative humidity of 50 percent for 24 hours. After 24 hours, the specimens were checked visually for settlement cracking.

The results show that settlement cracking increases with increased slump for all concrete mixtures. The concrete with low cement paste volume exhibits less settlement cracking than concrete with high cement paste volume. Adding fibers to the mixtures significantly reduces settlement cracking. This reduction ranged from 35 to 41 percent for fiber dosages between 1.5 and 7.5 lb/yd^3 (0.89 and 4.45 kg/m^3) at a 4-in. (100-mm) slump, and no significant difference in the cracking was observed for the different types of fibers. The reduction in the settlement can be attributed to an increase in the tensile strength of concrete, an increase in the cohesiveness of the mixtures, and a reduction in bleed water. The results also show that the addition of RMA decreases settlement cracking. Mixtures with 0.05 percent RMA based on the total weight of dry material exhibited a 19 percent reduction in settlement cracking compared with the control mixture at a 4-in. (100-mm) slump. Al-Qassag et al. stated that the RMA increased the cohesiveness and stability of the plastic concrete, resulting in less differential settlement and cracking.

1.5.3 Effect of Lightweight Aggregate on Plastic Settlement Cracking

Henkensiefken, Briatka, Bentz, Nantung, and Weiss (2010)

Henkensiefken, Briatka, Bentz, Nantung, and Weiss (2010) studied the effect of using pre-wetted lightweight aggregate (LWA) on settlement in mortar mixtures in a drying environment. The study replaced normalweight fine aggregate (sand) with different volumes (0, 11, 18.3, 23.7, and 33 percent) of pre-wetted LWA with a 24-hour absorption of 10.5 percent. The *w/c* ratio was 0.3. The sand plus LWA equaled 55 percent of the volume for all mixtures. The mixtures were cast in 3 × 4 in. (75 × 100 mm) cylindrical specimens and vibrated for 15 seconds before they were cured in a chamber at 73º F (23º C) and a relative humidity of 50 percent. A non-contact laser beam was used to measure the settlement of the surface at intervals of 1 minute during the first 6 hours.

The results indicate that less settlement occurs for the mortar containing LWA than for mortar with only sand; the reduction of settlement increases with increasing LWA volume replacement. Henkensiefken et al. believed that the improvement of settlement performance was due to internal curing, which supplied water to the mortar when moisture was lost due to evaporation and cement hydration, resulting in less consolidation and settlement.

1.5.4 Effect of Shrinkage-Reducing Admixtures on Plastic Settlement Cracking

Lura, Pease, Mazzota, Rajabipour, and Weiss (2007)

Lura, Pease, Mazzota, Rajabipour, and Weiss (2007) studied the effect of adding a shrinkage-reducing admixture (SRA) to mortar on settlement. This study evaluated mortars containing 0, 1, 2, and 5 percent SRA by weight of cement. For measuring settlement and mass loss through the evaporation, mortar with a *w/c* ratio of 0.5 was cast in 4 × 3 in. (100 × 75 mm) cylindrical molds. The mortar was placed in molds and vibrated externally, and then was cured at 86º ± 1.8º F (30º ± 1º C), a relative humidity 50 ± 2 percent, with wind velocity 15 ± 1 mph (24 ± 2 km/h). A non-contact laser was used to measure the vertical displacement of the mortar surface every 30 seconds for six hours.

The settlement of the mortar containing an SRA stopped 1.5 hours after placement, while settlement of the plain mortar stopped 2 hours after placement. In addition, the final settlement of the mortar containing an SRA was about 30 percent less than the settlement of the plain mortar. Lura et al. stated that the reduction in settlement resulted from the reduction in surface tension of pore water due to the use of the SRA, resulting in a reduction of capillary pressure. This reduction produced less consolidation of the particles and less bleed water rising to the surface, resulting in less settlement. The rate of evaporation for mixtures that contained the 5 percent dosage of SRA decreased after an hour of drying since an SRA reduces the surface tension of pore water and capillary pressure develops, which also had the effect of reducing settlement.

1.5.5 Effect of Silica Fume on Plastic Settlement Cracking

Hammer (2001)

Hammer (2001) evaluated the effect of silica fume as a replacement of cement on settlement, shrinkage, and pore water pressure in sealed and unsealed conditions. The study included concrete mixtures containing silica fume of 0, 5, 10, or 15 percent as a volume replacement of cement. The mixtures had a paste volume of 30 percent and a *w/cm* ratio of 0.4, and were cast in 12 × 4 × 4 in. (305 × 100 × 100 mm) steel molds. The molds were lined with two layers of plastic sheet with talcum powder in between the sheets to reduce the friction between the concrete and the molds. To measure concrete settlement, a 1.6 × 1.6 in. (40 × 40 mm) plastic mesh

was placed in the center of the specimen surface, and an inductive displacement transducer was used to measure the vertical displacement of the mesh. The mold was placed on a scale to measure water loss over time. Some specimens were sealed using a plastic sheet to reduce the moisture loss, while other specimens were exposed to 68º F (20º C), a relative humidity of 50 percent, and no wind.

For the sealed specimens, settlement started at a high rate, and no significant difference was observed in the settlement between the mixtures containing different dosages of silica fume. The mixture containing 0 percent silica fume was not tested in the sealed condition. After 6 to 7 hours, the sealed concrete specimens started to expand due to resorption of bleed water. This expansion increased as the dosage of silica fume increased (Hammer 1999). The settlement rate during the first four hours for the specimens exposed to 50 percent relative humidity was approximately equal for concrete containing 0, 5, and 10 percent of silica fume, while the settlement rate for concrete containing 15 percent of silica fume decreased compared to that of the mixtures with low silica fume content.

1.6 FREEZE-THAW DURABILITY

Concrete subjected to repeated freeze-thaw cycles is susceptible to damage. The development of cracks on bridge decks can contribute to this damage, because cracks allow water and chemicals to penetrate the concrete. Concrete deterioration can take different forms, including cracking and spalling of concrete due to the extreme expansion of the paste and surface scaling in the presence of moisture and deicing salts. Air entrainment is an effective means to reduce the risk of freeze-thaw damage in concrete. Further discussion of the air-void system is presented in Section 1.7. This study evaluates several concrete mixtures for freeze-thaw durability, scaling resistance, and air-void characteristics and examines the correlation between the first two and the latter. The following sections discuss the mechanism of freeze-thaw damage in cement paste and aggregates, and the mechanism of surface scaling.

1.6.1 Damage Mechanisms in Cement Paste under Freezing and Thawing

Freezing and thawing within the cement paste causes damage to non-air entrained concrete, while it causes no damage to properly air-entrained concrete. Freeze-thaw damage is caused by

two processes: desorption of water and osmotic pressure. As cement paste contains a variety of pore sizes and the freezing temperature of the water in pores drops as the diameter of the pore neck decreases, water in the smaller pores will freeze at lower temperatures than water in the larger pores. At temperatures below 32º F (0º C), water in the smaller pores supercools rather than freezes. As the chemical potential of ice is lower than that of supercooled water, higher vapor pressure forces water in small pores to flow toward the freezing sites (larger pores) to maintain equilibrium. This flow increases the volume of ice in the larger pores until there is no room to accommodate more ice, resulting in internal pressure and dilatation of the paste (Mindess et al. 2003, Mehta and Monterio 2006). Another process that contributes to the frost attack is osmotic pressure. The pore water in cement paste is not pure water, but ice is. As pore solution freezes in the larger pores, the concentration of the remaining solution increases, resulting in osmotic pressure that draws less dilute solution in the smaller adjacent pores to the freezing sites. The higher the concentration of pore solution, the greater the osmotic pressure, which, like the difference in vapor pressure, draws water to the freezing sites. Entrained air voids are larger than the pores in the cement paste, providing sites where pore water will freeze first (close to 32º F, 0º C). The formation of ice in the air voids allows osmosis and desorption to draw moisture from the surrounding cement paste, protecting it from damage.

1.6.2 Aggregate Freeze-Thaw Damage Mechanism

Most aggregates have larger pores than cement paste. The freezing temperature of water in aggregate pores is 32º F (0º C). The pores are large enough that desorption and osmosis play little part in the movement of water. When water freezes in aggregate, it expands about 9 percent, which will force water away from a freezing site, causing hydraulic pressure on the aggregate and the surrounding cement paste. The formation of ice within pores is the principal cause of freezing damage in aggregate (ACI Committee 201 2016). Freezing damage occurs when the distance that water must travel within the aggregate to reach the outside surface (an escape boundary) to relieve the pressure is too great or if the degree of saturation of the aggregate particles is high. The combination of this distance, the diameter of the pores, the degree of saturation, the absorption, and tensile strength of aggregate establishes the critical size of aggregate particles above which

the aggregate will be damaged upon freezing. Aggregates with fine pores and high absorption have a greater potential for undergoing freezing damage. Even if the aggregate particles are not damaged by freezing, the water that is forced from the pores of the aggregate due the hydraulic pressure can cause damage to the surrounding cement paste (Mindess et al. 2003). The role of entrained air in reducing freezing damage in aggregate is minimal (ACI Committee 201 2016).

1.6.3 Surface Scaling

Concrete subjected to freezing cycles in the presence of deicing salts is susceptible to damage due to scaling, even if it has an adequate air entrained and durable aggregate. Scaling is spalling of small pieces of mortar at the concrete surface, and it results from more than one process. Salt solutions have a lower vapor pressure than pure water. Therefore, concrete exposed to deicers exhibits a lower rate of evaporation and a higher degree of saturation than concrete that is not exposed. The use of deicing salts to melt ice, by reducing the freezing temperature of water, may cause an increase in moisture near the concrete surface, which can promote the growth of ice lenses and cause concrete damage. In addition, the use of deicing salts may also cause a rapid drop in temperature of the concrete just below the surface, resulting in tensile stresses and cracking from differential thermal strains (Mindess et al. 2003).

The addition of salt to the pore solution can also increase the effect of osmotic pressure. Scaling increases with the increase of the concentration of salts. Verbeck and Klieger (1956) demonstrated that greater scaling occurs at low to intermediate concentrations (2 to 4 percent) for both calcium chloride and sodium chloride. Further, overvibration and overfinishing concrete, which can bring excess paste to the surface, as well as raising the local *w*/*cm* ratio and causing insufficient air voids near the surface, can also increase scaling problems (Mindess et al. 2003).

1.7 AIR-VOID SYSTEM CHARACTERISTICS

A good air-void system, with closely spaced air voids, can protect the cement paste in concrete from freeze-thaw damage. As explained in Section 1.6.1, because entrained-air voids are larger than the pores in the surrounding paste, water in these voids starts freezing at a higher temperature than water in the pores. The formation of ice permits osmosis and desorption processes to draw water from the paste into air voids, which work as a reservoir for both ice and concentrated

pore solution (Mindess et al. 2003). The size and distribution of air voids within the concrete play a greater role in improving concrete durability than the air volume alone. In addition, no correlation exists between the air volume of fresh concrete and the distribution of the air-voids of hardened concrete. For this reason, analyzing air-void characteristics in hardened concrete is essential to understanding freeze-thaw durability.

The air-void parameters, which can be obtained from a microscopical analysis in accordance with ASTM C457, include the air content, spacing factor, and specific surface area. The air content is the total volume of the air voids in the cement paste. The spacing factor, perhaps the most important parameter, is a measure of the average distance from any point in the paste to the edge of the nearest void; it should not be greater than 0.008 in. (0.2 mm) to ensure sufficient frost resistance (Mindess et al. 2003, Russell 2004). The specific surface area is the surface area of air voids divided by the volume of these voids. In a good air-void system, the specific surface should be greater than 600 $in.^{-1}$ (25 mm^{-1}) (Mindess et al. 2003, Russell 2004). Figure 1.6 shows representations of two cement paste samples that have an air content of 12 percent, one with a smaller number of larger air voids (top image) than the other (bottom image). The air-void spacing factor for the paste in the bottom image is lower than the spacing factor of the paste in the top image, and thus, the degree of protection provided by the air voids to the paste illustrated in the bottom image is much greater than provided to the paste illustrated in the top image.

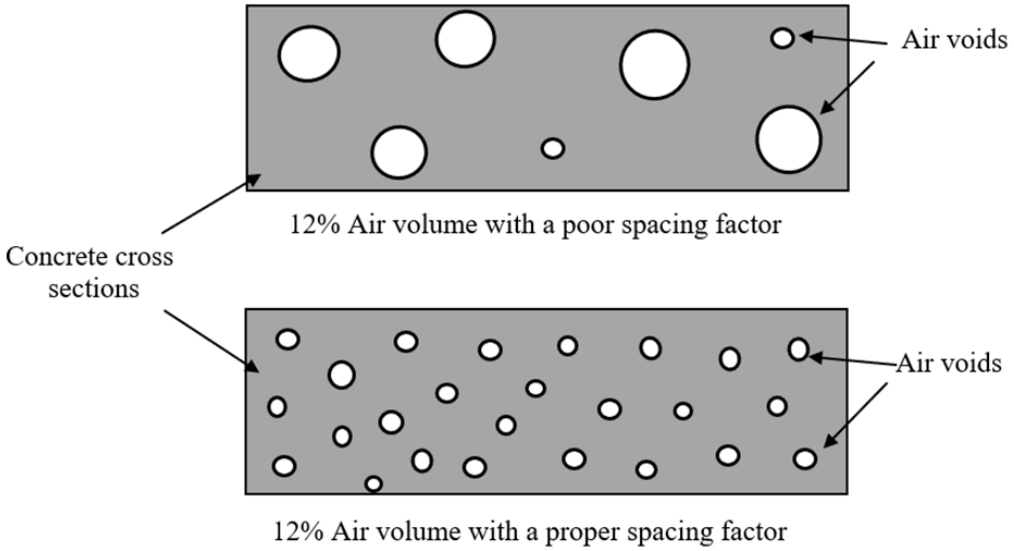

Figure 1.6 – Comparison between two cement pastes with the same air content but different size and distribution of air voids

1.7.1 Effect of Concrete Mixture Design on Air-Void Characteristics

Air-void characteristics are influenced by the concrete materials used and their proportions (Mindess et al. 2003). The use of fine materials, cementitious materials or aggregate, or different combinations of admixtures can reduce entrained air in concrete. The reason is that the increased surface area of the finer particles will attract a portion of the air-entraining admixture, which will not then be available to entrain air. The use of shrinkage-reducing admixtures (SRAs) in conjunction with an air-entraining admixture can reduce air-void stability. The reason is that both SRAs and air-entraining admixtures reduce the surface tension of water. This additional reduction in surface tension can reduce the stability of air voids in plastic concrete leading to the formation of fewer, larger air voids and, thus, reducing freeze-thaw durability (Pendergrass et al. 2014). Pendergrass et al. (2017) investigated the effect of incompatibility between SRAs and AEAs on the freeze-thaw durability, scaling resistance, and air-void characteristics of hardened concrete. The study included concretes containing two SRAs and two AEAs, one that was surfactant-based and one that was polymer-based. The concretes had either a cement content of 520 lb/yd^3 (308 kg/m^3) and a *w/cm* ratio of 0.45 or a cement content of 540 lb/yd^3 (320 kg/m^3) and a *w/cm* ratio of 0.44. The mixtures contained SRA dosages of 0, 0.5, 1, and 2 percent by weight of cement.

Freeze-thaw durability was evaluated in accordance with ASTM C666-Procedure B and ASTM C215 to determine the durability factor, which is based on the percentage of the initial dynamic modulus of elasticity remaining at the end of the test. The concrete was subjected to freeze-thaw cycles with a temperature range of 0 to 40 ºF (-18 to 4 ºC). Scaling resistance was evaluated in accordance with Canadian Test BNQ NQ 2621-900 Annex B, with modifications to the concentration of NaCl solution, the temperatures of freeze-thaw cycles, and the screen size to determine mass losses of the concrete specimens. The results revealed that for mixtures without an SRA, both types of AEA provided good freeze-thaw durability and scaling resistance. With either SRA, concrete containing the surfactant-based air-entraining admixture also provided good freeze-thaw durability and scaling resistance, but concrete containing the polymer-based-air did not. In all cases, the addition of an SRA resulted in a reduction in air content between plastic and hardened concrete, a reduction that increased with an increase in the SRA dosage. Mixtures with

a high air-void spacing factor, regardless of AEA, exhibited reduced durability, especially for mixtures with spacing factors greater than 0.008 in. (0.2 mm).

1.8 OBJECTIVE AND SCOPE

Previous studies have investigated the mechanism of plastic settlement cracking in concrete, and identified the factors that have the greatest effect on settlement cracking, including concrete cover, slump, reinforcing bar size, and spacing (Dakhil et al. 1975, Weyers at al. 1982, Qi et al. 2004, Combrinck and Boshoff 2013). Research has also addressed the mechanism of freeze-thaw durability, scaling resistance, and air-void system characteristics of hardened concrete and the effect of these characteristics on the durability of concrete, especially with concrete containing different admixtures (Powers and Helmuth 1953, Mindess et al. 2003, Pendergrass et al. 2014, Pendergrass et al. 2017 to name a few). This study evaluates the effect of supplementary cementitious materials (SCMs) and crack reduction technologies, including internal curing, shrinkage-reducing admixture (SRA), and aggregate gradation on settlement cracking in plastic concrete. The study also investigates the effect of various combinations of SRAs, fly ash, a rheology-modifying admixture (RMA), and shrinkage compensating admixtures (SCAs) on freeze-thaw durability, scaling resistance, and air-void characteristics, as well as the correlation between the air-void characteristics and the freeze-thaw durability and scaling resistance of these mixtures.

1.8.1 Settlement Cracking

1.8.1.1 Internal Curing Using Pre-Wetted LWA

Previous studies have shown that the use of internal curing in concrete improves durability and reduces cracking. Henkensiefken et al. (2010) investigated the effect of using pre-wetted LWA on settlement of mortar mixtures with a *w/cm* ratio of 0.3, with no reinforcement, measuring the settlement within the first few hours. This study examines the effect of internal curing using pre-wetted LWA in concrete mixtures with a *w/cm* ratio of 0.45, which is used to eliminate the any effect of autogenous shrinkage, an effect that may have affected the earlier mortar tests.

1.8.1.2 Supplementary Cementitious Materials, Including Slag Cement and Silica Fume

Few studies have evaluated the effect of supplementary cementitious materials (SCMs) on settlement cracking. Hammer (2001) studied the effect of silica fume on settlement, adding silica fume to concrete with a *w/cm* ratio of 0.4 under sealed and unsealed conditions. This study evaluates settlement cracking for concrete mixtures containing slag cement and silica fume.

1.8.1.3 Supplementary Cementitious Materials Used in Conjunction with Internal Curing

Previous studies have recommended the use of internal curing to enhance durability and reduce shrinkage cracking. Additional studies have investigated the effect of SCMs on the potential of settlement cracking. This study examines the effect of adding SCMs to the concrete in conjunction with pre-wetted LWA on settlement cracking performance.

1.8.1.4 Shrinkage-Reducing Admixtures

Some prior studies have examined the impact of a shrinkage-reducing admixture (SRA) on the reduction of bridge deck cracking. Lura et al. (2007) examined the effect of an SRA on settlement for mortar specimens that contained no reinforcement and were open to evaporation. This study investigates the effect of an SRA on settlement cracking for concrete specimens that are covered to eliminate evaporation.

1.8.1.5 Aggregate Gradation

Previous studies have determined that the use of well-graded aggregate in concrete can contribute to reduce bleeding and increase cohesiveness (Obla and Lobo 2007, Lindquist et al. 2008). This study evaluates the effect of the aggregate gradation on settlement cracking.

1.8.2 Freeze-Thaw Durability, Scaling Resistance, and Air-Void Characteristics of Air-Entrained Concrete Mixtures

Since the durability of concrete is influenced by the materials used and their proportions, this study includes an evaluation of mixtures containing different combinations of shrinkage-reducing admixtures (SRAs), fly ash, a rheology-modifying admixture (RMA), and shrinkage compensating admixtures (SCAs) on freeze-thaw durability, scaling resistance, and air-void

characteristics. The study also investigates the correlation between the air-void characteristics of the mixtures and their freeze-thaw durability and scaling resistance.

CHAPTER 2: EXPERIMENTAL PROGRAM

2.1 GENERAL

This chapter describes the experimental program for this study, which covers settlement cracking, freeze-thaw durability, scaling resistance, and air-void characteristics analysis.

Eighty-six concrete mixtures were evaluated to investigate the effects of supplementary cementitious materials (SCMs) and crack reduction technologies, including internal curing, a shrinkage-reducing admixture (SRA), and aggregate gradation on settlement cracking performance. The concrete mixtures had a water cementitious material ratio (*w/cm*) of 0.45 and a cement paste content of 24 or 27 percent by volume. Slumps ranged from $1^{3}/_{4}$ to $8^{1}/_{2}$ in. (45 to 215 mm). Three series of mixtures were evaluated, each with a different gradation of aggregate. Pre-wetted LWA was used to provide internal curing. Two SCMs, slag cement, and silica fume, were evaluated. Some mixtures included internally cured concrete containing SCMs. One mixture containing SRA was also evaluated.

Air-void analyses were conducted on mixtures that were also evaluated for freeze-thaw durability and scaling resistance. These mixtures contained different combinations of SRAs, fly ash, a rheology-modifying admixture (RMA), and shrinkage compensating admixtures (SCAs). The air-void characteristics of these mixtures were compared with the freeze-thaw durability and scaling resistance of the same mixtures to determine relationships between air-void parameters and durability performance.

This chapter describes the concrete material properties, concrete mixture proportions, the details of the settlement cracking, freeze-thaw, and scaling tests, as well as air-void system analysis, and the scope of the experimental program.

2.2 MATERIALS

The laboratory work in this study required approximately two years. During that period, the material sources were the same, while the physical and chemical properties of the materials changed slightly. The chemical and physical properties for the individual samples of cementitious material are provided in Appendix A. Likewise, a sieve analysis was performed, and specific

gravity and absorption were measured on each sample of aggregate. The following sections describe the properties of the materials used in this study.

2.2.1 Cement

All concrete mixtures in this study contained Type I/II portland cement. The cement was obtained in three samples over a period of the study and analyzed by the Ash Grove Cement Company Technical center in Overland Park, KS. The specific gravity according to ASTM C188 of the cement was either 3.15 or 3.12, and the Blaine fineness varied from 365 to 399 m^2/kg, based on ASTM C204. The chemical composition of each sample of the cement is shown in Table A.1 in Appendix A.

2.2.2 Supplementary Cementitious Materials

The supplementary cementitious materials used in this study were Grade 100 (G 100) slag cement, silica fume, and fly ash. The slag cement had a specific gravity of 2.86 and a blaine fineness of 584 m^2/kg. The slag cement was supplied by Skyway Cement Company in Chicago, IL. The silica fume had a specific gravity of 2.2 and was obtained from Euclid Chemical Company. Fly ash (Class F and Class C): Class F fly ash had a specific gravity of 2.55 and was supplied by Headwaters Resources in Underwood, ND. Class C fly ash had a specific gravity of 2.87 and was produced by Ash Grove Resources, LLC, Topeka, KS. The chemical composition of the supplementary cementitious materials is listed in Table A.1 in Appendix A.

2.2.3 Coarse Aggregates

Granite was used as the coarse aggregate. The granite was provided by Midwest Concrete Materials in Lawrence, KS, and satisfied Section 1102.2a of KDOT, Standard Specification, 2015 Edition. Two size fractions were used, referred to as A and B, to optimize the aggregate gradation and improve the concrete workability. A maximum size (MSA) of Granite A was either 3/4 or 1 in. (19 or 25 mm), and a MSA of Granite B was 1/2 in. (13 mm). Eleven and twelve samples of Granite A and B were used, respectively. The absorption (dry) of Granites A varied from 0.44 to 0.64 percent, and the absorption (dry) of Granites B varied from 0.58 to 0.75 percent. The specific

gravity (SSD) of Granite A and B varied from 2.6 to 2.64. The properties and the gradations of the coarse aggregates are listed in Table A.2 in Appendix A.

2.2.4 Normalweight Fine Aggregates

The normalweight fine aggregate consisted of Kansas River sand and pea gravel. Thirteen samples of sand and eight samples of pea gravel were obtained over the period of the study. The sand was supplied by Builder's Choice Aggregate, Topeka, KS, and satisfied Section 1102.2b of KDOT, Standard Specifications, 2015 Edition. The specific gravity (SSD) of the sand varied from 2.59 to 2.63, the absorption (dry) varied from 0.47 to 0.64 percent, and the fineness modulus varied from 2.75 to 3.19. Pea gravel was provided by Midwest Concrete Materials in Lawrence, KS, and is referred to as UD-1 in the material classification of KDOT. The specific gravities (SSD) of pea gravel varied from 2.61 to 2.63, the fineness modulus varied from 4.64 to 5.02, and the absorption (dry) varied from 0.84 to 1.42 percent. The properties and gradations of the fine aggregate are reported in Table A.3 in Appendix A.

2.2.5 Lightweight Aggregates

Two samples of pre-wetted LWA were used in this study to provide internal curing water in the concrete mixtures. The first was a pea-gravel-sized lightweight aggregate (LWA), and the second was a fine LWA. The absorption and pre-wetted surface-dry (PSD) specific gravity, determined after soaking the LWA in water for 72 hours were, respectively, 26.24 percent and 1.6, for the pea-gravel-sized LWA and 23.99 percent and 1.72 for the fine LWA. A centrifuge was used to place the aggregates in the PSD condition in accordance with a procedure developed by Miller et al. (2014). The properties and gradations of the pre-wetted LWA are reported in Table A.4 in Appendix A. Section 2.3.2 describes the centrifuge method in detail.

2.2.6 Chemical Admixtures

The chemical admixtures used in this study include shrinkage-reducing admixtures (SRAs), shrinkage-compensating admixtures (SCAs), air-entraining admixtures (AEAs), high-range water reducers (HRWRs), and rheology-modifying admixture (RMA).

Three shrinkage-reducing admixtures (SRAs) were used. SRA-2 is a propane-ethanol-based admixture consisting of 2,2-dimethylpropane-1,3-diol and 2-butylaminoethanol, and SRA-5 is an ethylpropane-based admixture consisting of 2-ethylpropane-1,3-diol and 5-ethyl-1,3,dioxane-5-methanol; both are produced by Sika Corporation. SRA-3 is a methylpentane-based admixture consisting of 2-methylpentane-2,4-diol; it is produced by Grace Construction Products. The specific gravity of SRA-2, SRA-3, and SRA-5 were 1.0, 1.01, and 0.93, respectively. These admixtures were used to minimize the surface tension of pore water, reducing capillary stresses and shrinkage. All admixtures conform to the requirements of an ASTM C494/AASHTO M194 Type S admixture.

Two types of shrinkage compensating admixtures (SCAs) were used. SCA-1 is produced by Premier Magnesia, LLC and contains magnesium oxide (MgO), which expands when reacting with water and converts to $Mg(OH)_2$. SCA-1 also contains an SRA, which provides additional shrinkage reduction. SCA-2 is produced by Euclid Chemical Company and consists of calcium oxide (CaO), which rapidly expands when reacting with water and converts to $Ca(OH)_2$. The specific gravity of SCA-1 and SCA-2 were 3.56 and 3.14, respectively.

Two air-entraining admixtures (AEAs) were used. AEA-1 is a tall oil-based surfactant, produced by BASF Construction Chemicals, LLC. AEA-3 is an alkaline solution of fatty acid salts, produced by W. R. Grace. The specific gravities of AEA-1 and AEA-3 are 1.01 and 1.0 respectively. The AEAs were used to provide an air contents between 6.5 and 9.5 percent for all concrete mixtures.

Two high-range water-reducing admixtures (HRWRs) were used. HRWR-1 is polycarboxylate, produced by BASF Construction Chemicals, LLC. HRWR-2 is carboxylate polyether, produced by W. R. Grace. The specific gravities of HRWR-1 and HRWR-2 were 1.05 and 1.07, respectively. HRWR is added to the concrete mixtures to obtain the desired slump.

The rheology-modifying admixture (RMA) is a thixotropic anti-setting and rheology agent containing magnesium aluminosilicate, produced by Active Minerals. The specific gravity is 2.62. An RMA increases the viscosity of mixing water, reduces bleeding, and improves the cohesiveness of concrete.

2.2.7 Mixture Proportioning

Optimized aggregate gradations containing four aggregates were used in most concrete mixtures. The gradations were determined using KU Mix, a program developed at the University of Kansas. Additional discussion of aggregate optimization is provided by Lindquist et al. (2008, 2015). KU Mix can be downloaded from http://www.iri.ku.edu/projects/concrete/phase2.html.

The proportions of the mixtures used to evaluate settlement performance are summarized in Tables A.5 through A.14. The mixtures had a *w/cm* ratio of 0.45 and a cement paste volume of 27 percent. These values were used to produce mixtures that consistently exhibited settlement cracking. This was needed because mixtures with lower cement paste contents often exhibited no settlement cracking (Al-Qassag et al. 2015) and, as such, could not be used to measure the benefits of mixture modifications. The dosage of AEA was varied to achieve an air content between 6.0 and 9.5 percent; the quantity was a function primarily of the combination of cementitious material in the mixture. A HRWR was added to most concrete mixtures to achieve the desired concrete slump. This study involved ten types of concrete. Three concretes served as controls, denoted Control-1, Control-2, and Control-3. Aggregate gradations were optimized for Control-1 and Control-2 but not for Control-3. Two concretes contained IC. One concrete contained a 10.3 percent volume replacement of total aggregate with pea-gravel size pre-wetted LWA, providing 5.9 lb of water per 100 lb of cementitious materials, and is designated "5.9 lb-IC." The other concrete contained 12.3 percent volume replacement of total aggregate with fine pre-wetted LWA, providing 7 lb of water per 100 lb of cementitious materials, and is designated "7 lb-IC."

Two concretes contained SCMs. One concrete contained a 30 percent volume replacement of cement with slag cement and is designated "30% Slag." The other concrete contained 30 and 3 percent volume replacements of cement with slag cement and silica fume, respectively, and is designated "30% Slag - 3% SF." Two other concretes contained SCMs and IC. One mixture contained a 30 percent volume replacement of cement with slag cement and a 12.3 percent volume replacement of total aggregate with pre-wetted fine LWA and is designated "30% Slag - 7 lb-IC." The other mixture contained 30 and 3 percent volume replacements of cement with slag cement and silica fume, respectively, and a 12.3 percent volume replacement of total aggregate with fine

pre-wetted LWA and is designated “30% Slag - 3% SF - 7 lb-IC.” One concrete contained 2 percent of SRA-5 by weight of cement and is designated “2% SRA.”

The proportions of mixtures evaluated for freeze-thaw durability, scaling resistance, and air-void analysis are tabulated in Tables A.15 through A.17 in Appendix A. The mixtures had a cement paste volume of 24 percent and a *w/cm* ratio of 0.45. The evaluation included 28 mixtures. Three mixtures served as controls, denoted as “Control.” Six mixtures containing 0.5, 1, and 2 percent of SRA-2 by weight of cement are designated “0.5% SRA-2, 1% SRA-2, and 2% SRA-2,” respectively, and two mixtures containing 0.75 and 2.25 percent of SRA-3 by weight of cement are designated “0.75% SRA-3 and 2.25% SRA-3,” respectively. Four mixtures containing 20 and 40 percent volume replacements of cement with Class F fly ash are designated “20% FA-F and 40% FA-F,” respectively. One mixture containing a 20 percent volume replacement of cement with Class C fly ash is designated “20% FA-C.” Two mixtures containing 0.05 and 0.075 percent of rheology-modifying admixture (RMA) by total weight of dry materials are designated “0.05 RMA and 0.075% RMA,” respectively. Three mixtures contained 0.05, 0.075, and 0.15 percent of RMA by total weight of dry materials and 40 percent volume replacements of cement with Class C fly ash; they are designated “0.05 RMA - 40% FA-C, 0.075 RMA - 40% FA-C, and 0.15 RMA - 40% FA-C,” respectively. One mixture contained 0.15 percent of RMA by total weight of dry materials and 20 percent volume replacements of cement with Class C fly ash is designated “0.15 RMA - 20% FA-C.” Five mixtures containing 2.5, 5, and 7.5 percent of SCA-1 by weight of cement are designated “2.5% SCA-1, 5% SCA-1, and 7.5% SCA-1,” respectively. Finally, one mixture contained 6 percent of SCA-2 by weight of cement and is designated “6% SCA-2.”

2.3 LABORATORY METHODS

The laboratory methods employed to produce the concrete used in the laboratory tests are described in the following sections.

2.3.1 Mixing Procedure

Before mixing, the coarse aggregate was soaked for approximately 24 hours and then placed in the saturated surface-dry (SSD) condition following ASTM C127. Normalweight fine aggregate, sand and pea gravel, were added to the mixture in a partially wet condition. Prior to

batching, the free surface moisture of the sand and pea gravel was measured in accordance with ASTM C70, and the batch water was adjusted accordingly. The pre-wetted lightweight aggregate (LWA) was oven dried, and then soaked for 72 hours prior to mixing. The volume of water used to soak the LWA included both the water absorbed by the LWA in 72 hours and 70% of mixing water. The excess water (water not absorbed in 72 hours) was decanted and used as the mixing water.

A counter-current pan mixer was used. The mixer pan and blades were dampened before mixing. The coarse aggregate and 80% of mixing water were added to the mixer. Silica fume (if used) was then added to the mixer and mixed for 1.5 minutes. The cement and slag cement (if used) were then added and mixed for an additional 1.5 minutes. The fine aggregate was added (including LWA, if used) and mixed for 2 minutes. After 5 minutes of mixing, the superplasticizer, combined with 10% of mixing water, was added to the mixer, and the concrete was mixed for one minute. The AEA, combined with 10% of the mixing water, was added to the mixture and mixed for an additional 2.5 minutes. The mixer was stopped for 5 minutes (for the concrete containing SRA, the rest period was 30 minutes instead of 5 minutes to provide more time for air void stabilization). During the rest period, the concrete temperature was measured. The concrete was then mixed for a final 3 minutes. Before specimens were cast, each concrete mixture is checked for air (ASTM C173), unit weight (ASTM C138), temperature (ASTM C1064), and slump (ASTM C143). Three 4 × 8 in. (100 × 205 mm) cylinders were cast to measure compressive strength in accordance with ASTM C39.

2.3.2 Lightweight Aggregate Preparation

A centrifuge was used to place the soaked LWA to a pre-wetted surface-dry (PSD) condition. This is in contrast to ASTM C1761, in which a paper towel is used to achieve to the PSD condition. The centrifuge used in the study (Figure 2.1) had a bowl radius of 4.5 in. (114 mm).

Following is ASTM C1761, an oven-dry sample of lightweight aggregate is soaked in water for 72 hours. To start the test, the excess water is then decanted from the sample, and the LWA is remixed to reduce any segregation that may have occurred. A representative sample with

a mass of (600 ± 10 g) is selected and designated M_W. The sample is then distributed inside the centrifuge bowl to achieve good balance and avoid excessive vibration during the test. The centrifuge bowl is placed in the centrifuge with 4 µm filter paper secured over the top of the bowl, and the upper housing is placed on the top of the centrifuge and secured with clamps. The centrifuge is operated at 2000 rpm for three minutes, at which time the PSD moisture condition is achieved. The mass of the PSD material, M_{PSD}, is measured. The PSD sample is placed in an oven for 24 hours, and the mass of the oven dry sample M_{OD} is measured (Miller et al. 2014).

The surface moisture is calculated using Eq. (2.1).

$$\text{Surface Moisture } (\%) = \frac{M_W - M_{PSD}}{M_{PSD}} \times 100\% \tag{2.1}$$

The absorption is determined using Eq. (2.2).

$$Absorption(\%) = \frac{M_{PSD} - M_{OD}}{M_{OD}} \times 100\% \tag{2.2}$$

Where:

M_W – Mass of pre-wetted LWA, g,

M_{PSD} – Mass of pre-wetted surface-dry LWA, g,

M_{OD} – Mass of oven-dry LWA, g.

Figure 2.1 – Centrifuge used for testing

2.4 Test Procedures

Laboratory testing in this study covers settlement cracking of plastic concrete, freeze-thaw durability, scaling resistance, and air-void system analysis of hardened concrete. Three specimens were tested from each batch of concrete for all tests, except air-void analysis, which used two specimens.

2.4.1 Settlement Cracking

Settlement cracking was measured using a test developed by Brettmann et al. (2015). For each concrete mixture, three specimens were cast, finished, cured, and checked for settlement cracking as described in Sections 2.4.1.1 through 2.4.1.4.

2.4.1.1 Test Specimens

To measure settlement cracking, concrete is cast in 12 × 12 × 8 in. (305 × 305 × 205 mm) wood molds, as shown in Figure 2.2. The molds consist of 0.75-in. (20-mm) thick plywood sheets. A 12 in. (305 mm) long No. 6 (No. 19) reinforcing bar is attached to the molds using machine screws to provide a nominal clear cover of $1^1/_8$ in. (30 mm). The molds are sealed inside with white latex caulk and oiled using mineral oil.

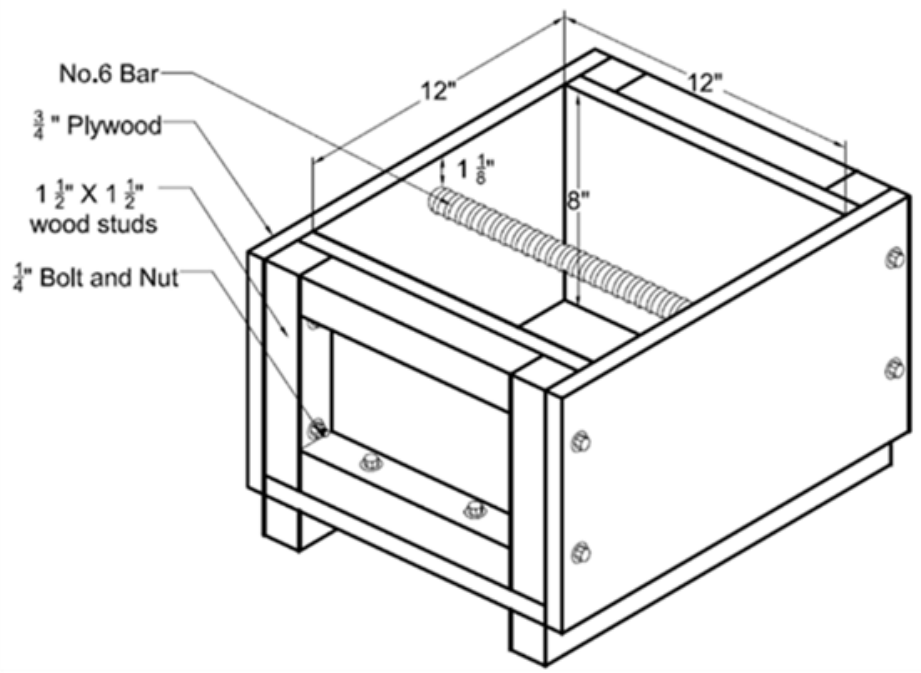

Figure 2.2 – Settlement cracking mold (Al-Qassag et al. 2015)

2.4.1.2 Casting

For each concrete mixture, three specimens are filled in two equal layers; after each layer is placed in the mold, the concrete is consolidated using an $1^1/_8$-in. (30-mm) diameter cordless spud vibrator, as shown in Figures 2.3a, 2.3b, and 2.3c. After the specimens are vibrated, the surface of each specimen is screeded using 20 × 2 × 0.75 in. (510 × 50× 20 mm) piece of plywood and finished with a 16 × 3 × 0.25 in. (405 × 75× 5 mm) metal hand float. Finished specimens are shown in Figure 2.3d.

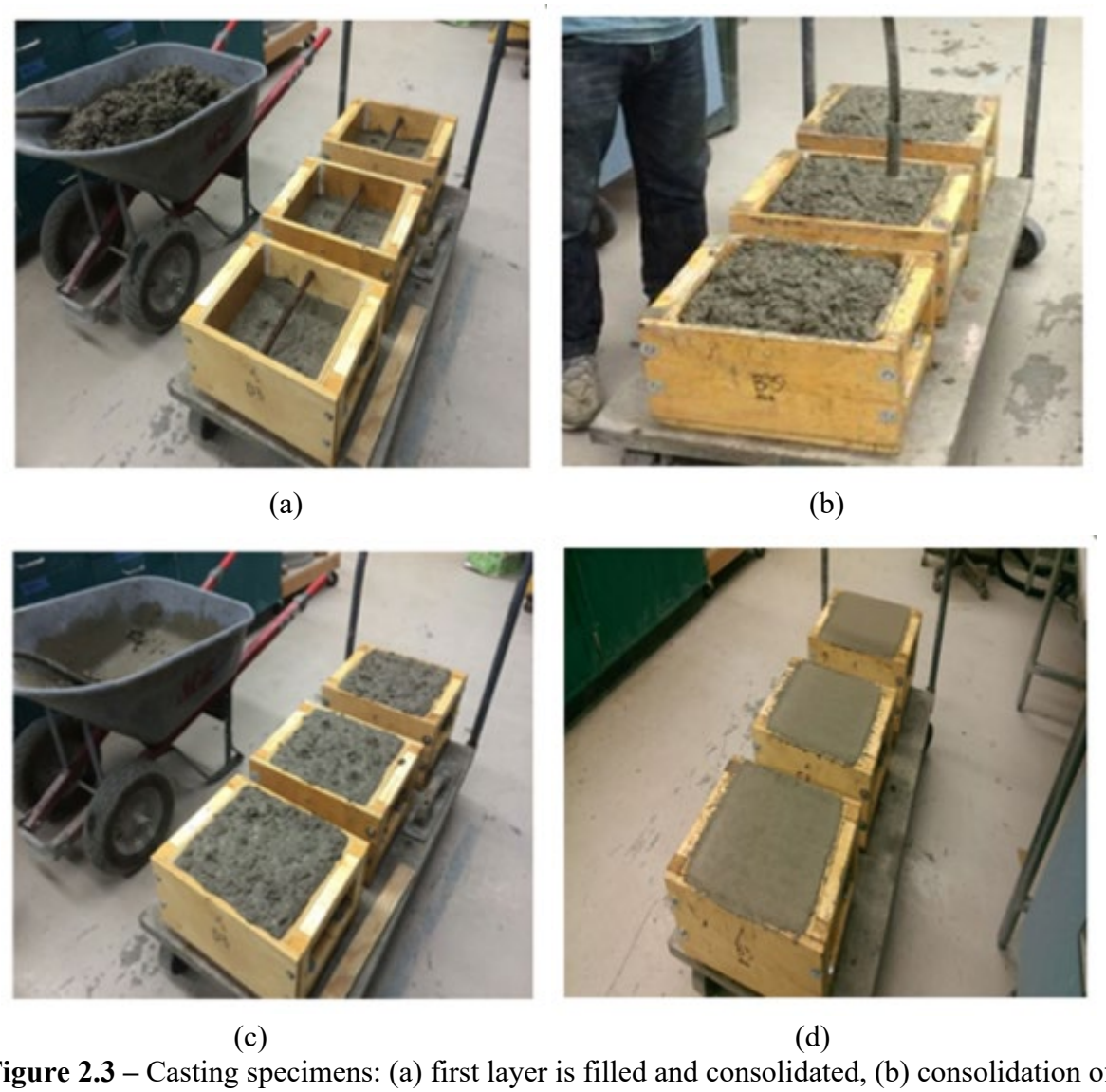

(a) (b)

(c) (d)

Figure 2.3 – Casting specimens: (a) first layer is filled and consolidated, (b) consolidation of second layer, (c) second layer is filled and consolidated, (d) specimens after finishing (Al-Qassag et al. 2015)

2.4.1.3 Curing

The curing procedure adopted in this study follows that developed by Brettmann et al. (2015) and is designed to minimize plastic shrinkage cracking and protect the concrete surface during the first 24 hours after casting.

After finishing the specimens, the concrete is covered using a Plexiglas plate sloped at 15° and then enclosed in a layer of plastic sheet, as shown in Figures 2.4a and b. The purpose of covering the specimens is to minimize plastic shrinkage cracking by providing sufficient humidity and reducing evaporation. The 15° slope on the Plexiglas allows water drops that condense on the plate to migrate to the lower edge of the plate and drop onto the sides of the form with no damage to the surface. The specimens are then moved to an environmentally-controlled laboratory and cured for 24 hours at 73° ± 3° F (23° ± 1.5° C) and relative humidity of 50 ± 4 percent.

(a) (b)

Figure 2.4 – Curing specimens: (a) place a sensor on the specimen surface and cover with sloped Plexiglas, (b) cover with plastic sheeting and cure at the environmentally controlled laboratory

To evaluate effectiveness of the procedure, a sensor (Figure 2.4a) is placed on the surface of selected specimens to measure the humidity during the curing period. The relative humidity during the first 24 hours after casting for a control mixture (Control-2), a mixture containing pre-

wetted lightweight aggregate (LWA), and a mixture containing shrinkage-reducing admixtures (SRA) is shown in Figure 2.5. As shown in the figure, the relative humidity of all mixtures was greater than 90 percent, preventing the formation of plastic shrinkage cracks; thus, the cracks that did form could be expected to be limited to those caused by settlement of the plastic concrete.

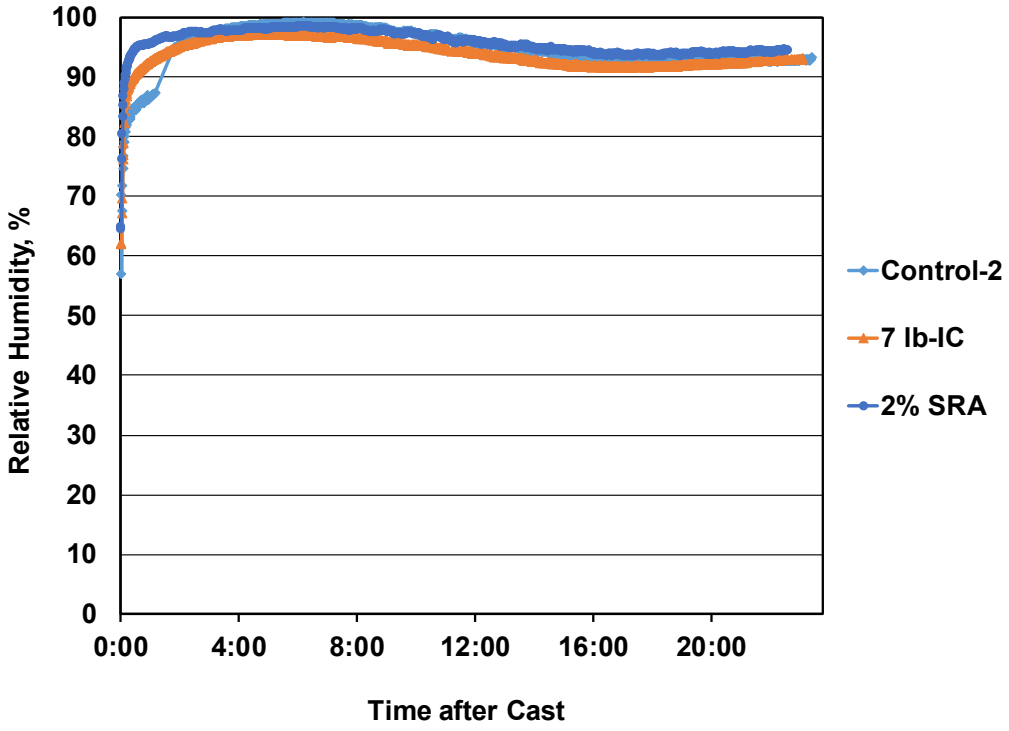

Figure 2.5 – Relative humidity versus time after cast for Control-2, IC, and SRA mixtures

2.4.1.4 Measuring Settlement Cracking

After 24 hours of curing, the specimens are removed from the environmentally controlled laboratory and checked for settlement cracking. Only cracks that form directly over and parallel to the reinforcing bar are considered to be settlement cracks. In this study, a small number of other cracks were observed on the surface of a few specimens. These cracks formed at random locations at some distance from the bar and were not counted as settlement cracks because they were not directly over the bar. Cracks are identified with unaided eye while using flashlight and recorded on the surface using a permanent marker. The total length of the cracks observed on the surface of each specimen is measured using a ruler. The settlement crack intensity of a concrete mixture is

then determined as the average total length of the cracks formed on the surface of three specimens of each mixture divided by the length of the reinforcement in a specimen [12 in. (305 mm)]. The greatest crack width observed on the surface of each individual specimen is measured using a magnifying crack comparator [with a minimum measure of 0.001 in. (0.025 mm)]. The crack width of a concrete mixture is taken as the average these widths for the three specimens of each mixture. Figure 2.6 shows a marked settlement cracking specimen.

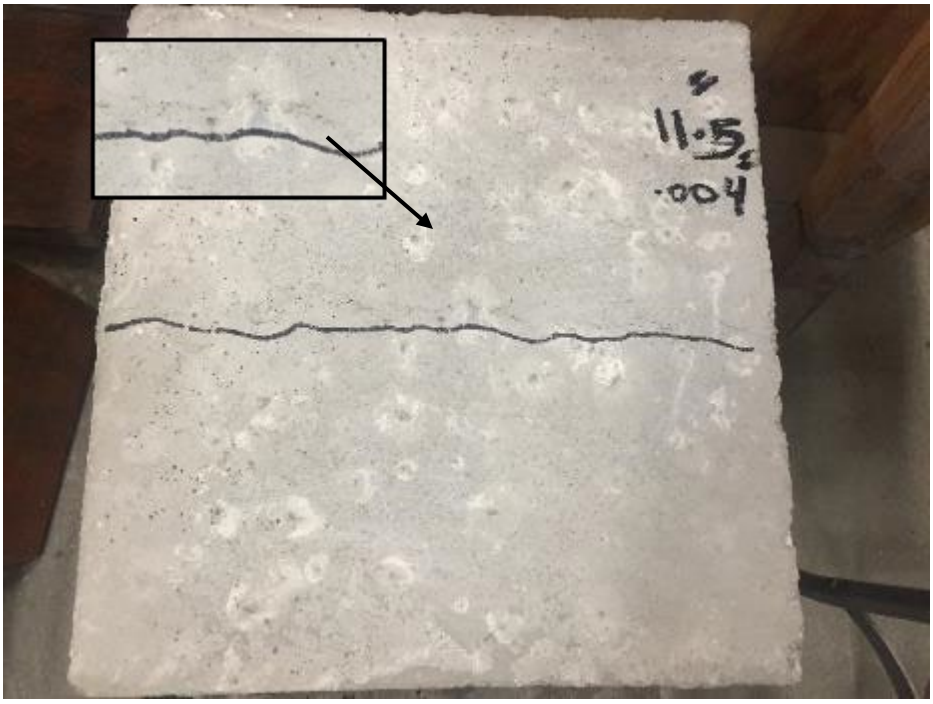

Figure 2.6 – Marked settlement cracking specimen

2.4.2 Freeze-Thaw Durability and Fundamental Transverse Frequency

The freeze-thaw durability and fundamental transverse frequency tests were performed in accordance with ASTM C666, using Procedure B, Rapid Freezing in Air and Thawing in Water, and ASTM C215, respectively. The tests were used to determine the resistance of concrete to rapidly repeated cycles of freezing and thawing in the laboratory. Three 16 × 3 × 4 in. (405 × 75 × 100 mm) specimens were cast for each batch using steel molds.

2.4.2.1 Demolding and Curing

The specimens are demolded 24 hours after casting, labeled, and cured in lime-saturated water. Following Kansas Department of Transportation (KDOT) Test Method KTMR-22, the specimens are cured in the lime water for 67 days, and then placed in an environmentally-controlled laboratory at 73° ± 3° F (23° ± 1.5° C) and relative humidity of 50 ± 4 percent for 21 days prior to testing. The specimens are placed in a water-filled, tempering tank maintained at 70° F (21° C) for 24 hours, and placed in a water-filled, insulated cooler maintained at 40° F (4.4° C) for 24 hours. The initial dynamic modulus of elasticity of each specimen is determined based on its initial mass and fundamental transverse frequency, as described in the following section.

2.4.2.2 Freezing and Thawing

Specimens are subjected to three-hour freeze-thaw cycles in accordance with ASTM C666 – Procedure B using a ScienTemp^{TM} 20-Block Concrete Freeze-Thaw Machine, shown in Figure 2.7. The procedure consists of alternately lowering the temperature from 40º to 0° F (4º to -18° C) in air and raising from 0 to 40° F (-18º to 4° C) in water for each freeze-thaw cycle. The specimens are removed from the machine in a thawed condition at intervals not exceeding 36 cycles to measure the mass and fundamental transverse frequency. The test continues until the specimens are subjected to 300 cycles or until the average dynamic modulus of elasticity of the specimens reaches 60 percent of the initial dynamic modulus.

Figure 2.7 – Freeze-Thaw machine (Pendergrass and Darwin 2014)

To measure the dynamic modulus of elasticity, specimens are dried to a surface-dry condition and weighed. The specimens are protected against loss of moisture during the test by placing them in a Styrofoam™ cooler. The fundamental transverse frequency is then measured in accordance with ASTM C215 – Impact Resonance Method, as illustrated in Figure 2.8.

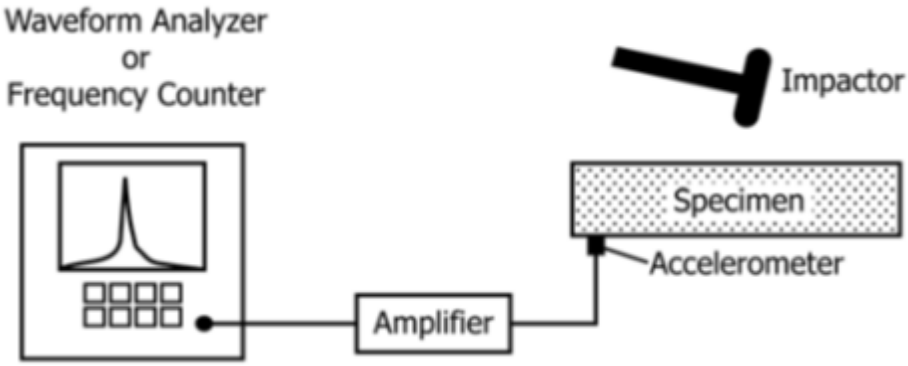

Figure 2.8 – Schematic of apparatus for impact Resonance Test (ASTM C215)

The transverse frequency is measured by placing the specimen on a pedestal made of rubber and foam. An accelerometer is mounted on the specimen near one end. The specimen is then struck by an impactor at the middle of the specimen perpendicular to the surface. The resonant frequency is measured using a frequency counter. The test is repeated two more times, and the average of transverse resonant frequency, along with the mass and specimen dimensions, is used to calculate the dynamic modulus of elasticity of the concrete using Eq. (3.2).

$$Dynamic\ E = C \times M \times n^2 \tag{3.2}$$

where:

Dynamic E = the dynamic modulus of elasticity (Pa),

C = 1083.6 m^{-1} for a prism, according to ASTM C125,

M = the mass of specimen,

n = the fundamental transverse frequency (Hz).

The freeze-thaw durability of the specimen is identified by the relative dynamic modulus (RDM), representing the percentage of the average dynamic modulus of elasticity of three specimens that are subjected to 300 freezing cycles, determined by the following equation:

$$RDM = \frac{P \times N}{M} \tag{4.2}$$

where:

P = the percentage of the dynamic modulus of elasticity remaining at N cycles,

N = the number of cycles at which P reached 60 percent or 300 cycles, whichever is less,

M = 300 cycles.

2.4.3 Scaling Resistance

The specimens were tested for scaling resistance following Canadian Test BNQ NQ 2621-900 Annex B rather than ASTM C672 since the Canadian test gives a better match with field studies (Bilodeau et al. 2008), with modifications to the concentration of NaCl solution and the temperature range used for the freeze-thaw cycle. Three 16 × 9 × 3 in. (405 × 230 × 75 mm) specimens were cast for each batch using steel molds.

2.4.3.1 Demolding and Curing

Specimens are demolded after 24 hours of casting, labeled, and cured in lime-saturated water for 14 days after casting. The specimens are then moved to an environmentally-controlled laboratory at 73° ± 3° F (23° ± 2° C) and a relative humidity of 50 ± 4 percent for an additional 14 days. After six days of air drying in the controlled room, a Styrofoam™ dike is attached to the surface of the specimen using a polyurethane sealant, as shown in Figure 2.9a. Twenty-eight days after casting, specimens are pre-saturated with a ¼-in. (6 mm) deep layer of 2.5 percent NaCl solution within the dike for 7 days in the controlled room and covered with a plastic sheet to avoid evaporation of the solution, as shown in Figure 2.9b. The 2.5 percent NaCl solution is used instead of 3 percent in accordance with BNQ NQ 2621-900 Annex B, based on the study of Verbeck and

Klieger (1957), who found that a 2.5 percent NaCl solution can cause greater scaling. As a result, this test is more severe than the BNQ test.

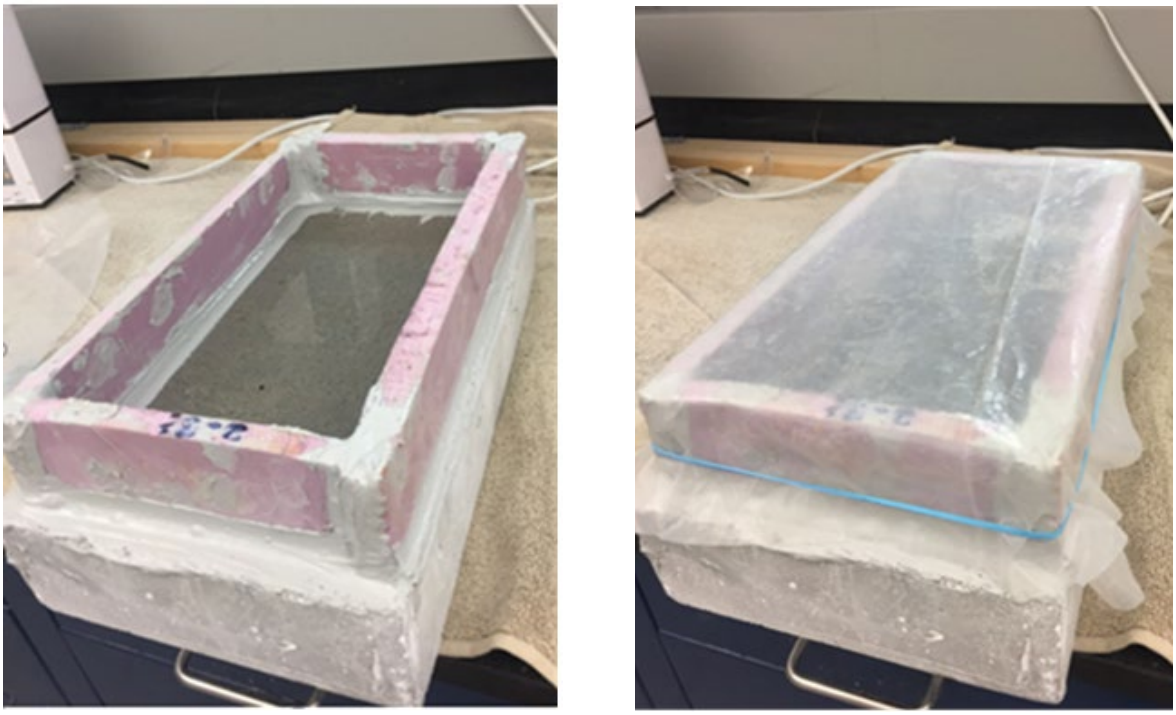

(a) (b)

Figure 2.9 – Scaling resistance test specimen: (a) attach Styrofoam™ dike to the surface of the specimen, (b) cover the specimen with plastic sheeting

2.4.3.2 Freezing and Thawing and Measuring of Mass Loss

The specimens are subjected to freeze-thaw cycles 35 days after casting. Each freeze-thaw cycle lasts 24 hours and consists of a freezing phase of 16 ± 1 hours at 0 ± 5º F (-18º ± 3º C) and a thawing phase of 8 ± 1 hours at 73º ± 3º F (23º ± 2º C). The freezing phase is performed each night in a walk-in freezer, and the thawing phase is performed each day in the environmentally-controlled room (73° ± 3° F (23° ± 2° C) and a relative humidity of 50 ± 4 percent). The temperature range of the cycles differs somewhat from that specified in BNQ NQ 2621-900 Annex B, which requires a freezing phase at -4º ± 5.4º F (-20º ± 3º C) and a thawing phase at 77º ± 5.4º F (25º ± 3º C). The scaled material is wet-sieved over a No. 200 (75-µm) sieve, and the mass loss of each specimen is measured after 7, 21, 35, and 56 cycles. Mass loss is expressed in lb/ft^2 of the

exposed surface. After measuring the mass loss, a fresh salt solution is placed on the surface to continue the test. At the end of the test (56 cycles), the average of mass cumulated of three specimens is considered the mass loss of the batch. The Canadian test permits a maximum average cumulative mass loss limit of 0.2 lb/ft^2 (1000 g/m^2) at test completion.

2.4.4 Air-Void System Analysis of Hardened Concrete

Air-void analysis of hardened concrete was performed in accordance with ASTM C457, Procedure A, Linear Traverse Method using an automated air-void analyzer. The analysis includes the determination of air-void parameters, including spacing factor, air content, and specific surface; these parameters were then compared with the freeze-thaw durability and scaling resistance of the same mixtures. The test was performed on two 4 × 8 in. (100 × 205 mm) cylindrical specimens cast in accordance with ASTM C192, demolded after 24 hours, cured in a moist-curing room with a minimum relative humidity of 95 percent and a temperature of 73º ± 3º F (23º ± 2º C) for 28 days, and moved to the environmentally controlled room at 73° ± 3° F (23° ± 2° C) and a relative humidity of 50 ± 4 percent until the date of the test.

2.4.4.1 Air-Void Sample Preparation

The steps used to prepare a sample for air-void analysis are as follows:

Sectioning

A cylinder is cut perpendicular to the longitudinal axis using a masonry saw. Each half is then cut longitudinally three times to form two parallel slabs, as shown in Figure 2.10a, using an 18 in. (450 mm) Rock Slab Lapidary saw. The outside of the samples is discarded. The slabs have dimensions of 4 × 4 × 3/4 in. (100 × 100 × 20 mm). In this study, some cylinders, which were cast from the concrete containing SCA-1, were cut perpendicular to the longitudinal axis; each half was then cut perpendicular to the longitudinal axis two times to form two parallel circular slabs with dimensions of 4 × 3/4 in. (100 × 20 mm), as shown in Figure 2.10b.

Polishing and Lapping

One surface of each slab is polished using an 18-in. (455-mm) ASW Diamond polishing machine, as shown in Figure 2.11a and 2.11b.

(a) (b)

Figure 2.10 – Sectioning air-void slab: (a) Square slab, (b) Circular slab

(a) (b)

Figure 2.11 – Polishing the surface: (a) ASW Diamond polishing machine, (b) Varying polishing discs

For each step in polishing, the slab is cleaned under running tap water, and dried using compressed air, a thin layer of lacquer is then applied to the surface to protect the edge of the air voids from damage during polishing. Each slab is polished, in order, using four diamond discs: 180, 260, 360, and 600 grit, then three pre-polish resin discs 180, 360, and 600 grit, with equal pressure applied by hand on the surface to ensure uniform polishing. After each step of polishing, the flatness of the slab is checked using a steel straightedge. After the last polishing step, a stereo microscope is used to check the quality of polishing to ensure the surface has no scratches, which can influence the results. At the end of these processes, the slab should have a flat and shiny surface. Figures 2.12a and 2.12b, respectively, show the surface of a slab before and after polishing. When polishing is completed, the slab is bathed in acetone for a few minutes to remove the remaining lacquer from the surface. The slab is then stored in a plastic bag to protect the surface from damage.

(a) (b)

Figure 2.12 – Polishing the surface: (a) Before polishing, (b) After polishing.

Surface Contrast Enhancement

Prior to using the air-void analyzer, the polished surfaces are treated to enhance the contrast between the air voids and the cement paste and aggregate, so that air voids appear as white regions on a black background. Figure 2.13 shows the surface contrast enhancement steps. First, the

surface is painted using a wide black permanent marker with the strokes oriented in a single direction (Figure 2.13a). The sample is then placed in an oven at 105°F (41ºC) for approximately 15 minutes to dry the surface. The surface is painted again in the direction perpendicular to that used for the first layer and allowed to dry in the oven for an additional 15 minutes. The sample is then placed on a board, and a layer of barium sulfate is spread over the surface (Figure 2.13b). The barium sulfate is pressed on the surface using a rubber stamper with sufficient force to fill the surface voids (Figure 2.13c), followed by a rubber stopper with a twisting motion to complete the process (Figure 2.13d). Excess barium sulfate is scraped from the surface using a metal straightedge (Figure 2.13e). To clean the surface from the remaining barium sulfate, the palm of a hand, which should be rubbed on the wet towel and then dry towel, is used to wipe the surface until the surface become shining with no white dust (Figure 2.13f). Voids in the aggregate that

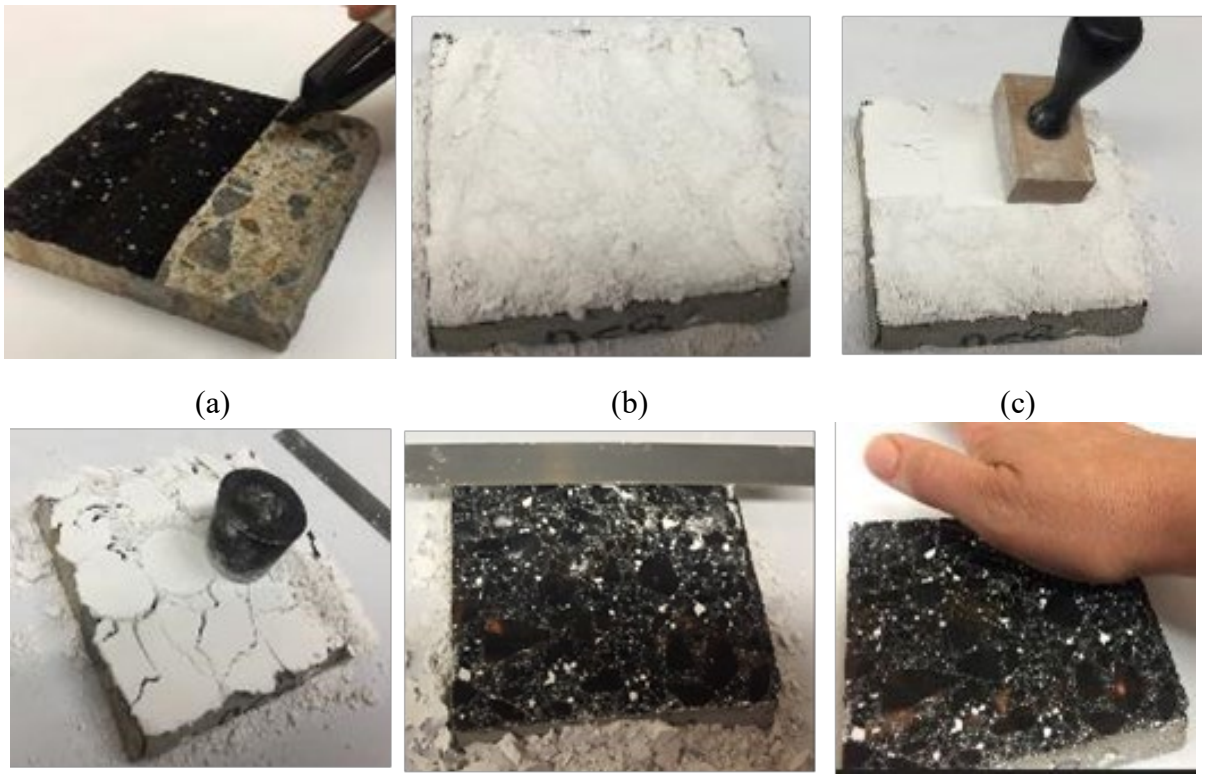

Figure 2.13 – Surface contrast enhancement steps: (a) Painting the surface using a black permanent marker, (b) Spreading barium sulfate over the surface, (c) Pressing barium sulfate on the surface using a rubber stamper, (d) Forcing barium sulfate in the voids using a rubber stopper, (e) Scraping the excess of barium sulfate from the surface using a metal straightedge, (f) Cleaning the surface from barium sulfate using the palm of a hand.

contain barium sulfate are then colored black using a fine point black permanent marker to avoid identifying them as entrained air during the analysis. A stereo microscope with cross lighting is used to check the small particles of aggregate, as shown in Figure 2.14a. Painter's tape is applied along the perimeter of the polished slab, providing four corners from which each of four analyses is initiated.

2.4.4.2 Air-Void Analysis System

The Rapid Air 457 is an automated analysis system for measuring the air-void characteristics of hardened concrete based on ASTM C457, Procedure-A, Linear Traverse Method. The Rapid Air 457 system is composed of a computerized control unit with a high-resolution LCD color monitor, a digital color camera, a microscope objective mounted on a moving stage and user analysis software (Murphy and Chao 2009). Figure 2.14b shows the configuration of the Rapid Air 457. The Linear Traverse Method uses a series of regularly spaced lines on which linear chords are measured for each material constituent. The data generated by the system, which includes the total length traversed (T_t), the length traversed through paste (T_p), the length traversed

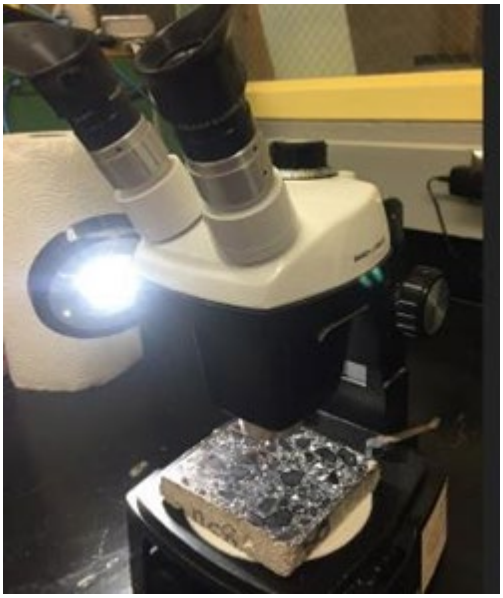

(a)

(b)

Figure 2.14 – (a) A stereo microscope with cross lighting to check and color black any voids in the aggregates, (b) The Rapid Air 457 system for automatic analysis of air-voids

through air voids (T_a), the number of air voids intersected by the lines (N), and the average chord length intersected for air voids (l_{mean}), are used to determine the parameters of the air-void system and are automatically saved within each test report. The Rapid Air 457 collects all white pixel chords, in accordance with ASTM C 457. Chords smaller than 30 μm, however, are not included in the analysis as they are not easily detected by a human during a standard test of ASTM C 457 and would, thus, not be counted in a manual survey of the surface. Using an automatic analysis system eliminates human judgment during the analysis. A Rapid Air 457 analysis requires approximately 15 minutes to perform, a major improvement compared to the manual method, which requires 5 to 6 hours (Carlson et al. 2006, Jakobsen et al. 2006).

To perform the ASTM C 457 test, the volume of the cement paste and the dimensions of the sample must be provided. A traverse-line with a length of 95 in. (2413 mm) per slab is used. A threshold value, which is the most important step in the analysis on a contrast-enhanced surface, is set for dividing line between what is and what is not classified as air. The threshold value of 160 is used for all slabs in the study. Each slab is then measured four times, the slab is rotated 90° between measurements. The average of the four readings of the slab is reported as the air-void parameters of that slab.

Following are the main air-void parameters determined by the analysis:

Air void content – Total volume fraction of air voids in the concrete.

Spacing factor – A measure of the average distance from any point in the cement paste to the edge of the nearest air void. The spacing factor is considered by some to be the most important factor for freeze-thaw durability.

Specific Surface – The surface area of the air voids divided by the volume of air voids.

2.5 EXPERIMENTAL PROGRAMS

The study involved six experimental programs. The objective and scope of the programs are described in this section. Programs 1 through 5 address the effects of different cementitious materials and shrinkage-reducing technologies on settlement cracking in concrete mixtures, while Program 6 addresses the effects of a range of shrinkage-reducing technologies on the air-void characteristics of concrete, freeze-thaw durability, and scaling resistance.

2.5.1 Program 1: Evaluation of Settlement Cracking for Control Mixtures with Different Aggregate Gradations

Program 1 examined control mixtures with different aggregate gradations to determine the effect of the gradation on settlement cracking. The program included three concrete mixtures, Control-1, Control-2, and Control-3. The Control-2 mixture contained an aggregate gradation that was finer than that of Control-1, while the Control-3 mixture contained non-optimized aggregate gradation. The proportions of each mixture are listed in Tables A.5 to A.7 in Appendix A.

2.5.2 Program 2: Evaluation of Settlement Cracking for Mixtures Containing Pre-Wetted Lightweight Aggregate

Program 2 examined two mixtures containing pre-wetted lightweight aggregate (LWA) to determine the effect of internal curing on settlement cracking: The 5.9 lb-IC mixture, with a 10.3 percent volume replacement of total aggregate with pea-gravel size pre-wetted LWA, providing 5.9 lb of water per 100 lb of cementitious material and the 7 lb-IC mixture, with a 12.3 percent volume replacement of total aggregate with fine pre-wetted LWA, providing 7 lb of water per 100 lb of cementitious materials. The proportions of these mixtures are listed in Tables A.8 and A.9 in Appendix A.

2.5.3 Program 3: Evaluation of Settlement Cracking for Mixtures Containing Supplementary Cementitious Materials, Slag Cement and Silica Fume

Program 3 examined two mixtures containing supplementary cementitious materials (SCMs), slag cement, and silica fume to investigate the effect of SCMs on settlement cracking: The 30% Slag mixture containing a 30 percent volume replacement of cement with slag cement and the 30% Slag - 3% SF mixtures containing 30 and 3 percent volume replacements of cement with slag cement and silica fume, respectively. The proportions of these mixtures are listed in Tables A.10 and A.11 in Appendix A.

2.5.4 Program 4: Evaluation of Settlement Cracking for Mixtures Containing Supplementary Cementitious Materials and Pre-Wetted Lightweight Aggregate

Program 4 examined two mixtures containing both supplementary cementitious materials (SCMs) and pre-wetted lightweight aggregate (LWA) to evaluate the combined effect of SCMs and internal curing on settlement cracking: The 30% Slag - 7 lb-IC mixture, with a 30 percent volume replacement of cement by slag cement and a 12.3 percent volume replacement of total

aggregate with pre-wetted LWA and the 30% Slag - 3% SF - 7 lb-IC mixture, with 30 and 3 percent volume replacements of cement by slag cement and silica fume, respectively and a 12.3 percent volume replacement of total aggregate with pre-wetted LWA. The proportions of these mixtures are listed in Tables A.12 and A.13 in Appendix A.

2.5.5 Program 5: Evaluation of Settlement Cracking for Mixtures Containing Shrinkage-Reducing Admixture

Program 5 examined one mixture containing shrinkage-reducing admixture (SRA-5) to determine its effect on settlement cracking: The 2% SRA mixture contained 2 percent of SRA-5 by weight of cement. The proportions of this mixture are listed in Tables A.14 in Appendix A.

2.5.6 Program 6: Evaluation the Air-Void Characteristics and Durability of the Concrete Mixtures Containing Shrinkage-Reducing Admixtures, Fly Ash, Rheology-Modifying Admixture, and Shrinkage-Compensating Admixtures

Program 6 evaluated concrete mixtures containing different combinations of shrinkage-reducing admixtures (SRAs), fly ash, a rheology modifying admixture (RMA), and shrinkage compensating admixtures (SCAs) based on the air-void parameters, freeze-thaw durability, and scaling resistance. The program also examined the correlation between the air-void parameters, freeze-thaw durability, and scaling resistance of these mixtures. The proportions of these mixtures are listed in Tables A.15 through A.17 in Appendix A.

CHAPTER 3: SETTLEMENT CRACKING RESULTS AND EVALUATION

3.1 GENERAL

Minimizing cracking in concrete structures provides many advantages tied to improved durability, not to mention appearance. Some crack-reducing technologies, such as fibers, internal curing, and shrinkage-reducing admixtures, are aimed at reducing shrinkage in hardened concrete. Replacing a portion of the portland cement in a mixture with one or more supplementary cementitious materials, such as fly ash, slag cement, and silica fume, is often used to improve the economy or properties of the resulting hardened concrete (Mindess et al. 2003). Minimizing plastic shrinkage cracking is usually addressed by limiting the rate of evaporation from a concrete surface (*Design and Control* 2016) and sometimes using fibers. Settlement cracking in plastic concrete, not the sole cause but often associated with transverse cracking in bridge decks, can be limited by using low slump (Dakhil et al. 1975, Weyers at al. 1982, and Al-Qassag et al. 2001), fibers, and rheology modifying admixtures (Al-Qassag et al. 2016), and by thorough consolidation, minimum finishing, and early curing (Darwin et al. 2004, 2010, 2016, Pendergrass and Darwin 2014, Khajehdehi and Darwin 2018). Transverse cracks in bridge decks tend to form parallel to and directly over reinforcing steel; minimizing cracking in bridge decks goes a long way toward improving their durability (Darwin et al. 2011). Because the effects of cracking in plastic and hardened concrete tend to be additive, the effects on settlement cracking of technologies developed to control concrete properties in other ways are investigated to more fully establish the role of these technologies in minimizing cracking in concrete structures. To date, this has been done for fibers and rheology modifying admixtures (Al-Qassag et al. 2016). This chapter presents the results and evaluation of the effects of aggregate gradation, internal curing (IC), supplementary cementitious materials (SCMs), and shrinkage-reducing admixture (SRA) on settlement cracking of plastic concrete. The study included two series; the aggregate gradation in Series 1 was coarser than that used in Series 2. The concrete of both series had a cement paste volume of 27 percent and a water to cementitious materials (*w/cm*) ratio of 0.45.

3.2 SERIES 1

Series 1 was used to evaluate the effect of internal curing (IC) water on settlement cracking of plastic concrete. Internal curing was provided by pre-wetted pea-gravel size LWA. The series involved two types of concrete: control mixtures, designated "Control-1," and mixtures with a 10.3 percent volume replacement of total aggregate with pea-gravel size pre-wetted LWA providing 5.9 lb of water per 100 lb of cementitious materials, designated "5.9 lb-IC." The concrete in this series used Type I/II portland cement with a specific gravity of 3.15 as the only cementitious material.

3.2.1 Control-1

Figure 3.1 compares the average settlement crack intensity, ratio of the average total crack length for the three specimens of a mixture to the bar length [12 in. (305 mm)], with slump for the Control-1 mixtures. The figure includes a trendline and two lines offset by ± 1 standard deviation of the trendline. The standard deviation is calculated by comparing the measured value of crack intensity x_i for each mixture to the value of crack intensity $\overline{x}_i$ given by the trendline, using the following equation:

$$\sigma = \sqrt{\frac{\sum_i \left(x_i - \overline{x}_i\right)^2}{n-1}} \tag{3.1}$$

where:

σ = standard deviation of the measured values of crack intensity about the trendline,

x_i = measured crack intensity of mixture i,

$\overline{x}_i$ = crack intensity given by the trendline,

n = number of mixtures in the set.

The figure shows that the crack intensity increased as slump increased. This finding agrees with the previous studies (Dakhil et al. 1975, Weyers at al. 1982, and Al-Qassag et al. 2015). In this case, the average crack intensity increased from 0.38 at a slump of $2^1/_2$ in. (65 mm) to 0.73 at a slump of 8 in. (205 mm). The average maximum crack width, which is based on the average of

the maximum crack width for each of the three specimens from a mixture, ranged from 0.0013 to 0.0047 in. (0.035 to 0.120 mm), also increases as slump increased, as shown in Figure 3.2. Control-1 is the only mixture to exhibit a maximum crack width greater than 0.004 in. (0.1 mm). The properties, including slump, air content, concrete temperature, unit weight, and compressive strength, as well as the settlement cracking results, the length and width of cracks, for these mixtures are summarized in Table B.1 in Appendix B.

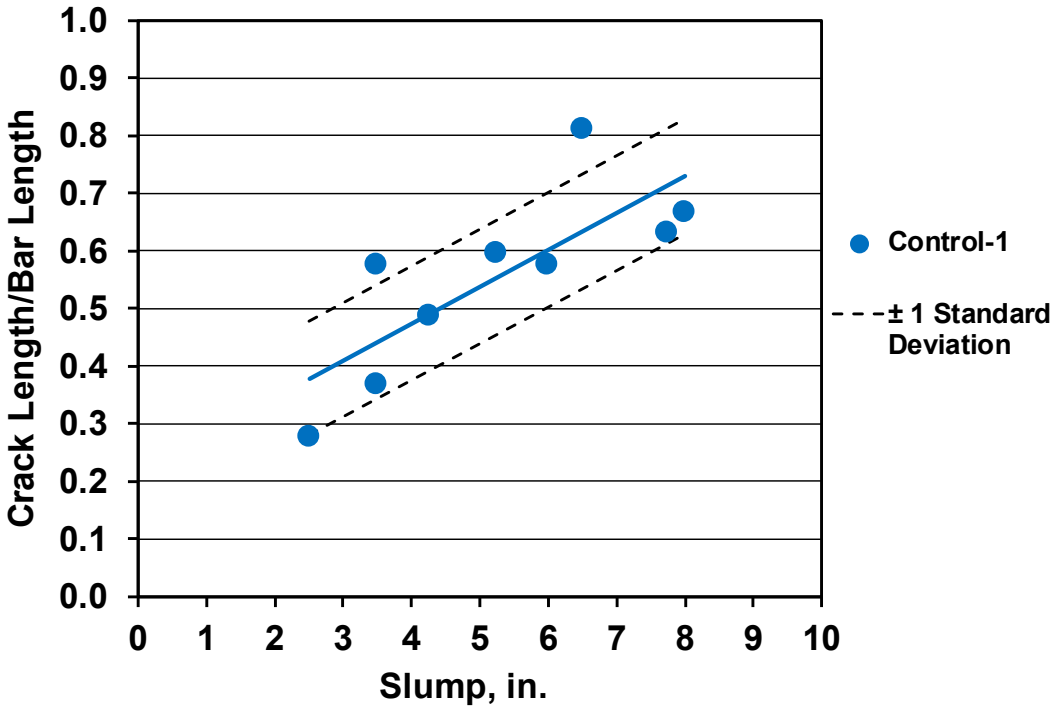

Figure 3.1 – Average settlement crack intensity (ratio of crack length to bar length) versus slump for the Control-1 mixtures

3.2.2 5.9 lb-IC

Figure 3.3 compares settlement crack intensity with slump for the 5.9 lb-IC mixtures. The average crack intensity increased from 0.22 at a slump of $2^1/_2$ in. (65 mm) to 0.44 at a slump of 7 in. (180 mm). The average maximum crack widths ranged from 0.0013 to 0.0030 in. (0.035 to 0.075 mm), increasing as slump increased, as shown in Figure 3.4. The properties and detailed settlement cracking results for these mixtures are summarized in Table B.4 in Appendix B.

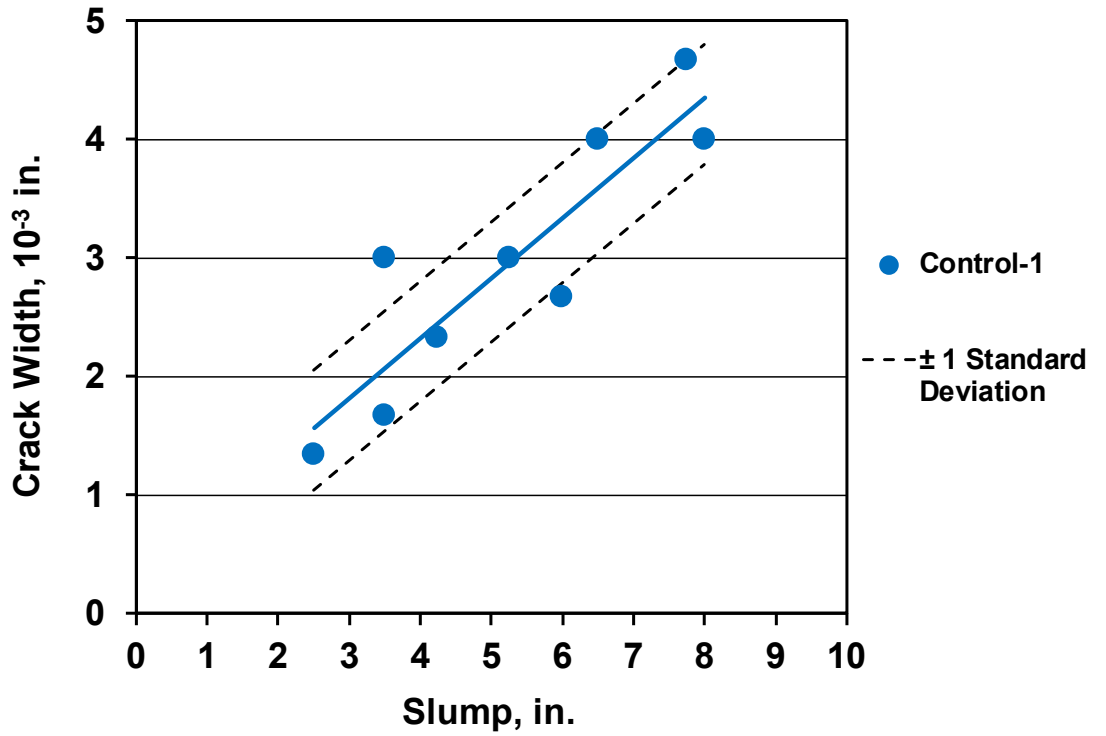

Figure 3.2 – Average maximum crack width versus slump for the Control-1 mixtures

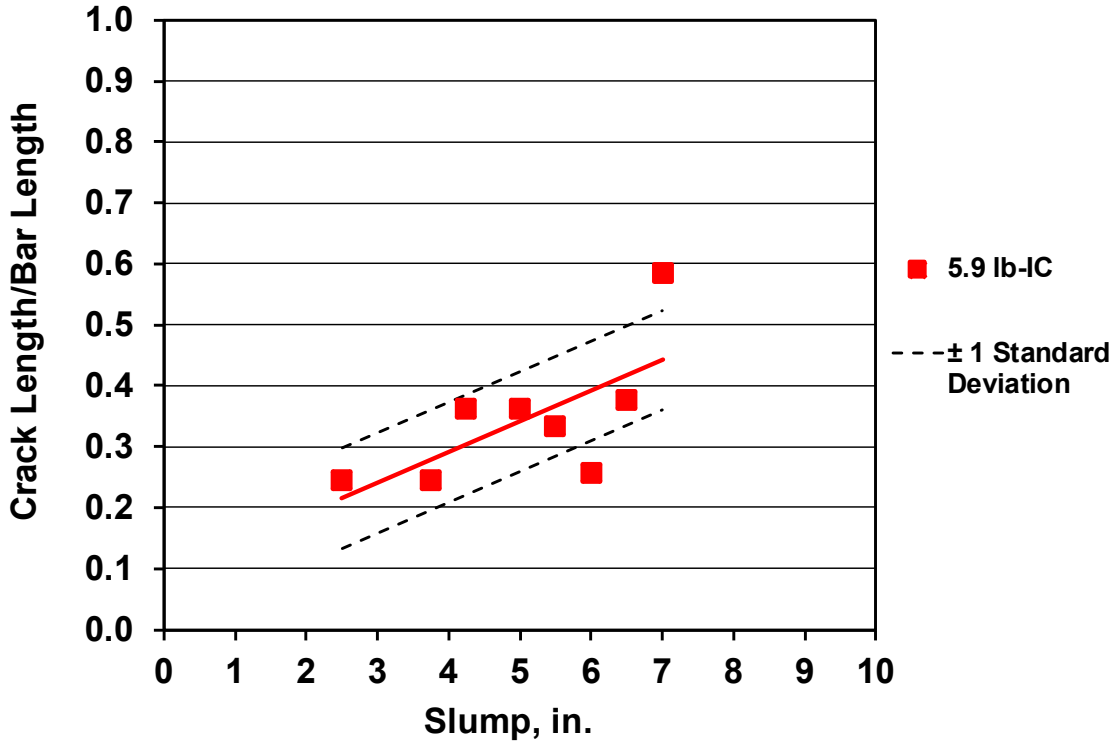

Figure 3.3 – Average settlement crack intensity (ratio of crack length to bar length) versus slump for the 5.9 lb-IC mixtures

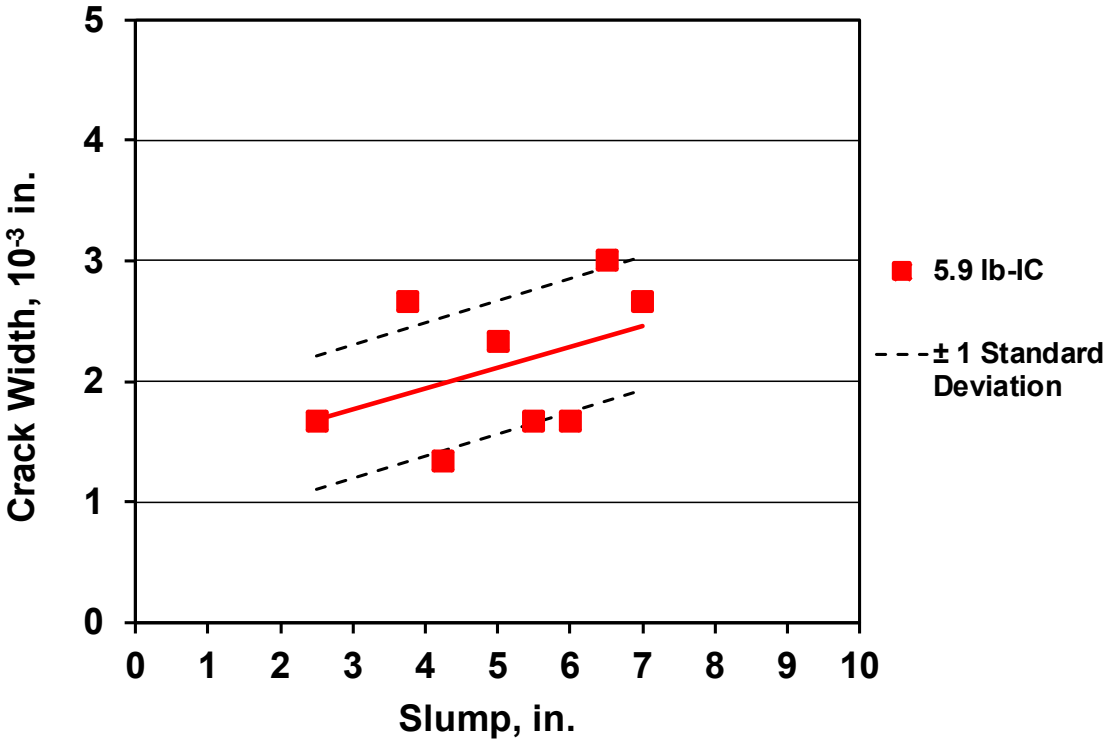

Figure 3.4 – Average maximum crack width versus slump for the 5.9 lb-IC mixtures

Figure 3.5 compares settlement crack intensity with slump for the Control-1 and 5.9 lb-IC mixtures. As shown in the figure, the concrete with internal curing exhibited less settlement cracking than the control mixture at all slumps. The average crack intensity of the 5.9 lb-IC mixture is about 34 percent lower than that of Control-1 at a 7-in. (180-mm) slump. To identify the statistical significance of the differences in crack intensity for these two types of concrete, Student's t-test was used. Student's t-test is a parametric analysis that can determine whether the difference in the means, $\overline{x}_1$ and $\overline{x}_2$, of two sets of data, x_1 and x_2, is statistically significant at a specified level of significance, p. The comparison between two types of concrete was performed at slumps between 1 and 8 in. (25 and 205 mm) at 1-in. (25-mm) interval. The analysis depends on the mean $\overline{x}$, the number of samples n, and the standard deviation σ of each set. The mean $\overline{x}$ of each interval of slump is taken as the value of the trendline equation derived based on the slump and the corresponding crack intensity for each mixture in the set. The standard deviation is calculated using an Eq. (3.1), as described in Section 3.2.1. The significance level p is then

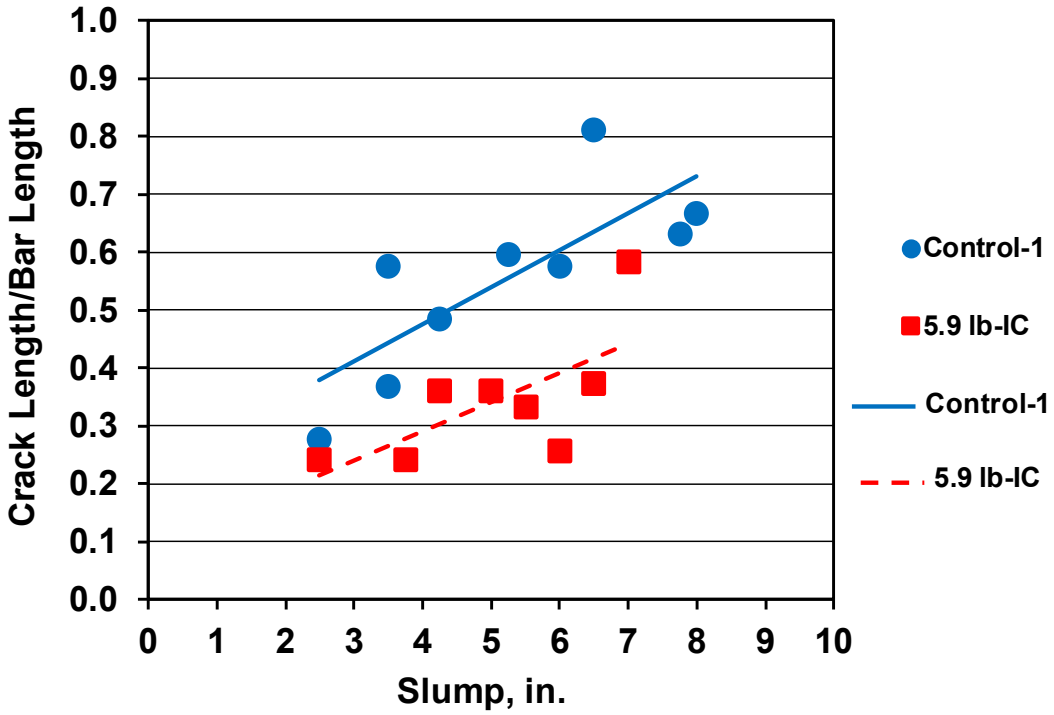

Figure 3.5 – Average settlement crack intensity (ratio of crack length to bar length) versus slump for the Control-1 and 5.9 lb-IC mixtures

calculated to determine the probability that the difference in the sets does not occur due to random variation in the test. In this study, a value of p less than or equal to 0.05 is used as the threshold for statistical significance, indicating that there is a 5 percent probability (or less) that the observed difference in the mean of two sets would occur by chance. The results of Student's t-test show that the significance level, p, was less than 0.05 for all slumps, indicating that the differences in the crack intensity between the Control-1 and 5.9 lb-IC mixtures are statistically significant. Student's t-test results for the mixtures of these two types of concrete are listed in Table C.1 in Appendix C. The reason for this reduction in settlement crack intensity is attributed to the internal curing provided by the pre-wetted lightweight aggregate (LWA). Henkensiefken et al. (2010) hypothesized that water is lost due to bleeding that is accelerated by evaporation on the concrete surface. The bleeding causes capillary pressure, resulting in consolidation and settlement. Because LWA has larger pores than cement paste, water is drawn out of the rigid LWA before it is drawn out of the deformable cement paste. The water supplied by the LWA during this time allows the maintenance of a greater degree of saturation of the plastic concrete, resulting in less consolidation

of the particles and less settlement. The current study indicates that the process may be somewhat different because, while IC had a similar effect to that observed by Henkensiefken et al. (2010), the reduced settlement cracking in this study occurred without significant evaporation; as described in Chapter 2, the relative humidity at the surface of the specimens exceeded 90 percent throughout the first 24 hours after casting and typically reached 97 percent within the first hour. This seems to suggest that water lost to hydration contributes to consolidation and settlement. Thus, the role of pre-wetted LWA appears to much as suggested by Henkensiefken et al. (2010), but hydration appears to be a driving force for consolidation that is counteracted by IC.

The average maximum crack widths of the Control-1 and 5.9 lb-IC concrete are compared in Figure 3.6. There is overlap in the data. The concrete with internal curing, in general, exhibited narrower average maximum crack widths than the control concrete at the slumps greater than or equal to 4 in. (100 mm). Below a slump of 4 in. (100 mm), these two types of concrete had approximately same average maximum crack widths. The figure shows that the crack widths in the concrete with internal curing increased less rapidly with increasing slump than the control concrete.

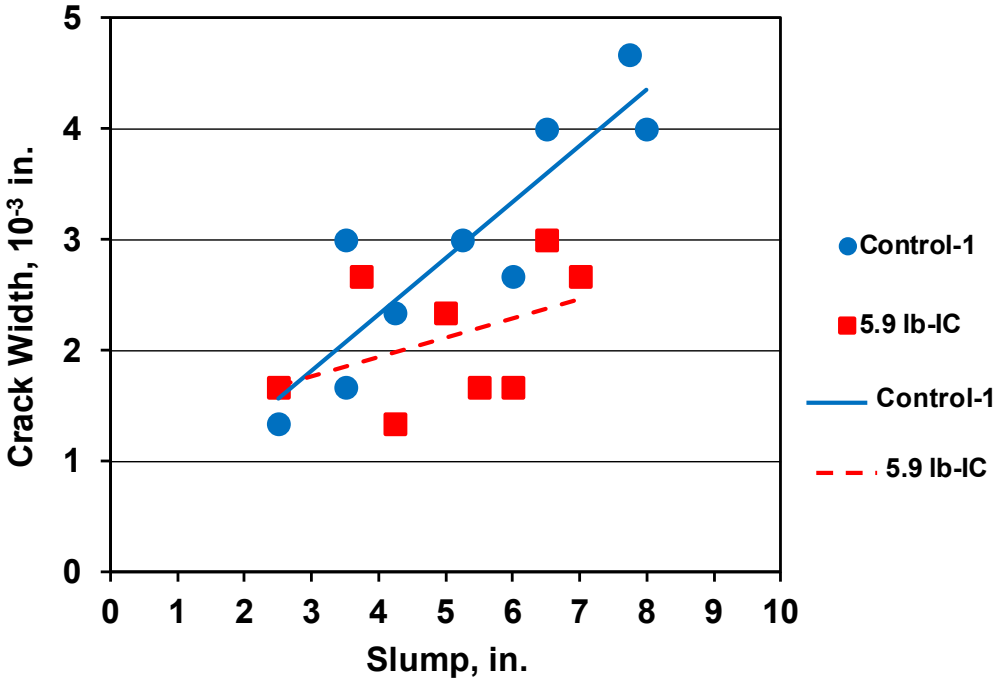

Figure 3.6 – Average maximum crack width versus slump for the Control-1 and the 5.9 lb-IC mixtures

3.3 SERIES 2

This series consisted of eight types of concrete and included two control mixtures, designated as Control-2 and Control-3; the aggregate gradation was optimized for Control-2 but not for Control-3. One concrete contained a 12.3 percent volume replacement of total aggregate with pre-wetted fine LWA, providing 7 lb of water per 100 lb of cementitious materials, and is designated 7 lb-IC. Two concretes contained supplementary cementitious materials (SCMs), one with a 30 percent volume replacement of cement with slag cement, designated as 30% Slag, and the other with 30 and 3 percent volume replacements of cement with slag cement and silica fume, respectively, designated as 30% Slag - 3% SF. Two other concretes contained SCMs and IC, one concrete contained a 30 percent volume replacement of cement with slag cement and a 12.3 percent volume replacement of total aggregate with pre-wetted fine LWA and is designated as 30% Slag - 7 lb-IC, and the other concrete contained 30 and 3 percent volume replacements of cement with slag cement and silica fume, respectively, and a 12.3 percent volume replacement of total aggregate with pre-wetted fine LWA and is designated as 30% Slag - 3% SF - 7 lb-IC. The final concrete contained 2 percent of SRA-5 by weight of cement and is designated 2% SRA.

The concrete in this series used Type I/II portland cement with a specific gravity of 3.12. The aggregate gradations in Series 2 were finer than those used in Series 1.

3.3.1 Control-2

Figure 3.7 compares settlement crack intensity with slump for the Control-2 mixtures. The average crack intensity increased from 0.33 at a slump of $3^1/_4$ in. (85 mm) to 0.55 at a slump of $8^1/_2$ in. (215 mm). The crack widths of the Control-2 mixtures ranged from 0.0010 to 0.0027 in. (0.025 to 0.070 mm), increasing as slump increased, as shown in Figure 3.8. The concrete properties and settlement cracking results for these mixtures are listed in Table B.2.

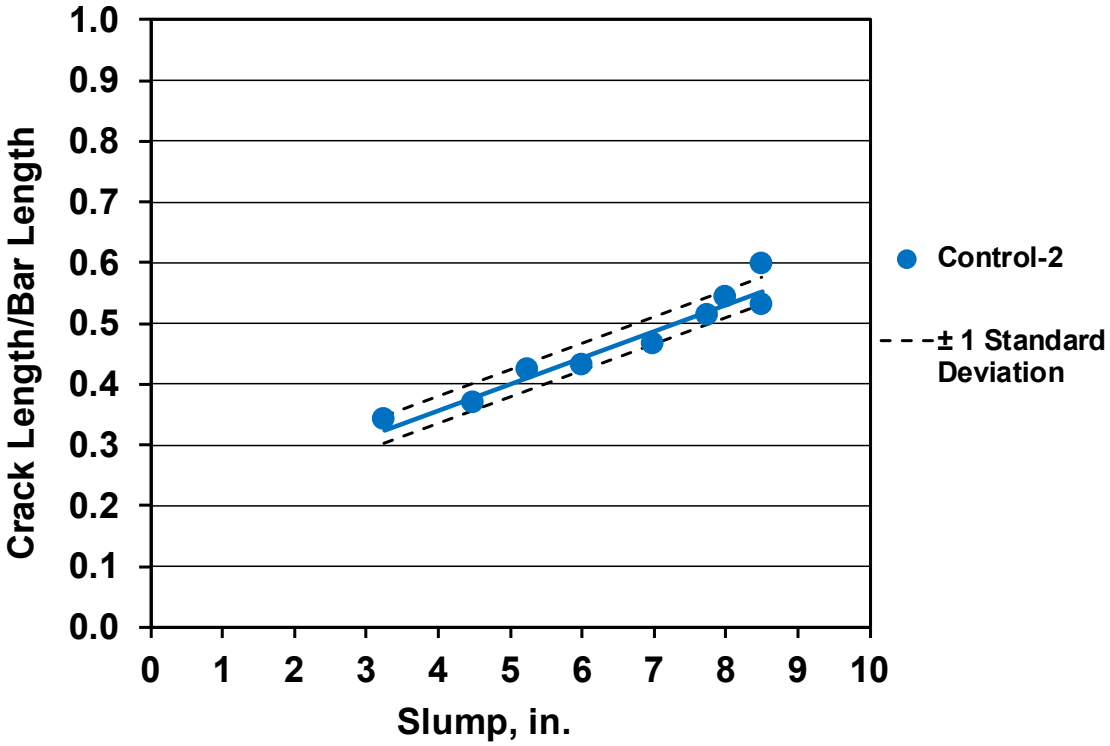

Figure 3.7 – Average settlement crack intensity (ratio of crack length to bar length) versus slump for the Control-2 mixtures

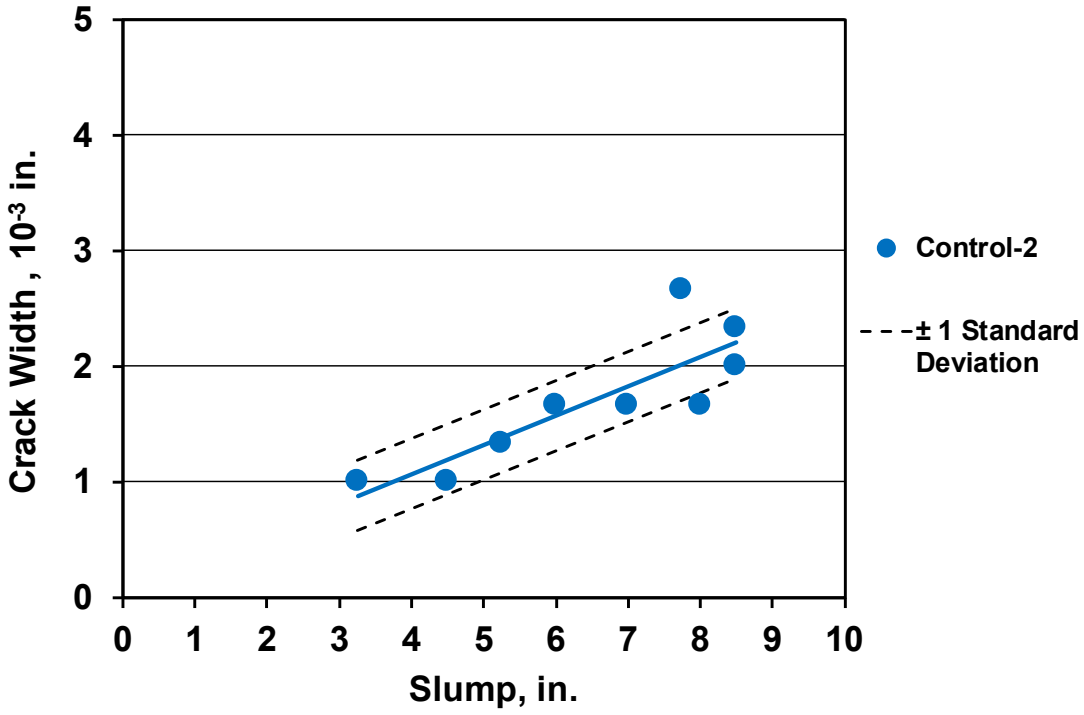

Figure 3.8 – Average maximum crack width versus slump for the Control-2 mixtures

3.3.2 Control-3

Figure 3.9 compares settlement crack intensity with slump for the Control-3 mixtures. The average crack intensity increased from 0.44 at a slump of $3^1/_2$ in. (90 mm) to 0.67 at a slump of $8^1/_4$ in. (210 mm), as shown in the figure.

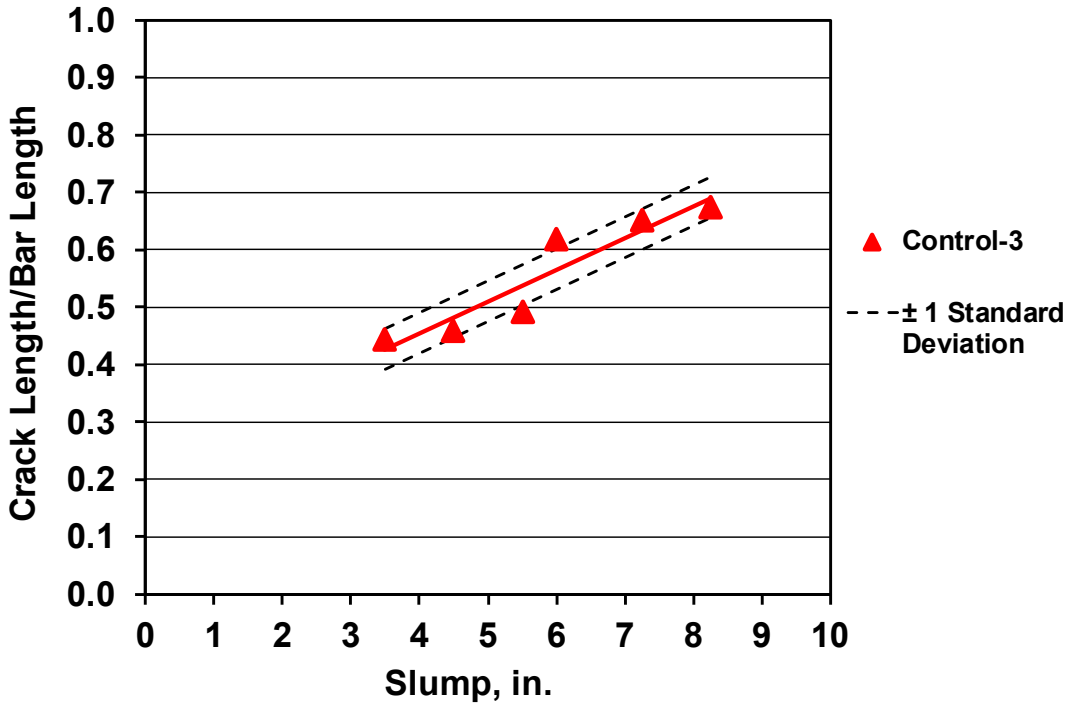

Figure 3.9 – Average settlement crack intensity (ratio of crack length to bar length) versus slump for the Control-3 mixtures

The average maximum crack widths of the Control-3 mixtures ranged from 0.0017 to 0.0027 in. (0.045 to 0.070 mm), increasing as slump increased, as shown in Figure 3.10. The properties and detailed cracking results for these mixtures are summarized in Table B.3.

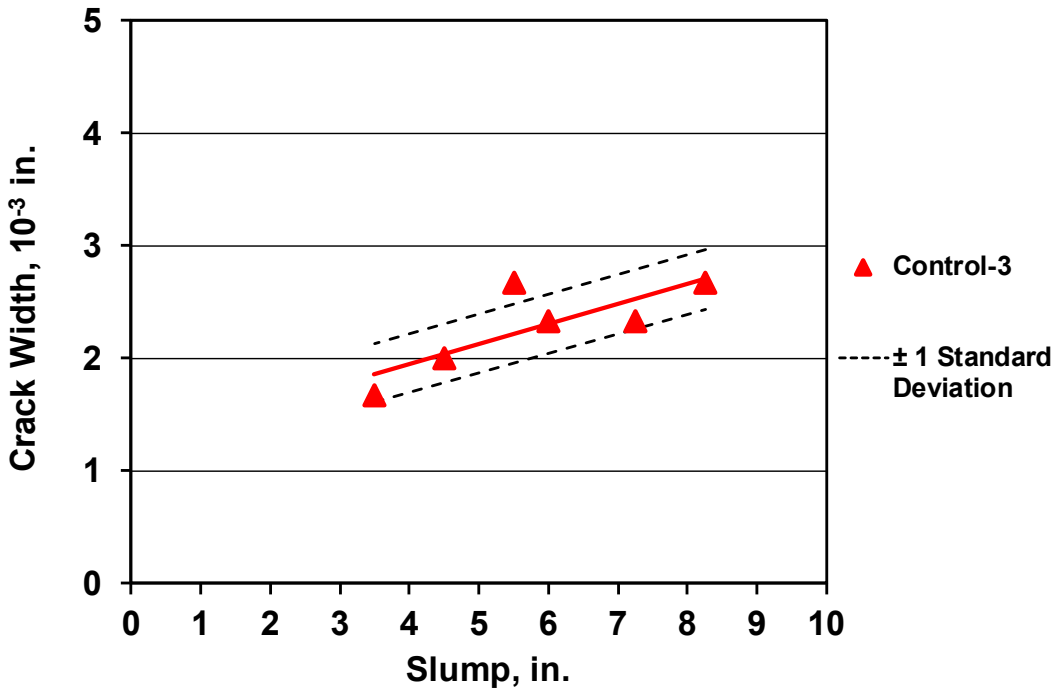

Figure 3.10 – Average maximum crack width versus slump for the Control-3 mixtures

Figure 3.11 compares settlement crack intensity with slump for the Control-2 and Control-3 mixtures. The results show that the concrete with non-optimized aggregate gradation (Control-3) exhibited more cracking than the concrete with optimized aggregate gradation (Control-2). The average crack intensity of Control-3 is 21 percent higher than the average crack intensity of Control-2 at a 7-in. (180-mm) slump. Based on Student's t-test, the difference in crack intensity between these two types of concrete is statistically significant at all slumps. Student's t-test results for these mixtures are presented in Table C.2 in Appendix C. The increase in crack intensity is likely due to the use of non-optimized aggregate gradation, which has a larger volume of the voids between aggregate particles than the optimized aggregate gradation. The use of non-optimized aggregate gradations in concrete with the same cement paste content can reduce cohesiveness, and increase segregation and bleeding of the plastic concrete (Scholer and Baker 1973, Mindess et al. 2003, Lindquist et al. 2008, Rangaraju et al. 2013), leading to more settlement and cracking. The average maximum crack widths for these two types of concrete are compared in Figure 3.12. The concrete containing the non-optimized aggregate gradation (Control-3) exhibited wider crack

widths than the concrete containing the optimized aggregate gradation (Control-2) at all slumps, as shown in Figure 3.12.

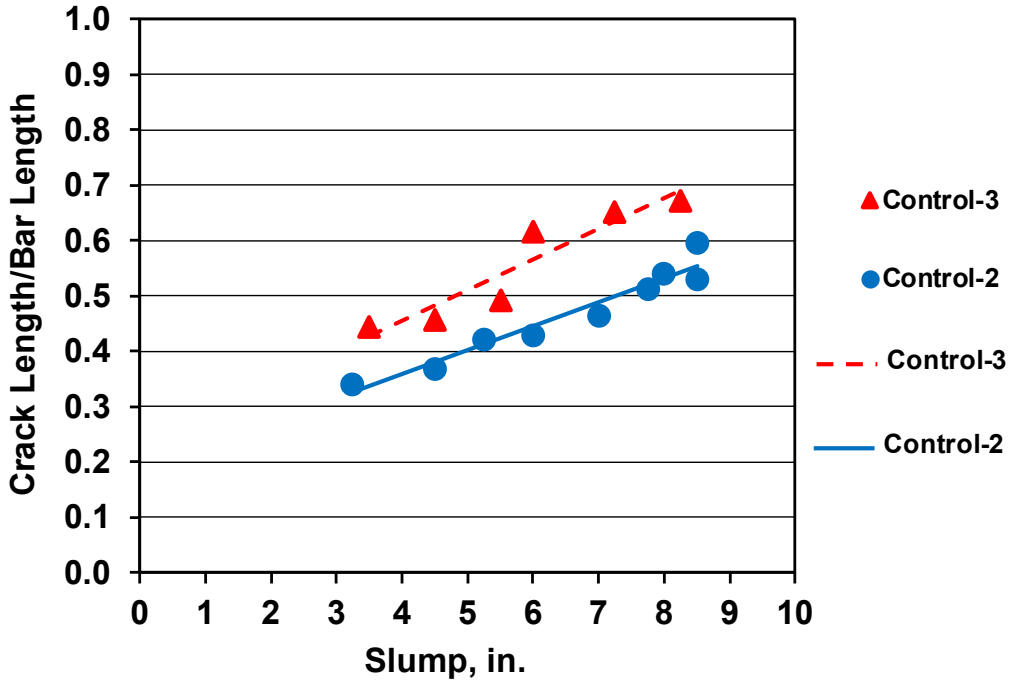

Figure 3.11 – Average settlement crack intensity (ratio of crack length to bar length) versus slump for the Control-2 and Control-3 mixtures

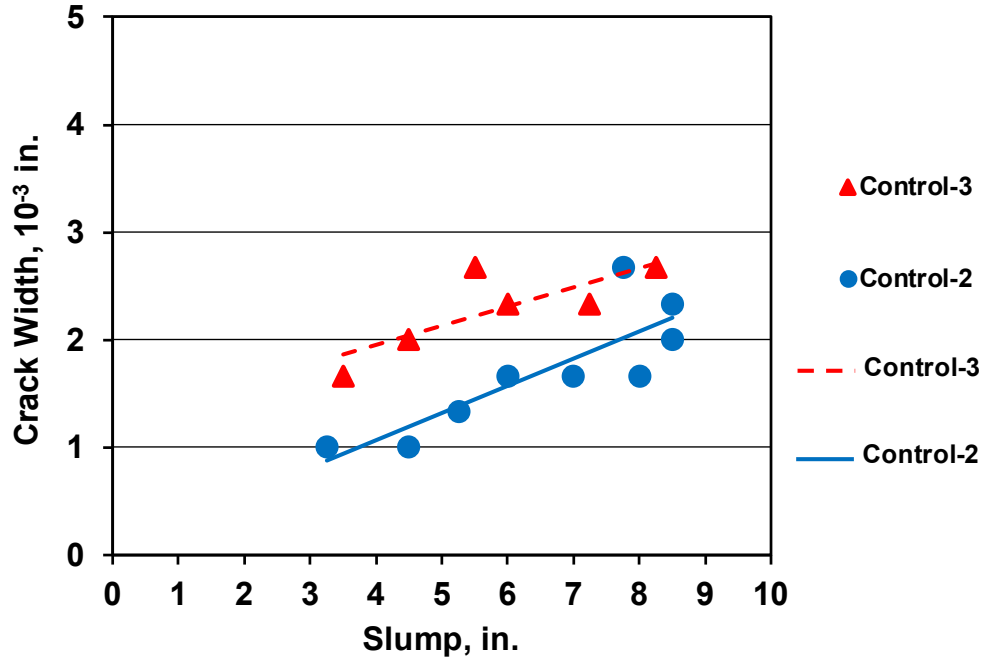

Figure 3.12 – Average maximum crack width versus slump for the Control-2 and Control-3 mixtures

3.3.3 7 lb-IC

Figure 3.13 compares settlement crack intensity with slump for the 7 lb-IC mixtures. As shown in the figure, the average crack intensity increased from 0.18 at a slump of 3 in. (75 mm) to 0.36 at a slump of $8^1/_2$ in. (215 mm). The average maximum crack widths of these mixtures ranged from 0.0010 to 0.0020 in. (0.025 to 0.050 mm), increasing as slump increased, as shown in Figure 3.14. The properties and detailed cracking results for these mixtures are summarized in Table B.5.

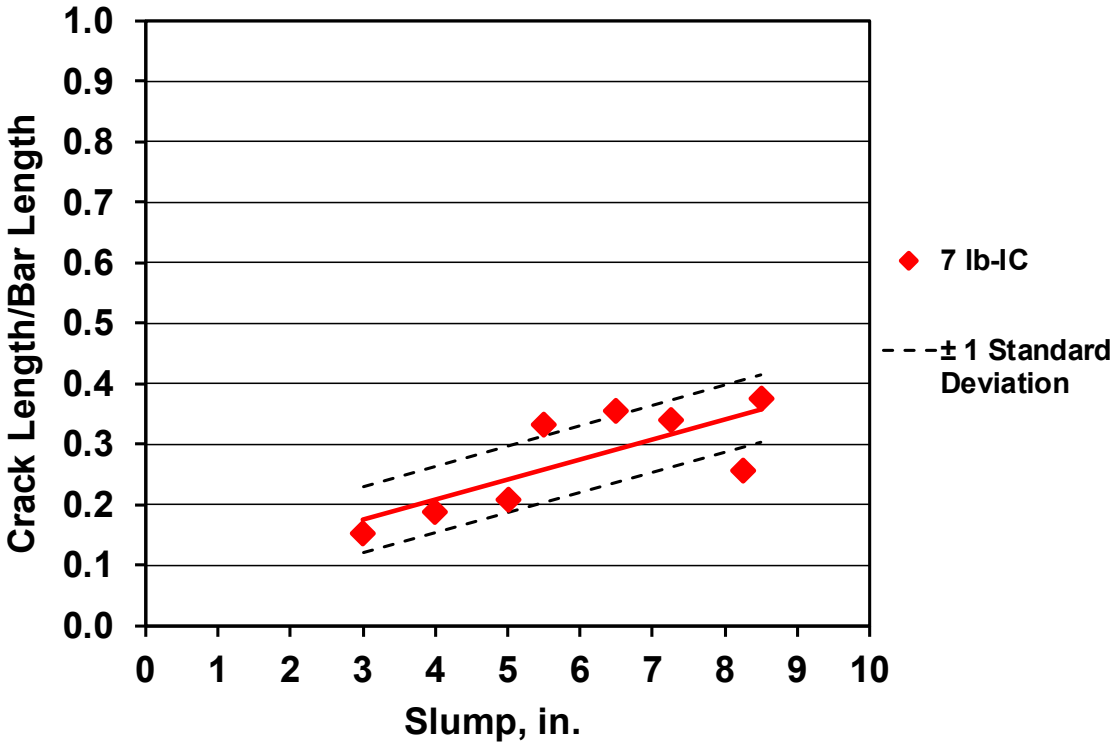

Figure 3.13 – Average settlement crack intensity (ratio of crack length to bar length) versus slump for the 7 lb-IC mixtures

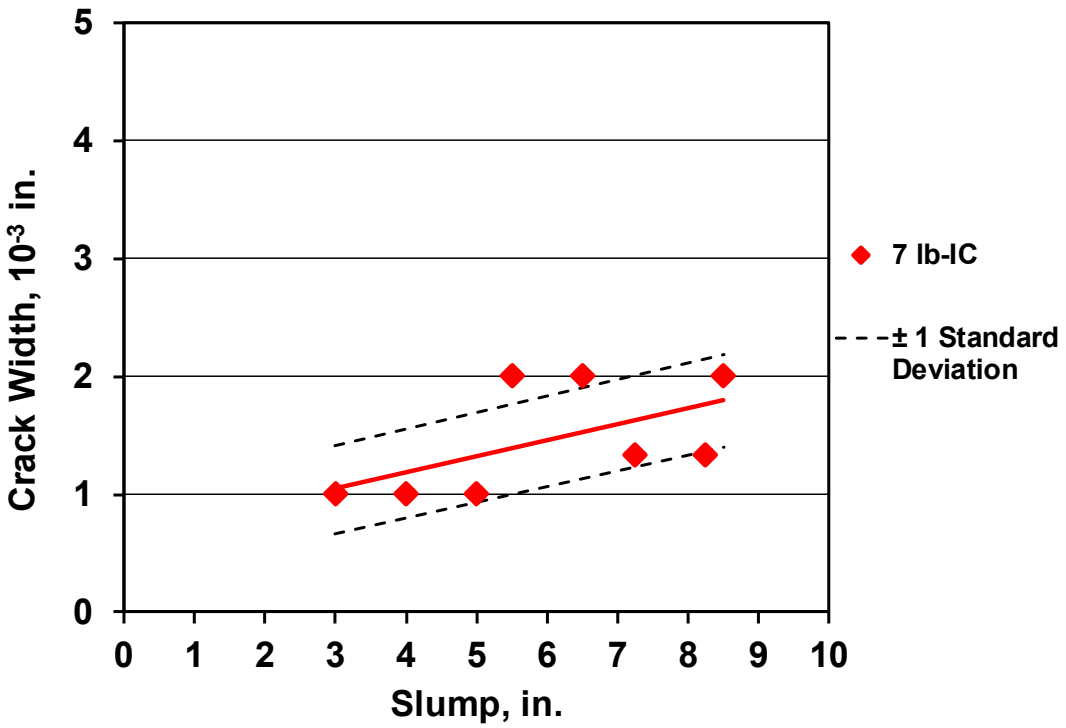

Figure 3.14 – Average maximum crack width versus slump for the 7 lb-IC mixtures

Figure 3.15 compares average settlement crack intensity with slump for the Control-2 and 7 lb-IC mixtures. The mixtures with internal curing exhibited less settlement cracking than the control mixtures at all slumps. As described for the 5.9-IC mixture, this reduction in cracking can be attributed to the water released from the LWA before it is released from the cement paste. The average crack intensity of the 7 lb-IC (with fine size LWA) is 37 percent lower than the average crack intensity of the Control-2 at a slump of 7 in. (180 mm). The reduction in crack intensity is similar to the reduction of 34 percent exhibited by the 5.9 lb-IC (with pea-gravel size LWA) mixtures.

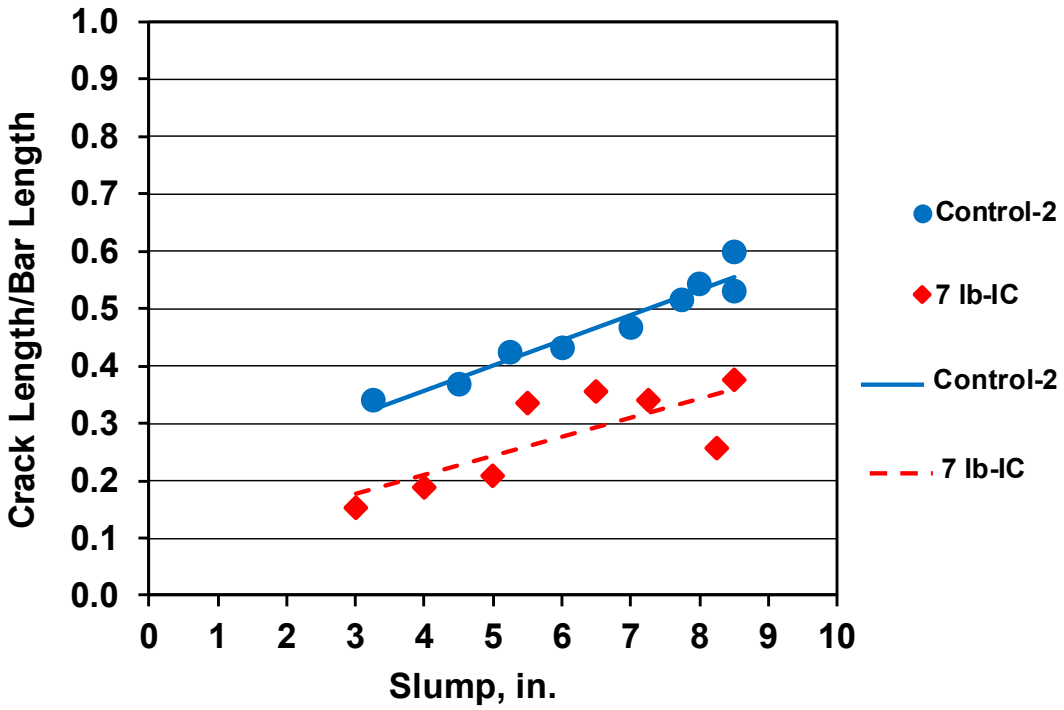

Figure 3.15 – Average settlement crack intensity (ratio of crack length to bar length) versus slump for the Control-2 and 7 lb-IC mixtures

The average maximum crack widths for the Control-2 and 7 lb-IC concretes are compared in Figure 3.16. There is overlap in the data. At the slumps less than 5 in. (125 mm), the average maximum crack widths for the concrete with internal curing are same as the control. At the slumps greater than 7 in. (180 mm), the concrete with internal curing exhibited narrower crack widths than the control. The figure shows that the crack widths for both mixtures increased as slump increased.

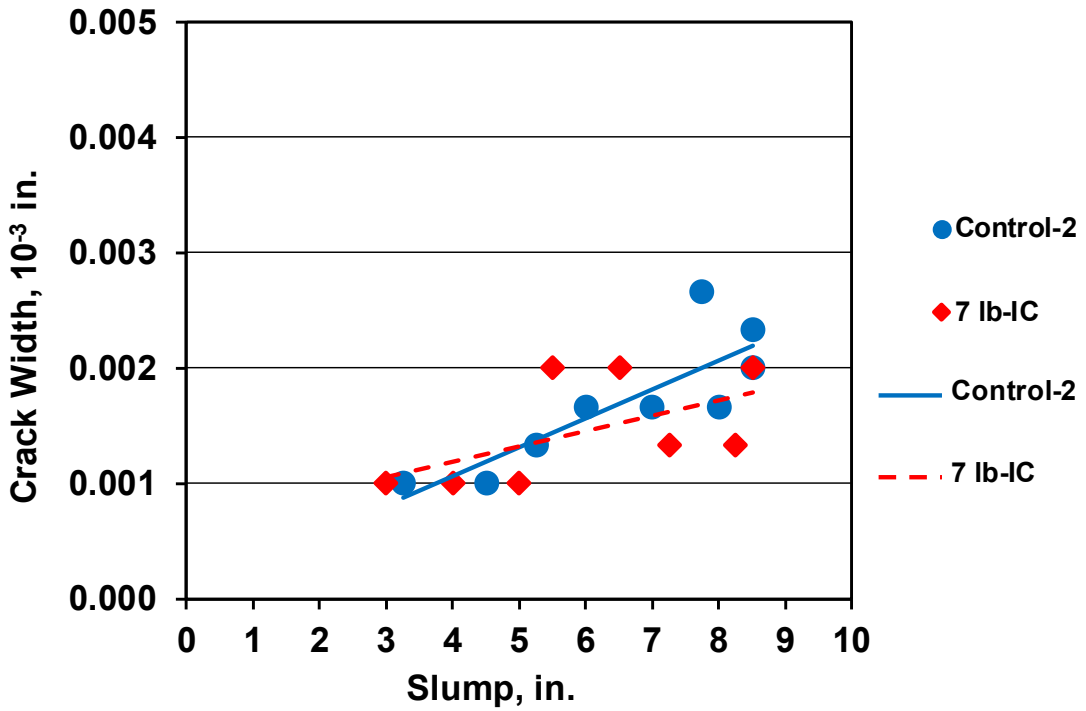

Figure 3.16 – Average maximum crack width versus slump for the Control-2 and 7 lb-IC mixtures

3.3.4 30% Slag

Figure 3.17 compares settlement crack intensity with slump for the 30% Slag mixtures. Crack intensity slightly increased as slump increased. The average crack intensity increased from 0.18 at a slump of 3 in. (75 mm) to 0.34 at a slump of 8 in. (205 mm). Two mixtures with the slumps of $7^1/_4$ (185 mm) and 8 in. (205 mm) experienced crack intensities (0.56 and 0.13, respectively) that appear to be outliers. As a result, a mixture with a slump of $7^3/_4$ (195 mm) was then cast and tested for settlement cracking to verify cracking at the slump greater than 7 in. (180 mm). The average maximum crack widths of the 30% Slag mixtures ranged from 0.0010 to 0.0027 in. (0.025 to 0.070 mm), increasing as slump increased, as shown in Figure 3.18. The properties and detailed cracking results for these mixtures are summarized in Table B.6.

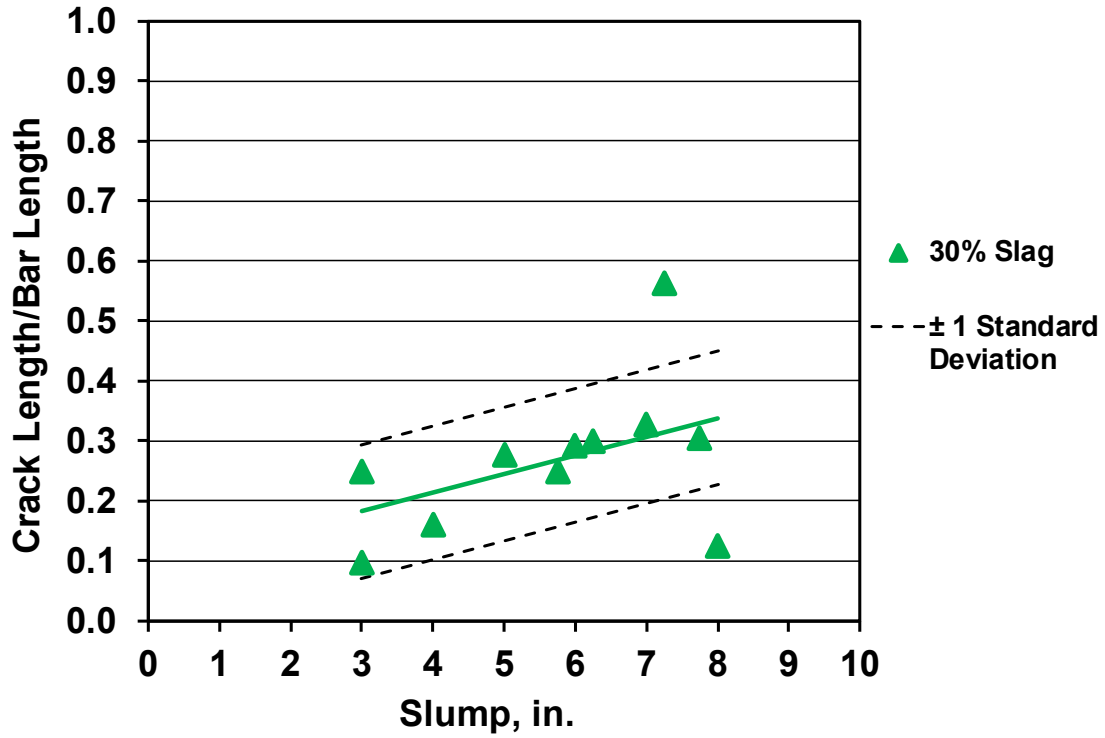

Figure 3.17 – Average settlement crack intensity (ratio of crack length to bar length) versus slump for the 30% Slag mixtures

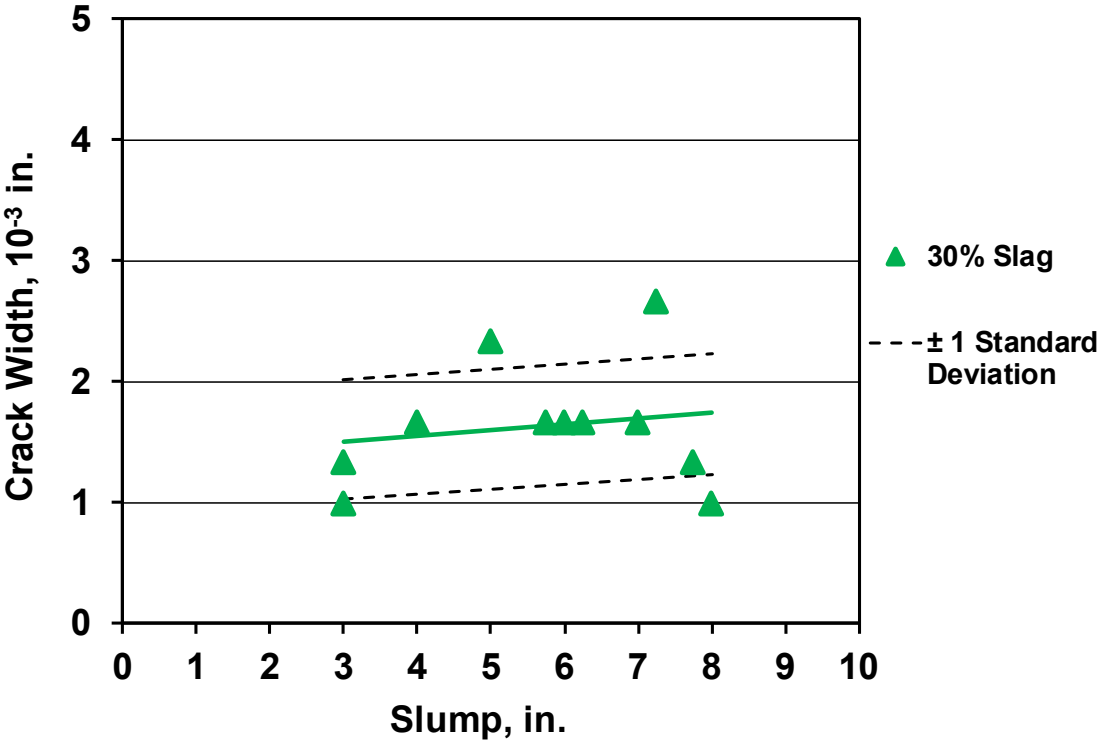

Figure 3.18 – Average maximum crack width versus slump for the 30% Slag mixtures

Figure 3.19 compares settlement crack intensity with slump for the Control-2 and 30% Slag mixtures. The concrete containing a 30 percent volume replacement of cement with slag cement, with one exception – an apparent outlier, experienced less cracking than the control at all slumps. The average crack intensity of the 30 % Slag mixture is 37 percent lower than the average crack intensity of the Control-2 mixture at a 7-in. (180-mm) slump. The reduction in crack intensity occurs because the slag cement, with a Blaine fineness of (5840 m^2/kg), is finer than the cement, with the Blaine fineness of (3986 m^2/kg). Because the bleed capacity and bleeding rate of concrete are influenced by the ratio of surface area of particles to the unit volume of water, using a finer cementitious material will reduce bleeding (ACI Committee 233 2017), leading to less settlement. In addition, since slag cement has a lower lime content than portland cement, the composition of calcium silicate hydrate (C-S-H) resulting from the hydration of slag cement has a lower C/S ratio than obtained with portland cement, leading to some pozzolanic behavior. The excess silica in the slag cement reacts with calcium hydroxide ($Ca(OH)_2$) produced during cement hydration, resulting in C-S-H filling pores and refining the pore size in the cement paste, causing less bleeding and settlement (Bakker 1980, Roy and Idron 1983, Mindess et al. 2003). Based on Student's t-test, this reduction in crack intensity is statistically significant for all slumps. Student's t-test results of these mixtures are listed in Table C.4.

The average maximum crack widths of the Control-2 and 30% Slag concrete are compared in Figure 3.20. There is overlap in the data, with the 30% Slag concrete exhibiting wider average maximum crack widths than the Control-2 concrete at the slumps less than 5 in. (125 mm) and the Control-2 concrete exhibiting wider maximum crack widths at the slumps greater than $7^1/_2$ in. (190 mm). The two concretes exhibited similar crack widths for the slumps between $5^3/_4$ and 7 in. (145 and 180 mm).

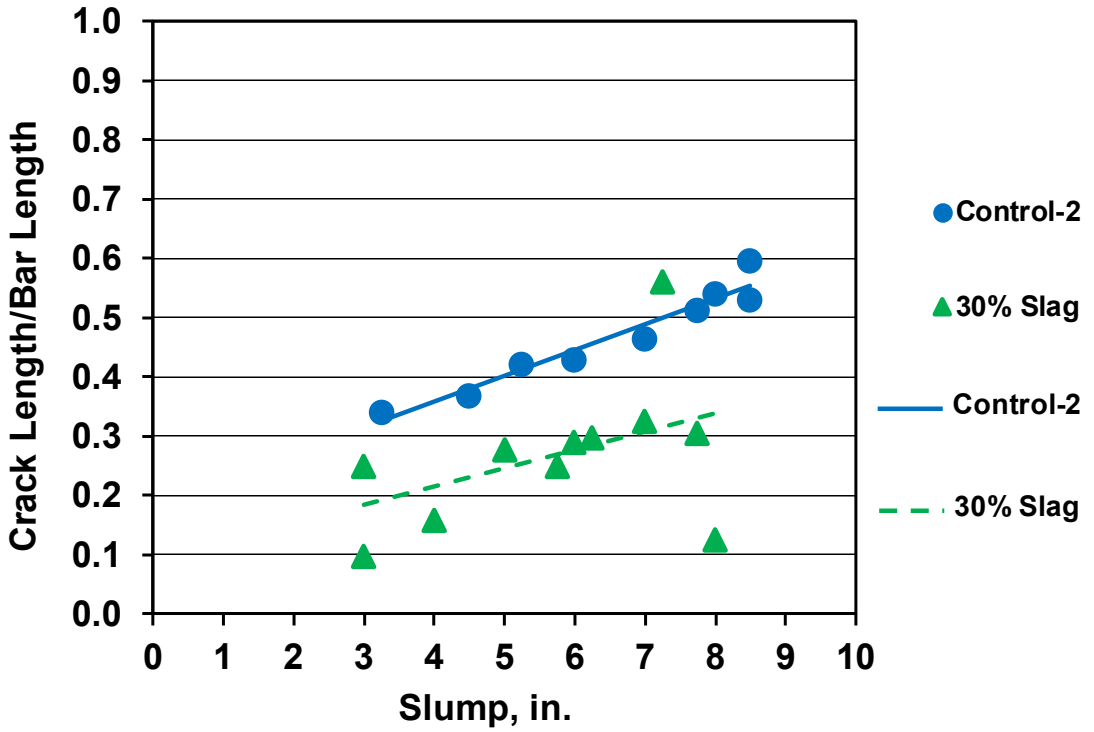

Figure 3.19 – Average settlement crack intensity (ratio of crack length to bar length) for the Control-2 and 30% Slag mixtures

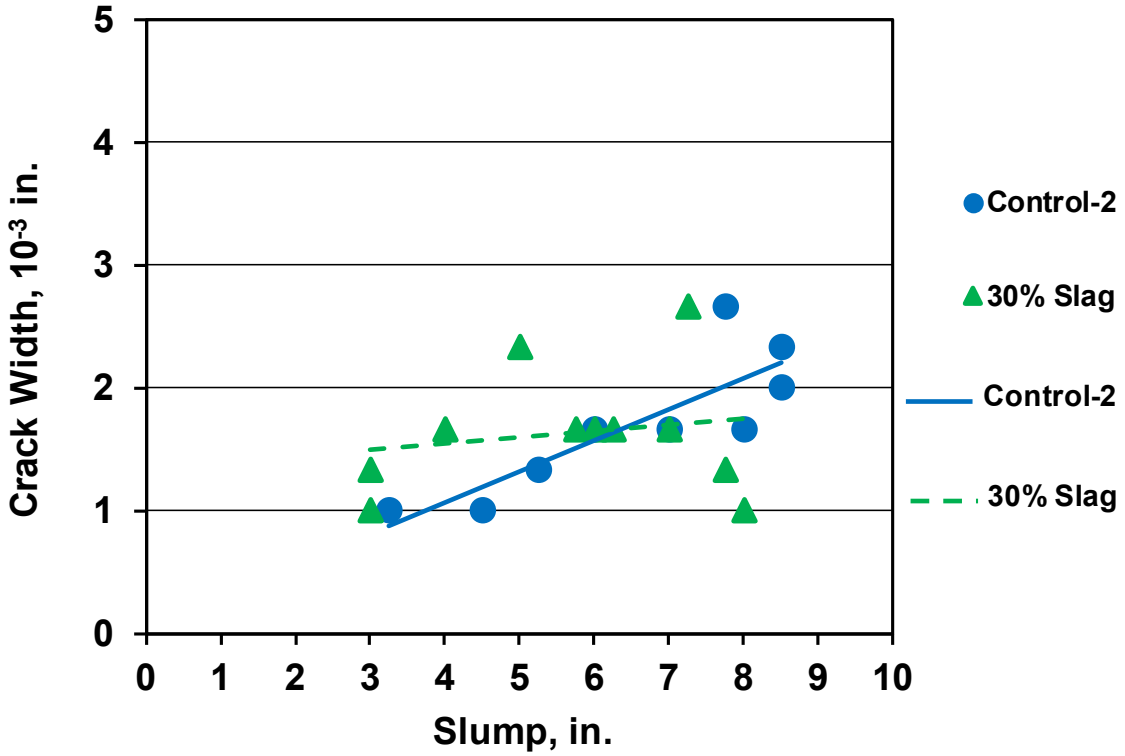

Figure 3.20 – Average maximum crack width for the Control-2 and 30% Slag mixtures

3.3.5 30% Slag - 3% SF

Figure 3.21 compares crack intensity with slump for the 30% Slag - 3% SF mixtures. The figure shows a very low average crack intensity that increased from 0.04 at a slump of $1^{3}/_{4}$ in. (45 mm) to just 0.1 at a slump of $8^{1}/_{2}$ in. (215 mm). The slope of the trendline for these mixtures is also low, indicating that the slump had only slight effect on settlement. This insensitively is likely due to the extreme fineness of the silica fume particles, which plays a role in enhancing the strength of the bond between the cement paste and the aggregate particles, increasing the cohesiveness of plastic concrete, and reducing bleeding (Mindess 1987, Butler 1997, Mindess et al. 2003). In addition, the high silica content and extreme fineness of silica fume particles make it a very reactive pozzolan. The pozzolanic reaction results in the formation of calcium-silicate hydrate (C-S-H), which forms in the voids between C-S-H paricles producing a very dense structure (Mindess et al. 2003), leading to less bleeding and settlement cracking. The average maximum crack widths for these mixtures ranged from 0.0003 to 0.0013 in. (0.008 to 0.035 mm) showing essentially no increase with increasing slump, as shown in Figure 3.22. The properties and detailed cracking results for these mixtures are summarized in Table B.7.

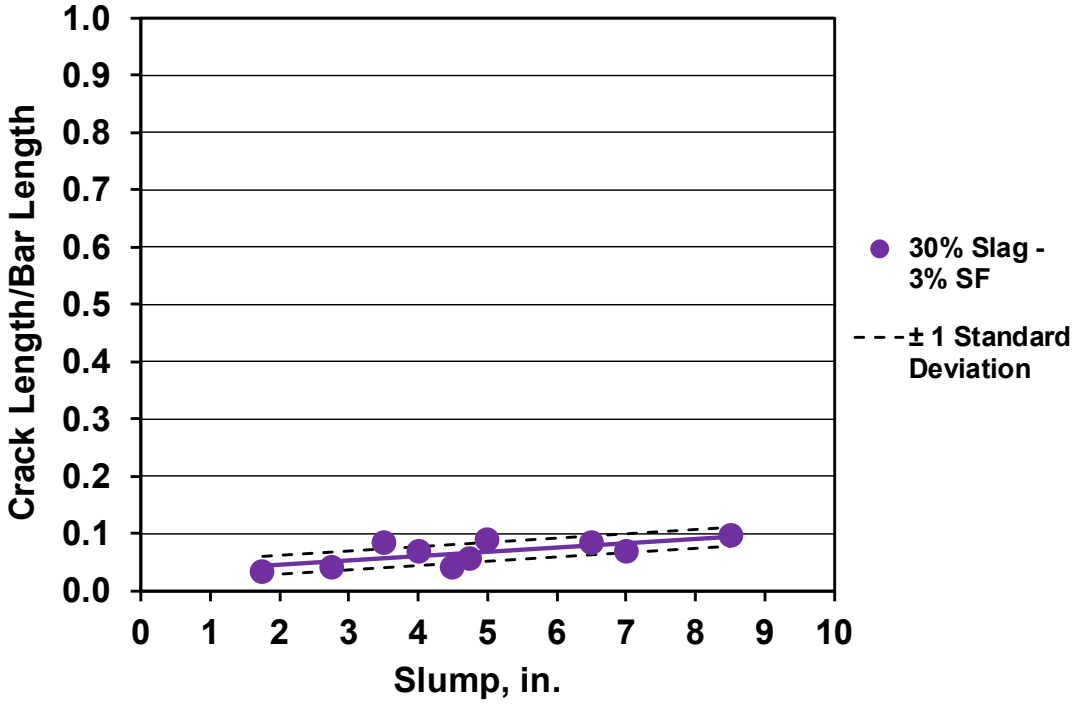

Figure 3.21 – Average settlement crack intensity (ratio of crack length to bar length) versus slump for the 30% Slag - 3% SF mixtures

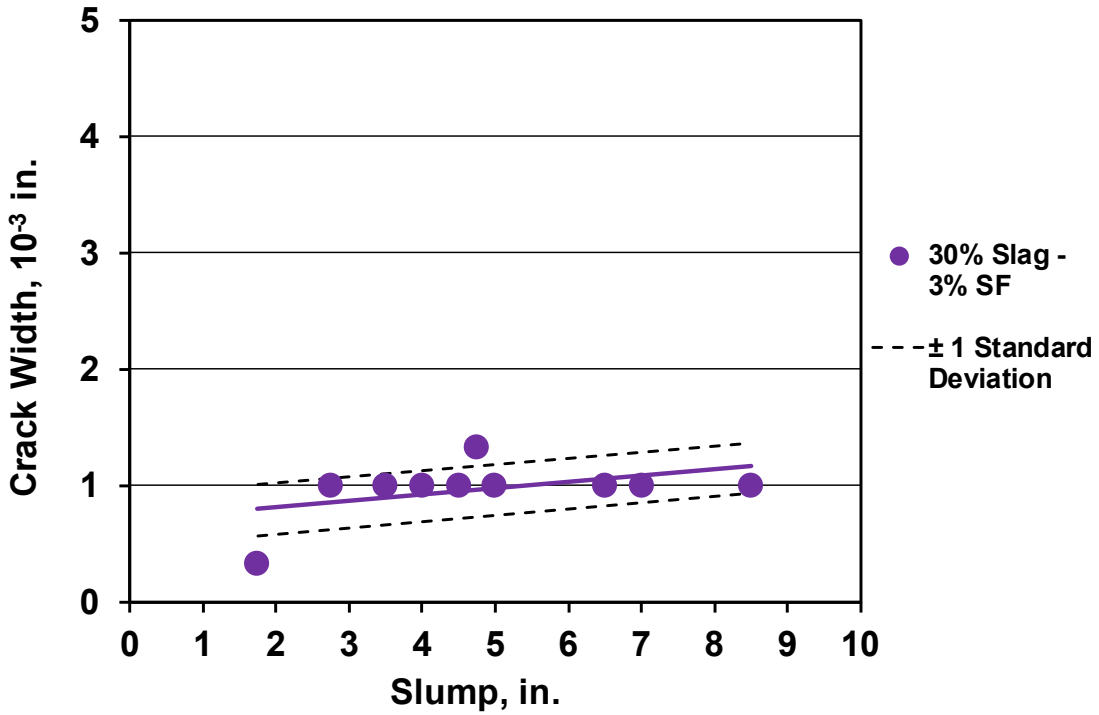

Figure 3.22 – Average maximum crack width versus slump for the 30% Slag - 3% SF mixtures

Figure 3.23 compares settlement crack intensity with slump for the Control-2, 30% Slag, and 30% Slag - 3% SF mixtures. The concrete containing slag cement and silica fume exhibited the lowest crack intensity at all slumps. The average crack intensity of the 30% Slag concrete is 37 percent lower than the average crack intensity of the Control-2 at a 7-in. (180-mm) slump; while the average crack intensity of the 30% Slag - 3% SF concrete is 83 percent lower than the average crack of the Control-2 at the 7-in. (180-mm) slump. The larger reduction in crack intensity due to the use of silica fume is likely the results of the high silica content and extreme fineness of silica fume particles. Based on Student's t-test, the differences in crack intensity between the mixtures shown in Figure 3.23 are statistically significant at all slumps. The average maximum crack widths for the three mixtures are compared in Figure 3.24. The concrete containing slag cement and silica fume exhibited the narrowest crack widths at all slumps followed by the 30% Slag and Control-2 mixtures, again indicating that the use of very fine cementitious materials is effective in reducing the width of settlement cracks especially.

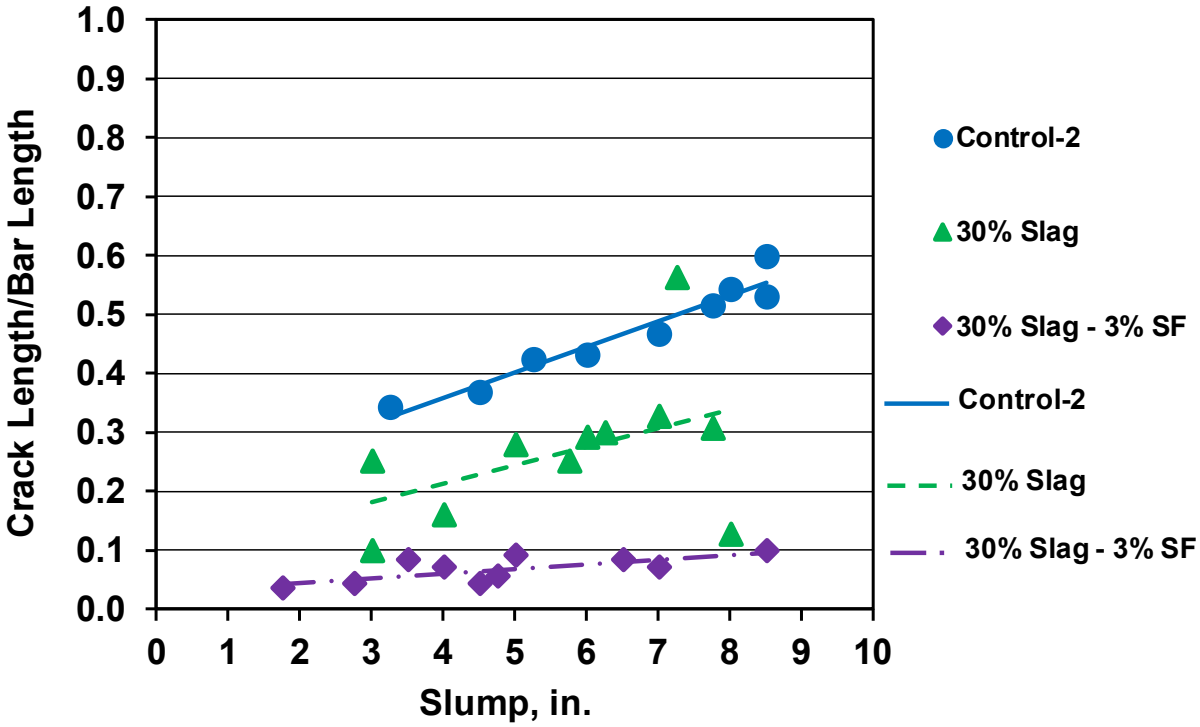

Figure 3.23 – Average settlement crack intensity (ratio of crack length to bar length) versus slump for the Control-2, 30% Slag, and 30% Slag - 3% SF mixtures

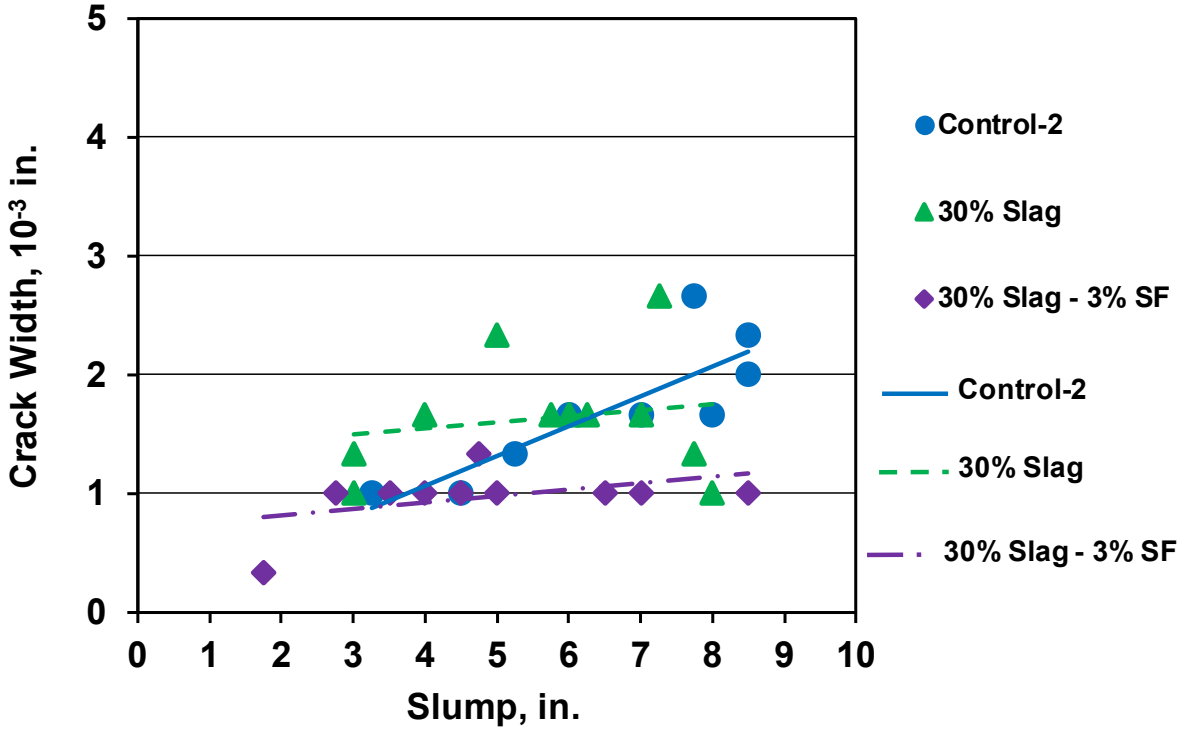

Figure 3.24 – Average maximum crack width versus slump for the Control-2, 30% Slag, and 30% Slag - 3% SF mixtures

3.3.6 30% Slag - 7 lb-IC

Figure 3.25 compares crack intensity with slump for the 30% Slag - 7 lb-IC mixtures. The average crack intensity of these mixtures with internal curing increased from 0.12 at a slump of $3^1/_2$ in. (90 mm) to 0.26 at a slump of $8^1/_4$ in. (210 mm). The average maximum crack widths of the 30% Slag - 7 lb-IC mixtures ranged from 0.0010 to 0.0013 in. (0.025 to 0.035 mm) at all slumps, decreasing slightly as slump increased, but, in fact, remaining nearly constant, as shown in Figure 3.26. The properties and detailed cracking results for these mixtures are summarized in Table B.8 in Appendix B.

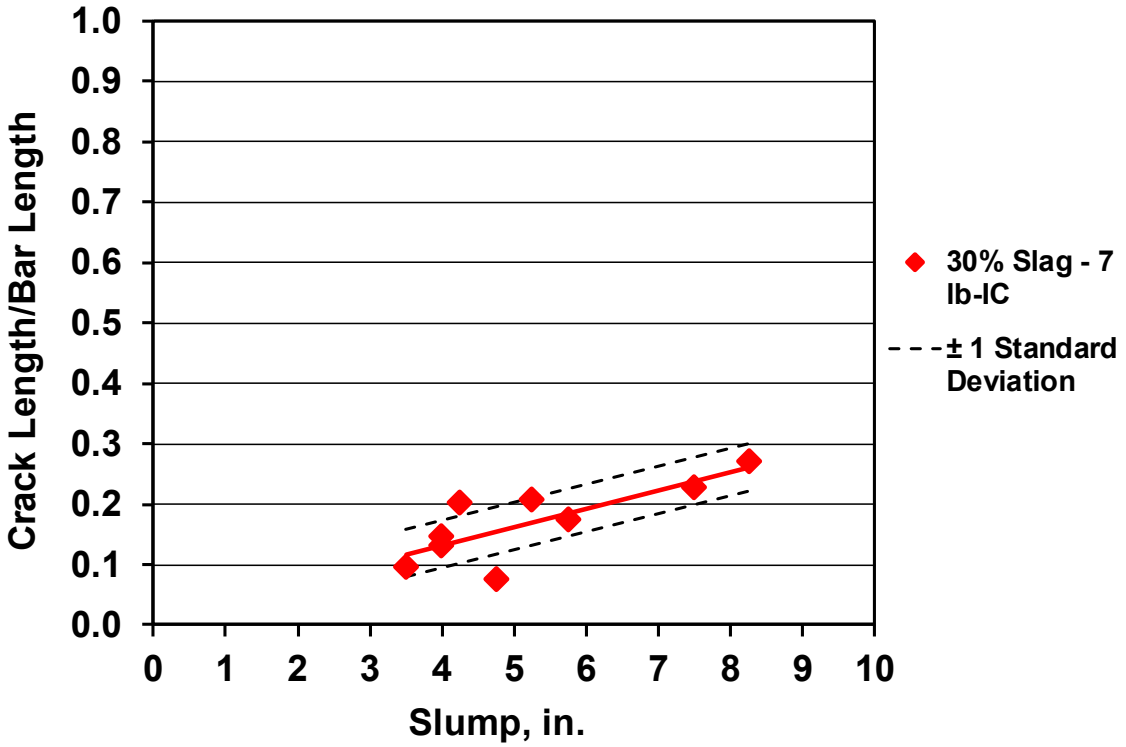

Figure 3.25 – Average settlement crack intensity (ratio of crack length to bar length) versus slump for 30% Slag - 7 lb-IC mixtures

Figure 3.27 compares settlement crack intensity with slump for the Control-2, 30% Slag, and 30% Slag - 7 lb-IC mixtures. For this group, the mixtures containing slag cement with internal curing (IC) water exhibited the lowest crack intensity at all slumps. The average crack intensity of

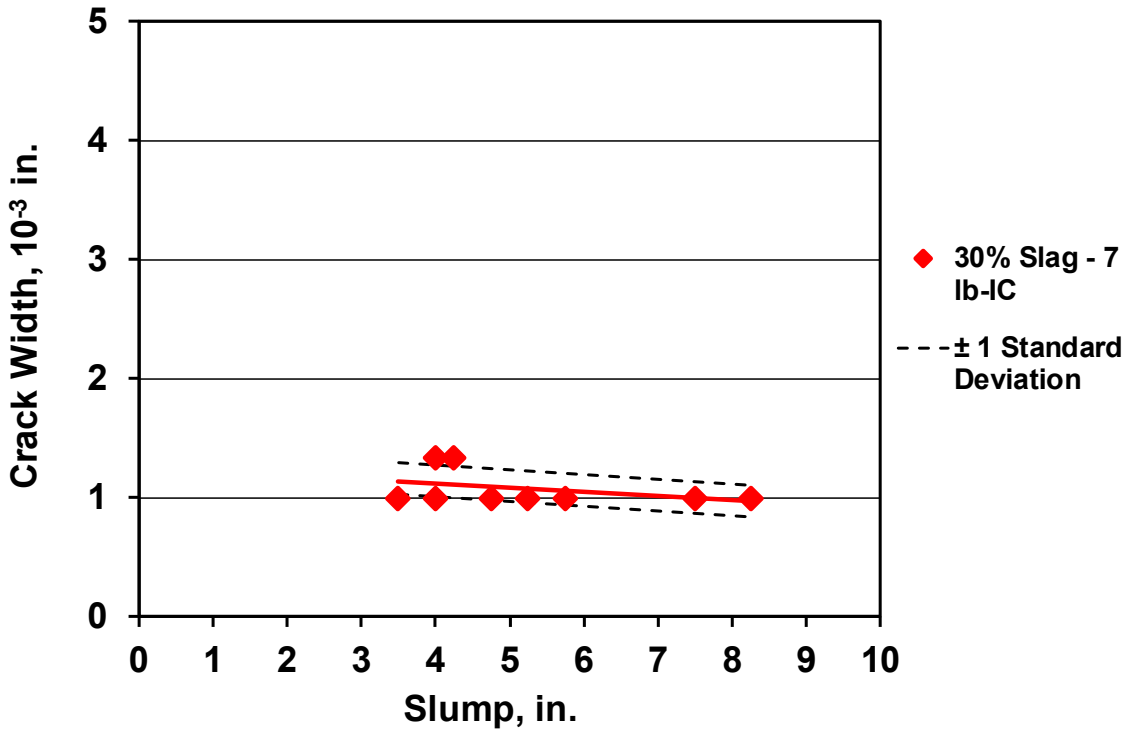

Figure 3.26 – Average maximum crack width versus slump for the 30% Slag - 7 lb-IC mixtures

the 30% Slag concrete is 37 percent lower than the average crack intensity of the Control-2 concrete; while the average crack intensity of the 30% Slag - 7 lb-IC concrete is 45 percent lower than that of the Control-2 concrete at a 7-in. (180-mm) slump. The comparison illustrates the advantage of combining IC water with slag cement. Based on Student's t-test, the reduction in crack intensity between the Control-2 and 30% Slag - 7 lb-IC concrete is statistically significant at all slumps. Student's t-test results of these two types of concrete are listed in Table C.6 in Appendix C. The average maximum crack widths of the Control-2, 30% Slag, and 30% Slag - 7 lb-IC mixtures are compared in Figure 3.28. The mixture containing slag cement and IC water, in general, exhibited the narrowest crack widths, followed by the mixture containing slag cement without IC and the control mixture. The average maximum crack widths of the mixtures containing slag cement, with and without IC, were largely unaffected by slump, while the maximum crack widths of the control mixture increased as slump increased.

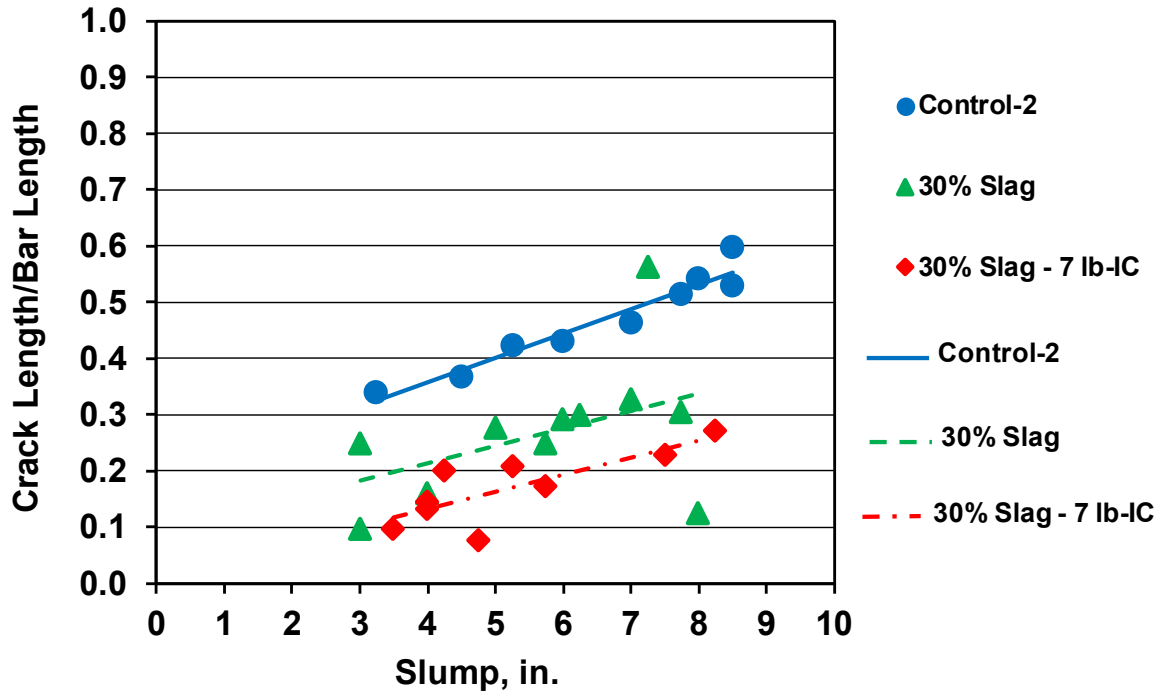

Figure 3.27 – Average settlement crack intensity (ratio of crack length to bar length) versus slump for the Control-2, 30% Slag, and 30% Slag - 7 lb-IC mixtures

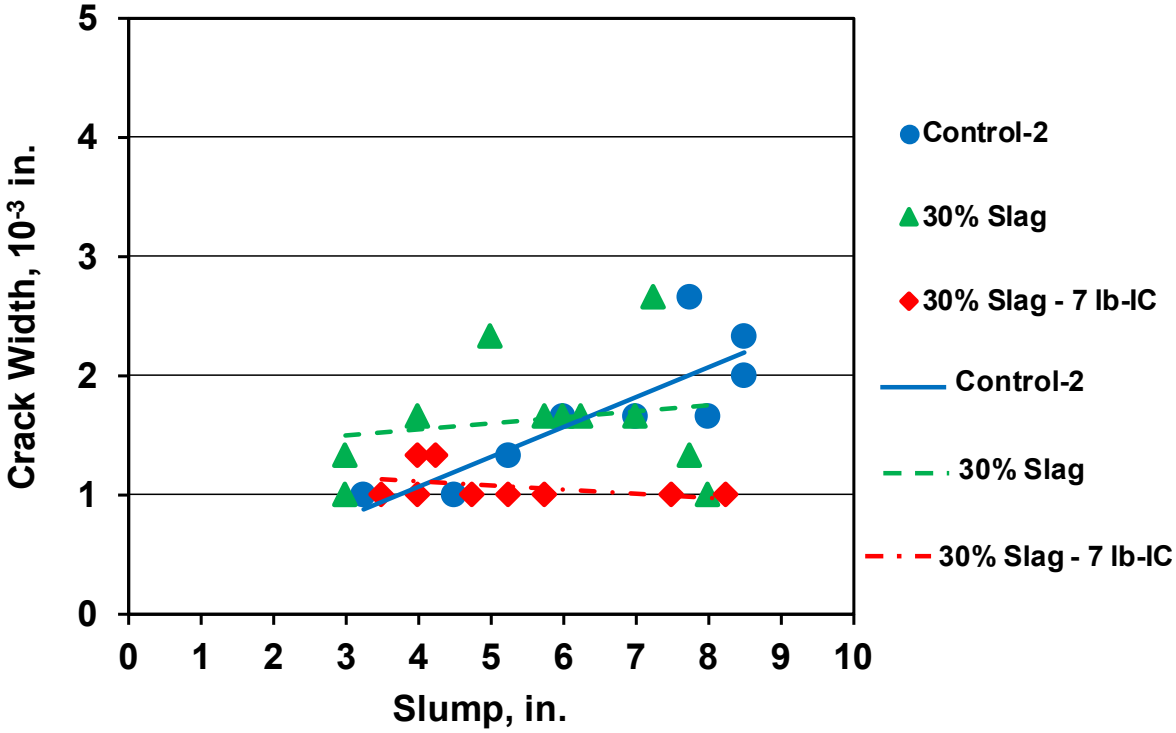

Figure 3.28 – Average maximum crack width versus slump for the Control-2, 30% Slag, and 30% Slag - 7 lb-IC mixtures

3.3.7 30% Slag - 3% SF - 7 lb-IC

Figure 3.29 compares settlement crack intensity with slump for the 30% Slag - 3% SF - 7 lb-IC mixtures. The average crack intensity ranged from 0.04 at a slump of $2^{3}/_{4}$ in. (70 mm) to just 0.08 at a slump of $8^{1}/_{4}$ in. (210 mm). The slope of the trendline of these mixtures is low, indicating that the slump had only slight effect on settlement. Again, this is insensitively may attributed to the extreme fineness and the pozzolanic action of silica fume. The average maximum crack widths of the mixture are approximately constant at all slumps, with values between 0.0010 to 0.0013 in (0.025 to 0.035 mm), as shown in Figure 3.30. of this type of concrete are summarized in Table B.9 in Appendix B.

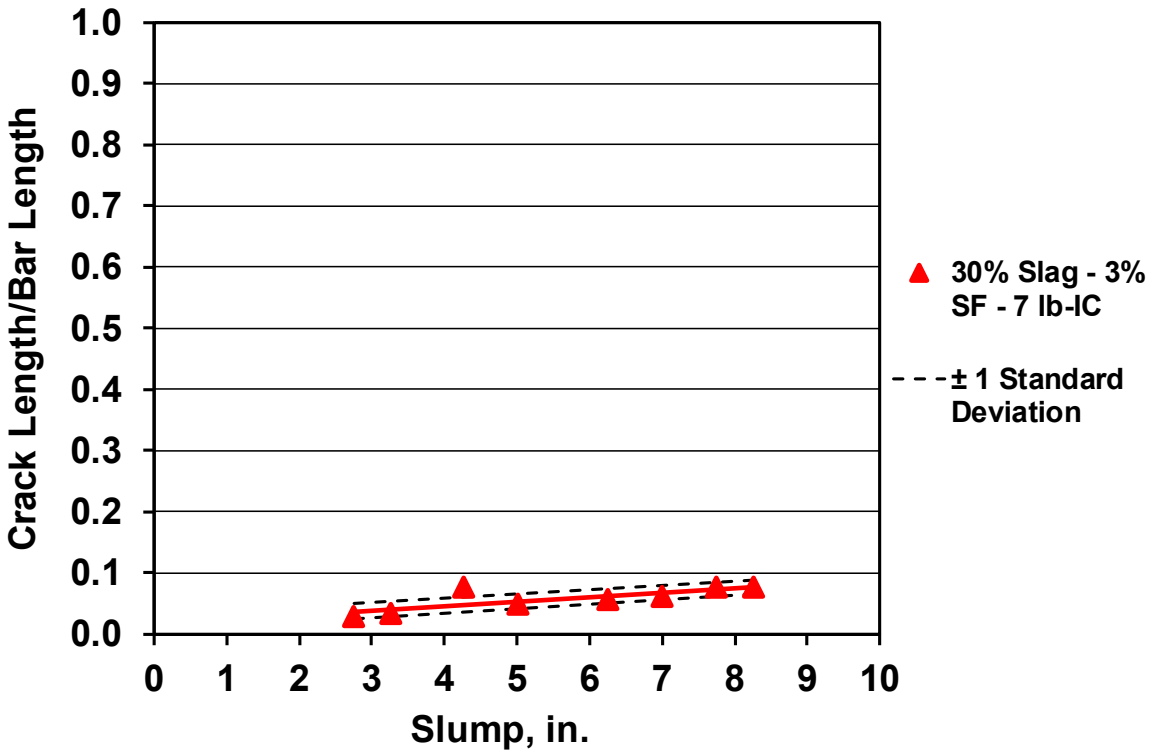

Figure 3.29 – Average settlement crack intensity (ratio of crack length to bar length) versus slump for the 30% Slag - 3% SF - 7 lb-IC mixtures

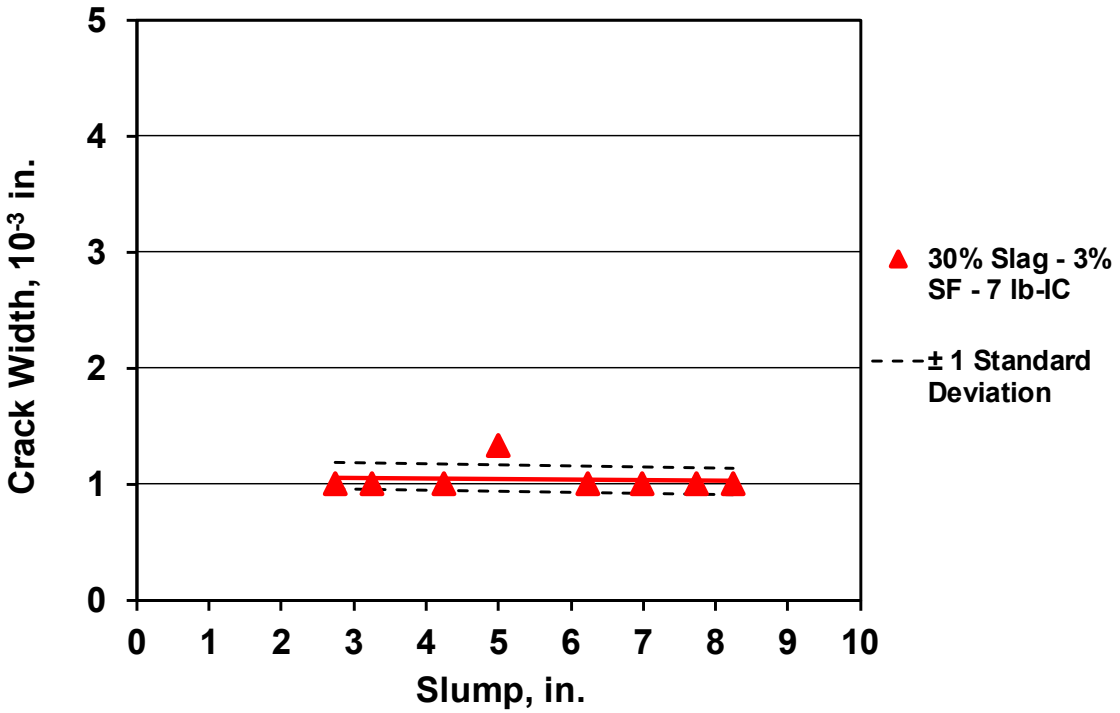

Figure 3.30 – Average maximum crack width versus slump for the 30% Slag - 3% SF - 7 lb-IC mixtures

Figure 3.31 compares settlement crack intensity for the Control-2, 30% Slag - 3% SF, and 30% Slag - 3% SF- 7 lb-IC concrete. The concrete containing slag cement and silica fume without and with IC water exhibited extremely lower crack intensity compared to the control at all slumps, with average crack intensities 83 and 86 percent, respectively, lower than the average crack intensity of the Control-2 at 7-in. (180-mm) slump. This extreme reduction in the crack intensity occurs due to the combined effects of the SCMs slag cement and silica fume, with perhaps a small assist from the IC water. As stated earlier, the fineness of SCMs particles and their pozzolanic reaction increase the cohesiveness and reduce bleeding in the plastic concrete, resulting in less settlement and cracking. In addition, the IC water released from the LWA provides a high degree of saturation of the plastic concrete, resulting in less consolidation of the particles and less settlement (Henkensiefken et al. 2010). Based on Student's t-test, the reductions in crack intensity between the Control-2 and the two mixtures containing slag cement and silica fume concrete are statistically significant over all slumps, as listed in Table C.7 in Appendix C. As could be predicted based on the results shown in Figure 3.31, the differences between the 30% Slag - 3% SF and 30% Slag - 3% SF- 7 lb-IC mixtures are not statistically significant. The maximum crack widths for the

Control-2, 30% Slag - 3% SF, and 30% Slag - 3% SF- 7 lb-IC mixtures are compared in Figure 3.32. The mixtures containing slag cement and silica fume without and with IC water exhibited narrower cracks than the control mixtures for slumps greater than 4 in. (100 mm). The average crack width for the mixtures containing SCMs without and with IC is approximately constant and equal 0.0010 in. (0.025 mm) at all slumps.

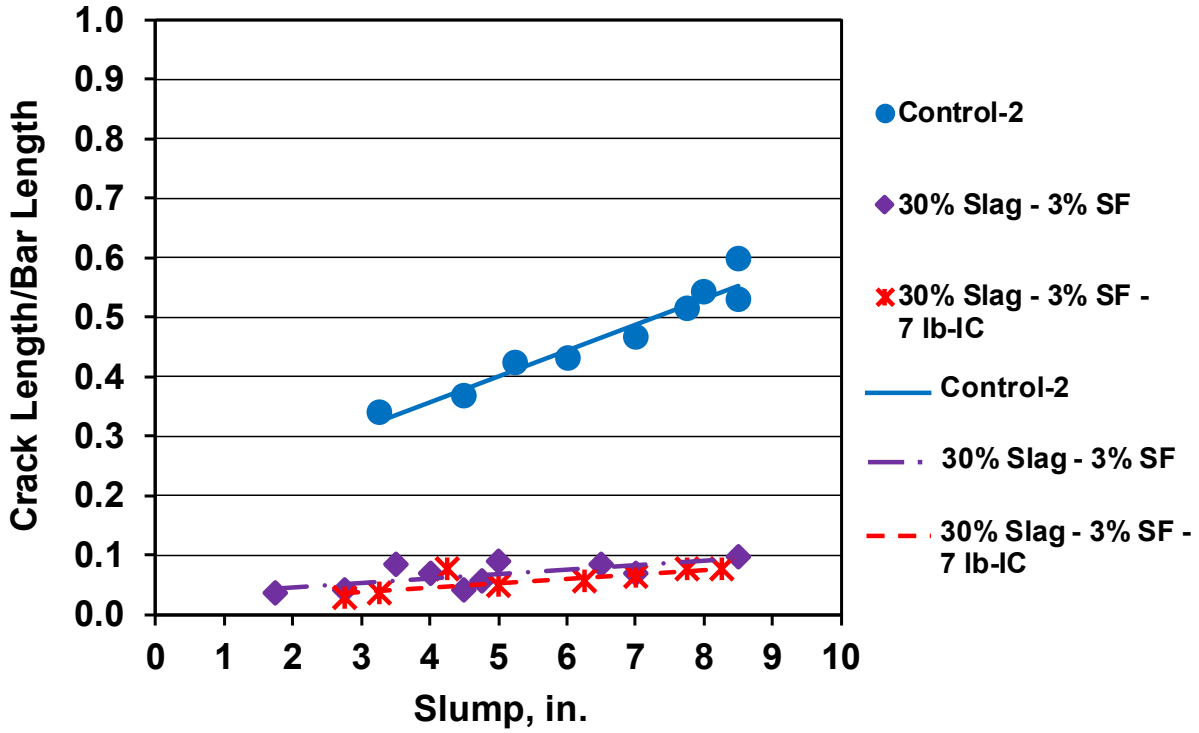

Figure 3.31 – Average settlement crack intensity (ratio of crack length to bar length) versus slump for the Control-2, 30% Slag - 3% SF, and 30% Slag - 3% SF - 7 lb-IC mixtures

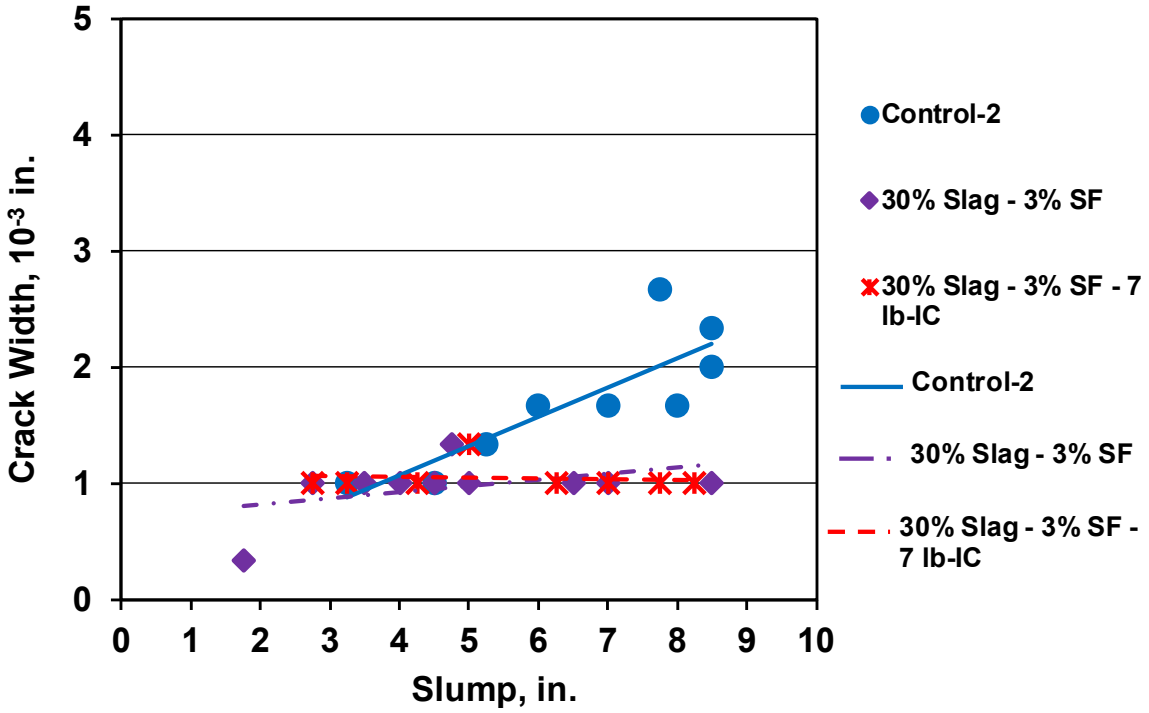

Figure 3.32 – Average maximum crack width versus slump for the Control-2, 30% Slag - 3% SF, and 30% Slag - 3% SF - 7 lb-IC mixtures

3.3.8 2% SRA

Figure 3.33 compares settlement crack intensity with slump for the concrete containing shrinkage-reducing admixture SRA-5. The figure shows that the average crack intensity increased from 0.14 at a slump of $2^{3}/_{4}$ in. (70 mm) to 0.44 at a slump of $8^{1}/_{4}$ in. (210 mm). As shown in Figure 3.34, the average maximum crack width of the concrete containing an SRA is constant and equal 0.0010 in. (0.025 mm) at all slumps. The properties and detailed cracking results for this type of concrete are summarized in Table B.10 in Appendix B.

Figure 3.35 compares settlement crack intensity with slump for the Control-2 and 2% SRA concrete. The concrete containing the shrinkage-reducing admixture exhibited lower crack intensity than the control at all slumps. No overlap in the data is shown. The average crack intensity of the 2% SRA is 23 percent lower than the average crack intensity of the Control-2 at a 7-in. (180-mm) slump. The reduction in crack intensity occurs because an SRA increases the viscosity of the pore water in the plastic concrete (Bentz 2006, Sant et al. 2010), leading to less bleeding and

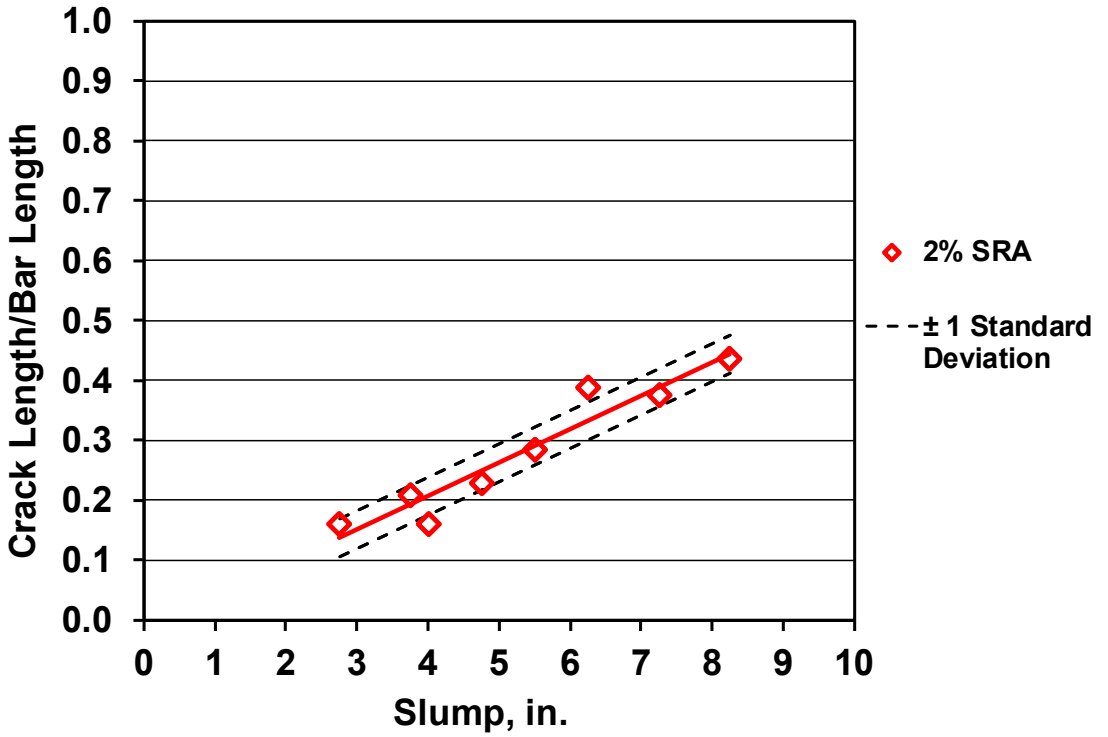

Figure 3.33 – Average settlement crack intensity (ratio of crack length to bar length) versus slump for the 2% SRA mixtures

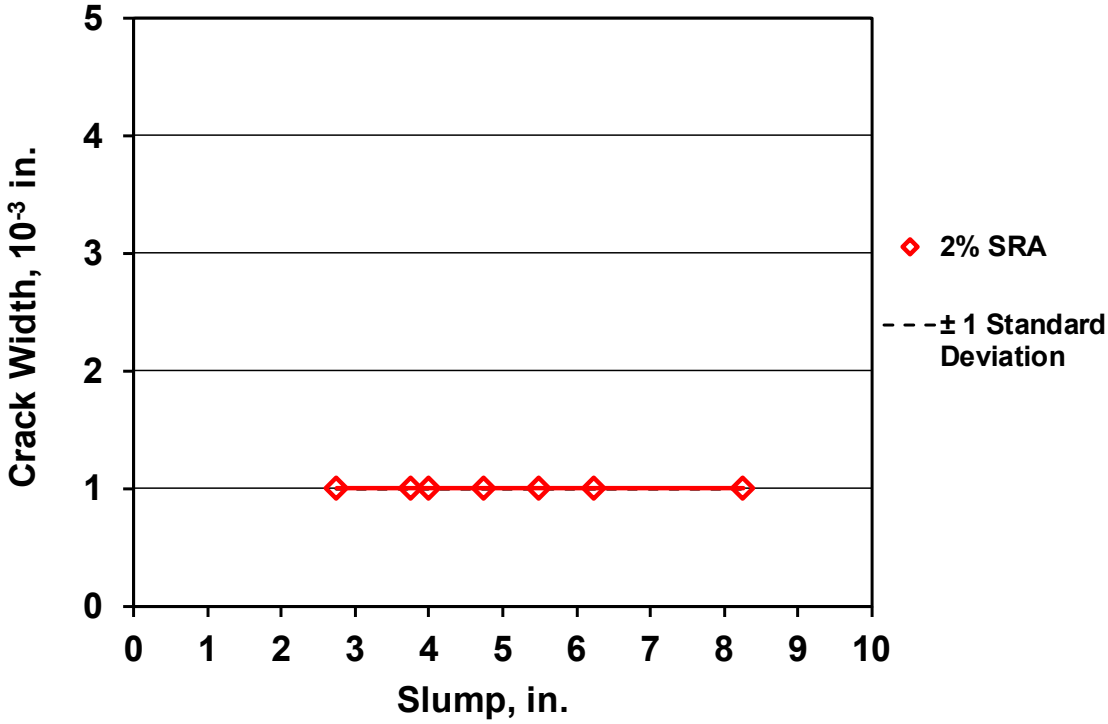

Figure 3.34 – Average maximum crack width versus slump for the 2% SRA mixtures

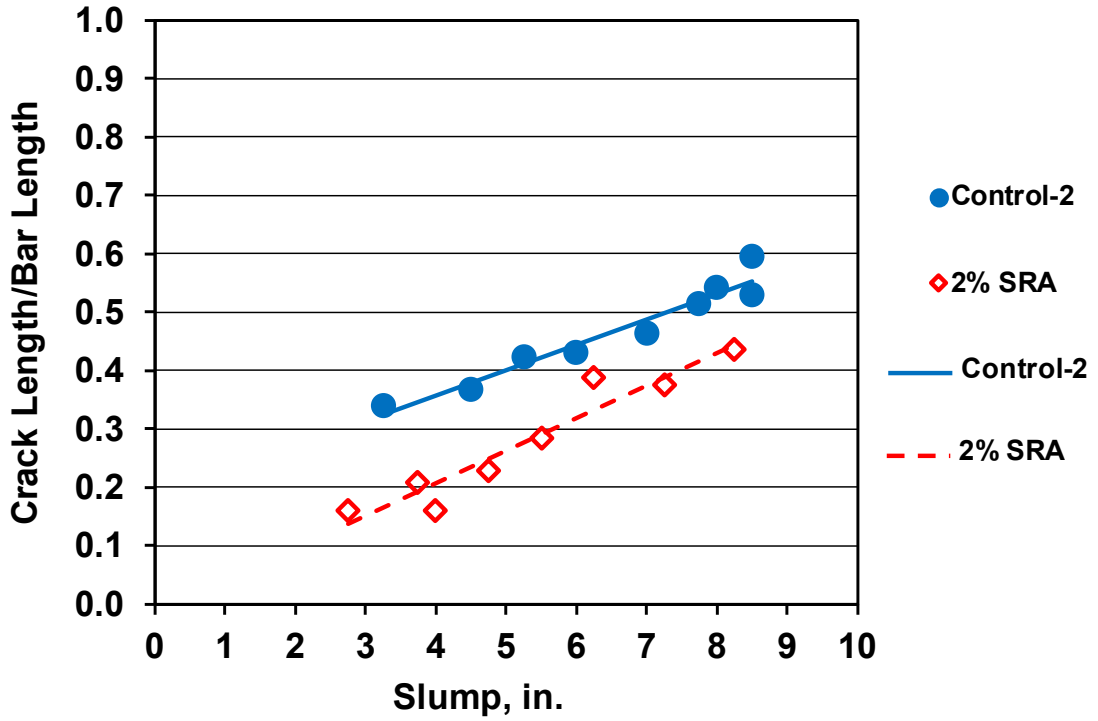

Figure 3.35 – Average settlement crack intensity (ratio of crack length to bar length) versus slump for the Control-2 and 2% SRA mixtures

settlement. The SRA also causes expansion of the concrete during the first 24 hours. This expansion may reduce settlement cracking (Sant et al. 2011). Based on Student's t-test, this reduction in the crack intensity is statistically significant at all slumps. Student's t-test results for this comparison are listed in Table C.8. The average maximum crack widths of the Control-2 and 2% SRA concrete are compared in Figure 3.36. The concrete containing the SRA exhibited narrower crack widths than the control for all but the lowest slumps.

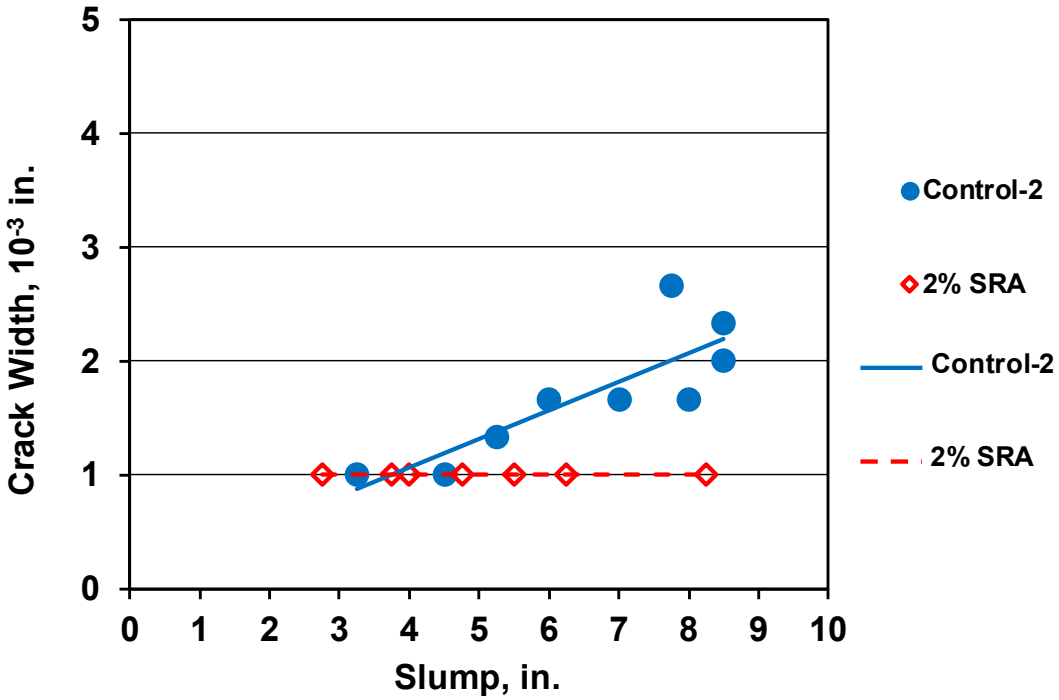

Figure 3.36 – Average maximum crack width versus slump for the Control-2 and 2% SRA mixtures

3.3.9 Summary

The mixtures in Series 2 contained the same cement and aggregate gradations, except Control-3, the only mixture with a non-optimized aggregate gradation. The study evaluated the effects of aggregate gradation, internal curing (IC), the supplementary cementitious materials (SCMs) slag cement and silica fume, and a shrinkage-reducing admixture (SRA-5) on the settlement crack intensity of plastic concrete. As shown in Figure 3.37, all mixtures experienced increased settlement crack intensity as slump increased; this is compatible with the previous studies (Dakhil et al. 1975, Weyers at al. 1982, and Al-Qassag et al. 2015). The increase, however, was very low for the two concretes containing both slag cement and silica fume, one with and one without IC; these concretes also exhibited the lowest crack densities, due largely to the fineness of both the slag cement and, especially, the silica fume particles, which increased the cohesiveness of plastic concrete and reduced bleeding (Mindess 1987, Mindess et al. 2003).

The concrete containing the non-optimized aggregate gradation (Control-3) exhibited the greatest crack intensity, likely because of the larger voids between the aggregate particles, reducing

cohesiveness, and increasing segregation and bleeding in the plastic concrete relative to that of the other mixtures, all of which contained aggregate with an optimized gradation (Scholer and Baker 1973, Mindess et al. 2003, Rangaraju et al. 2013, Lindquist et al. 2008).

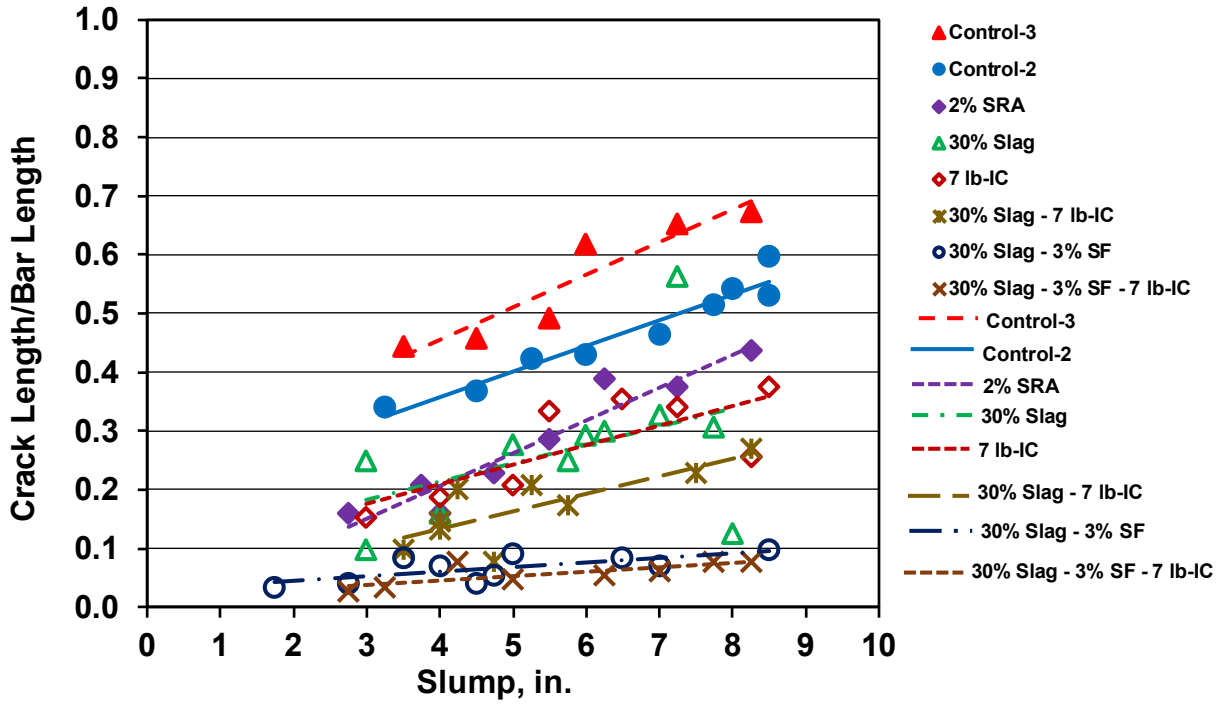

Figure 3.37 – Average settlement crack intensity (ratio of crack length to bar length) versus slump for the Control-3, Control-2, 2% SRA, 30% Slag, 7 lb-IC, 30% Slag - 7 lb-IC, 30% Slag - 3% SF, and 30% Slag - 3% SF - 7 lb-IC mixtures

The concretes containing the crack-reducing technologies IC and SRA and the SCMs slag cement and silica fume exhibited less settlement cracking than the control mixtures. As shown in Figure 3.37, the concrete containing the SRA (2% SRA) exhibited a reduction in crack intensity compared to the Control-2 mixtures. This occurs because the SRA increases the viscosity of the pore water in the plastic concrete (Bentz 2006, Sant et al. 2010) leading to less bleeding and settlement. The concrete containing slag cement without silica fume (30% Slag) or internal curing (7 lb-IC) exhibited nearly the same reduction in crack intensity compared to the control. The use of slag cement in concrete reduces bleeding because the slag cement particles are finer than cement particles. Since the bleed capacity and bleeding rate of concrete are influenced by the ratio of surface area of particles to the unit volume of water, using a finer cementitious material reduces

the bleeding (ACI Committee 233 2017), leading to less settlement. In addition, the higher silica content in the slag cement compared to portland cement reacts with calcium hydroxide ($Ca(OH)_2$), produced during cement hydration, resulting in C-S-H filling cement pores and refining the pore size of the concrete, causing less bleeding and settlement. The use of IC water provided by pre-wetted lightweight aggregate (LWA) can contribute to reduced settlement. Because LWA contains larger pores than cement paste, during the early hydration, water is drawn out of the LWA before it is drawn out of the deformable cement paste. The IC water allows the maintenance of a greater degree of saturation of the plastic concrete, resulting in less consolidation of the particles and less settlement. The concrete containing slag cement and IC water (30% Slag - 7 lb-IC) exhibited an even greater reduction in settlement crack intensity compared to the Control-2 mixture. This additional reduction in settlement cracking occurs due to the combined effect of slag cement and IC in reducing bleeding and settlement, as explained early. Finally, Figure 3.37 shows that the mixtures containing SCMs, slag cement and silica fume, without and with IC (30% Slag - 3% SF) and (30% Slag - 3% SF - 7 lb - IC), respectively, exhibited the greatest reduction in settlement crack intensity compared to the Control-2 mixtures. This most likely occurs because of the greater fineness of the supplementary cementitious materials, especially the silica fume, compared to portland cement.

Based on Student's t-test, the reduction in settlement crack intensity between the other concretes and Control-2 is statistically significant at all slumps. The increase in crack intensity in Control-3, with its non-optimized aggregate gradation, compared to the Control-2 is also statistically significant at all slumps. Overall, the use of any of the crack-reducing technologies studied, the SCMs slag cement and silica fume, or an optimized aggregate gradation will significantly reduce settlement cracking, even though materials or technologies are used principally for reasons other than settlement crack reduction. The use of combined methods, such as two of supplementary cementitious materials, slag cement and silica fume, or slag cement and IC, or slag cement and silica fume with IC in concrete can be used to achieve even greater reductions in crack intensity.

The study also compared the widths of settlement cracks for the mixtures in Series 2, Control-2, Control-3, 30% Slag, 7 lb-IC, 2% SRA, 30% Slag - 7 lb-IC, 30% Slag - 3% SF, and

30% Slag - 3% SF - 7 lb-IC, as shown in Figure 3.38. The Control (Control-2 and Control-3) mixtures exhibited increasing crack widths as slump increased, with those for the Control-3, with its non-optimized aggregate gradation, much wider than those of the Control-2 at all slumps. The concrete with IC (7 lb-IC) exhibited crack widths that increased only slightly as slump increased, with narrower cracks than the Control-2 at the slumps greater than 5 in. (125 mm). The concrete containing slag cement (30% Slag) exhibited crack widths that were approximately constant at all slumps. The crack widths for 30% Slag were wider than Control-2 at the slumps less than 6 in. (150 mm), but narrower at the slumps greater than 7 in (180 mm). The mixtures containing an SRA, slag cement with IC, slag cement with silica fume without and with IC exhibited crack widths equal to 0.0010 in. (0.025 mm), the minim width measured, at all slumps. Mixtures with SCMs, IC, SCMs and IC, or an SRA, in general, exhibited narrower crack widths than the Control-2 mixtures specifically at high slumps. The results indicate that SCMs, slag cement and silica fume, and the crack-reducing technologies, SRA and IC, not only reduce settlement crack intensity but also the width of these cracks.

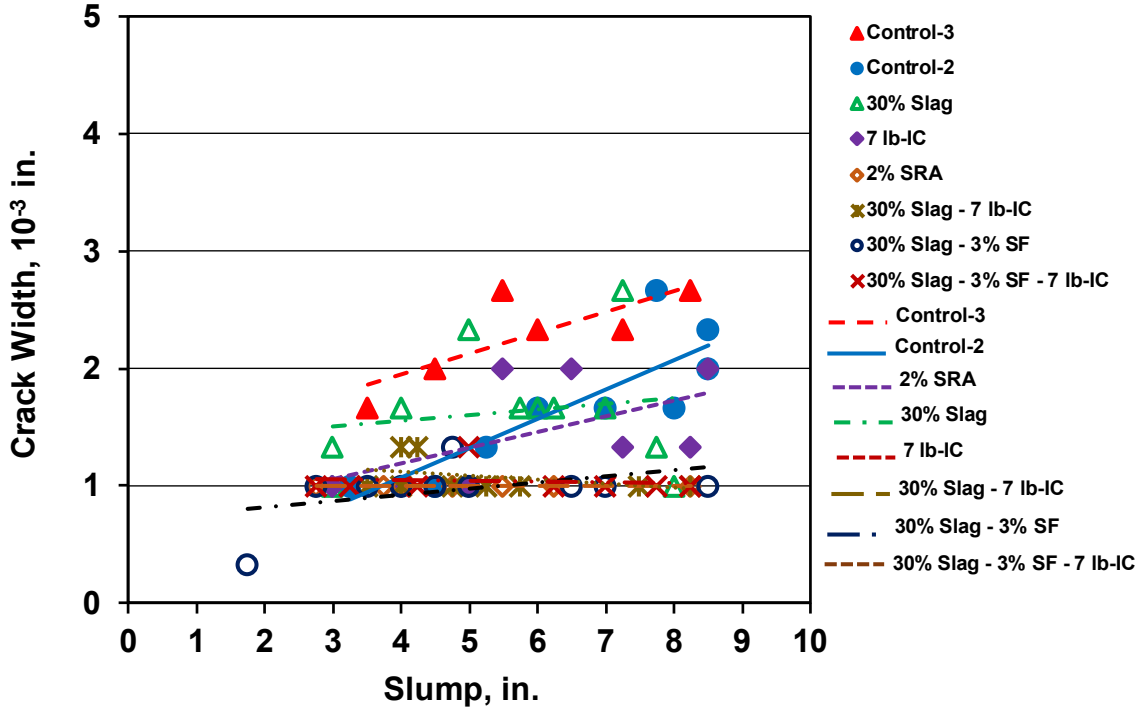

Figure 3.38 – Average maximum crack width versus slump for the Control-3, Control-2, 2% SRA, 30% Slag, 7 lb-IC, 30% Slag - 7 lb-IC, 30% Slag - 3% SF, and 30% Slag - 3% SF - 7 lb-IC mixtures

CHAPTER 4: DURABILITY OF MIXTURES CONTAINING SHRINKAGE-REDUCING, RHEOLOGY-MODIFYING, AND SHRINKAGE-COMPENSATING ADMIXTURES, AND FLY ASH

4.1 GENERAL

Cracking in bridge decks can increase the risk of the freeze-thaw damage; this damage can be minimized by providing an adequate air-void system for concrete. Shrinkage-reducing, rheology-modifying, and shrinkage-compensating admixtures, and fly ash have been used in bridge decks to minimize cracking. The effect of these materials on the freeze-thaw durability, scaling resistance and air-void system characteristics of hardened concrete is not completely understood. A study conducted at the University of Kansas has addressed the effect of incompatibility between shrinkage-reducing admixtures (SRAs) and air-entraining admixtures (AEAs) on the durability and air-void characteristics of hardened concrete (Pendergrass et al. 2017). The current study examined freeze-thaw durability, scaling resistance, and air-void characteristics for twenty-eight mixtures containing different combinations of shrinkage-reducing admixtures (SRAs), a rheology-modifying admixture (RMA), and shrinkage-compensating admixtures (SCAs), and fly ash. The mixtures had a cement paste volume of 24 percent and a water-to-cementitious materials ratio (*w/cm*) of 0.45. The study also examined the variability and repeatability of the air-void characteristics resulting from the air-void system analysis. This chapter describes three programs. Program 1 evaluated mixtures containing one of two SRAs (SRA-2 and SRA-3), Program 2 evaluated mixtures containing fly ash, with and without an RMA, and Program 3 evaluated mixtures containing one of two SCAs (SCA-1 and SCA-2). The mixture proportions of these three programs are presented, respectively, in Tables A-15, A-16, and A-17 in Appendix A. The properties of the mixtures, including slump, concrete temperature, air content in plastic concrete, unit weight, and 28-day compressive strength, are listed in Table E-1 in Appendix E.

RESEARCH SIGNIFICANCE

Crack-reducing technologies and supplementary cementitious materials, including fly ash, have been used in bridge decks to minimize cracking and improve the performance and reduce the cost of the concrete. The use of these materials in concrete, however, may influence the stability of the air-void system of hardened concrete and cause durability problems. The current research

evaluates the effect of shrinkage-reducing, rheology-modifying, and shrinkage-compensating admixtures, and fly ash on the freeze-thaw durability, scaling resistance, and stability of the air-void characteristics of hardened concrete. This study also addresses the correlation between the air-void characteristics, compressive strength, freeze-thaw durability, and scaling resistance for concrete containing these materials.

4.2 PROGRAM 1: EVALUATION OF MIXTURES CONTAINING SHRINKAGE - REDUCING ADMIXTURES

4.2.1 General

Program 1 examined the effects of two shrinkage-reducing admixtures (SRA-2 and SRA-3) on freeze-thaw durability, scaling resistance, and air-void characteristics in hardened concrete. The program included 11 mixtures. Three mixtures containing 0 percent SRA are denoted as Control. Six mixtures containing 0.5, 1.0, or 2.0 percent of SRA-2 by weight of cement are denoted as 0.5% SRA-2, 1% SRA-2, and 2% SRA-2, respectively. Two mixtures containing 0.75 or 2.25 percent of SRA-3 by weight of cement are denoted as 0.75% SRA-3 and 2.25% SRA-3, respectively. The measured air content in plastic concrete for these mixtures ranged from 5.75 to 9.75 percent. As discussed in Section 1.7.1, the use of SRAs in air-entrained concrete reduces the surface tension of water. Concrete containing both admixtures is susceptible to a reduction in the stability of the air-void system in plastic concrete and a reduction in the air content of hardened concrete, increasing the spacing factor and reducing freeze-thaw durability (Schemmel et al. 1999, Pendergrass et al. 2017) and scaling resistance (Cope and Ramey 2001).

The mixtures were evaluated for freeze-thaw durability in accordance with ASTM C666-Procedure B and ASTM C215 to determine the relative dynamic modulus and for scaling resistance using Canadian Test BNQ NQ 2621-900 Annex B to determine mass loss of the concrete specimens. A hardened air-void analysis was performed in accordance with ASTM C457-Procedure A to determine the air-void characteristics of hardened concrete. The procedures of these tests are discussed in detail in Chapter 2. The results of these evaluations are presented in the following sections.

4.2.2 Freeze-Thaw Durability

As discussed in Section 1.6, concrete with an inadequate air-void system may be damaged by repeated cycles of freezing-thawing because of water movement from the surrounding paste to the freezing sites, resulting in internal tensile stresses and cracking. When air voids are closely spaced, they protect the concrete from damage by providing empty spaces within the paste for water to move and freeze without causing damage.

In this program, 10 mixtures, four of which were duplicated, were subjected to freezing-thawing cycles to determine the effect of the type and dosage of SRA on freeze-thaw durability. These mixtures included three Control mixtures with no SRA, five containing 0.5, 1, or 2 percent of SRA-2 by weight of cement and two containing 0.75 or 2.25 percent of SRA-3 by weight of cement. As discussed in Section 2.4.2, three specimens from each batch were tested in accordance with ASTM C666 Procedure B; the test was terminated when the specimens were subjected to 300 freeze-thaw cycles or when the average dynamic modulus of elasticity of the three specimens dropped to 60 percent or less of the initial dynamic modulus of elasticity. Linear interpolation between dynamic modulus and freeze-thaw cycles was used to calculate the number of freeze-thaw cycles when the dynamic modulus of a specimen dropped to 60 percent of its initial dynamic modulus before reaching 300 cycles, and the dynamic modulus at 300 cycles for specimens subjected to more than 300 cycles. The relative dynamic modulus, representing the percentage of the average initial dynamic modulus of elasticity of three specimens that are subjected to 300 freezing cycles, serves as a measure of the freeze-thaw durability of the mixtures. Following the Kansas Department of Transportation (KDOT) requirements, a relative dynamic modulus of 95 percent is the acceptable lower limit for a durable concrete in this test. The results of this test are summarized in Table D.1 in Appendix D.

The average relative dynamic modulus of elasticity for the three specimens from each batch is plotted as a function of the number of freeze-thaw cycles in Figures 4.1 and 4.2 for the mixtures containing SRA-2 and SRA-3, respectively. The dashed line in the figures represents a relative dynamic modulus of 95 percent, to show the limit for acceptable freeze-thaw durability. The mixtures are listed in the legends of the figures in order of descending relative dynamic modulus at 300 cycles. Table 4.1 shows the relative dynamic moduli for the Control, SRA-2, and SRA-3

mixtures and the number of freeze-thaw cycles completed. All mixtures were subjected to 300 cycles, except one mixture containing 2.25 percent of SRA-3, which was subjected to 268 cycles. The latter is a duplicated mixture and its durability performance was close to the durability performance of the original mixture under freezing cycles; therefore, the test was terminated when the relative dynamic modulus of the duplicated mixture dropped below the failure limit.

Based on the results, the mixtures containing SRA-2, by maintaining 98 percent or more of their initial dynamic modulus of elasticity, satisfied the KDOT criterion of 95 percent. The mixture containing SRA-3 with a dosage of 2.25 percent by weight of cement did not, dropping to 94 percent of its initial dynamic modulus of elasticity after 268 freeze-thaw cycles. Thus, while SRA-2 had no noticeable effect on the freeze-thaw durability at all dosages of the SRA-2, SRA-3 resulted in a measurable reduction in freeze-thaw durability when used at the highest dosage used in this study.

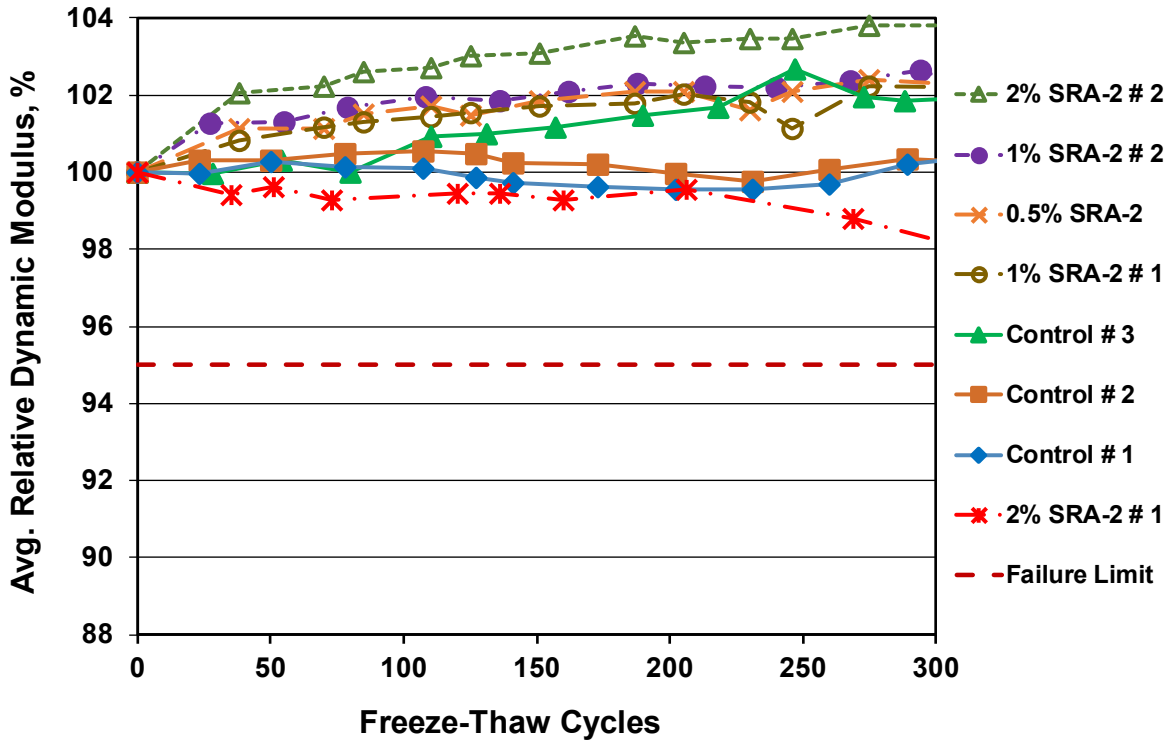

Figure 4.1 – Average relative dynamic modulus of elasticity versus freeze-thaw cycles for the Control and SRA-2 mixtures of Program 1

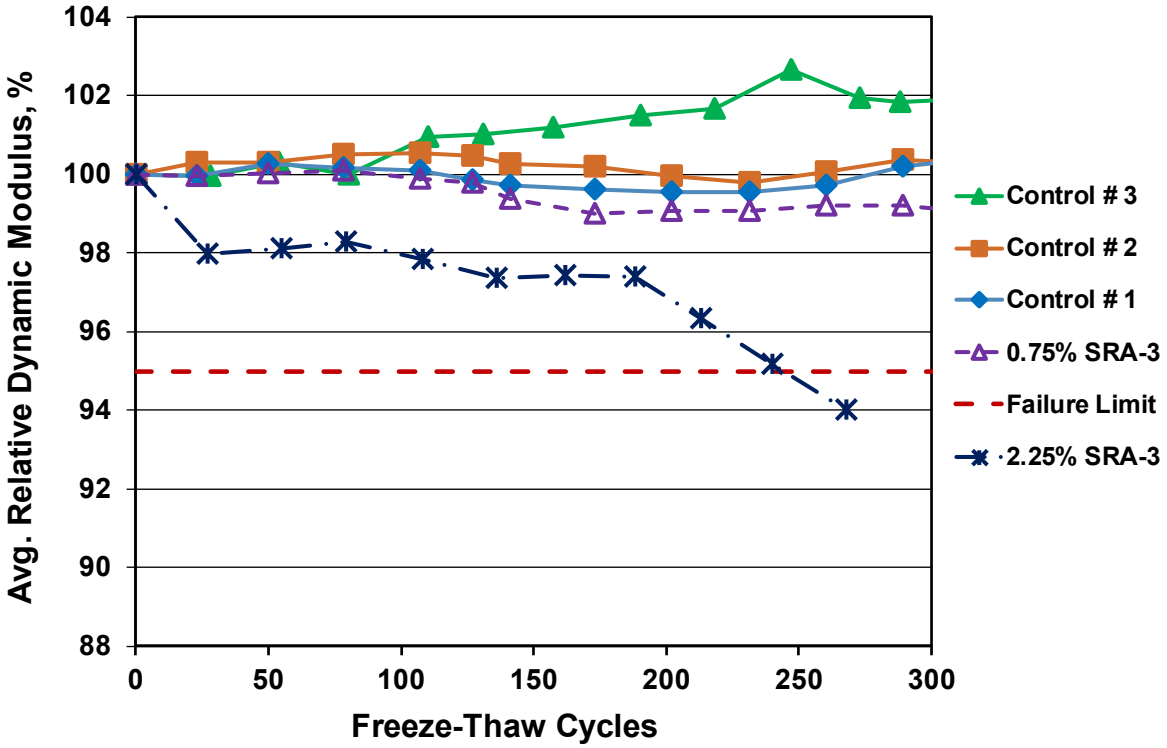

Figure 4.2 – Average relative dynamic modulus of elasticity versus freeze-thaw cycles for the Control and SRA-3 mixtures of Program 1

Table 4.1 – Average relative dynamic modulus versus freeze-thaw cycles for the Control, SRA-2, and SRA-3 mixtures of Program 1

Mixture	Average Relative Dynamic Modulus, %*	Freeze-Thaw Cycles Completed
Control # 1	100.3	300
Control # 2	100.3	300
Control # 3	101.9	300
0.5% SRA-2	102.3	300
1% SRA-2 # 1	102.2	300
1% SRA-2 # 2	†	†
1% SRA-2 # 3	102.5	300
2% SRA-2 # 1	098.2	300
2% SRA-2 # 2	103.8	300
0.75% SRA-3	099.1	300
2.25% SRA-3	094.0[$]	268

[#]*Relative Dynamic Modulus* is the percentage (*P*) of the average dynamic modulus remaining at *N* cycles. *N* is the smallest of either the number of cycles at which *P* reached 60 percent of initial dynamic modulus or 300 cycles.

†Mixture not tested

[$] Mixture exhibited relative dynamic modulus lower than of 95 percent at 300 cycles.

4.2.3 Scaling Resistance

Like freeze-thaw resistance, the scaling resistance of concrete is also affected by the air-void system. A good air-void system can improve the scaling resistance of concrete, and concrete containing a shrinkage-reducing admixture (SRA) may be susceptible to scaling if the SRA reduces the stability of the air-void system.

Eleven mixtures, five of which were duplicated, were evaluated for scaling resistance. These mixtures included three Control mixtures with no SRA, six mixtures containing 0.5, 1, and 2 percent of SRA-2 by weight of cement and two containing 0.75 and 2.25 percent of SRA-3 by weight of cement. Three specimens from each batch were evaluated for scaling resistance. As described in Section 2.4.3, a 2.5 percent NaCl solution was used in place of the 3 percent solution specified in Canadian Test BNQ NQ 2621-900 because a 2.5 percent solution causes greater scaling, as observed by Verbeck and Klieger (1957). Scaling resistance was based on the average cumulative mass losses of the surface for three specimens from each batch. Canadian Test BNQ NQ 2621-900 sets an upper limit of 0.2 lb/ft^2 (977 g/m^2) for the average cumulative mass loss. The results of the scaling resistance test for the mixtures of this program are presented in Table D.4 in Appendix D.

The average cumulative mass loss for the three specimens from each batch is plotted as a function of freeze-thaw cycles in Figures 4.3 and 4.4 for the mixtures containing SRA-2 and SRA-3, respectively. The dashed line in the figure represents the mass loss limit of 0.2 lb/ft^2 (977 g/m^2). The mixtures are listed in the legends of the figures in order of descending cumulative mass loss at 56 freeze-thaw cycles. Table 4.2 summarizes the average cumulative mass losses of the Control, SRA-2, and SRA-3 mixtures at 7, 21, 35, and 56 cycles. As shown in Figures 4.3 and 4.4 and Table 4.2, the mixtures containing the dosage of 2.25% SRA-3 by weight of cement exhibited the greatest mass loss. This mixture (2.25% SRA-3) was the only mixture in Program 1 to fail in the freeze-thaw test. Figure 4.3 shows that the three Control mixtures and three SRA-2 mixtures, one containing 0.5 percent SRA-2 and two containing 1 percent SRA-2 by weight of cement, exhibited a cumulative mass loss below the specified failure limit [0.2 lb/ft^2 (977 g/m^2)] after 56 cycles. One of the SRA-2 mixtures containing 1 percent SRA-2 and both mixtures containing 2 percent SRA-2 by weight of cement, however, exceeded the specified failure limit for mass loss after 56 cycles.

Figure 4.4 shows that four mixtures, three Controls and one containing 0.75 percent SRA-3 by weight of cement, exhibited a cumulative mass loss below the failure limit after 56 cycles. One mixture containing 2.25 percent SRA-3 by weight of cement exceeded the failure limit after 21 cycles. The results indicate that the mixtures containing the highest dosage of SRA-3 used in this study exhibited the greatest reduction in scaling resistance.

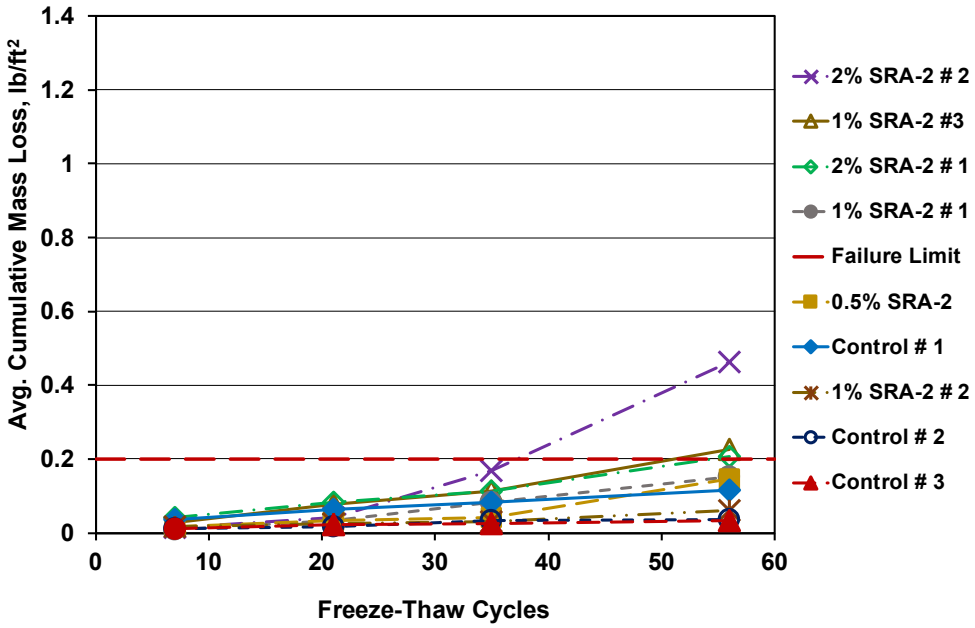

Figure 4.3 – Average cumulative mass loss versus freeze-thaw cycles for the Control and SRA-2 mixtures of Program 1

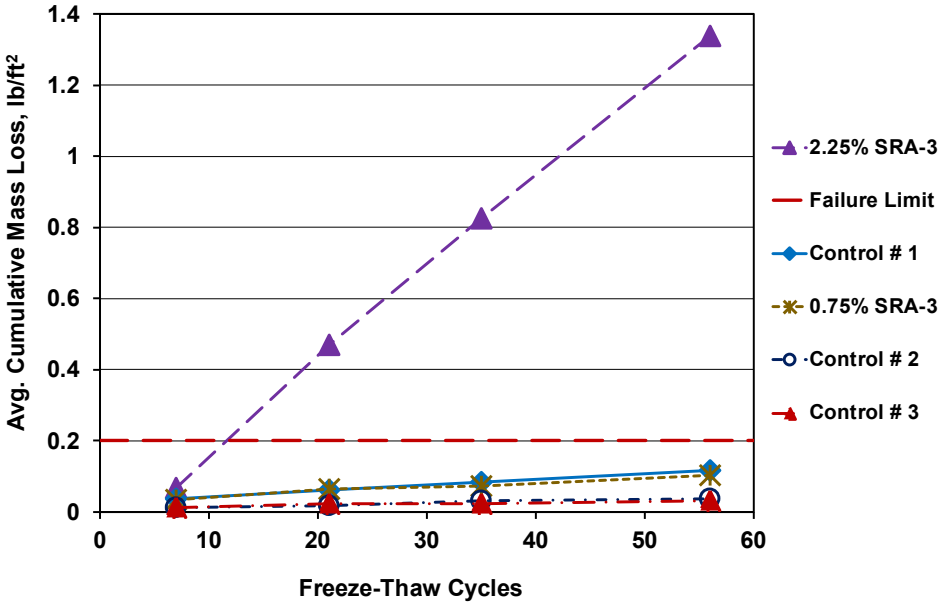

Figure 4.4 – Average cumulative mass loss versus freeze-thaw cycles for the Control and SRA-3 mixtures of Program 1

Table 4.2 – Summary of average cumulative mass loss at different freeze-thaw cycles for the Control, SRA-2, and SRA-3 mixtures of Program 1

Mixture	Average Cumulative Mass Loss, lb/ft^2			
	7 cycles	21 cycles	35 cycles	56 cycles
Control # 1	0.036	0.063	0.083	0.117
Control # 2	0.013	0.017	0.032	0.036
Control # 3	0.012	0.022	0.025	0.032
0.5% SRA-2	0.016	0.032	0.041	0.147
1% SRA-2 # 1	0.008	0.034	0.084	0.152
1% SRA-2 # 2	0.016	0.026	0.030	0.060
1% SRA-2 # 3	0.029	0.076	0.011	0.226[#]
2% SRA-2 # 1	0.043	0.084	0.113	0.207[#]
2% SRA-2 # 2	0.013	0.041	0.170	0.464[#]
0.75% SRA-3	0.035	0.064	0.073	0.102
2.25% SRA-3	0.067	0.047	0.083	1.339[#]

[#]Mixture with cumulative mass loss exceeded the failure limit of 0.2 lb/ft^2 (977 g/m^2),
10^{-3} lb/ft^2 = 4.884 g/m^2

4.2.4 Hardened Concrete Air-Void Analysis

As discussed in Section 4.2.2, a proper air-void system with closely spaced air voids, can protect concrete from freezing and scaling damage. The spacing of the air-voids, represented by the air-void spacing factor, is considered the key parameter affecting the ability of the air-void system to protect concrete. An air-void spacing factor of no greater than 0.008 in. (0.20 mm) is recommended for concrete subjected to freezing cycles (Mindess et al. 2003, Russell 2004). American Concrete Institute (ACI) Committee 201 recommends an air volume within the range of 5 to 6 percent to help ensure sufficient frost resistance for the concrete with a maximum size aggregate of 1 in. (25.4 mm). Low-cracking high-performance concrete (LC-HPC) specifications require air contents between 6.5 to 9.5 percent, but these higher values are based on mixture proportions to minimize cracking in bridge decks (Kansas Department of Transportation 2014). Another parameter, the specific surface area, representing the surface area of air voids divided by their volume, should be greater than 600 in.$^{-1}$ (25 mm^{-1}) to protect the concrete from frost attack (Mindess et al. 2003, Russell 2004).

In this study, the air contents of the mixtures were measured in plastic concrete using the Volumetric Method (ASTM C173) and in hardened concrete using the linear traverse method in

accordance with Procedure A of Microscopically Determination of Parameters of the Air-Void System (ASTM C457). To evaluate the effect of the dosage and type of shrinkage-reducing admixture (SRA) on the stability of the air-void system, the program included eleven mixtures, five of which were duplicated, three Control mixtures, six mixtures containing 0.5, 1, and 2 percent of SRA-2 by weight of cement, and two mixtures containing 0.75 and 2.25 percent of SRA-3 by weight of cement. As discussed in Section 2.4.4.2, the air-void system was measured using two slabs from each of two cylinders specimens from each mixture, and the average air-void parameters of the four slabs are reported as the air-void parameters of that mixture. The results of the hardened air-void analysis for the mixtures of Program 1 are summarized in Tables E.2 to E.12 in Appendix E.

The air contents in plastic and hardened concrete for the mixtures of Program 1 for the concrete containing different dosages of the SRA-2 and SRA-3 are presented in Figures 4.5 and 4.6, respectively. The numbers on the bars indicate the reduction in the air content between the plastic and hardened concrete. Based on the results, all mixtures exhibited a lower air content in hardened concrete than in plastic concrete. The reduction in air content may attributed to the loss of large air voids due to handling, transport, or consolidation of concrete; this does not influence freeze-thaw durability. The reduction may also be due to dissolution of small air voids in the water or merging of small air voids to larger voids; this can cause a reduction in freeze-thaw durability (Fagerlund 1991). The reduction in air content increased when an SRA was used, increasing with the SRA dosage; this observation is compatible with previous studies (Schemmel et al. 1999, Pendergrass et al. 2017). As shown in the figure, the decline in the air content increased from 0.2 to 3.1 percent as the dosage of the SRA-2 increased from 0.5 to 2 percent by weight of cement, while the decline in the air content increased from 0.5 to 2.9 percent as the dosage of the SRA-3 increased from 0.75 to 2.25 percent by weight of cement. A summary of the air-void parameters, including air content, average air-void spacing factor, and specific surface for the Control, SRA-2, and SRA-3 mixtures is reported in Table 4.3. As shown in the table, the average air-void spacing factor ranged from 0.0039 to 0.0078 in. (0.1 to 0.2 mm), and the average specific surface ranged from 612 to 768 $in.^{-1}$ (24.5 to 30.7 mm^{-1}). The two mixtures containing the highest dosage (2 %) of SRA-2 used in this study exhibited the greatest reduction in air content between the plastic and

hardened concrete. The mixtures also had an air-void spacing factor lower than the recommended 0.008 in. (0.2 mm) for concrete subjected to freezing cycles. This suggests that the reduction in air content in these mixtures occurred due to the loss of large air voids, which would have little or no effect on freeze-thaw durability of the concrete. The mixture containing the highest dosage (2.25 %) of the SRA-3 used in this program had the lowest air content (4.65%) in hardened concrete, the highest air-void spacing factor [0.0078 in. (0.2 mm)], and the lowest specific surface (612 in.$^{-1}$). This observation indicates that the reduction in air content occurred in this mixture may be due to merging of small air voids to the larger voids, which can influence freeze-thaw durability. This is consistent with observations by Battaglia et al. (2008) who recommended that SRA-3 is not be used in concrete bridge decks because of its effect on the stability of the air-void system.

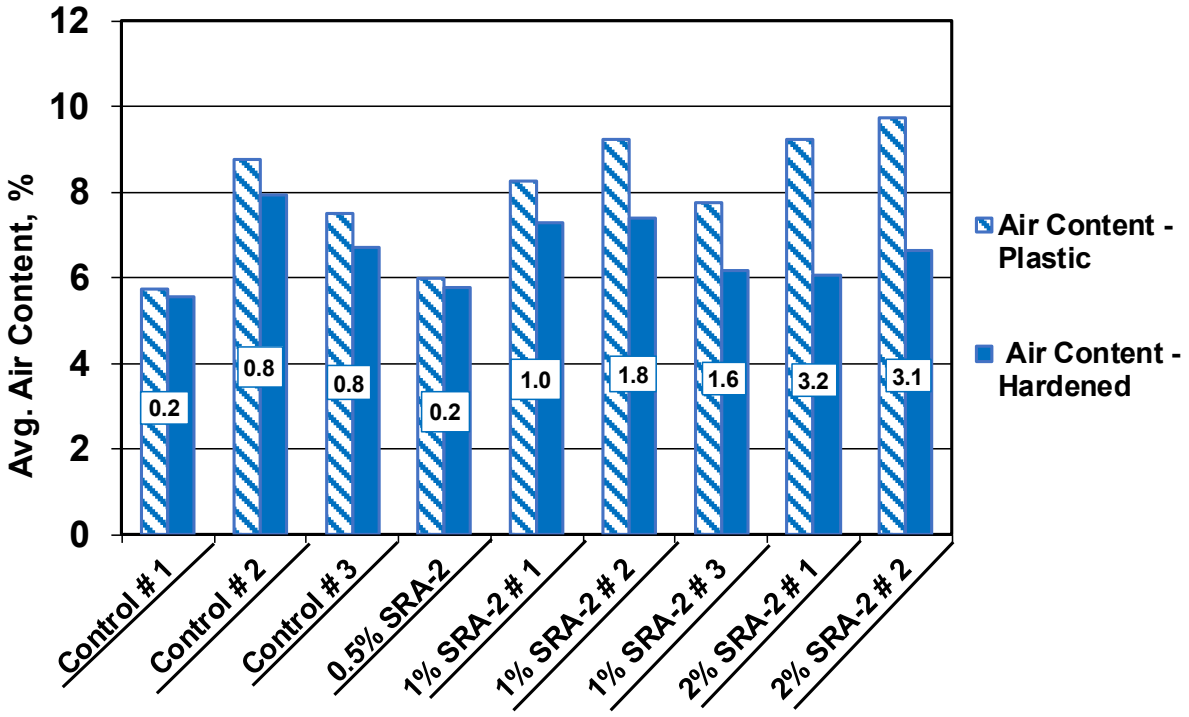

Figure 4.5 – Average air contents in plastic and hardened concrete for the Control and SRA-2 mixtures of Program 1

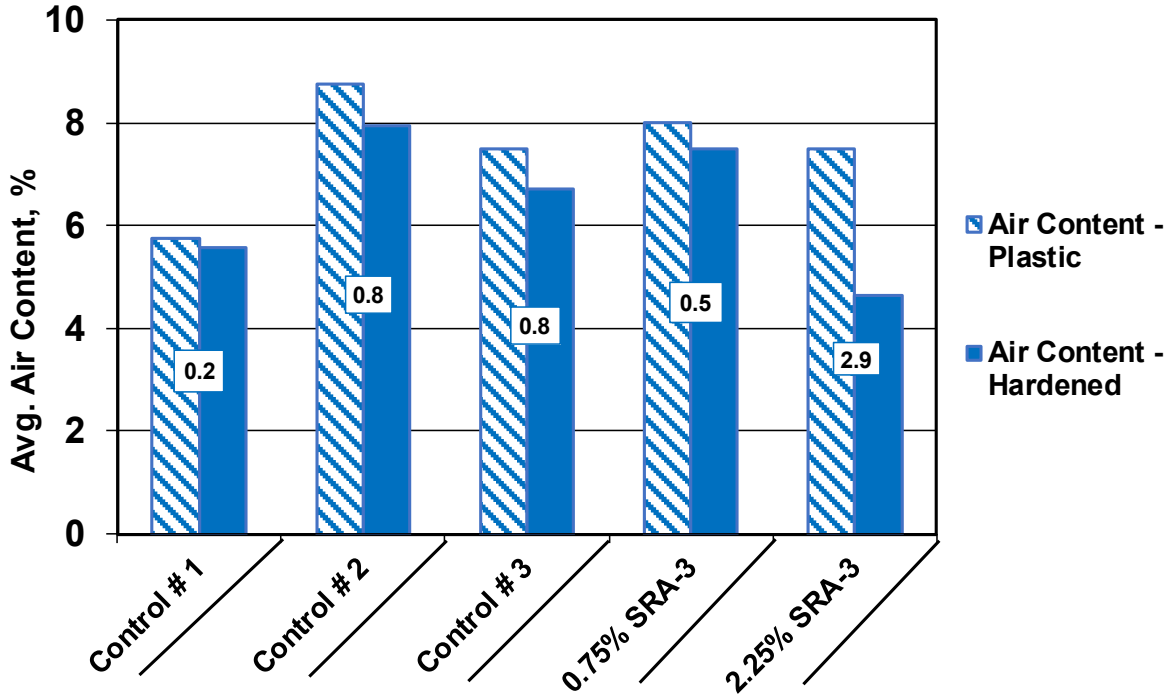

Figure 4.6 – Average air contents in plastic and hardened concrete for the Control and SRA-3 mixtures of Program 1

Table 4.3 – Average air content, air-void spacing factor, and specific surface for the Control, SRA-2, and SRA-3 mixtures of Program 1

Mixture	Average Air Content, %			Average Air-Void Spacing Factor in. (mm)	Average Specific Surface ($in.^{-1}$) (mm^{-1})
	Plastic, %	Hardened, %	Difference, %†		
Control #1	5.75	5.56	-0.19	0.0056 (0.14)	711 (28.4)
Control #2	8.75	7.93	-0.82	0.0039 (0.10)	768 (30.7)
Control #3	7.50	6.71	-0.79	0.0052 (0.13)	695 (27.8)
0.5% SRA-2	6.00	5.78	-0.22	0.0066 (0.17)	622 (24.9)
1% SRA-2 #1	8.25	7.28	-0.97	0.0050 (0.01)	659 (26.4)
1% SRA-2 #2	9.25	7.41	-1.84	0.0048 (0.12)	686 (26.4)
1% SRA-2 #3	7.75	6.17	-1.58	0.0058 (0.15)	671 (26.8)
2% SRA-2 #1	9.25	6.07	-3.18	0.0063 (0.16)	628 (25.1)
2% SRA-2 #2	9.75	6.65	-3.10	0.0055 (0.14)	648 (25.9)
0.75% SRA-3	8.00	7.49	-0.51	0.0047 (0.12)	679 (27.2)
2.25% SRA-3	7.50	4.65	-2.85	0.0078 (0.20)	612 (24.5)

Note: Air contents in plastic and hardened concrete measured through ASTM C173 and C457, respectively.
† Percentage difference in air content between values measured in plastic and hardened concrete.
Spacing Factor – is the average distance from any point in the paste to the edge of the nearest air void.
Specific Surface – The surface area of the air voids divided by the volume of air voids.

4.2.5 Correlation Between Air-Void Characteristics, Compressive Strength, and Concrete Durability

This study also evaluated the correlation between air-void characteristics, compressive strength, and the durability of concrete based on freeze-thaw and scaling resistance for concrete containing SRA-2 and SRA-3. A summary of the average air-void spacing factor, 28-day compressive strength, dynamic moduli, and mass loss after 56 freeze-thaw cycles for the mixtures of Program 1 is presented in Table 4.4. The average air-void spacing factors for these mixtures ranged from 0.0039 to 0.0078 in. (0.1 to 0.2 mm). The average compressive strength for these mixtures ranged from 3530 to 6790 psi (24.3 to 46.8 MPa). Ten mixtures had a spacing factor less than 0.007 in. (0.18 mm) and all of them passed the freeze-thaw durability test by maintaining a relative dynamic modulus above 95 percent. The only mixture that had spacing factor greater than 0.007 in. (0.18 mm) had a relative dynamic modulus below 95 percent; this mixture also exhibited the greatest mass loss in the scaling test. Seven of the ten mixtures that had a spacing factor less than 0.007 in. (0.18 mm) exhibited a mass loss below the failure limit [0.2 lb/ft^2 (977 g/m^2)]; and the other three mixtures had a mass loss that exceeded the failure limit. The latter three mixtures had a compressive strength less than or equal to 4000 psi (27.6 MPa). The mass loss of these mixtures may have been due to their low strength, which can contribute to reduce scaling resistance (Langan et al. 1990, Bouzoubaa et al. 2011).

Table 4.4 – Average air-void spacing factor, 28-day compressive strength, relative dynamic modulus, and average cumulative mass loss at 56 cycles for the Control, SRA-2, and SRA-3 mixtures of Program 1

Mixture	Average Air-Void Spacing Factor		Average 28-Day Compressive Strength		Average Relative Dynamic Modulus*	Average Cumulative Mass Loss @ 56 cycles (lb/ft^2)
	(in.)	(mm)	(psi)	(MPa)		
Control # 1	0.0056	0.14	6790	46.8	100.3	0.117
Control # 2	0.0039	0.10	5330	36.8	100.3	0.036
Control # 3	0.0052	0.13	4860	33.5	101.9	0.032
0.5% SRA-2	0.0066	0.17	4240	29.2	102.3	0.147
1% SRA-2 # 1	0.0050	0.01	4160	28.7	102.2	0.152
1% SRA-2 # 2	0.0048	0.12	4560	31.4	†	0.060
1% SRA-2 # 3	0.0058	0.15	4000	27.6	102.0	0.226[#]
2% SRA-3 # 1	0.0063	0.16	3530	24.3	098.2	0.207[#]
2% SRA-3 # 2	0.0055	0.14	3840	26.5	103.8	0.464[#]
0.75% SRA-3	0.0047	0.12	5400	37.2	099.1	0.102
2.25% SRA-3	0.0078	0.20	4370	30.1	094.0[$]	1.339[#]

[#]*Relative Dynamic Modulus* is the percentage (*P*) of the average dynamic modulus remaining at *N* cycles.
N is the smallest of either the number of cycles at which *P* reached 60 percent of initial dynamic modulus or 300 cycles.
†Mixture not testing
[$] Mixture exhibited relative dynamic modulus lower than of 95 percent at 300 cycles.
[#]Mixture exhibited cumulative mass loss exceeded 0.2 lb/ft^2 (977 g/m^2) prior to 56 cycles.

Figure 4.7 shows the relative dynamic modulus in the freeze-thaw test as a function of the average air-void spacing factors. The dashed line in the figure represents a relative dynamic modulus of 95 percent. Nine of the ten mixtures had a relative dynamic modulus greater than 95 percent. These mixtures, all, had an air-void spacing factor less than 0.007 in. (0.18 mm). One mixture (2.25% SRA-3) had a relative dynamic modulus below the failure limit; this mixture had a spacing factor greater than 0.007 in. (0.18 mm). Figure 4.8 shows the relative dynamic modulus in the freeze-thaw test as a function of the average 28-day compressive strength. The results show nine mixtures had a relative dynamic modulus greater than the failure limit; two of these had a compressive strength less than or equal to 4000 psi (27.6 MPa). One mixture had a relative dynamic modulus below the failure limit; this mixture, however, had a compressive strength greater than 4000 psi (27.6 MPa). The results indicate that the air-void spacing factor, but not compressive strength, influenced the freeze-thaw durability of the concretes containing SRA-2 or SRA-3.

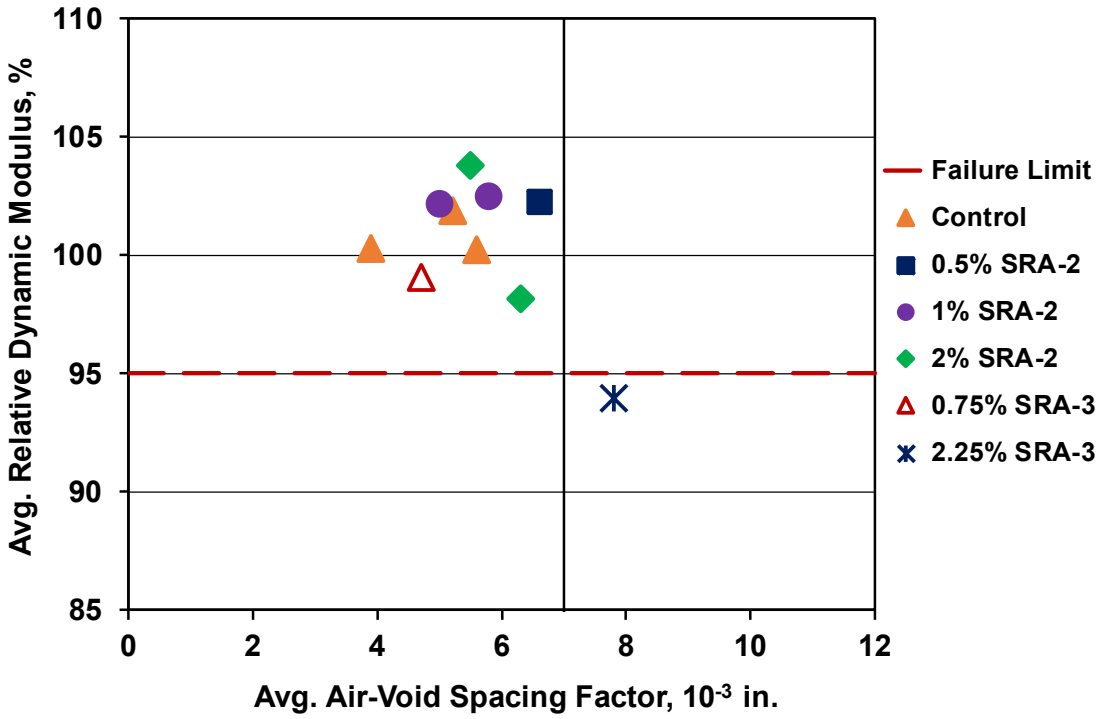

Figure 4.7 – Average relative dynamic modulus versus air-void spacing factor for the mixtures of Program 1

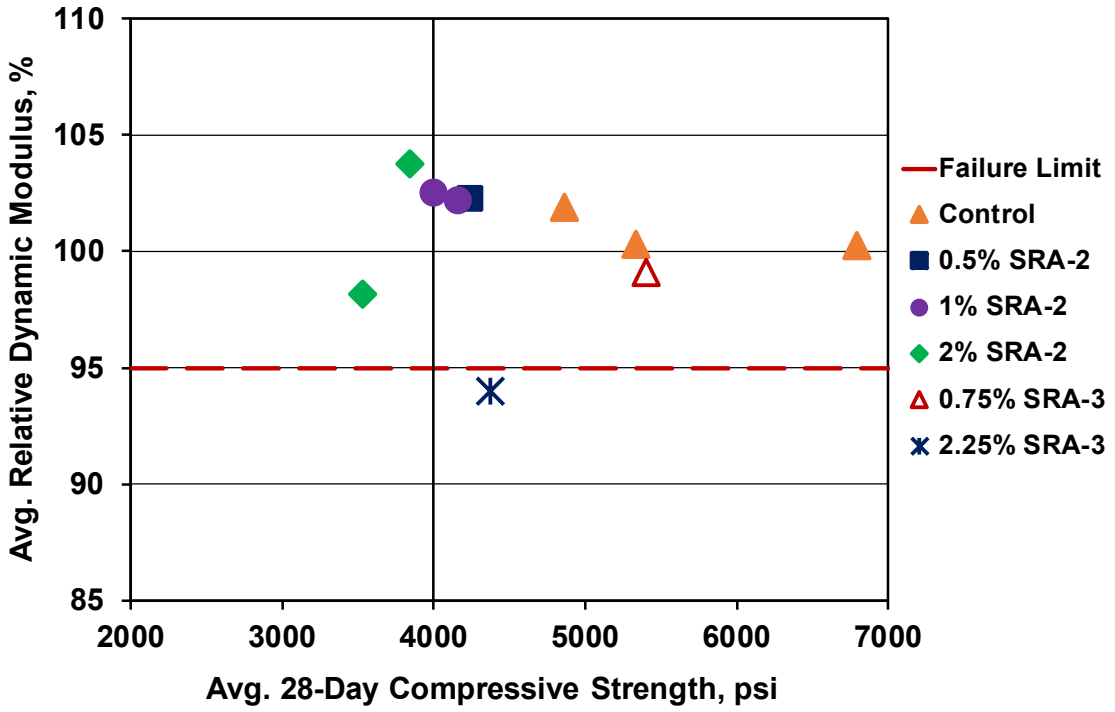

Figure 4.8 – Average relative dynamic modulus versus average 28-day compressive strength for the mixtures of Program 1

Figure 4.9 compares the average cumulative mass loss after 56 freeze-thaw cycles with the average air-void spacing factor. The dashed line in the figure represents a mass loss limit of 0.2 lb/ft^2 (977 g/m^2). Ten of the eleven mixtures had spacing factors less than 0.007 in. (0.18 mm). Seven of the ten exhibited mass loss below the failure limit, while the other three mixtures (1% SRA-2 #3, 2% SRA-2 #1, and 2% SRA-2 #2) exceeded the failure limit. The latter three mixtures had an average compressive strength of [4000, 3530, and 3840 psi (27.6, 24.3, and 26.5 MPa)], respectively, as shown in the figure 4.10. The results indicate that only mixtures that had either an air-void spacing factor greater than 0.007 in. (0.18 mm) or a compressive strength of 4000 psi (27.6 Ma) or less exhibited a mass loss that exceeded the failure limit, indicating that both the air-void spacing factor and compressive strength can influence the scaling resistance of the concrete containing SRA-2 or SRA-3. The mixture containing the highest dosage (2.25%) of SRA-3 by weight of cement had the highest spacing factor [0.0078 in. (0.2 mm)] and exhibited the greatest mass loss, 1.34 lb/ft^2 (6544 g/m^2).

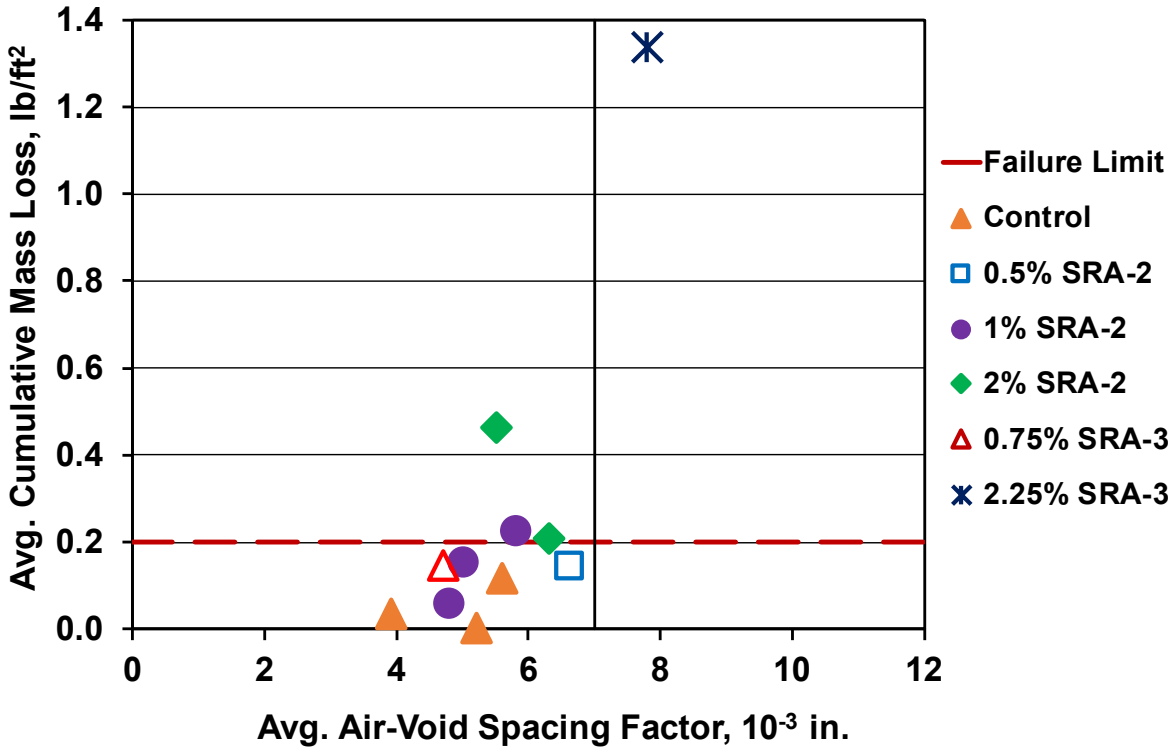

Figure 4.9 – Average cumulative mass loss at 56 freeze-thaw cycles versus average air-void spacing factor for the mixtures of Program 1

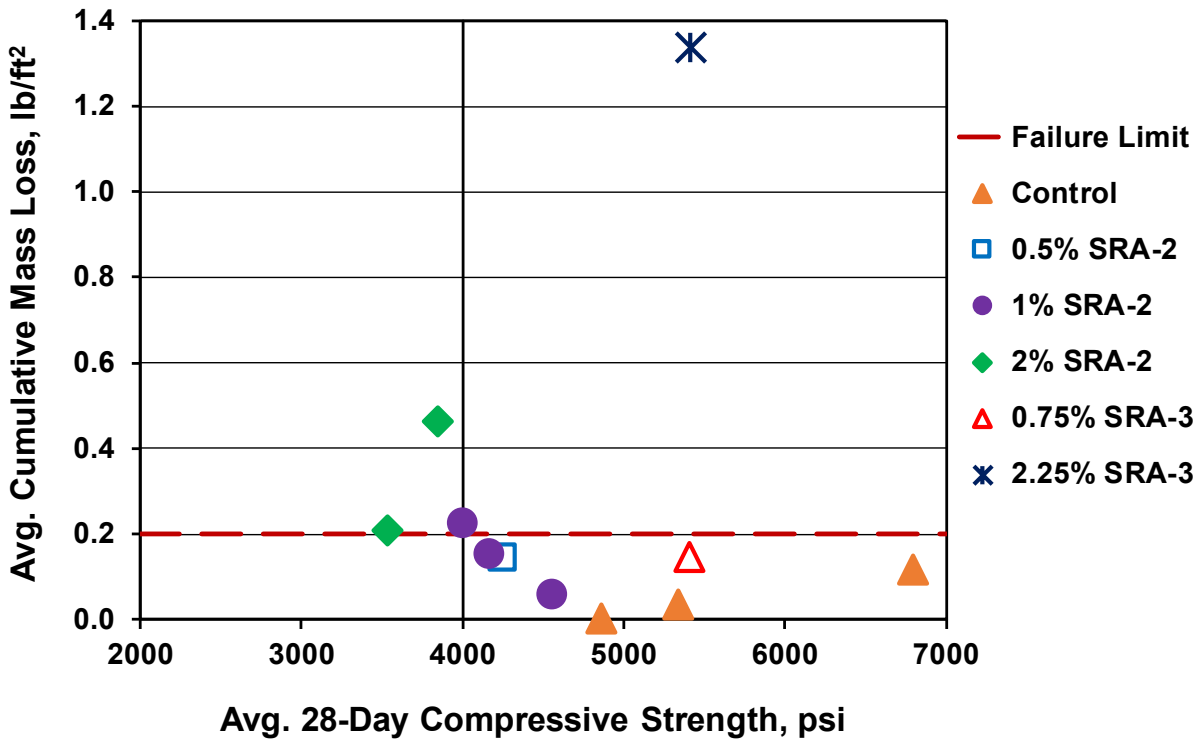

Figure 4.10 – Average cumulative mass loss at 56 freeze-thaw cycles versus average 28-day compressive strength for the mixtures of Program 1

4.2.6 Program 1 Summary

The results of Program 1 indicate that all mixtures containing SRA-2 passed the freeze-thaw test, maintaining at least 98 percent of their initial relative dynamic modulus; the mixture containing the highest dosage (2.25%) of SRA-3 used in this study did not, dropping to 94 percent of its initial dynamic modulus before the test was terminated after 268 cycles. Three mixtures containing 1 or 2 percent SRA-2 exhibited mass loss exceeding the failure limit [0.2 lb/ft^2 (977 g/m^2)]; and single mixture containing 2.25 percent SRA-3 exhibited the highest mass loss. All mixtures exhibited a reduction in air content between the plastic and hardened concrete. This reduction increased when an SRA was used, increasing with the SRA dosage. In addition, all mixtures that had an average air-void spacing factor less than 0.007 in. (0.18 mm) exhibited a relative dynamic modulus greater than 95 percent. The only mixture that had the average air-void spacing factor greater than 0.007 in. (0.18 mm) exhibited a relative dynamic modulus below the failure limit. Seven of the ten mixtures that had an air-void spacing factor less than 0.007 in. (0.18 mm) exhibited mass loss below the failure limit; the other three mixtures exhibited mass loss

exceeded the failure limit. These three mixtures had an average compressive strength less than or equal to 4000 psi (27.6 MPa).

4.3 PROGRAM 2: EVALUATION OF MIXTURES CONTAINING FLY ASH WITHOUT AND WITH A RHEOLOGY-MODIFYING ADMIXTURE (RMA)

4.3.1 General

Program 2 examined the effects of Class F and Class C fly ash and a rheology-modifying admixture (RMA) on freeze-thaw durability, scaling resistance, and air-void characteristics in hardened concrete. The program included fourteen mixtures; three mixtures contained no fly ash or RMA and are denoted as Control. Four mixtures contained a 20 or 40 percent volume replacement of cement with Class F fly ash and are denoted as 20% FA-F and 40% FA-F, respectively. One mixture contained a 20 percent volume replacement of cement with Class C fly ash and is denoted as 20% FA-C. Two mixtures contained 0.05 or 0.075 percent of RMA by total weight of dry materials and are denoted as 0.05% RMA and 0.075% RMA, respectively. Three mixtures contained a 40 percent volume replacement of cement with Class C fly ash in conjunction with 0.05, 0.075, and 0.15 percent of RMA by total weight of dry materials and are denoted as 0.05% RMA - 40% FA-C, 0.075% RMA - 40% FA-C, and 0.15% RMA - 40% FA-C, respectively. One mixture contained a 20 percent volume replacement of cement with Class C fly ash in conjunction with 0.15 percent of RMA and is denoted as 0.15% RMA - 20% FA-C. The measured air content in plastic concrete for these mixtures ranged from 2.75 to 10 percent. The mixtures were evaluated based on freeze-thaw durability, scaling resistance, and air-void characteristics, and the results of these evaluations are presented in the following sections.

4.3.2 Freeze-Thaw Durability

In this program, thirteen mixtures, four of which were duplicated, were evaluated to determine the effect of the type and dosage of fly ash and RMA on freeze-thaw durability. These mixtures included three Control mixtures containing no fly ash or RMA. Three contained a 20 or 40 percent volume replacement of cement with Class F fly ash; one mixture containing 20 percent volume replacements of cement with Class C fly ash. Two mixtures contained 0.05 or 0.075 percent of RMA by total weight of dry materials. Three mixtures contained a 40 percent volume

replacement of cement with Class C fly ash in conjunction with 0.05, 0.075, and 0.15 percent of RMA by total weight of dry materials. One mixture contained a 20 percent volume replacement of cement with Class C fly ash in conjunction with 0.15 percent of RMA by total weight of dry materials. As described in Section 2.4.2, three specimens from each batch were tested in accordance with ASTM C666 Procedure B. The results of this test are summarized in Table D.2 in Appendix-D.

The average relative dynamic modulus of elasticity for the three specimens from each batch is plotted versus the number of freeze-thaw cycles in Figure 4.11 for the mixtures containing fly ash and RMA. Table 4.5 shows the relative dynamic moduli of elasticity for these mixtures and the number of freeze-thaw cycles completed. Based on the results, the mixtures containing Class F fly ash, RMA, and Class C fly ash with RMA passed the test – all maintaining at least 98 percent of their initial dynamic modulus of elasticity. One mixture containing Class C fly ash (20% FA-C) and no RMA failed the test, dropping below a relative dynamic modulus of 95 percent after 164 freeze-thaw cycles. After the 300 cycles the relative dynamic modulus had dropped to 91.6 of its initial dynamic modulus of elasticity. The freeze-thaw test results in Figure 4.11 and Table 4.5 show that the mixtures containing Class F fly ash, RMA, and Class C fly ash with RMA had acceptable durability at 300 cycles, with the exception of mixture 20% FA-C. The reason for the poor performance of mixture 20% FA-C is described in Section 4.3.5 and does not appear to be related to the use of Class C fly ash, indicate that the use of fly ash or RMA in concrete had no noticeable effect on freeze-thaw durability. This finding is compatible with the study by Naik et al. (1994), which stated that a high volume, specifically at 40 percent, replacement of cement with Class F or Class C fly ash does not reduce freeze-thaw durability. The use of fly ash in conjunction with the RMA also had no effect on the freeze-thaw durability at the dosages of fly ash and RMA evaluated in this study.

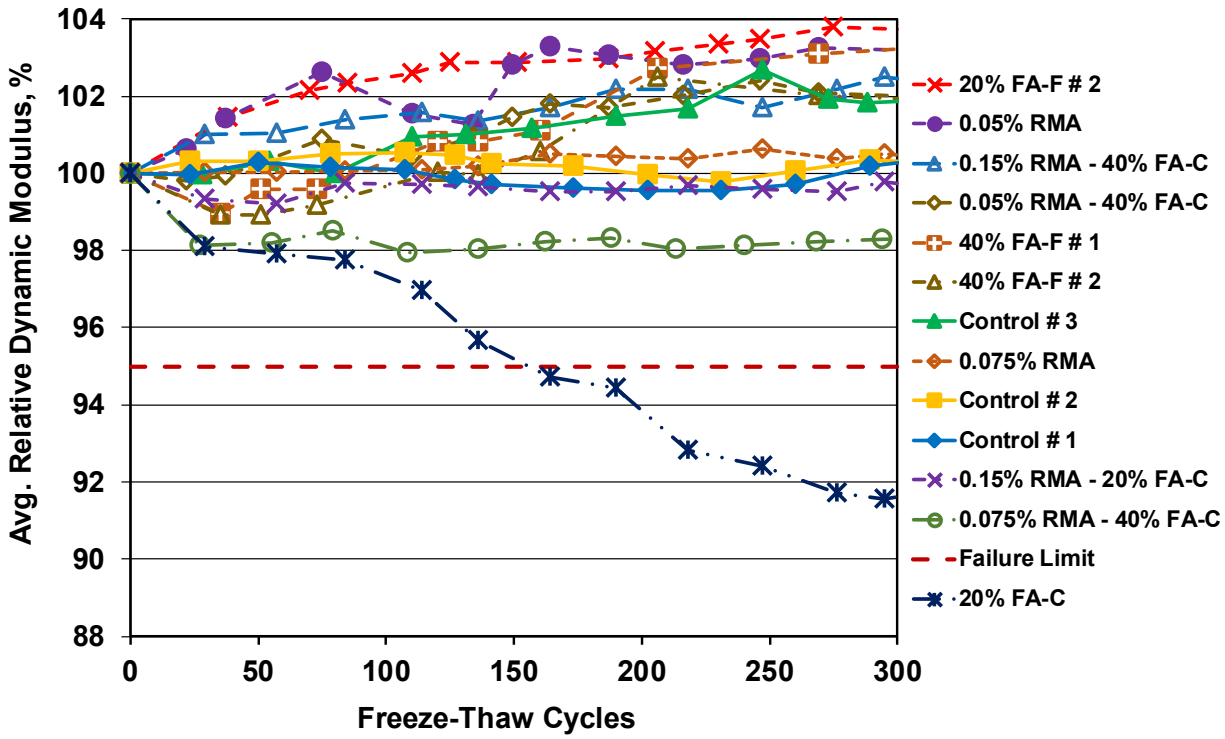

Figure 4.11 – Average relative dynamic modulus of elasticity versus freeze-thaw cycles for the Control, Class F and Class C fly ash, RMA, and Class C fly ash with RMA mixtures of Program 2.

4.3.3 Scaling Resistance

Fourteen mixtures, four of which were duplicated, were evaluated for scaling resistance to determine the effects of the type and dosage of fly ash and RMA. These mixtures included three Control mixtures with no fly ash or RMA. Four mixtures contained a 20 or 40 percent volume replacement of cement with Class F fly ash; one mixture contained a 20 percent volume replacement of cement with Class C fly ash. Two mixtures contained 0.05 or 0.075 percent of RMA by total weight of dry materials. Three mixtures contained a 40 percent volume replacement of cement with Class C fly ash in conjunction with 0.05, 0.075, or 0.15 percent of RMA by total weight of dry materials. One mixture contained a 20 percent volume replacement of cement with Class C fly ash in conjunction with 0.15 percent of RMA by total weight of dry materials. Three specimens from each batch were tested in accordance with Canadian Test BNQ NQ 2621-900. The results of this test are summarized in Table D.5 in Appendix D.

Table 4.5 – Average relative dynamic modulus versus freeze-thaw cycles for the Control, Class F, and Class C fly ash, RMA, and Class C fly ash with RMA mixtures of Program 2

Mixture	Average Relative Dynamic Modulus, %*	Freeze-Thaw Cycles Completed
Control # 1	100.3	300
Control # 2	100.3	300
Control # 3	101.9	300
20% FA-F # 1	†	†
20% FA-F # 2	103.7	300
40% FA-F # 1	103.2	300
40% FA-F # 2	101.9	300
20% FA-C	091.6[$]	300
0.05% RMA	103.2	300
0.075% RMA	100.5	300
0.05%RMA - 40% FA-C	102.0	300
0.075% RMA - 40% FA-C	098.3	300
0.15% RMA - 40% FA-C	102.4	300
0.15% RMA - 20% FA-C	099.7	300

[#]*Relative Dynamic Modulus* is the percentage (*P*) of the average dynamic modulus remaining at *N* cycles. *N* is the smallest of either the number of cycles at which *P* reached 60 percent of initial dynamic modulus or 300 cycles

†Mixture not tested

[$] Mixture exhibited relative dynamic modulus lower than of 95 percent at 300 cycles.

The average cumulative mass loss for the three specimens from each batch is plotted as a function of freeze-thaw cycles in Figure 4.12 for the Control, Class F and Class C fly ash, RMA, and Class C fly ash with RMA mixtures. The dashed line in the figure represents the mass loss limit of 0.2 lb/ft^2 (977 g/m^2). The mixtures are listed in the legends of the figure in order by descending cumulative mass loss at 56 freeze-thaw cycles. Table 4.6 presents the average cumulative mass loss of the mixtures at 7, 21, 35, and 56 cycles. As shown in the figures and the table, the mixture containing the 20 percent volume replacement with cement by Class F fly ash (20% FA-F #1) exhibited the greatest mass loss; the test was terminated at 21 freeze-thaw cycles. This mass loss in all likelihood occurred due to the low air content (2.75%) of this mixture, which is insufficient to protect the concrete from freezing cycles based on the previous studies (ACI Committee 201, Kansas Department of Transportation 2014). This mixture was not subjected to freeze-thaw testing. Two mixtures containing Class C fly ash in conjunction with RMA (0.15% RMA - 40% FA-C and 0.075% RMA - 40% FA-C) exceeded the specified failure limit for mass

loss after 21 cycles. Two other mixtures (0.075% RMA and 0.05% RMA - 40% FA-C) exceeded the failure limit for mass loss after 35 cycles. One mixture (0.15% RMA - 20% FA-C) exceeded the failure limit for mass loss at 56 cycles. The high mass loss may have occurred due to the combined effects of fly ash and RMA on cement hydration. All five mixtures that exhibited mass loss above the failure limit had a compressive strength of 4000 psi (27.6 MPa) or less (Table E.1 in Appendix E). Low strength can contribute to reduced scaling resistance of concrete. These five mixtures, however, performed well in freeze-thaw durability test. The Control mixtures, mixtures containing a 20 or 40 percent volume replacement of cement with Class F or Class C fly ash without an RMA, and the mixture containing 0.05 percent of RMA without fly ash exhibited mass losses below the failure limit. The results indicate that fly ash by itself or the RMA by itself does not lower scaling resistance. All but one of these mixtures had a relative dynamic modulus greater than 95 percent at 300 cycles; the relative dynamic modulus of 20% FA-C decreased to below 95 percent at 164 cycles.

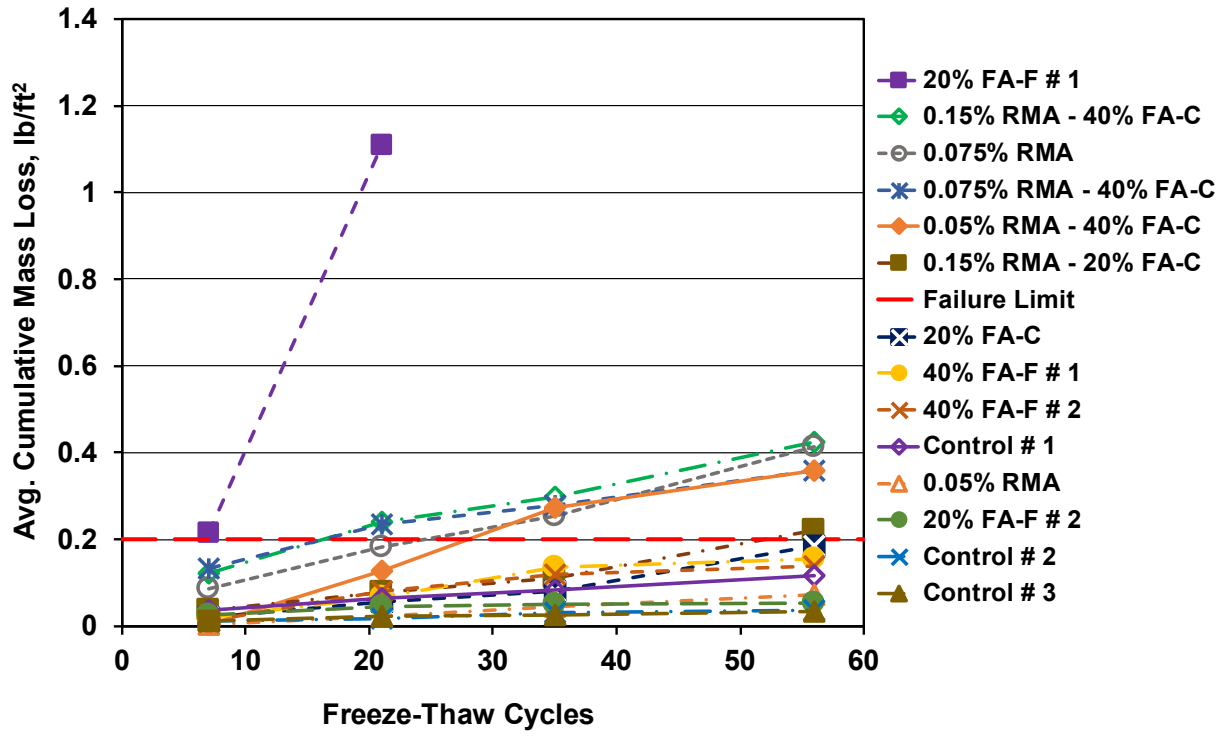

Figure 4.12 – Average cumulative mass loss versus freeze-thaw cycles for the Control, Class F and C fly ash, RMA, and Class C fly ash with RMA mixtures of Program 2.

Table 4.6 – Summary of the average cumulative mass loss at different freeze-thaw cycles for the Control, Class F and C fly ash, RMA, and Class C fly ash with RMA mixtures of Program 2

Mixture	Average Cumulative Mass Loss, lb/ft^2			
	7 cycles	21 cycles	35 cycles	56 cycles
Control # 1	0.036	0.063	0.083	0.117
Control # 2	0.013	0.017	0.032	0.036
Control # 3	0.012	0.022	0.025	0.032
20% FA-F # 1	0.214[#]	1.110[#]	----	----
20% FA-F # 2	0.026	0.044	0.045	0.053
40% FA-F #1	0.021	0.066	0.135	0.154
40% FA-F #2	0.012	0.081	0.118	0.137
20% FA-C	0.020	0.055	0.082	0.186
0.05% RMA	0.004	0.023	0.046	0.071
0.075% RMA	0.086	0.183	0.253[#]	0.412[#]
0.05% RMA - 40% FA-C	0.002	0.126	0.273[#]	0.357[#]
0.075% RMA - 40% FA-C	0.132	0.235[#]	0.279[#]	0.357[#]
0.15% RMA - 40% FA-C	0.122	0.240[#]	0.298[#]	0.424[#]
0.15% RMA - 20% FA-C	0.036	0.077	0.111	0.221[#]

[#]Mixture with cumulative mass loss exceeded the failure limit of 0.2 lb/ft^2 (977 g/m^2),
10^{-3} lb/ft^2 = 4.884 g/m^2

4.3.4 Hardened Concrete Air-Void Analysis

This program evaluated the effect of the dosage and type of fly ash and a rheology-modifying admixture (RMA) on the air-void characteristics. The program included fourteen mixtures, four of which were duplicated. Three Control mixtures contained no fly ash or RMA, four contained a 20 or 40 percent volume replacement of cement with Class F fly ash; one mixture contained a 20 percent volume replacement of cement with Class C fly ash. Two mixtures contained 0.05 or 0.075 percent of RMA by total weight of dry materials. Three mixtures contained a 40 percent volume replacement of cement with Class C fly ash in conjunction with 0.05, 0.075, or 0.15 percent of RMA by total weight of dry materials. One mixture contained a 20 percent volume replacement of cement with Class C fly ash in conjunction with 0.15 percent of RMA by total weight of dry materials. The results of the hardened air-void analysis for the mixtures of Program 2 are summarized in Tables E.13 to E.23 in Appendix E.

Figure 4.13 compares the air contents in plastic and hardened concrete for the Control, Class F and Class C fly ash, RMA, and Class C fly ash with RMA mixtures. The numbers on the bars indicate the reduction in air content between the plastic and hardened concrete. All mixtures

exhibited lower air content in the hardened concrete than in the plastic concrete. This reduction increased slightly for mixtures containing Class F or Class C fly ash. The reduction may have occurred due to the carbon in the fly ash, which reduces the effectiveness of air-entraining admixtures (AEAs) in plastic concrete (Mindess et al. 2003, Folliard et al. 2009). The mixtures containing the RMA exhibited the greatest decrease in the air content, a reduction that increased with RMA dosage. This reduction in air content was reduced when Class C fly ash was used in conjunction with RMA. As shown in Figure 4.13, the decline in the air content increased from 0.3 to 1.5 percent as the volume replacement of cement with fly ash increased from 20 to 40 percent. The decline in the air content increased from 2.4 to 2.9 percent as the dosage of RMA increased from 0.05 to 0.075 percent by total weight of dry materials. While the decline in the air content increased from 0.1 to 0.9 percent as the dosage of RMA increased from 0.05 to 0.15 percent in conjunction with 20 or 40 percent volume replacement of cement with Class C fly ash.

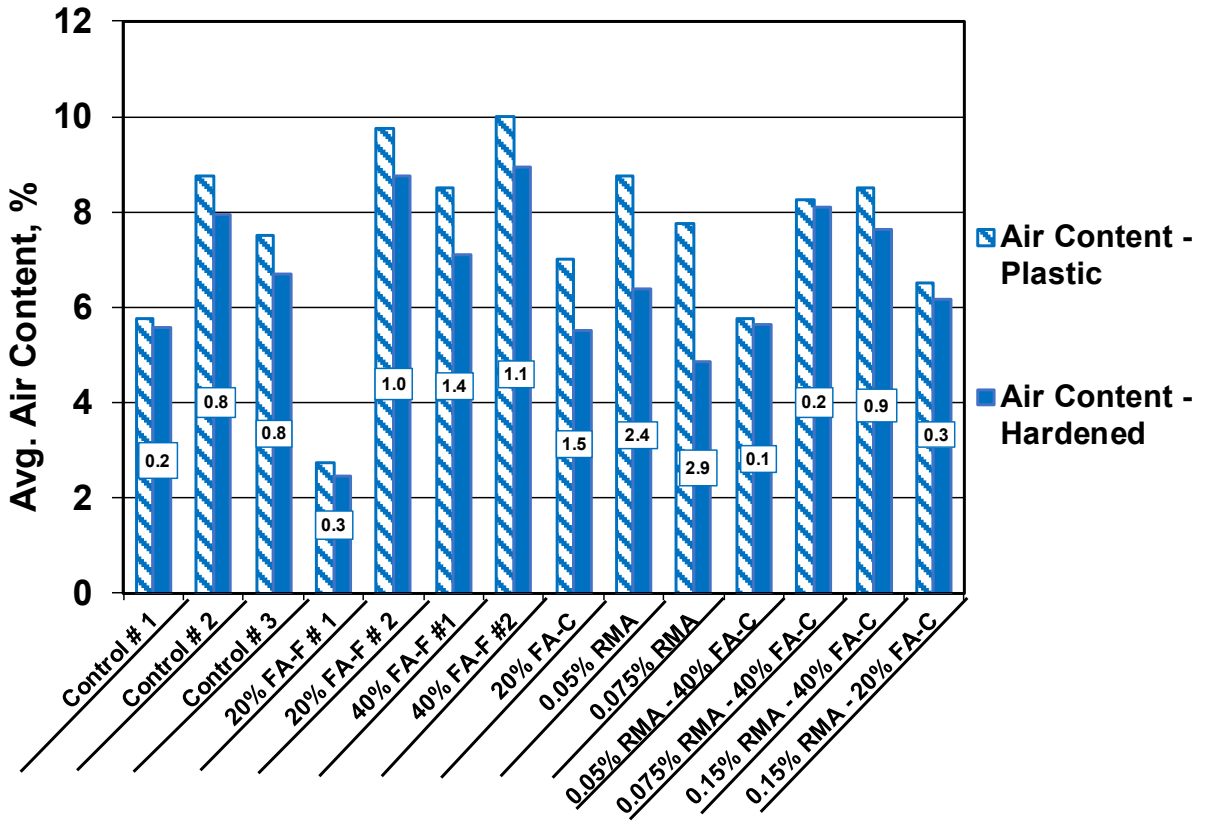

Figure 4.13 – Average air contents in plastic and hardened concrete for the Control, Class F and Class C fly ash, RMA, and Class C fly ash with RMA mixtures of Program 2

A summary of the air-void parameters, including air content in the plastic and hardened concrete, air-void spacing factor, and specific surface for the Control, Class F and Class C fly ash, RMA, and Class C fly ash with RMA mixtures is presented in Table 4.7. As shown in the table, the average air-void spacing factor ranged from 0.0039 to 0.011 in. (0.1 to 0.28 mm), and the average specific surface ranged from 569 to 784 $in.^{-1}$ (22.8 to 31.4 mm^{-1}). The mixture 20% FA-F #1 had the lowest air content (2.45%) in hardened concrete, the highest spacing factor [0.011 in. (0.28 mm)], and the lowest specific surface [569 $in.^{-1}$ (22.8 mm^{-1})]. The mixtures containing RMA that exhibited the greatest reduction in air content between the plastic and hardened concrete still had an air-void spacing factor lower than the recommended 0.008 in. (0.2 mm). This observation indicates that, as it did for the highest dosage (2 %) of SRA-2 mixtures described in Section 4.2.4, the reduction in air content occurred due to the loss of large air voids and would have little effect on freeze-thaw durability of concrete. These two mixtures passed the freeze-thaw test.

Table 4.7 – Average air content, air-void spacing factor, and specific surface for the Control, Class F and C fly ash, RMA, and Class C fly ash with RMA mixtures of Program 2

Mixture	Average Air Content, %			Average Air-Void Spacing Factor in. (mm)	Average Specific Surface ($in.^{-1}$) (mm^{-1})
	Plastic, %	Hardened, %	Difference, %†		
Control # 1	5.75	5.56	-0.19	0.0056 (0.14)	711 (28.4)
Control # 2	8.75	7.93	-0.82	0.0039 (0.10)	768 (30.7)
Control # 3	7.50	6.71	-0.79	0.0052 (0.13)	695 (27.8)
20%FA-F # 1	2.75	2.45	-0.30	0.0109 (0.28)	569 (22.8)
20%FA-F # 2	9.75	8.77	-0.98	0.0042 (0.10)	657 (26.3)
40% FA-F # 1	8.50	7.11	-1.39	0.0053 (0.13)	635 (25.4)
40% FA-F # 1	10.00	8.94	-1.06	0.0042 (0.11)	644 (25.8)
20%FA-C	7.00	5.51	-1.49	0.0071 (0.18)	602 (24.1)
0.05% RMA	8.75	6.40	-2.35	0.0053 (0.13)	719 (28.8)
0.075% RMA	7.75	4.86	-2.89	0.0066 (0.17)	701 (28.0)
0.05% RMA - 40% FA-C	5.75	5.63	-0.12	0.0055 (0.14)	768 (30.7)
0.075% RMA - 40% FA-C	8.25	8.10	-0.15	0.0040 (0.10)	735 (29.4)
0.15% RMA - 40% FA-C	8.50	7.62	-0.88	0.0043 (0.11)	737 (29.5)
0.15% RMA - 20% FA-C	6.50	6.16	-0.34	0.0049 (0.12)	784 (31.4)

Note: Air contents in plastic and hardened concrete measured through ASTM C173 and C457, respectively.
† Percentage difference in air content between values measured in plastic and hardened concrete.
Spacing Factor – is the average distance from any point in the paste to the edge of the nearest air void
Specific Surface – The surface area of the air voids divided by the volume of air voids.

4.3.5 Correlation Between Air-Void Characteristics, Compressive Strength, and Concrete Durability

This study evaluated the correlation between air-void characteristics, compressive strength, and the durability of concrete based on freeze-thaw and scaling resistance for the concrete containing Class F and Class C fly ash, RMA, and Class C fly ash with RMA. A summary of the average air-void spacing factors, 28-day compressive strength, relative dynamic modulus, and mass loss after 56 freeze-thaw cycles for the mixtures of Program 2 is presented in Table 4.8. The average air-void spacing factors for these mixtures ranged from 0.0039 to 0.011 in. (0.1 to 0.28 mm); and the average 28-day compressive strength ranged from 2890 to 6790 psi (19.9 to 46.8 MPa). Mixture 20% Fly Ash-F # 1 with the highest spacing factor [0.011 in. (0.28 mm)] exhibited the greatest mass loss; this mixture was not subjected to freeze-thaw testing. Mixture 20% Fly Ash-C, with the spacing factor of 0.0071 in. (0.18 mm), had a relative dynamic modulus lower than the failure limit (95 percent), but exhibited a mass loss below the failure limit [0.2 lb/ft^2 (977 g/m^2)] after 56 cycles. The other mixtures had a spacing factor lower than 0.007 in. (0.18 mm) and a relative dynamic modulus greater than the failure limit. Five of these mixtures (0.075% RMA, 0.05% RMA - 40% FA-C, 0.075% RMA - 40% FA-C, 0.15% RMA - 40% FA-C, and 0.15% RMA - 20% FA-C), however, exceeded the failure limit for mass loss after 56 cycles. As pointed out in Section 4.3.4, four of the mixtures contained both Class C fly ash and the RMA, and the combination may have negatively affected the hydration reaction. All five mixtures had a compressive strength below 4000 psi (27.6 MPa).

Table 4.8 – Average air-void spacing factor, 28-day compressive strength, relative dynamic modulus, and average cumulative mass loss at 56 cycles for the Control, Class F and C fly ash, RMA, and Class C fly ash with RMA mixtures of Program 2

Mixture	Average Air-Void Spacing Factor		Average 28-Day Compressive Strength		Average Relative Dynamic Modulus*	Average Cumulative Mass Loss @ 56 cycles (lb/ft^2)
	(in.)	(mm)	(psi)	(MPa)		
Control # 1	0.0056	0.14	6790	46.8	100.4	0.117
Control # 2	0.0039	0.10	5330	36.8	101.9	0.036
Control # 3	0.0052	0.13	4860	33.5	100.3	0.032
20% FA-F # 1	0.0109	0.28	5410	37.3	†	1.110[#]
20% FA-F # 2	0.0042	0.10	3590	24.8	103.8	0.053
40% FA-F # 1	0.0053	0.13	3260	22.5	103.2	0.154
40% FA-F # 2	0.0042	0.11	3450	23.8	102.0	0.137
20% FA-C	0.0071	0.18	4720	32.5	91.8[$]	0.186
0.05% RMA	0.0053	0.13	4040	27.9	103.2	0.071
0.075% RMA	0.0066	0.17	3480	24.0	100.4	0.412[#]
0.05% RMA - 40% FA-C	0.0055	0.14	3920	27.0	102.0	0.357[#]
0.075% RMA - 40% FA-C	0.0040	0.10	3250	22.4	98.3	0.357[#]
0.15% RMA - 40% FA-C	0.0043	0.11	2890	19.9	102.3	0.424[#]
0.15% RMA - 20% FA-C	0.0049	0.12	2940	20.3	99.6	0.221[#]

[#]*Relative Dynamic Modulus* is the percentage (*P*) of the average dynamic modulus remaining at *N* cycles.
N is the smallest of either the number of cycles at which *P* reached 60 percent of initial dynamic modulus or 300 cycles
†Mixture not subjected to testing
[$] Mixture exhibited relative dynamic modulus lower than failure limit of 95 percent at 300 cycles.
[#] Mixture with cumulative mass loss exceeded the failure limit of 0.2 lb/ft^2 (977 g/m^2),
10^{-3} lb/ft^2 = 4.884 g/m^2

Figure 4.14 shows the relative dynamic modulus in the freeze-thaw test as a function of average air-void spacing factor. The dashed line in the figure represents a relative dynamic modulus of 95 percent. Twelve of the thirteen mixtures had a relative dynamic modulus greater than 95 percent; these mixtures had an air-void spacing factor less than 0.007 in. (0.18 mm). The only mixture (20% Fly Ash-C) that had a relative dynamic modulus below 95 percent had an air-void spacing factor of 0.0071 in. (0.18 mm), which is still less than the critical limit, 0.008 in. (0.2 mm) for adequate freeze-thaw durability based on previous studies (Mindess et al. 2003, Russell 2004). Figure 4.15 shows the relative dynamic modulus in the freeze-thaw test as a function of the 28-day compressive strength for the mixtures of Program 2. Twelve of the 13 mixtures had a relative dynamic modulus greater than the failure limit, eight of the 12 had a compressive strength below 4000 psi (27.6 MPa). One mixture had a relative dynamic modulus below the failure limit;

this mixture had a compressive strength greater than 4000 psi (27.6 MPa). The results indicate that the air-void spacing factor, but not compressive strength, affects the freeze-thaw durability of concrete containing fly ash, RMA, or fly ash with RMA.

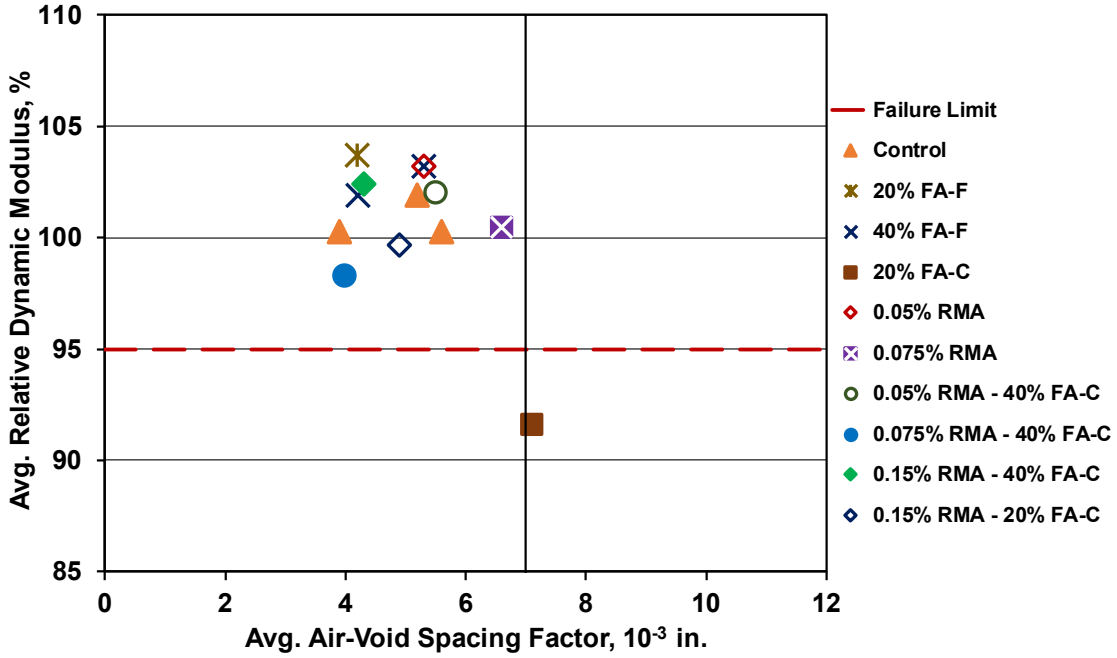

Figure 4.14 – Average relative dynamic modulus versus average air-void spacing factor for the mixtures of Program 2

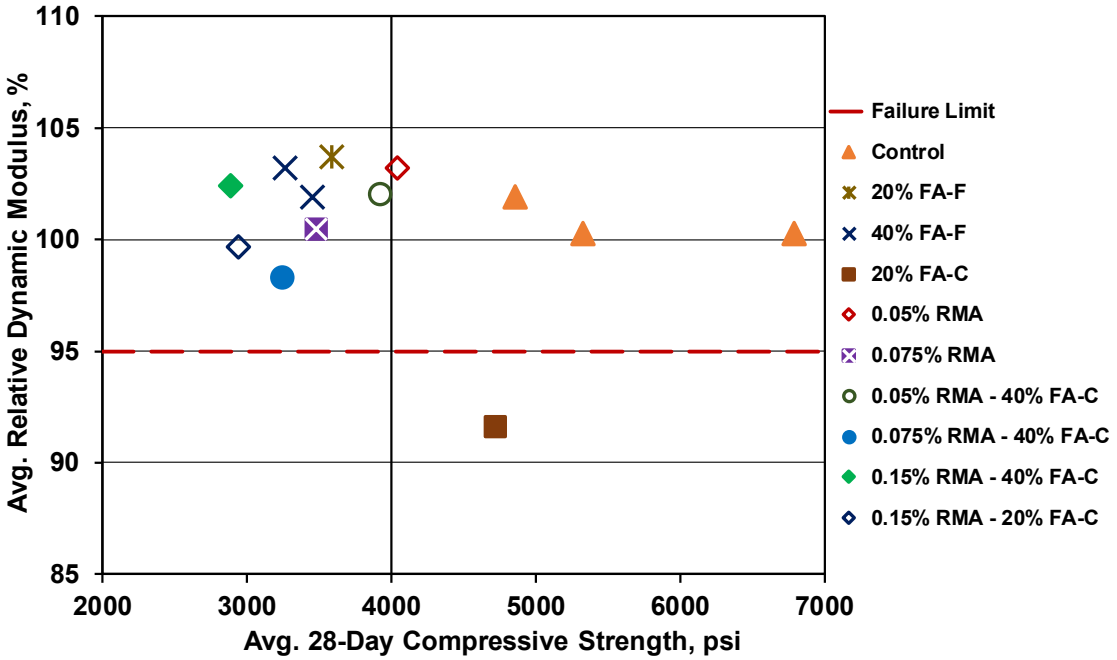

Figure 4.15 – Average relative dynamic modulus versus average 28-day compressive strength for the mixtures of Program 2

Figure 4.16 shows the average cumulative mass loss after 56 freeze-thaw cycles with the average air-void spacing factor. The dashed line in the figure represents the mass loss limit of 0.2 lb/ft^2 (977 g/m^2). Twelve of the fourteen mixtures had spacing factors less than 0.007 in. (0.18 mm). Seven of the twelve exhibited mass loss below the failure limit, while the other five mixtures exceeded the failure limit. As discussed earlier, these five mixtures included four containing Class C fly ash in conjunction with RMA and one mixture containing 0.075 percent of RMA. These five mixtures had an average compressive strength below 4000 psi (27.6 MPa), as shown in Figure 4.17. This finding indicates that the mass loss of these mixtures may have occurred due to a combination of low compressive strength and hydration products with poor resistance to scaling. The argument in favor of the effect of the combined of materials on the hydration products is strengthen by the observation that three other low-strength mixtures contained fly ash (Class C) and no RMA. The mixture 20% Fly Ash-F #1 that had the lowest air content (2.75 percent) and the highest spacing factor [10.9 in. (0.28 mm)] exhibited the greatest mass loss.

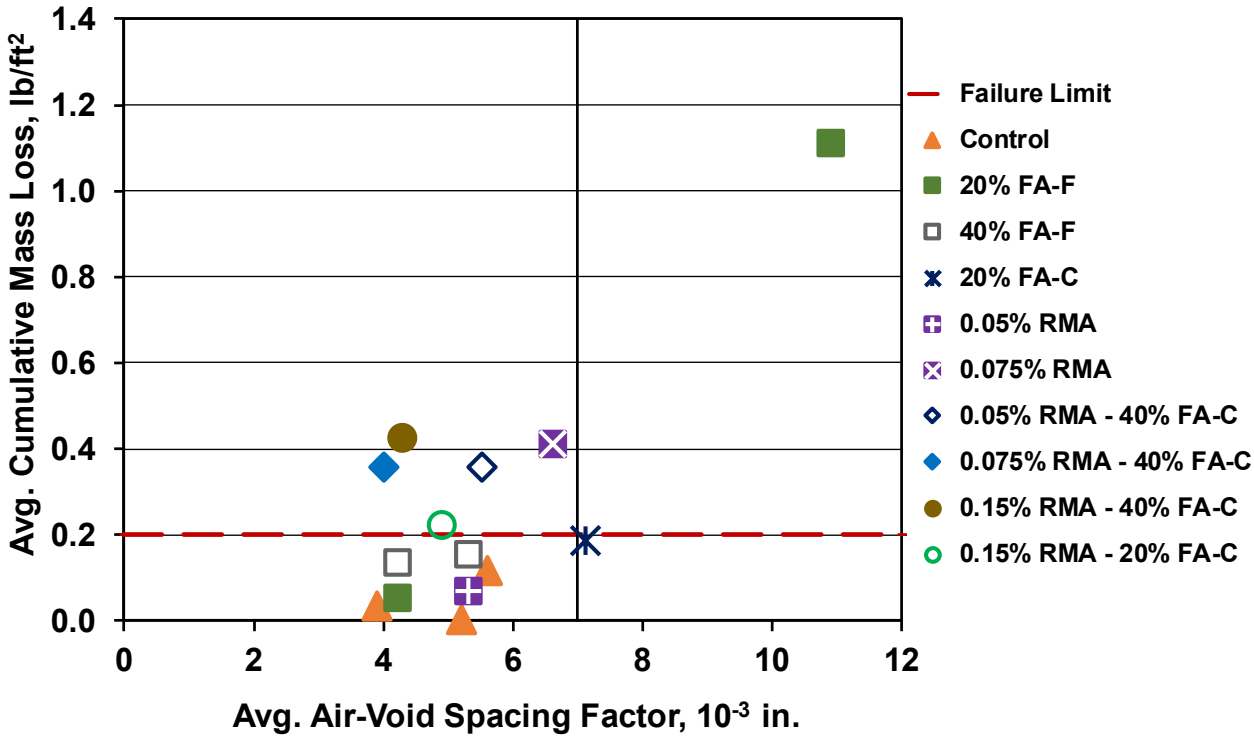

Figure 4.16 – Average cumulative mass loss at 56 freeze-thaw cycles versus air-void spacing factors for the mixtures of Program 2

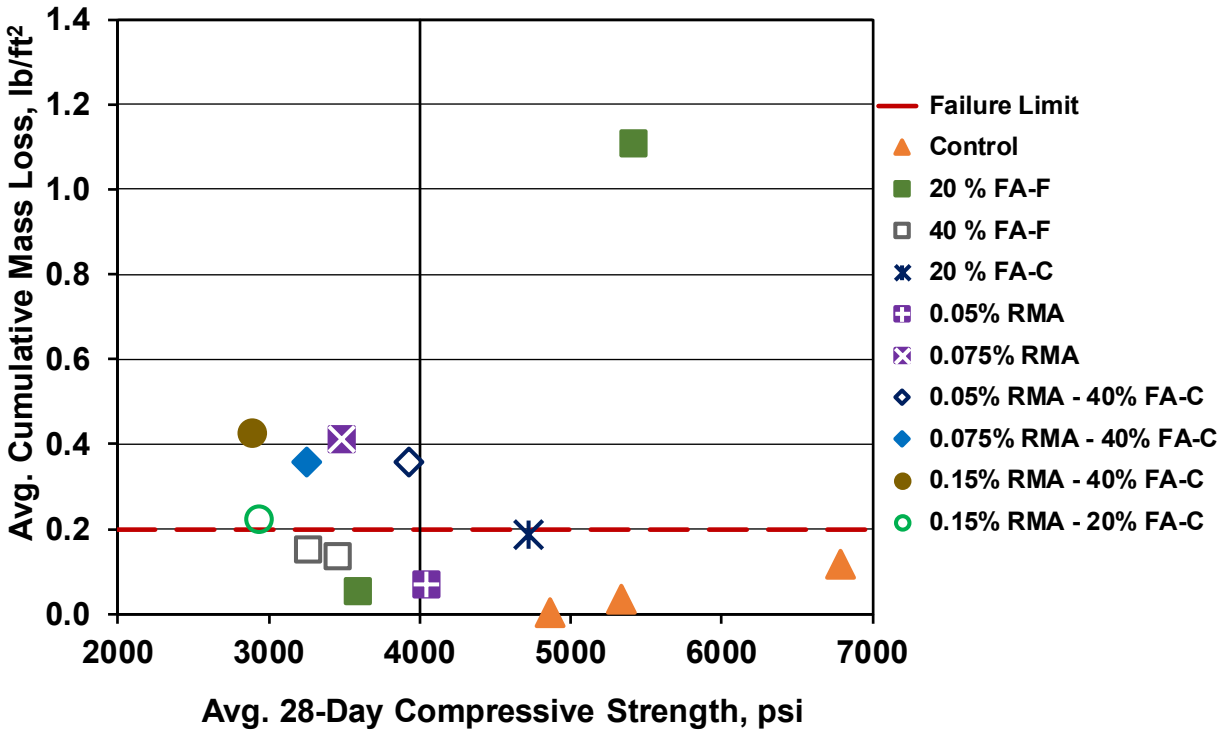

Figure 4.17 – Average cumulative mass loss at 56 freeze-thaw cycles versus average 28-day compressive strength for the mixtures of Program 2

4.3.6 Program 2 Summary

The results of Program 2 indicate that all mixtures containing Class F fly ash, RMA, or Class C fly ash with RMA passed the freeze-thaw test, maintaining at least 98 percent of their initial dynamic modulus of elasticity. One mixture containing Class C fly ash (20% FA-C) failed, dropping below 95 percent of its initial dynamic modulus after 164 freeze-thaw cycles and maintaining only 91.8 percent of its initial dynamic modulus after 300 cycles. One mixture (20% FA-F #1) that had low air content (2.75%) exhibited the greatest mass loss; this mixture was not subjected to the freeze-thaw test. One mixture containing RMA and four mixtures containing Class C fly ash in conjunction with RMA exhibited a mass loss exceeded the failure limit. All mixtures exhibited lower air contents in the hardened concrete than in the plastic concrete; this reduction increased slightly when Class F or Class C fly ash used. The mixtures containing RMA exhibited the greatest decrease in air content, a reduction that increased with the RMA dosage; this reduction, however, decreased when Class C fly ash was used in conjunction with the RMA. All mixtures that had an average air-void spacing factor less than 0.007 in. (0.18 mm) passed the freeze-thaw

test; and the only mixture that had the average air-void spacing factor greater than 0.007 in. (0.18 mm) failed in the freeze-thaw test. Two of the 14 mixtures had spacing factors greater than 0.007 in. (0.18 mm); one mixture (20% FA-F #1), with 2.75% air content, exhibited the greatest mass loss, but the other mixtures (20% FA-C), with 7% air content, exhibited mass loss below the failure limit. The other twelve mixtures that had spacing factors less than 0.007 in. (0.18 mm), seven of them exhibited mass loss below the failure limit, while the other five mixtures exceeded the failure limit. The latter five mixtures, including four mixtures containing Class C fly ash in conjunction with RMA and one mixture containing 0.075 percent of RMA, had a compressive strength less than 4000 psi (27.6 MPa).

4.4 PROGRAM 3: EVALUATION OF MIXTURES CONTAINING SHRINKAGE COMPENSATING ADMIXTURES

4.4.1 General

Program 3 evaluated the effect of two types of shrinkage compensating admixture (SCA-1 and SCA-2) on freeze-thaw durability, scaling resistance, and air-void characteristics in hardened concrete. The program included nine mixtures. Three mixtures containing no SCA are denoted as Control. Five mixtures containing 2.5, 5, or 7.5 percent of SCA-1 by weight of cement are denoted as 2.5% SCA-1, 5% SCA-1, and 7.5% SCA-1, respectively. One mixture containing 6 percent, the maximum recommended dosage, of SCA-2 by weight of cement is denoted as 6% SCA-2. The measured air content in plastic concrete for these mixtures ranged from 4.75 to 9 percent. As discussed in Section 2.2.6, SCA-1 contains a shrinkage-reducing admixture (SRA) that reduces the surface tension of pore water, potentially causing a reduction in the stability of the air-void system. The results of the evaluations are presented in the following sections.

4.4.2 Freeze-Thaw Durability

In this program, nine mixtures, four of which were duplicated, were subjected to freeze-thaw testing to determine the effect of the type and dosage of SCA on freeze-thaw durability. These mixtures included three Control mixtures with no SCA, five containing 2.5, 5, or 7.5 percent of SCA-1 by weight of cement, and one containing 6 percent of SCA-2 by weight of cement. Three

specimens from each batch were tested in accordance with ASTM C666-Procedure B. The results of this test are summarized in Table D.3 in Appendix-D.

The average relative dynamic modulus of elasticity for the three specimens from each batch is plotted as a function of the number of freeze-thaw cycles in Figure 4.18 for the mixtures containing SCA-1 and SCA-2. The dashed line in the figures represents a relative dynamic modulus of 95 percent, the acceptable lower limit for a durable concrete in this test. The mixtures are listed in the legends of the figures in order of descending relative dynamic modulus at 300 cycles. Table 4.9 shows the relative dynamic modulus for these mixtures and the number of freeze-thaw cycles completed. Based on the results, two mixtures containing SCA-1 with dosages of 2.5 and 7.5 percent by weight of cement, and one mixture containing the SCA-2 with a dosage of 6 percent by weight of cement passed the freeze-thaw test, maintaining at least 98 percent of their initial dynamic modulus of elasticity. These three mixtures had air contents between 8.5 to 9 percent. Three mixtures containing SCA-1 with dosages of 2.5, 5, and 7.5 percent by weight of cement failed the freeze-thaw test, dropping below 95 percent their initial dynamic modulus of elasticity after 197, 263, and 40 freeze-thaw cycles, respectively. One of these mixtures (2.5% SCA-1 #2) had an air content of 7.5 percent, while other two mixtures (5% SCA-1 and 7.5% SCA-1 # 1) had air contents of 4.75 and 5 percent, respectively – air contents that are insufficient to protect the concrete from freezing cycles (Kansas Department of Transportation 2014). The three mixtures that failed the test contained the lowest dosage of AEA for the mixtures containing SCA, as shown in Table A.17 in Appendix A.

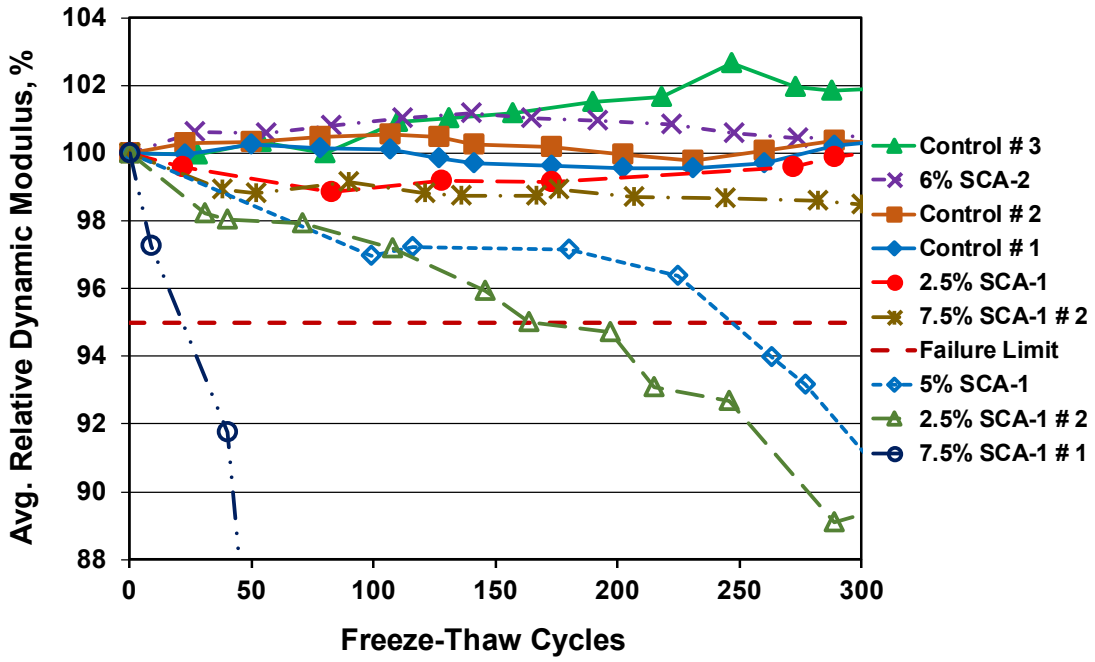

Figure 4.18 – Average relative dynamic modulus of elasticity versus freeze-thaw cycles for the Control, SCA-1, and SCA-2 mixtures of Program 3

Table 4.9 – Average relative dynamic modulus versus freeze-thaw cycles for the Control, SCA-1, and SCA-2 mixtures of Program 3

Mixture	Average Relative Dynamic Modulus, %*	Freeze-Thaw Cycles Completed
Control # 1	100.3	300
Control # 2	100.3	300
Control # 3	101.9	300
2.5% SCA-1 # 1	100.0	300
2.5% SCA-1 # 2	89.3$	300
5% SCA-1	91.2$	300
7.5% SCA-1 # 1	16.4$	133
7.5% SCA-1 # 2	98.5	300
6% SCA-2	100.5	300

**Relative Dynamic Modulus* is the percentage (*P*) of the average dynamic modulus remaining at *N* cycles. *N* is the smallest of either the number of cycles at which *P* reached 60 percent of initial dynamic modulus or 300 cycles.

$ Mixture exhibited relative dynamic modulus lower than of 95 percent at 300 cycles.

4.4.3 Scaling Resistance

The evaluation of scaling resistance in Program 3 included nine mixtures, four of which were duplicated, to determine the effects of the type and dosage of SCA-1 and SCA-2. These mixtures included three Control mixtures with no SCA, five mixtures containing 2.5, 5, and 7.5 percent of SCA-1 by weight of cement, and one mixture containing 6 percent of SCA-2 by weight of cement. Three specimens from each batch were evaluated for scaling resistance in accordance with Canadian Test BNQNQ2621-900 Annex B. The results of the scaling resistance test for the mixtures of this program are presented in Table D.6 in Appendix D.

The average cumulative mass loss for the three specimens from each batch is plotted as a function of freeze-thaw cycles in Figure 4.19 for the mixtures containing SCA-1 and SCA-2. The dashed line in the figure represents the mass loss limit of 0.2 lb/ft^2 (977 g/m^2). The mixtures are listed in the legend of the figure in order of descending cumulative mass loss at 56 freeze-thaw cycles. Table 4.10 summarizes the average cumulative mass losses of the Control, SCA-1, and SCA-2 mixtures at 7, 21, 35, and 56 cycles. The figure shows that all mixtures of this program, except one, exhibited a cumulative mass loss below the failure limit of 0.2 lb/ft^2 (977 g/m^2) after 56 cycles. One of the two mixtures containing 7.5 percent SCA-1 by weight of cement exhibited mass loss exceeded the failure limit after 21 cycles. This mixture had an air content of just 5% compared to 9% in the other mixture. This mixture, with 5% air, contained the highest dosage (7.5%) of SCA-1, which contains SRA that may reduce the stability of the air-void system, resulting in a reduction in scaling resistance. This mixture also failed the freeze-thaw test after 40 cycles, by maintaining only 16.4 percent of its initial dynamic modulus of elasticity.

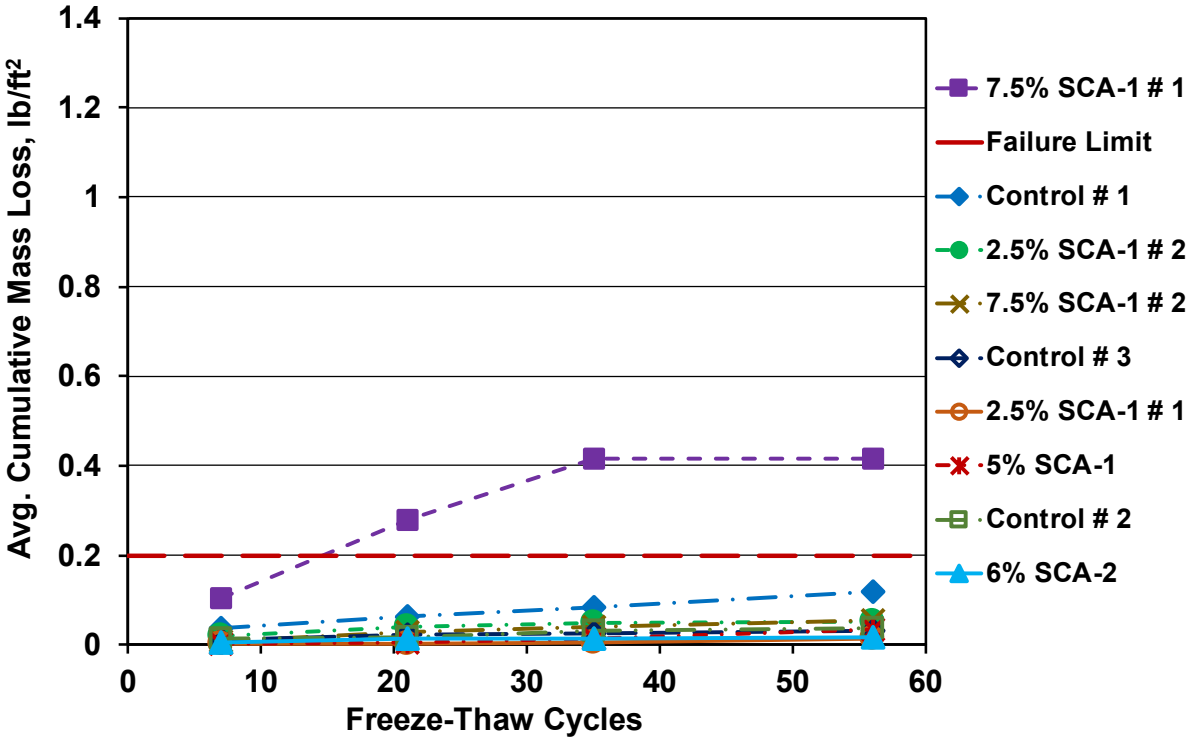

Figure 4.19 – Average cumulative mass loss versus freeze-thaw cycles for the Control, SCA-1, and SCA-2 mixtures of Program 3

Table 4.10 – Summary of average cumulative mass loss at different freeze-thaw cycles for the Control, SCA-1, and SCA-2 mixtures of Program 3

Mixture	Average Cumulative Mass Loss, lb/ft²			
	7 cycles	21 cycles	35 cycles	56 cycles
Control # 1	0.036	0.063	0.083	0.117
Control # 2	0.013	0.017	0.032	0.036
Control # 3	0.012	0.022	0.025	0.032
2.5% SCA-1 # 1	0.002	0.003	0.005	0.015
2.5% SCA-1 # 2	0.021	0.039	0.048	0.052
5% SCA-1	0.004	0.005	0.014	0.034
7.5% SCA-1 # 1	0.105	0.278	0.415	0.415[#]
7.5% SCA-1 # 2	0.008	0.029	0.040	0.054
6% SCA-2	0.004	0.013	0.014	0.016

[#]Mixture with cumulative mass loss exceeded the failure limit of 0.2 lb/ft² (977 g/m²),
10^{-3} lb/ft² = 4.884 g/m²

4.4.4 Hardened Concrete Air-Void Analysis

Hardened concrete air-void analysis was used to evaluate the effect of the dosage of SCA-1 and SCA-2 on the stability of the air-void characteristics. The program included nine mixtures, four of which were duplicated. Three Control mixtures contained no SCA, five mixtures contained 2.5, 5, or 7.5 percent of SCA-1 by weight of cement, and one mixture contained 6 percent of SCA-2 by weight of cement. The results of the hardened air-void analysis for the mixtures in Program 3 are presented in Tables E.24 to E.29 in Appendix E.

The air content in plastic and hardened concrete of the Control, SCA-1, and SCA-2 mixtures are presented in Figure 4.20. The numbers on the bars indicate the reduction in the air content between the plastic and hardened concrete. All mixtures exhibited lower air content in the hardened concrete than in the plastic concrete. The reduction in air content occurred likely, as stated earlier, due to the loss of large air voids or dissolution of small air voids in the water or merging of small air voids to larger voids (Fagerlund 1991). A summary of the air-void parameters, including air content, air-void spacing factor, and specific surface for the Control, SCA-1, and SCA-2 mixtures is reported in Table 4.11. As shown in the table, the average air content in plastic concrete ranged from 4.75 to 9 percent, the average air-void spacing factor ranged from 0.0039 to 0.0096 in. (0.1 to 0.24 mm), and the average specific surface ranged from 495 to 768 $in.^{-1}$ (19.8 to 30.7 mm^{-1}). The two mixtures (7.5% SCA-1 #2 and 6% SCA-2) with the highest air contents (9 and 8 %, respectively,) exhibited slightly greater reductions in air content than the other mixtures in this program. These two mixtures, however, had average air-void spacing factors of 0.0048 and 0.0049 in. (0.12 mm), indicating that the reduction in air content of these two mixtures was likely due to the loss of large air voids, which does not influence freeze-thaw durability. Three mixtures (2.5% SCA-1 # 2, 5% SCA-1, and 7.5% SCA-1 #1) had the highest air-void spacing factors [0.0074, 0.0087, and 0.0096 in. (0.19, 0.22, and 0.24 mm)] and the lowest specific surfaces [539, 565, 495 $in.^{-1}$ (21.6, 22.6, and 19.8 mm^{-1})]. Two of these mixtures had the lowest air contents in plastic concrete, 4.75 and 5 percent, while the third mixture had an air content of 7.5 percent.

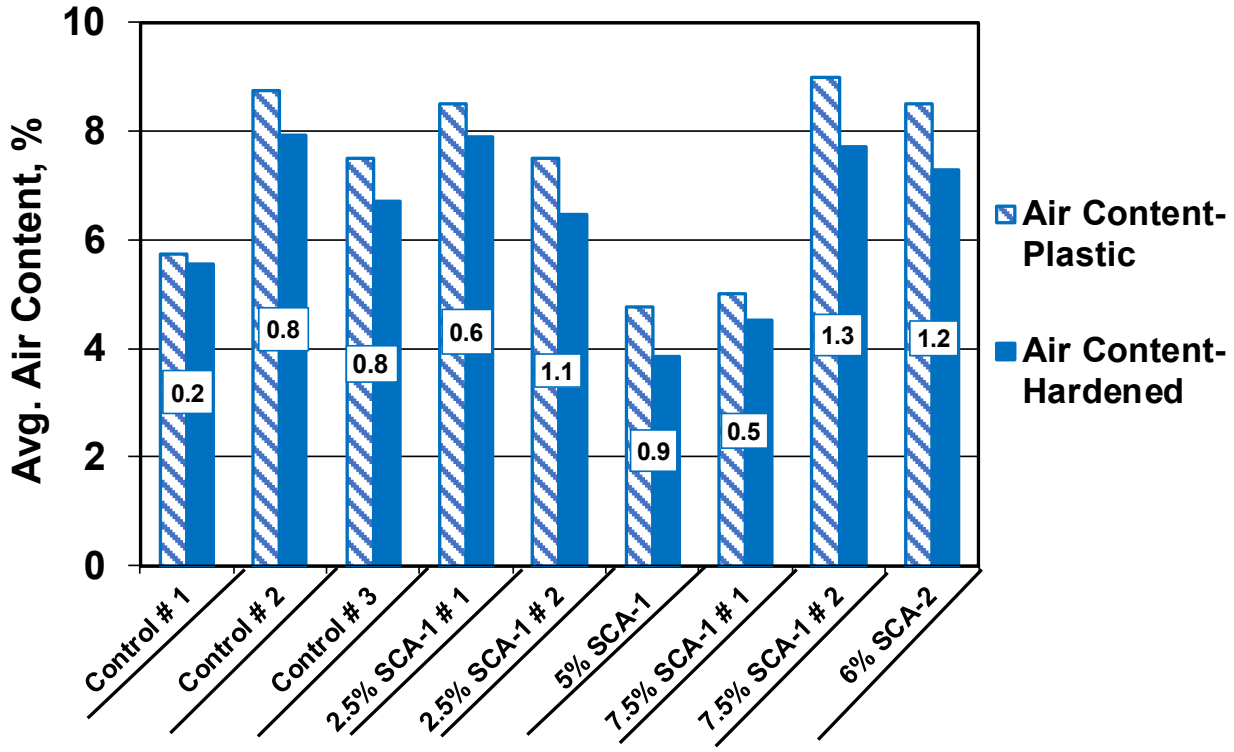

Figure 4.20 – Average air contents in the plastic and hardened concrete for the Control, SCA-1, and SCA-2 mixtures of Program 3

Table 4.11 – Average air content, air-void spacing factor, and specific surface for the Control, SCA-1, and SCA-2 mixtures of Program 3

Mixture	Average Air Content, %			Average Air-Void Spacing Factor (in.) (mm)	Average Specific Surface ($in.^{-1}$) (mm^{-1})
	Plastic, %	Hardened, %	Difference, %†		
Control # 1	5.75	5.66	-0.19	0.0056 (0.14)	711 (28.4)
Control # 2	8.75	7.93	-0.82	0.0039 (0.10)	768 (30.7)
Control # 3	7.50	6.71	-0.79	0.0052 (0.13)	695 (27.8)
2.5% SCA-1 # 1	8.50	7.89	-0.61	0.0047 (0.12)	650 (26.0)
2.5% SCA-1 # 2	7.50	6.45	-1.05	0.0074 (0.19)	539 (21.6)
5% SCA-1	4.75	3.86	-0.89	0.0087 (0.22)	565 (22.6)
7.5% SCA-1 # 1	5.00	4.52	-0.48	0.0096 (0.24)	495 (19.8)
7.5% SCA-1 # 2	9.00	7.72	-1.28	0.0048 (0.12)	644 (25.8)
6% SCA-2	8.50	6.98	-1.52	0.0049 (0.12)	847 (33.9)

Note:
Air contents in plastic and hardened concrete measured through ASTM C173 and C457, respectively.
† Percentage difference in air content between values measured in plastic and hardened concrete.
Spacing Factor – The average distance from any point in the paste to the edge of the nearest air void.
Specific Surface – The surface area of the air voids divided by the volume of air voids.

4.4.5 Correlation Between Air-Void Characteristics, Compressive Strength, and Concrete Durability

In this section, the correlation between air-void characteristics, compressive strength, and the durability of concrete based on freeze-thaw and scaling resistance is evaluated for the concretes containing SCA-1 or SCA-2. A summary of the air-void spacing factors, 28-day compressive strength, relative dynamic moduli, and mass loss after 56 freeze-thaw cycles for the mixtures of Program 3 is presented in Table 4.12. The average air-void spacing factors of these mixtures ranged from 0.0039 to 0.0096 in. (0.1 to 0.24 mm), and the average compressive strengths ranged from 3020 to 6790 psi (20.8 to 46.8 MPa). The mixture with the highest spacing factor [0.0096 in. (0.24 mm)], 7.5% SCA-1 #1, exhibited the lowest freeze-thaw durability and scaling resistance. Two mixtures (2.5% SCA-1 and 5% SCA-1 # 2) with spacing factors of 0.0074 and 0.0087 in. (0.19 and 0.22 mm), respectively, failed in the freeze-thaw durability test but not the scaling resistance test. All other mixtures that had the spacing factors lower than 0.007 in. (0.18 mm) performed well in both the freeze-thaw and scaling tests. The compressive strength of the concrete containing SCA-1 and SCA-2 had no observed effect on freeze-thaw durability and scaling resistance.

Table 4.12 – Average air-void spacing factor, 28-day compressive strength, relative dynamic modulus, and cumulative mass loss at 56 cycles for the Control, SCA-1, and SCA-2 mixtures of Program 3

Mixture	Average Air-Void Spacing Factor		Average 28-Day Compressive Strength		Average Relative Dynamic Modulus*	Average Cumulative Mass Loss @ 56 Cycles (lb/ft^2)
	(in.)	(mm)	(psi)	(MPa)		
Control # 1	0.0056	0.14	6790	46.8	100.4	0.117
Control # 2	0.0039	0.10	5330	36.8	101.9	0.036
Control # 3	0.0052	0.13	4860	33.5	100.3	0.032
2.5% SCA-1 # 1	0.0047	0.12	3700	25.5	100.2	0.015
2.5% SCA-1 # 2	0.0074	0.19	4240	29.2	89.7[$]	0.052
5% SCA-1	0.0087	0.22	5250	36.2	91.8[$]	0.034
7.5% SCA-1 # 1	0.0096	0.24	4950	34.1	16.4[$]	0.415[#]
7.5% SCA-1 # 2	0.0048	0.12	3020	20.8	98.6	0.054
6% SCA-2	0.0049	0.12	4400	30.3	100.5	0.016

*Relative dynamic modulus is the percentage (P) of the initial dynamic modulus remaining at N cycles, N is either the number of cycles at which P reached 60 percent or 300 cycles (whichever is smaller).
[$] Mixture exhibited relative dynamic modulus lower than failure limit of 95 percent at 300 cycles.
[#] Mixture with cumulative mass loss exceeded the failure limit of 0.2 lb/ft^2 (977 g/m^2),
10^{-3} lb/ft^2 = 4.884 g/m^2

Figure 4.21 shows the average relative dynamic modulus in the freeze-thaw test as a function of the average air-void spacing factor for the Control, SCA-1, and SCA-2 mixtures in Program 3. The dashed line in the figure represents a relative dynamic modulus of 95 percent. Six of the nine mixtures had a relative dynamic modulus greater than 95 percent, these mixtures had an average air-void spacing factor less than 0.007 in. (0.18 mm). Three mixtures (2.5% SCA-1, 5% SCA- 1, and 7.5% SCA-1) had a relative dynamic modulus below the failure limit; all of these mixtures had the average air-void spacing factor greater than 0.007 in. (0.18 mm). The mixture with the highest air-void spacing factor exhibited the greatest reduction in freeze-thaw durability. Figure 4.22 shows the relative dynamic modulus in the freeze-thaw test as a function of the average 28-day compressive strength for the mixtures of Program 3. The results show six mixtures had a relative dynamic modulus greater than the failure limit; two of these mixtures had a compressive strength less than 4000 psi (27.6 MPa). Three mixtures had a relative dynamic modulus below the failure limit; these mixtures, however, had a compressive strength greater than 4000 psi (27.6

MPa). The results indicate that the air-void spacing factor, but not compressive strength, influenced freeze-thaw durability of the concrete containing SCA-1 or SCA-2.

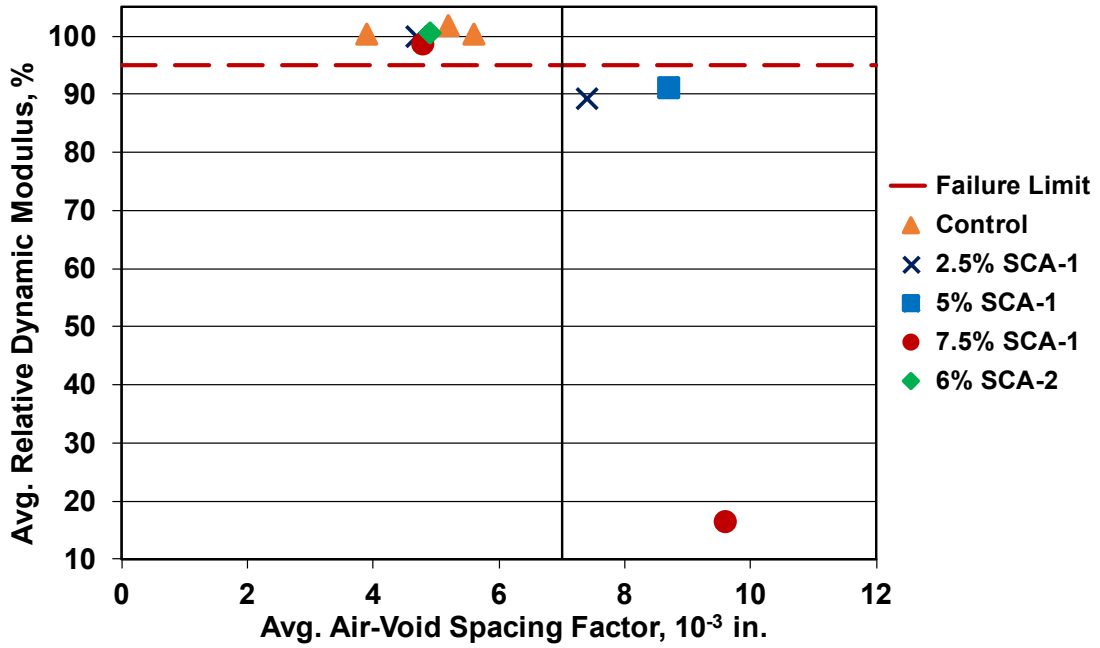

Figure 4.21 – Average relative dynamic modulus versus average air-void spacing factor for the mixtures of Program 3

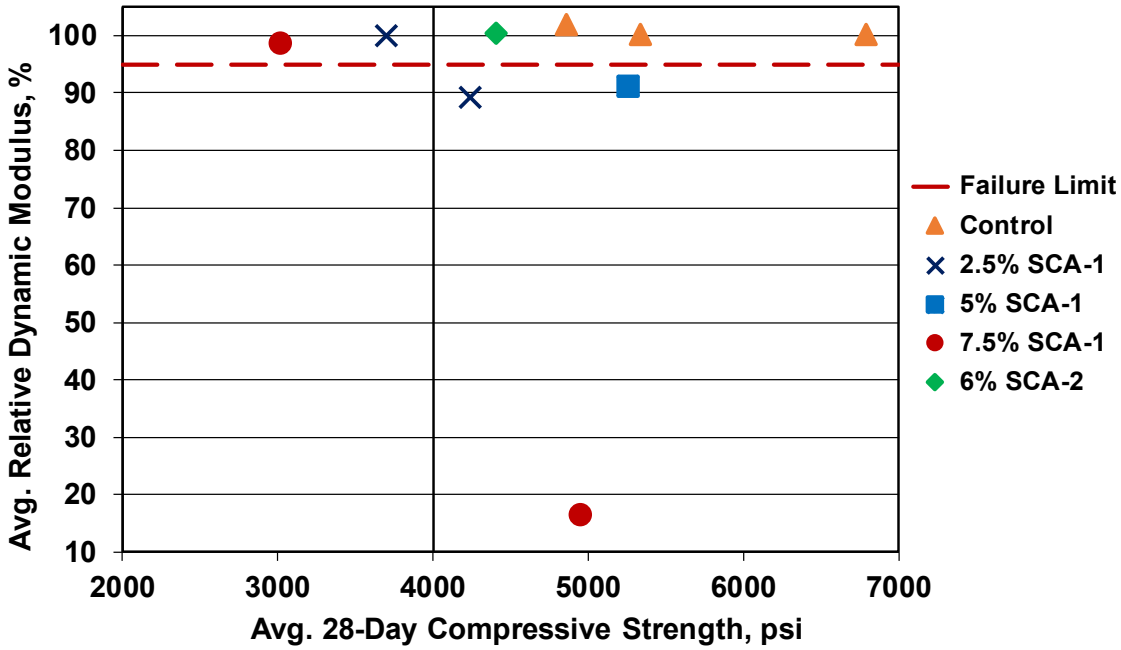

Figure 4.22 – Average relative dynamic modulus versus average 28-day compressive strength for the mixtures of Program 3

Figure 4.23 compares the average cumulative mass loss after 56 freeze-thaw cycles with the average air-void spacing factor for the Control, SCA-1, and SCA-2 mixtures in Program 3. The dashed line in the figure represents a mass loss limit of 0.2 lb/ft^2 (977 g/m^2). Eight of the nine mixtures exhibited mass loss below the failure limit. The only mixture that exceeded the failure limit of mass loss (7.5% SCA-1 # 1) had the highest spacing factor [0.0096 in. (0.24 mm)]. Figure 4.24 shows the average cumulative mass loss after 56 freeze-thaw cycles with the 28-day compressive strength for the Control, SCA-1, and SCA-2 mixtures. The results show that the two mixtures containing SCA-1 that had the compressive strength less than 4000 psi (27.6 MPa) exhibited mass loss below the failure limit. This observation indicates that compressive strength of the concrete containing SCA-1 had no effect on scaling resistance.

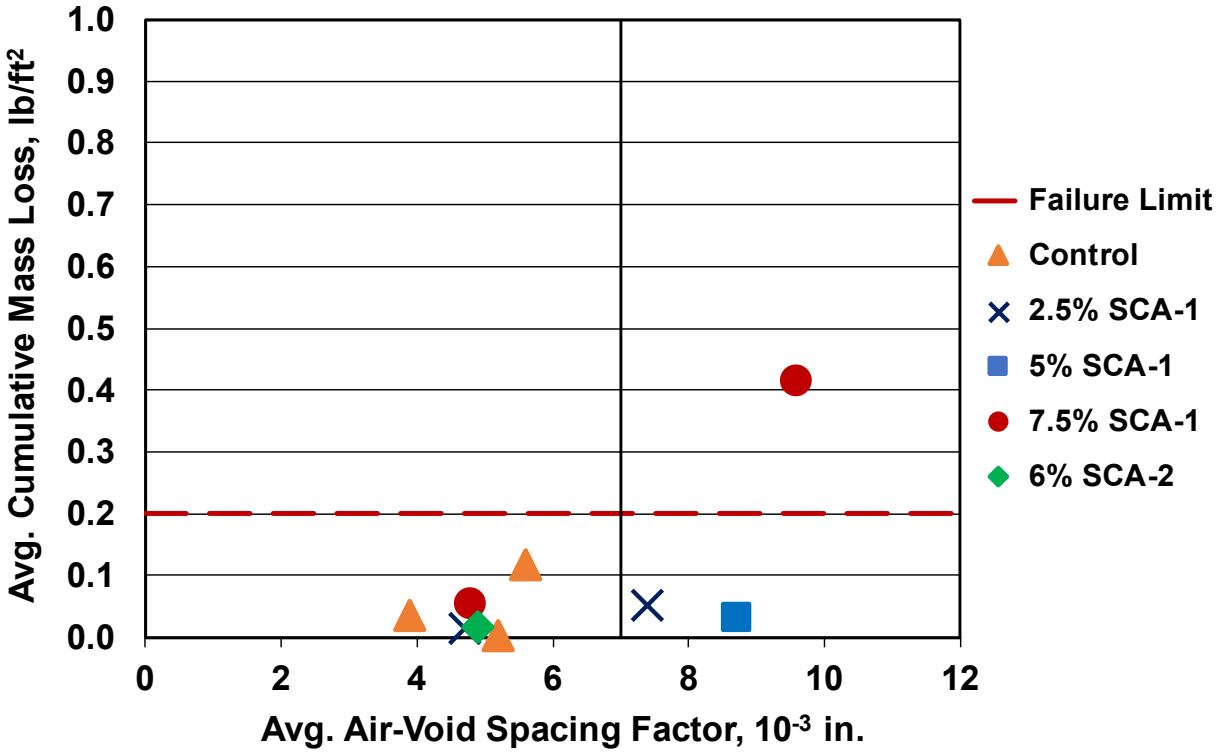

Figure 4.23 – Average cumulative mass loss at 56 freeze-thaw cycles versus the air-void spacing factor for the mixtures of Program 3

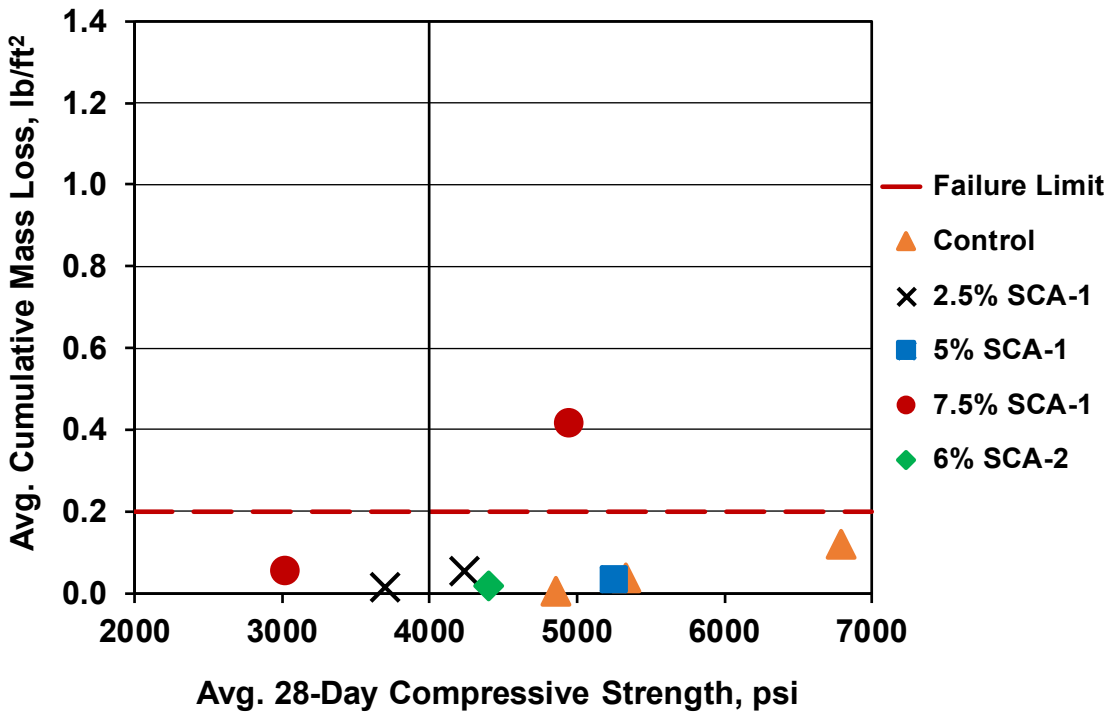

Figure 4.24 – Average cumulative mass loss at 56 freeze-thaw cycles versus average 28-day compressive strength for the mixtures of Program 3

4.4.6 Program 3 Summary

The results of the evaluations in Program 3 indicate that two mixtures containing SCA-1 with dosages of 2.5 and 7.5 percent by weight of cement and one mixture containing SCA-2 passed the freeze-thaw test, maintaining at least 98 percent of their initial relative dynamic modulus. These three mixtures had an air content ranged between 8.5 to 9 percent. Three mixtures containing SCA-1 with dosages of 2.5, 5, and 7.5 percent by weight of cement failed in freeze-thaw test, dropping below 95 percent of their initial dynamic modulus of elasticity after 197, 263, and 40 freeze-thaw cycles, respectively. Two of the latter mixtures had air contents of 4.75 and 5 percent while other mixture had an air content of 7.5 percent. All mixtures, except one, containing SCA-1 and one mixture containing SCA-2 exhibited mass loss below the failure limit [0.2 lb/ft^2 (977 g/m^2)]. A single mixture, containing 7.5 percent SCA-1 by weight of cement, exhibited a mass loss that exceeded the failure limit. It did so after 21 cycles; the mixture had an air content of 5 percent. As for the mixtures in the other programs, all mixtures in Program 3 exhibited a lower air content in the hardened concrete than in the plastic concrete. Six of the nine mixtures had a relative dynamic

modulus greater than the failure limit (95 percent) after 300 cycles; these mixtures had an air-void spacing factors less than 0.007 in. (0.18 mm). Three mixtures had a relative dynamic modulus below the failure limit; these mixtures had the air-void spacing factor greater than 0.007 in (0.018 mm). The compressive strength of the concrete containing SCA-1 had no observed effect on the relative dynamic modulus and mass loss of that concrete.

4.5 SUMMARY OF THE RESULTS FOR THE MIXTURES OF ALL PROGRAMS

The study examined concrete mixtures containing different combinations of SRA-2, SRA-3, Class F and Class C fly ash, an RMA, Class C fly ash with RMA, SCA-1, and SCA-2 based on freeze-thaw durability, scaling resistance, and air-void characteristics in hardened concrete. The objective was to determine the effect of these materials on the durability of concrete and stability of an air-void system of hardened concrete. All mixtures exhibited a lower air content in hardened concrete than in plastic concrete. This reduction in air content increased with increasing the dosage of SRA-2, SRA-3, and RMA, as shown in Figure 4.25.

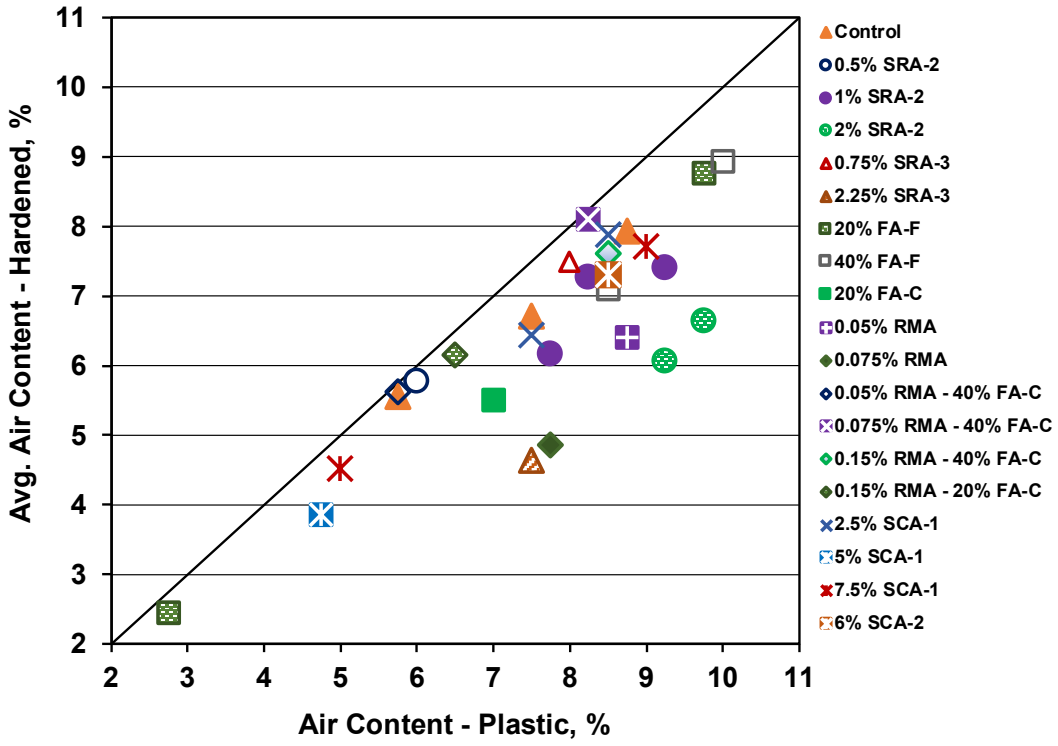

Figure 4.25 – Average air content in hardened concrete versus air content in plastic concrete for the mixtures of all programs

Correlation between an average air-void spacing factor and air content: As would be expected, the average air-void spacing factor of the mixtures drops consistently with increasing the air content. The figure shows that there is scatter in the relationship. For example, for air contents between 6.16 and 6.45 percent, the average air-void spacing factor ranged from 0.0049 to 0.0074 in. (mm). The mixture 2.5% SCA-1 #2 exhibited a greater air-void spacing factor than the mixture 0.05% RMA by about 0.0021 in. (0.053 mm) at the same air content, indicating that the 2.5% SCA-1 #2 mixture had fewer but larger air voids than the 0.05% RMA mixture. A similar observation can be for the air contents between 4.52 and 4.65 percent; the 7.5% SCA-1 #1 mixture exhibited a greater air-void spacing factor than the 2.25% SRA-3 by about 0.0018 in. (0.046 mm). Overall, however, the correlation is good, with the coefficient of determination $R^2 = 0.86$.

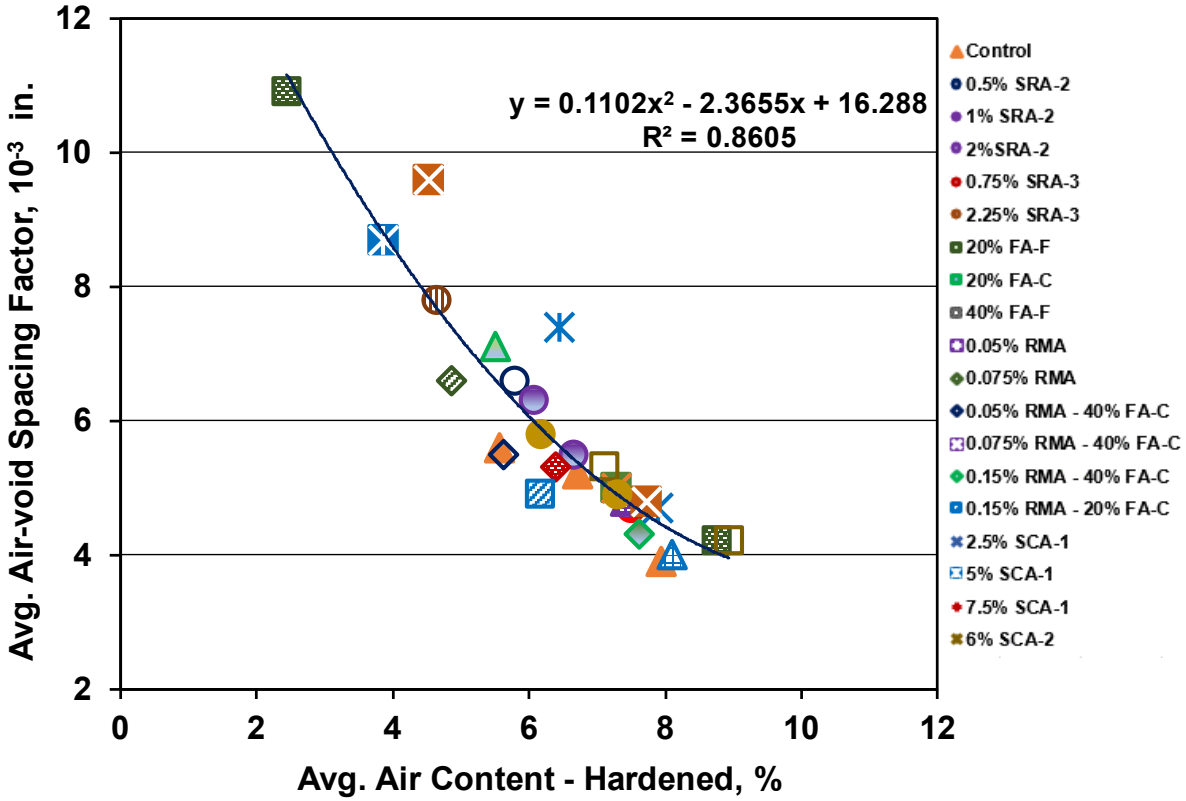

Figure 4.26 – Average air-void spacing factor versus average air content in the hardened concrete for the mixtures of all programs

Correlation between air-void spacing factor or compressive strength and relative dynamic modulus: All mixtures with an average air-void spacing factor less than 0.007 in. (0.18 mm)

exhibited a relative dynamic modulus greater than the failure limit (95 percent). All mixtures that had an average air-void spacing factor greater than 0.007 in. (0.18 mm), however, exhibited a relative dynamic modulus below the failure limit, as shown in Figure 4.27. The results indicate that an air-void spacing factor of 0.007 in. (0.18 mm) is needed, rather than 0.008 in. (0.2 mm), for adequate freeze-thaw protection for concrete – at least for the materials evaluated in this study. Figure 4.28 shows the relative dynamic modulus in the freeze-thaw test as a function of the average 28-day compressive strength for the mixtures of all programs. The results show that 23 mixtures had a relative dynamic modulus greater than the failure limit; 13 of these mixtures had a compressive strength less than or equal to 4000 psi (27.6 MPa). Five mixtures had a relative dynamic modulus below the failure limit; these mixtures, however, had a compressive strength greater than 4000 psi (27.6 MPa). The results indicate that for the range of variable evaluated in this study, air-void spacing factor, but not compressive strength, influenced freeze-thaw durability. This point is illustrated graphically in Figure 4.29.

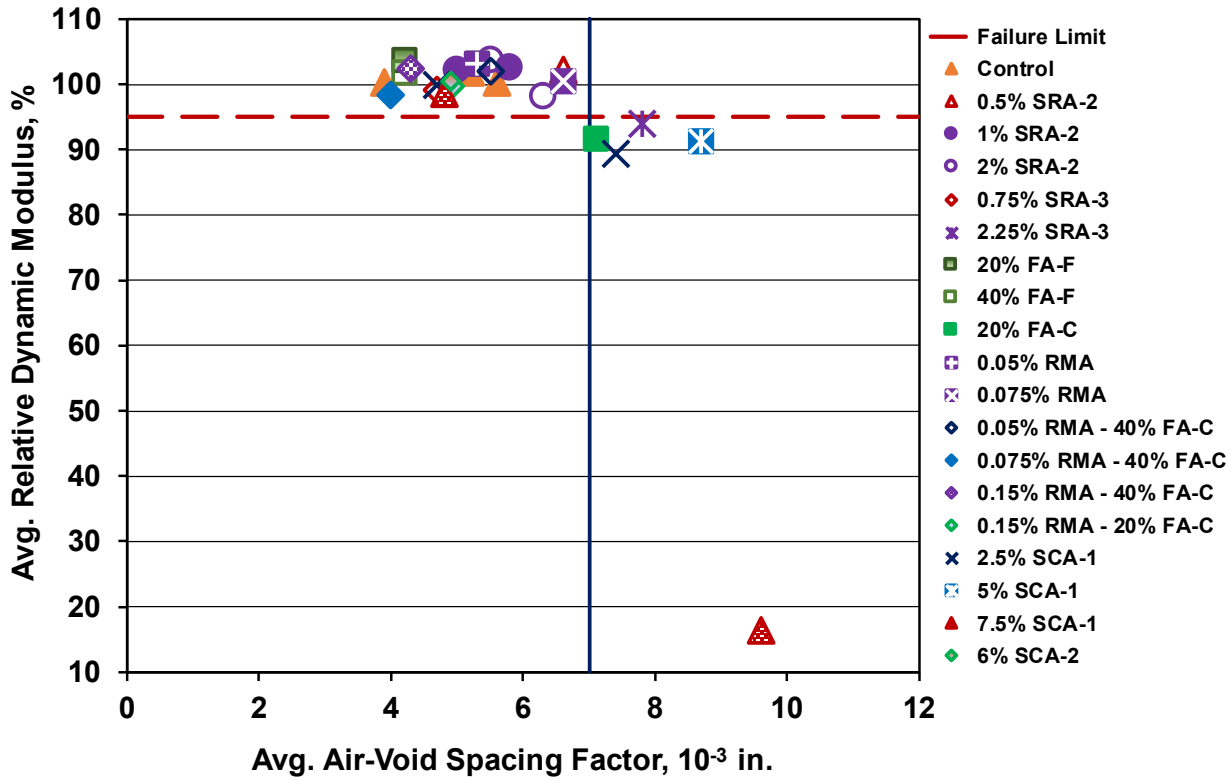

Figure 4.27 – Average relative dynamic modulus versus air-void spacing factors for the mixtures of all programs

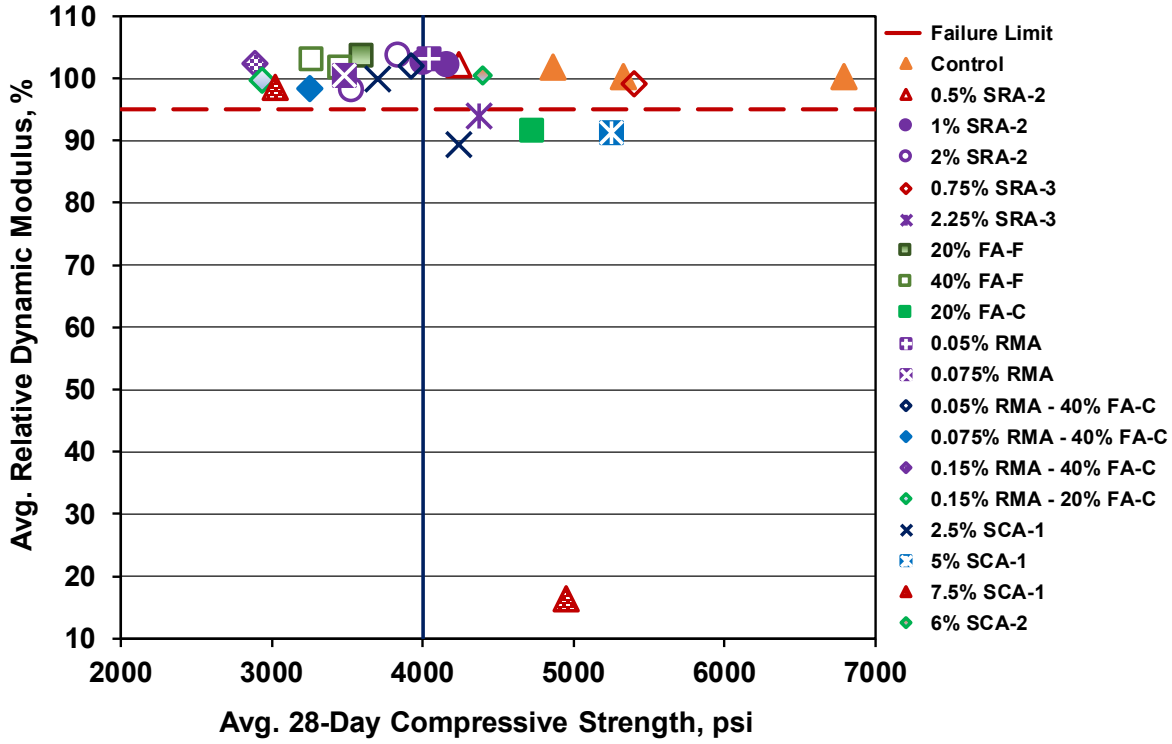

Figure 4.28 – Average relative dynamic modulus versus average 28-day compressive strength for the mixtures of all programs

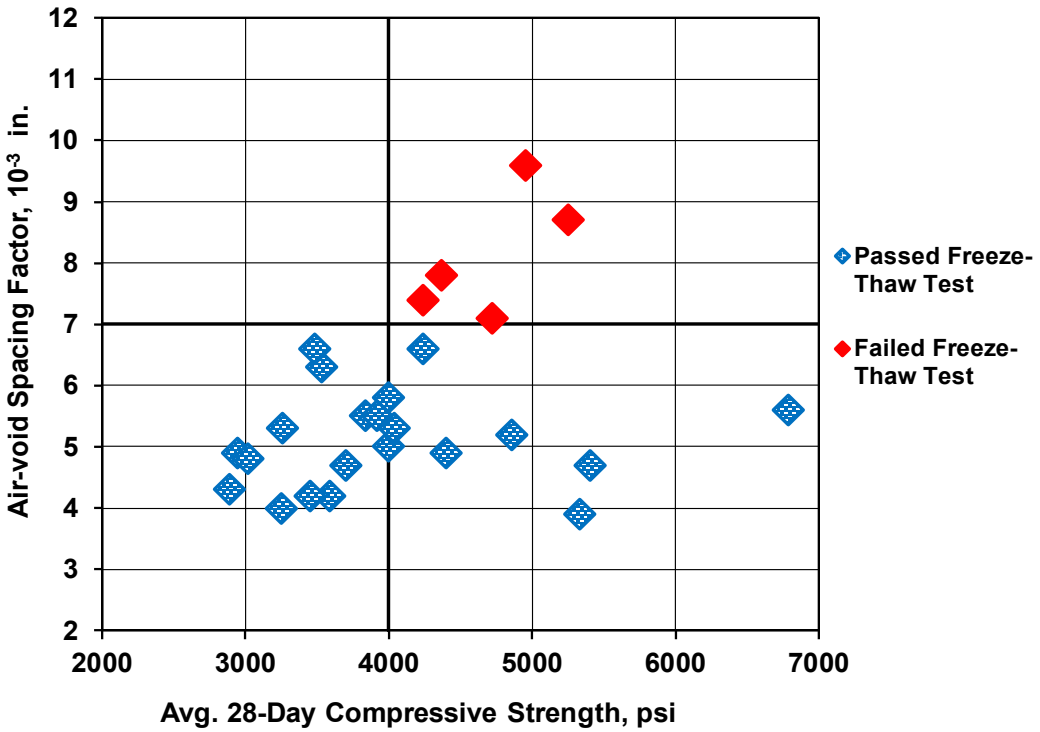

Figure 4.29 – Average air-void spacing factor versus average 28-day compressive strength for the mixtures of all Programs

Correlation between air-void spacing factor or compressive strength and mass loss: The results also show that three of the six mixtures that had an air-void spacing factor greater than 0.007 in. (0.18 mm) exhibited mass loss that exceeded the failure limit, as shown in Figure 4.30. Eight of the twenty-two mixtures that had the average air-void spacing factor less than 0.007 in. (0.0018 mm), however, also exhibited a mass loss that exceeded the failure limit. These eight mixtures, including mixtures containing SRA-2, Class C fly ash in conjunction with RMA, and RMA, had an average compressive strength less than or equal to 4000 psi (27.6 MPa), as shown in Figure 4.31. The results show that all mixtures that failed in scaling had either a spacing factor greater than 0.007 in. (0.0018 mm) or an average compressive strength less than or equal to 4000 psi (27.6 MPa), suggesting that both air-void spacing factor and compressive strength can influence the scaling resistance for concrete. This point is illustrated in Figure 4.32.

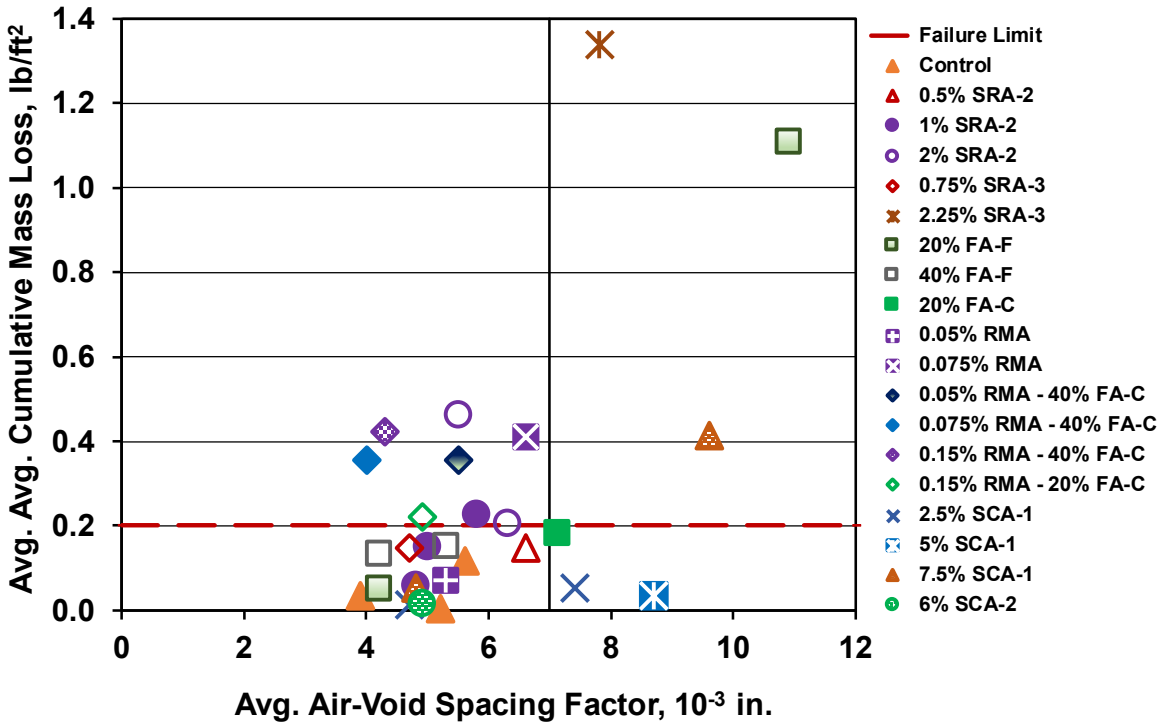

Figure 4.30 – Average cumulative mass loss at 56 freeze-thaw cycles versus the air-void spacing factors for the mixtures of all programs

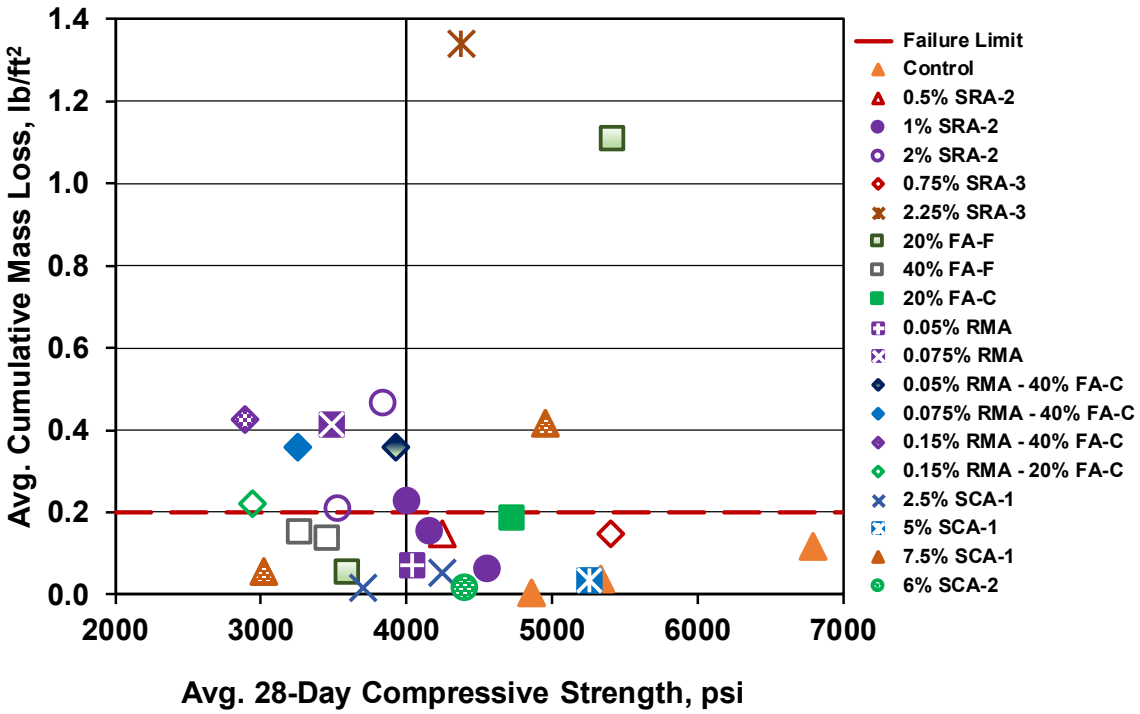

Figure 4.31 – Average cumulative mass loss at 56 freeze-thaw cycles versus average 28-day compressive strength for the mixtures of all Programs

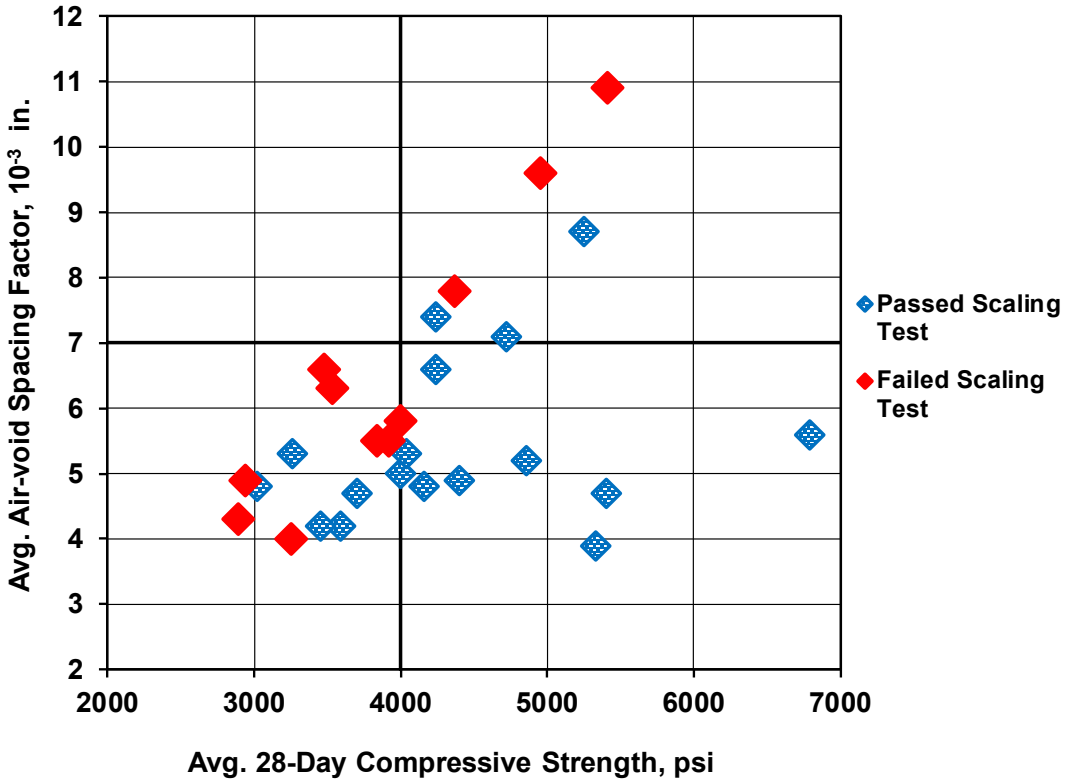

Figure 4.32 – Average air-void spacing factor versus average 28-day compressive strength for the mixtures of all Programs

4.6 EVALUATION AIR-VOID ANALYSIS RESULTS

This section examines the variability of the average air contents and air-void spacing factors obtained from the air-void analyses for all the mixtures in this study, including the repeatability of the results of the air-void parameters for two specimens, picked randomly, from two different mixtures. As discussed in Section 4.1, two slabs from each of two cylinders for each mixture were tested, and the average results were reported.

4.6.1 Variability of the Air-Void Analysis Results

This section evaluates the variation of the results for the average air contents and air-void spacing factors of the four slabs analyzed from each mixture in this study to estimate the variability of the results that were obtained using the Rapid Air 457. The variation found is then compared to variations obtained by Sommer (1979), whose work was used to develop the precision and bias statements in ASTM C457. The average air contents and air-void spacing factors for the four slabs analyzed for each mixture are listed in Tables E.30 and E.31, respectively, in Appendix E. Table 4.13 shows the average, maximum, minimum, standard deviation (SD), and coefficient of variation (COV) of the air content in hardened concrete for the mixtures obtained by combining the results for the four slabs. The results show that the SDs for the air content ranged from 0.08 to 0.39 percent. The maximum SD for air content for four slabs in this study, 0.39 percent, compares favorably to values of 0.39 and 0.54 percent obtained by Sommer for *ten* specimens. Table 4.14 shows the average, maximum, minimum, SD, and COV of the air-void spacing factor of the four slabs analyzed for each mixture. The SDs of the air-void spacing factor for the four slabs ranged from 0.06 to 0.76×10^{-3} in. The value of 0.76×10^{-3} in. may be an outlier, since the next highest value is 0.59×10^{-3} in. As with air content, these values compare favorably to values of 0.24×10^{-3} and 0.47×10^{-3} in. obtained by Sommer for 10 specimens.

Table 4.13 – Average, maximum, minimum, standard deviation, and coefficient of variation of air content in the hardened concrete for the mixtures of all programs

	Air Content - Hardened, %													
Mixtures	**Control # 1**	**Control # 2**	**Control # 3**	**0.5% SRA-2**	**1% SRA-2 # 1**	**1% SRA-2 # 2**	**1% SRA-2 # 3**	**2% SRA-2 # 1**	**2% SRA-2 # 2**	**0.75% SRA-3**	**2.25% SRA-3**	**20% FA-F # 1**	**20% FA-F # 2**	**20% FA-C**
Average of 4 Readings	5.56	7.94	6.71	5.78	7.27	7.41	6.17	6.07	6.65	7.44	4.65	2.45	8.77	5.52
Maximum	5.72	8.20	6.89	5.90	7.50	7.75	6.57	6.35	6.90	7.55	4.80	2.57	8.87	5.93
Minimum	5.37	7.58	6.36	5.68	7.13	7.00	5.78	5.82	6.06	7.21	4.55	2.38	8.57	5.24
Standard Deviation	0.15	0.26	0.25	0.10	0.16	0.38	0.32	0.23	0.39	0.15	0.11	0.08	0.13	0.31
Coefficient of Variation	0.03	0.03	0.04	0.02	0.02	0.05	0.05	0.04	0.06	0.02	0.02	0.03	0.02	0.06

Table 4.13 (Cont'd) – Average, maximum, minimum, standard deviation, and coefficient of variation of air content in the hardened concrete for the mixtures of all programs

	Air Content - Hardened, %													
Mixtures	**40% FA-F # 1**	**40% FA-F # 2**	**0.05% RMA**	**0.075% RMA**	**0.05% RMA - 40% FA-C**	**0.075% RMA - 40% FA-C**	**0.15% RMA - 40% FA-C**	**0.15% RMA – 20% FA-C**	**2.5% SCA-1 # 1**	**2.5% SCA-1 # 2**	**5% SCA-1**	**7.5% SCA-1 # 1**	**7.5% SCA-1 # 2**	**6% SCA-2**
Average of 4 Readings	7.11	8.95	6.40	4.88	5.63	8.11	7.64	6.18	7.88	6.45	3.87	4.53	7.72	7.30
Maximum	7.45	9.26	6.64	5.20	6.01	8.35	7.90	6.30	8.00	6.70	4.14	4.62	7.79	7.62
Minimum	6.58	8.56	6.12	4.70	5.12	7.70	7.40	6.00	7.70	6.30	3.65	4.44	7.61	7.10
Standard Deviation	0.39	0.30	0.23	0.24	0.37	0.30	0.23	0.13	0.13	0.22	0.25	0.09	0.10	0.28
Coefficient of Variation	0.05	0.03	0.04	0.05	0.07	0.04	0.03	0.02	0.02	0.03	0.06	0.02	0.01	0.04

Table 4.14 – Average, maximum, minimum standard deviation, and coefficient of variation of the air-void spacing factor in the hardened concrete for the mixtures of all programs

	Air-Void Spacing Factors, 10^{-3} in.													
Mixtures	**Control # 1**	**Control # 2**	**Control # 3**	**0.5% SRA-2**	**1% SRA-2 # 1**	**1% SRA-2 # 2**	**1% SRA-2 # 3**	**2% SRA-2 # 1**	**2% SRA-2 # 2**	**0.75% SRA-3**	**2.25% SRA-3**	**20% FA-F # 1**	**20% FA-F # 2**	**20% FA-C**
Average of 4 Readings	5.60	3.90	5.20	6.60	5.00	4.80	5.80	6.30	5.50	4.70	7.80	10.90	4.20	7.10
Maximum	5.80	4.30	5.70	6.80	5.20	5.40	6.70	6.60	6.20	5.30	8.10	12.00	4.20	7.40
Minimum	5.40	3.40	4.90	6.30	4.90	4.20	5.40	5.90	5.00	4.40	7.50	10.40	4.10	6.80
Standard Deviation	0.16	0.40	0.37	0.24	0.14	0.49	0.59	0.36	0.51	0.41	0.25	0.76	0.06	0.32
Coefficient of Variation	0.03	0.10	0.07	0.04	0.03	0.10	0.10	0.06	0.09	0.09	0.03	0.07	0.01	0.04

Table 4.14 (Cont'd) – Average, maximum, minimum, standard deviation, and coefficient of variation of the air-void spacing factor in the hardened concrete for the mixtures of all programs

	Air-Void Spacing Factors, 10^{-3} in.													
Mixtures	**40% FA-F # 1**	**40% FA-F # 2**	**0.05% RMA**	**0.075% RMA**	**0.05% RMA - 40% FA-C**	**0.075% RMA - 40% FA-C**	**0.15% RMA - 40% FA-C**	**0.15% RMA - 20% FA-C**	**2.5% SCA-1 # 1**	**2.5% SCA-1 # 2**	**5% SCA-1**	**7.5% SCA-1 # 1**	**7.5% SCA-1 # 2**	**6% SCA-2**
Average of 4 Readings	5.30	4.20	5.30	6.60	5.50	4.00	4.30	4.90	4.70	7.40	8.70	9.60	4.80	4.90
Maximum	6.10	4.30	5.70	7.30	6.10	4.20	4.50	5.30	5.20	8.10	9.10	10.20	5.30	5.10
Minimum	4.80	3.80	4.90	6.20	4.90	3.80	4.10	4.50	4.40	7.00	8.30	9.30	4.50	4.60
Standard Deviation	0.51	0.25	0.33	0.48	0.49	0.18	0.17	0.39	0.36	0.59	0.40	0.52	0.44	0.26
Coefficient of Variation	0.10	0.06	0.06	0.07	0.09	0.05	0.04	0.08	0.08	0.08	0.05	0.05	0.09	0.05

4.6.2 Repeatability of the Air-Void System Analysis Results

To assess the repeatability of the measurements of the air-void parameters, this suction compares the air content and air-void spacing factor obtained from two series of measurements on four slabs. As described in Section 2.4.4.2, air-void parameters are obtained using measurements with the specimens rotated by 90º between each measurement. The measurements were performed on slabs picked randomly from two concrete mixtures, one mixture containing 2 percent SRA-2 by weight of cement and the other mixture containing a 40 percent volume replacement of cement with Class F fly ash, with two slabs from each mixture. The results of the repeated measurements of the air-void parameters are presented in detail in Tables E.33 and E.34 in Appendix E. Table 4.15 shows the results of the repeated measurements for each orientation for each slab. The results show that the maximum difference between two measurements of the same slab is 0.12% for air content and 0.0001 in. (0.0025 mm) for the air-void spacing factor, indicating that there is good agreement in the number and the length of air voids intersected and that the results are satisfactory if they are obtained using single series of measurements.

Table 4.15 - Air contents and air-void spacing factors in hardened concrete of the four measurements, repeated two times, for specimens from two different mixtures

Slab No.	Orientation	Air content, %		Difference, %	Air-Void Spacing Factor, in.		Difference, %
		Test 1	Test 2		Test 1	Test 2	
1*	0º	7.81	7.85	0.04	0.0031	0.0030	0.0001
	90º	7.88	7.88	0.00	0.0026	0.0027	0.0001
	180º	8.12	8.12	0.00	0.0024	0.0024	0.0000
	270º	7.58	7.58	0.00	0.0028	0.0028	0.0000
2*	0º	6.72	6.66	0.06	0.0029	0.0030	0.0001
	90º	6.33	6.26	0.07	0.0031	0.0032	0.0001
	180º	6.39	6.42	0.03	0.0032	0.0033	0.0001
	270º	6.08	6.10	0.02	0.0029	0.0030	0.0001
3#	0º	6.76	6.78	0.02	0.0034	0.0035	0.0001
	90º	7.29	7.3	0.01	0.0033	0.0033	0.0000
	180º	6.86	6.95	0.09	0.0030	0.0029	0.0001
	270º	7.43	7.44	0.01	0.0036	0.0036	0.0000
4#	0º	8.07	7.95	0.12	0.0025	0.0026	0.0001
	90º	7.82	7.71	0.11	0.0027	0.0028	0.0001
	180º	7.48	7.56	0.08	0.0031	0.0030	0.0001
	270º	7.25	7.28	0.03	0.0030	0.0030	0.0000

*Specimens from concrete containing 2 percent SRA-2 by weight of cement.
Specimens from concrete containing 40 percent volume replacements of cement with Class F fly ash.

CHAPTER 5: SUMMARY, CONCLUSIONS, AND RECOMMENDATIONS

5.1 SUMMARY

The effects of crack-reducing technologies and supplementary cementitious materials on plastic settlement cracking and the durability of concrete subjected to freezing and thawing are evaluated. The study of settlement cracking included 86 concrete mixtures containing internal curing, a shrinkage-reducing admixture, optimized and non-optimized aggregate gradations, or the supplementary cementitious materials slag cement and silica fume. Some concrete mixtures contained combinations of these technologies, such as supplementary cementitious materials and internal curing. The study evaluated the effect of these methods in terms of both crack length and width.

The study of durability included 28 concrete mixtures, divided into three programs. Program 1 involved concrete containing different dosage rates of one of two shrinkage-reducing admixtures. Program 2 involved concrete containing different volume replacements of Class F and Class C fly ash and different combinations of a rheology-modifying admixture with and without Class C fly. Program 3 involved concrete containing different dosage rates of one of two shrinkage compensating admixtures, one based on MgO that also incorporated a shrinkage-reducing admixture and one based on CaO. This study evaluated the effect of the technologies and materials on freeze-thaw durability, based on ASTM C666 Procedure B, scaling resistance, based on a modified version of Canadian Test BNQ NQ 2621-900 Annex B, and characteristics of the air-void system, obtained following ASTM C457. The research also examined the correlation between air-void characteristics, compressive strength, freeze-thaw durability, and scaling resistance for the mixtures.

5.2 CONCLUSIONS

The following conclusions are drawn from the test results and analyses presented in this report.

5.2.1 Settlement Cracking

1. All the crack-reducing technologies, including internal curing, the shrinkage-reducing admixture, an optimized aggregate gradation, and the supplementary cementitious materials, slag cement and silica fume, resulted in a significant reduction in settlement cracking compared to mixtures without these technologies (control mixtures) at all slumps.
2. All mixtures experienced increased settlement cracking as slump increased. This increase, however, was very low for the concrete containing both slag cement and silica fume, without and with internal curing. This suggests that high slump may not be as detrimental to settlement cracking for mixtures slag cement and silica fume and internal curing.
3. Crack widths greatly increased as slump increased for all control mixtures. Crack width increased slightly as slump increased for concrete containing internal curing or slag cement. Crack width remained constant with increasing slump for the concrete containing the shrinkage-reducing admixture, slag cement and silica fume, without and with internal curing.
4. The mixtures with a non-optimized aggregate gradation exhibited increased settlement cracking compared to mixtures with an optimized aggregate gradation.
5. The use of internal curing water, provided by partial replacement of total aggregate with pre-wetted fine lightweight aggregate, reduced settlement cracking. The size of pre-wetted fine lightweight aggregate did not affect the reduction in settlement cracking. In addition, using two different quantities of internal curing water (5.9 or 7 percent of the weight of cementitious material) caused resulted in the about same reduction in cracking.
6. The combination of slag cement and silica fume in concrete provided a greater reduction in settlement cracking than slag cement alone.

5.2.2 Durability Performance and Air-Void System

1. One shrinkage-reducing admixture had no effect on freeze-thaw durability at all dosages, while a second shrinkage-reducing admixture caused reduced durability at the highest dosage used in this study, indicating that SRAs should be individually checked for effects on durability.

2. Mixtures containing Class F fly ash, the rheology modifying admixture, or Class C fly ash in conjunction with the rheology modifying admixture at all dosages studied performed well in the freeze-thaw durability test if the air-void spacing factor was 0.007 in. (0.18 mm) or less.
3. The shrinkage compensating admixture based on CaO had no effect on the freeze-thaw durability of concrete at the dosage used in this study. The shrinkage compensating admixture based on MgO resulted in lower freeze-thaw durability mixtures, but only in mixtures that had increased air-void spacing; the increased air-void spacing may have been due to the shrinkage-reducing admixture incorporated in the admixture, which can reduce the stability of the air-void system.
4. Mixtures containing a shrinkage-reducing admixture exhibited a reduction in scaling resistance.
5. Class F and Class C fly ash had no effect on scaling resistance when the concrete has an air-void spacing factor of 0.0071 in. or less. The rheology modifying admixture without and with Class C fly ash resulted in reduced scaling resistance of concrete. This reduction was in all cases associated with a concrete compressive strength below 4000 psi (27.6 MPa).
6. With the exception of one mixture with high air-void spacing factor [0.0096 in. (0.24 mm)], the two shrinkage compensating admixtures had no deleterious effect on scaling resistance at all dosages used in this study.
7. All mixtures exhibited a lower air content in the hardened concrete than in the plastic concrete. This reduction in air content was significantly greater for mixtures containing high dosages of a shrinkage-reducing admixture or the rheology modifying admixture.
8. All mixtures with an average air-void spacing factor of 0.007 in. (0.18 mm) or less performed well in the freeze-thaw test (relative dynamic modulus above 95 percent after 300 cycles).
9. All mixtures with an average air-void spacing factor of 0.007 in. (0.18 mm) or less and a compressive strength greater than 4000 psi (27.6 MPa) performed well in the scaling test (mass loss below 0.2 lb/ft^2 (977 g/m^2) after 56 cycles).
10. The air-void spacing factor was the only property in this study that influenced the freeze-thaw durability of concrete. Both the air-void spacing factor and compressive strength influenced scaling resistance.

5.3 RECOMMENDATIONS

The following recommendations to reduce settlement cracking and improve the durability of concrete are based on the results of this study.

1. Optimized aggregate gradations, internal curing, shrinkage-reducing admixtures, and slag cement, with or without silica fume, are recommended to minimize both the length and width of settlement cracks.
2. Combining multiple supplementary cementitious materials or using supplementary cementitious materials in conjunction with internal curing is recommended to achieve reductions in settlement cracking.
3. Concrete must have an adequate air-void system when subjected to freezing-thawing cycles. Careful attention to the dosage of air-entraining agent and the resulting air content is needed.
4. To provide adequate protection for concrete from freezing-thawing cycles, an air-void spacing factor of 0.007 in. (0.18 mm) or less is recommended.
5. To provide adequate scaling resistance for concrete subjected to freezing-thawing cycles, an air-void spacing factor of 0.007 in. (0.18 mm) or less and a compressive strength greater of at least 4000 psi (27.6 MPa) are recommended.

REFERENCES

AASHTO, (2013). *AASHTO LRFD Bridge Design Specifications*, Sixth Edition, Washington, DC, 1308 pp.

ACI Committee 201, (2016). *Guide to Durable Concrete,* ACI 201.2R-16, American Concrete Institute, Farmington Hills, MI, 84 pp.

ACI Committee 231, (2010). *Report on Early-Age Cracking: Causes, Measurement and Mitigation*, ACI 231R-10, American Concrete Institute, Farmington Hills, MI, 46 pp.

ACI Committee 233, (2017). *Guide for the Use of Slag Cement in Concrete and Mortar,* ACI 233R-17, American Concrete Institute, Farmington Hills, MI, 37 pp.

ACI Committee 234, (2006). *Guide for the Use of Silica Fume in Concrete,* ACI 234R-06, American Concrete Institute, Farmington Hills, MI, 63 pp.

ACI Committee 305, (2010*). Guide to Hot weather concereting,* ACI 305R-10, American Concrete Institute, Farmington Hills, MI, 23 pp.

ACI Committee 308, (2016). *Guide to External Curing of Concrete,* ACI 308-16, American Concrete Institute, Farmington Hills, MI, 36 pp.

Al-Qassag, O., Darwin, D., and O'Reilly, M. (2015). "Effect of Synthetic Fibers and a Rheology Modifier on Settlement Cracking of Concrete," *SM Report* No. 116, University of Kansas Center for Research, Inc. Lawrence, KS, December, 130 pp.

ASTM C39/C39M (2018). *Standard Test Method for Compressive Strength of Cylindrical Concrete Specimens,* ASTM International*,* West Conshohocken, PA, 8 pp.

ASTM C70-13 (2013). *Standard Test Method for Surface Moisture in Fine Aggregate,* ASTM International, West Conshohocken, PA, 3 pp.

ASTM C127-15 (2015). *Standard Test Method for Relative Density (Specific Gravity) and Absorption of Coarse Aggregate,* ASTM International, West Conshohocken, PA, 5 pp.

ASTM C138/C138M-17 (2017). *Standard Test Method for Density (Unit Weight), Yield, and Air Content (Gravimetric) of Concrete,* ASTM International, West Conshohocken, PA, 5 pp.

ASTM C143/C143M-15 (2015). *Standard Test Method for Slump of Hydraulic-Cement Concrete,* ASTM International, West Conshohocken, PA, 4 pp.

ASTM C173/C173M-16 (2016). *Standard Test Method for Air Content of Freshly Mixed Concrete by the Volumetric Method,* ASTM International, West Conshohocken, PA, 9 pp.

ASTM C188-17 (2017). *Standard Test Method for Density of Hydraulic Cement,* ASTM International, West Conshohocken, PA, 3 pp.

ASTM C192/C192M-18 (2018). *Standard Practice for Making and Curing Concrete Test Specimens in the Laboratory,* ASTM International, West Conshohocken, PA, 8 pp.

ASTM C204-17 (2017). *Standard Test Method for Fineness of Hydraulic Cement by Air-Permeability Apparatus,* ASTM International, West Conshohocken, PA, 10 pp.

ASTM C215-14 (2014). *Standard Test Method for Fundamental Transverse, Longitudinal, and Torsional Resonant Frequencies of Concrete Specimens,* ASTM International, West Conshohocken, PA, 7 pp.

ASTM C457/C457M-16 (2016). *Standard Test Method for Microscopical Determination of Parameters of the Air-Void System in Hardened Concrete,* ASTM International, West Conshohocken, PA, 18 pp.

ASTM C494/C494M-17 (2017). *Standard Specification for Chemical Admixtures for Concrete,* ASTM International, West Conshohocken, PA, 10 pp.

ASTM C666/C666M-15 (2015). *Standard Test Method for Resistance of Concrete to Rapid Freezing and Thawing,* ASTM International, West Conshohocken, PA, 7 pp.

ASTM C1064/C1064M-17 (2017). *Standard Test Method for Temperature of Freshly Mixed Hydraulic-Cement Concrete,* ASTM International, West Conshohocken, PA, 3 pp.

ASTM C1761/C1761M-17 (2017). *Standard Specification for Lightweight Aggregate for Internal Curing of Concrete,* ASTM International, West Conshohocken, PA, 8 pp.

Babaei, K., and Purvis, R. L. (1995). "Prevention of Cracks in Concrete Bridge Decks: Report on Surveys of Existing Bridges," *Report,* PA-FHWA-95-001+89-01, 100 pp.

Babaei, K., and Purvis, R. L. (1996). "Prevention of Cracks in Concrete Bridge Decks Summary Report," *Report* No. 233, Wilbur Smith Associates Report, Falls Church, VA, 30 pp.

Babaei, K., and Fouladgar, A. M. (1997). "Solutions to Concrete Bridge Deck Cracking," *Concrete International Magazine*, Vol. 19, No. 7, July, pp. 34-37.

Bakker, R. F. M. (1980). "On the Cause of Increased Resistance of Concrete Made from Blast-Furnace Cement to Alkali Reaction and to Sulfate Corrosion," *Thesis*, RWTH-Aachen, 118 pp.

Battaglia, I., Whited, G., and Swank, R. (2008). "Eclipse® Shrinkage Reducing Admixtures Product Evaluation," *Final Report,* Washington Department of Transportation, February, 18 pp.

Bentz, D. P. (2006). "Influence of Shrinkage-Reducing Admixtures on Early-Age Properties of Cement Pastes," Advanced Concrete Technology, Vol. 4, No. 3, September, pp. 1-7.

Bentz, D. P. (2006). "Ten Observations from Experiments to Quantify Water Movement and Porosity Percolation in Hydrating Cement Pastes," *Proceedings of Transport Properties and Concrete Quality Workshop*, American Ceramic Society, Westerville, OH, December, pp. 3-18.

Bilodeau, A., Fournier, B., Hooton, D., Gagne, R., Jolin, M., and Bouzoubaa, N. (2008). "Deicing Salt Scaling Resistance of Concrete Incorporating Supplementary Cementing Materials: Laboratory and Field Test Data," *Canadian Journal of Civil Engineering,* Vol. 35, No. 11, November, pp. 1261- 1275.

Bouzoubaa, N., Bilodeau, A., Fournier, B., Hooton, D., Gagne, R., Jolin, M. (2011). "Deicing Salt Scaling Resistance of Concrete Incorporating Fly Ash and (or) Silica Fume: Laboratory and Field Sidewalk Test Data," *Canadian Journal of Civil Engineering*, Vol. 38, No. 4, April, pp. 373-382.

Breitenbucher, R., and Mangold, M. (1994). " Minimization of Thermal Cracking in Concrete at Early Ages," *RILEM Proceeding 25, Thermal Cracking in Concrete at Early Ages,* R. Springenschmid, ed., E&FN Spon, London, pp. 205-212.

Brettmann, R., Darwin, D., and O'Reilly, M. (2015). "Developing a Test Procedure to Evaluate Settlement Cracking Performance," *SL Report* No. 15-2*,* University of Kansas Center for Research, Inc. Lawrence, KS, May, 44 pp.

Brown, M. D., Sellers, G., Folliard, K., and Fowler, D. (2001). "Restrained Shrinkage Cracking of Concrete Bridge Decks: State-of-the-Art Review," *Report*, Research Project 0-4098, Texas Department of Transportation, June, 50 pp.

Butler, B. (1997). "Durable Concrete Containing Three or Four Cementitious Materials," *ACI Journal*, special publication, Vol. 170, July, pp. 309-330.

Carlson J., Sutter L., Peterson K., and Van Dam T. (2006). "Comparison of Flatbed Scanner and RapidAir 457 System for Determining Air Void System Parameters of Hardened Concrete," *Transportation Research Record: Journal of the Transportation Research Board*, No. 1979, January, pp. 54-59.

Chariton, T., and Weiss, W. J. (2001). "Using Acoustic Emission to Monitor Damage Development in Mortars Restrained from Volumetric Changes," *ACI Special Publication,* SP-206, December, pp. 205-218.

Cheng, T. T. H., and Johnston, D. W. (1985). "Incidence Assessment of Transverse Cracking in Concrete Bridge Decks: Construction and Material Considerations," *Report* No. FHWA/NC/85-002, Vol. 1, North Carolina State University, Raleigh, Department of Civil Engineering, 232 pp.

Chui, J., and Dilger, W. (1993). "Temperature Stress and Cracking Due to Hydration Heat," Creep and Shrinkage of Concrete, E&FN Spon, London, pp. 271-276.

Combrinck, R., and Boshoff, W. P. (2013). "Fundamentals of Plastic Settlement Cracking in Concrete," *Construction Materials and Structures:* Stellenbosch, Department of Civil Engineering, Stellenbosch University, IOS Press, December, 354 pp.

Cong, X., Gong, S., Darwin, D., and McCabe, S. (1992). "Role of Silica Fume in Compressive Strength of Cement Paste, Mortar, and Concrete," *ACI Materials Journal*, Vol. 89, No. 4, July, pp. 375-387.

Cope, B. L., and Ramey, G. E. (2001). "Reducing Drying Shrinkage of Bridge Deck Concrete," *Concrete International*, Vol.23, No. 8, August, pp. 76-82.

Cramer, S. M., Hall, M., and Parry, J. (1995). "Effect of Optimized Total Aggregate Gradation on Portland Cement Concrete for Wisconsin Pavements," *Transportation Research Board Record* No. 1478, National Research Council, July, pp. 100-106.

Dakhil, F. H., Cady, P. D., and Carrier, R. E. (1975). "Cracking of Fresh Concrete as Related to Reinforcement," *ACI Journal,* Proceedings, Vol. 72, No. 8, August, pp. 421-428.

Darwin, D., and Slate, F. O. (1970). "Effect of Paste-Aggregate Bond Strength on Behavior Concrete," *Journal of Materials*, Vol. 5, No. 1, March, pp. 86-98.

Darwin, D., Browning, J., and Lindquist, W. D. (2004). "Control of Cracking in Bridge Decks: Observations from the Field," *Cement, Concrete and Aggregates*, Vol. 26, No. 2, December, pp. 148-154.

Darwin, D., Browning, J., Lindquist, W., McLeod, H. A. K., Yuan, J., Toledo, M., and Reynolds, D. (2010). "Low-Cracking, High-Performance Concrete Bridge Decks – Case Studies Over the First 6 Years," *Transportation Research Record*, No. 2202, pp. 61-69.

Darwin, D., Browning, J., O'Reilly, M., Locke, C. E., and Virmani, Y. P. (2011). "Multiple Corrosion Protection Systems for Reinforced Concrete Bridge Components," Publication No. FHWA-HRT-11-060, Federal Highway Administration, also *SM Report* No. 101, University of Kansas Center for Research, Inc. Lawrence, KS, November, 255 pp.

Darwin, D., Khajehdehi, R., Alhmood, A., Feng, M., Lafikes, J., Ibrahim, E., and O'Reilly, M., "Construction of Crack-Free Bridge Decks: Final Report," *SM Report* No. 121, University of Kansas Center for Research, Inc., Lawrence, Kansas, December 2016, 143 pp.

Design and Control of Concrete Mixtures, 16th Ed., Portland Cement Association, Skokie, IL, 2016.

Durability of Concrete Bridge Decks – A Cooperative Study, Final Report. (1970). The State Highway Departments of California, Illinois, Kansas, Michigan, Minnesota, Missouri, New Jersey, Ohio, Texas, and Virginia; Bureau of Public Roads; and Portland Cement Association, 35 pp.

Fagerlund, G. (1991). "Air-Pore Instability and its Effects on the Concrete Properties," *Nordic Concrete Research*, Vol. 9, pp. 34-52.

Folliard, K., Hover, K., Harris, N., Ley, M., and Naranjo, A., (2009). "Effect of Texas Fly Ash on Air-Entrainment in Concrete: Comprehensive Report," *Report* No. FHWA/TX-08/0-5207-1, Center for Transportation Research, University of Texas, Austin, January, 577 pp.

Freeman, J. (2009). "Stability and Quality of Air-Void Systems in Concrete with Superplasticizers," *Master's Thesis*, Oklahoma State University, OK, 57 pp.

FHWA. (2016). "Area on Deficient Bridges by Functional Classification," National Bridge Inventory, http://www.fhwa.dot.gov/bridge/britab.cfm.

French, C., Eppers L., Le, Q., and Hajjar, J. F. (1999). "Transverse Cracking in Concrete Bridge Decks," *Transportation Research Record* 1688, Paper No. 99-0888, January, pp. 21-29.

Frosch, R. J., Blackman, D. T., and Radabaugh, R. D. (2003). "Investigation of Bridge Deck Cracking in Various Bridge Superstructure Systems," Publication FHWA/IN/JTRP-2002/25. Joint Transportation Research Program, Indiana Department of Transportation and Purdue University, West Lafayette, IN. 265 pp.

Grutzeck, M. W., Roy, D. M., and Wolfe-Confer, D. (1982). "Mechanism of Hydration of Portland Cement Composites Containing Ferrosilicon Dust," *Proceedings*, 4th International Conference on Cement Microscopy, Las Vegas, International Cement Microscopy Association, Duncanville, TX, pp. 193-202.

Hammer, T. A. (1999). "Test Methods for Linear Measurement of Autogenous Shrinkage Before Setting," *Autogenous Shrinkage of Concrete,* E & FN Spon, London, pp. 143–154.

Hammer, T. A. (2001). "Effect of Silica Fume on the Plastic Shrinkage and Pore Water Pressure of High Strength Concrete," *Materials and Structures,* Vol. 34, June, pp. 273-278.

Henkensiefken, R. Briatka, P., Bentz, D., Nantung, T., and Weiss, J. (2010). "Plastic Shrinkage Cracking in Internally Cured Mixtures Made with Pre-Wetted Lightweight Aggregate," *Concrete International,* No. 32, January, pp. 49-54.

Holt, E. E. (2001). "Early Age Autogenous Shrinkage of Concrete," *Technical Research Centre of Finland*, *VTT Publications* 446, 184 pp.

Horn, M. W., Stewart, C. F., and Boulware, R. L. (1972). "Factors Affecting the Durability of Concrete Bridge Decks: Normal vs. Thickened Deck," *Interim Report* No. 3, Bridge Department, California Division of Highways, CA-HY-4101-3-72-11, May.

Horn, M. W., Stewart, C. F., and Boulware, R. L. (1975). "Factors Affecting the Durability of Concrete Bridge Decks: Construction Practices," *Interim Report* No. 4, Bridge Department, California Division of Highways, CA-DOT-ST-4104-4-75-3, March, 142 pp.

Huang, C. and Feldman, R. F. (1985). "Hydration Reactions in Portland Cement-Silica Fume Blends," *Cement and Concrete Research*, Vol. 15, No. 4, July, pp. 585-592.

Issa, M. (1999). "Investigation of Cracking in Concrete Bridge Decks at Early Ages," *ASCE Journal of Bridge Engineering*, Vol. 4, No. 2, May, pp. 116-124.

Jakobsen, U., Pade, C., Thaulow, N., Brown, D., Sahu, S., Magnusson, O., De Buck, S., and De Schutter, G. (2006). "Automated Air-Void Analysis of Hardened Concrete - a Round Robin Study," *Cement and Concrete Research,* Vol. 36, No. 8, August, pp. 1444-1452

Kansas Department of Transportation (2014). "Low-Cracking High-Performance Concrete," *Standard Specifications for State Road and Bridge Construction*, Topeka, KS.

Kayir, H., and Weiss. J. (2002). "A Fundamental Look at Settlement in Fresh Systems: Role of Mixing Time and High Range Water Reducers," *First North American Conference on the Design and Use of Self-Consolidating Concrete*. Chicago, IL, November, pp. 27-32.

Khajehdehi, R., Feng, M., Darwin, D., Lafikes, J., Ibrahim, E., and O'Reilly, M. (2018). "Combined Effects of Internal Curing, SCMs, and Expansive Additives on Concrete Shrinkage," *Advances in Civil Engineering Materials,* Vol. 7, No. 4, November, pp. 644–659, https://doi.org/10.1520/ACEM20170145. ISSN 2379-1357

Khajehdehi, R., and Darwin, D. (2018). "Controlling Cracks in Bridge Decks," *SM Report* No. 129, University of Kansas Center for Research, Inc. Lawrence, KS, December, 218 pp.

Khayat, K. H., and Yahia, A. (1997). "Effect of Welan Gum-High-Range Water Reducer Combinations on Rheology of Cement Grout," *ACI Materials Journal,* Vol. 94, No. 5, September, pp. 365-372.

Kirk, R., and Mallett, W. (2013). "Highway Bridge Conditions: Issues for Congress," *Congressional Research Service (CRS) Report Prepared for Members and Committees of Congress*, December, 18 pp.

Klieger, P. (1955). "Effect of Atmospheric Conditions During the Bleeding Period and Time of Finishing on the Scale Resistance of Concrete," *ACI Journal*, Proceedings Vol. 52, No. 11, November, pp. 309-326.

Krauss, P. D., and Rogalla, E. A. (1996). "Transverse Cracking in Newly Constructed Bridge Decks," *National Cooperative Highway Research Program Report* 380, Transportation Research Board, Washington, DC, October, 132 pp.

Langan, B., Joshi, R., Ward, M. (1990). "Strength and Durability of Concrete Containing 50% Portland Cement Replacement by Fly Ash and Other Materials," *Canadian Journal of Civil Engineering*, Vol. 17, No. 1, February, pp. 19-27.

Ley, M. T. (2010). "Determining the Air-Entraining Admixture Dosage Response for Concrete with a Single Concrete Mixture." *ASTM Journal of Testing and Evaluation*, Vol. 7, February, pp. 155-169.

Lindquist, W. D., Darwin, D., and Browning, J. (2005). "Cracking and Chloride Contents in Reinforced Concrete Bridge Decks," *SM Report* No. 78, University of Kansas Center for Research, Inc. Lawrence, KS, February, 482 pp.

Lindquist, W. D., Darwin, D., and Browning, J. (2008). "Development and Construction of Low-Cracking High-Performance Concrete (LC-HPC) Bridge Decks: Free Shrinkage, Mixture Optimization, and Concrete Production," *SM Report* No. 92, University of Kansas Center for Research, Inc. Lawrence, KS, November, 540 pp.

Lindquist, W., Darwin, D., Browning, J., McLeod, H. A. K., Yuan, J., and Reynolds, D. (2015). "Implementation of Concrete Aggregate Optimization," *Construction & Building Materials*, Vol. 74, No. 15, January, pp. 49-56.

Lura, P., Pease, B., Mozzata, G., Rajabipour, F., and Wiess, J. (2007). "Influence of Shrinkage Reducing Admixtures on Development of Plastic Shrinkage Cracks," *ACI Materials Journal*, Vol. 104, No. 2, March, pp. 187-194.

Maage, M., and Sellevold, E., (1987). "Effect of Microsilica on the Durability of Concrete Structures," *Concrete International*, V. 9, No. 12, December, pp. 39-43.

Malisch, W. R., Raecke, D. A., Fischer, D. M., Lott, J. L., Kennedy, T. W., and Kessler, C. E. (1966). "Physical Factors Influencing Resistance of Concrete to Deicing Agents," *National Cooperative Highway Research Program (NCHRP) Report* No. 27, Transportation Research Board, Washington, DC, 41 pp.

Marcotte, T. D., and C. Hansson. (2003). "The Influence of Silica Fume on the Corrosion Resistance of Steel in High-Performance Concrete Exposed to Simulated Sea Water," *Journal of Materials Science*, Vol. 38, No, 23, December, pp. 4765–4776.

Mehta, P. K., and Monterio, P. J. M. (2006). *Concrete: Microstructure, Properties, and Materials*, Third Edition, McGraw-Hill Education, NY, 659 pp.

Meusel, J. W., and Rose, J. H. (1983). "Production of Granulated Blast Furnace Slag at Sparrows Point, and the Workability and Strength Potential of Concrete Incorporating the Slag," *1st International Conference on Fly Ash, Silica Fume, and Slag in Concrete*, ACI Special Publication SP-79, Vol. 2, May, pp. 867-890.

McDonald, J. E. (1991). "The Potential for Cracking of Silica-Fume Concrete," *Repair, Evaluation, Maintenance, and Rehabilitation Bulletin*, Vol. 8, No. 3, August, pp. 8-11.

McLeod, H., Darwin, D., and Browning, J. (2009). "Development and Construction of Low-Cracking High-Performance Concrete Bridge Decks: Construction Methods, Temperature Effects, and Resistance to Chloride Ion Penetration," *SM Report* No. 94*,* University of Kansas Center for Research, Inc. Lawrence, KS, September, 848 pp.

Mindess, S. (1987). "Bonding in Cementitious Composites: How Important is It?," *Proceedings*, Symposium on Bonding in Cementitious Composites, V. 114, Materials Research Society, Pittsburgh, pp. 3-10.

Mindess, S., Young, F. and Darwin, D. (2003). *Concrete*, second edition, Prentice-Hall., Englewood Cliffs, NJ, 644 pp.

Miller, G. G., and Darwin, D. (2000). "Performance and Constructability of Silica Fume Bridge Deck Overlays," *SM Report* No. 57, University of Kansas Center for Research, Inc. Lawrence, KS, January, 423 pp.

Miller, A., Albert, E., Spragg, R., Antico, F. C., Ashraf, W., Barrett, T., Behnood, A., Bu, Y., Chiu, Y., Desta, B., Farnam, Y., Jeong, H., Jone, W., Lucero, C., Luo, D., Nickel, C., Panchmatia, P., Pin, K., Qiang, S., Qiao, C., Shagerdi, H., Tokpatayeva, R., Villani, C., Wiese, A., Woodard, S., and Weiss, J. (2014). "Determining the Moisture Content of Pre-Wetted Lightweight Aggregate: Assessing the Variability of the Paper Towel and Centrifuge Methods," *4th International Conference on the Durability of Concrete Structures*, Purdue University, West Lafayette, IN, January, 5 pp.

Miller, A., Barrett, T., Zander, A., and Weiss, J. (2014). "Using a Centrifuge to Determine Moisture Propertes of Lightweight Fine Aggregate for Use in Internal Curing," *Advances in Civil Engineering Materials*, Vol. 3, No. 1, January, pp. 142-157.

Mora-Ruacho, J., Gettu, R., and Aguado, A. (2009). "Influence of Shrinkage-Reducing Admixtures on the Reduction of Plastic Shrinkage Cracking in Concrete," *Cement and Concrete Research*, Vol. 39, No. 3, March, pp. 141-146.

Murphy, M. and Chao, X. (2009). "Technology Evaluation on Characterization of the Air Void System in Concrete," *Final Report*, Pennsylvania Department of Transportation, Project No. PSU 020, September, 122 pp.

Naik, T. R., Ramme, B. W., and Tews, J. H. (1994). "Use of High Volume of Class C and Class F Fly Ash in Concrete," *Cement, Concrete, and Aggregates,* CCAGPD, Vol. 16, No. 1, June, pp. 12-20.

National Bridge Inventory (NBI), (2016). ASCE Analysis of U.S. Department of Transportation, Federal Highway Administration.

Obla, K., Kim, H., and Lobo, C. (2007). "Effect of Continuous (Well-Graded) Combined Aggregate Grading on Concrete Performance," Phase B: Concrete Performance, *NRMCA Research Laboratory, Project D340*, May, 45 pp.

Paillere, A. M., Buil, M., and Serrano, J. J. (1989). "Effect of Fiber Addition on the Autogenous Shrinkage of Silica Fume Concrete," *ACI Materials Journal*, Vol. 86, No. 2, March, pp 139-144.

Pendergrass, B., Darwin, D., and Browning, J. (2011). "Crack Surveys of Low-Cracking High-Performance Concrete Bridge Decks in Kansas 2009-2010," *SL Report* No. 11-3, University of Kansas Center for Research, Inc. Lawrence, KS, October, 103 pp.

Pendergrass, B., and Darwin, D. (2014). "Low-Cracking High-Performance Concrete (LC-HPC) Bridge Decks: Shrinkage-Reducing Admixtures, Internal Curing, and Cracking Performance," *SM Report* No. 107, University of Kansas Center for Research, Inc. Lawrence, KS, February, 664 pp.

Pendergrass, B., Darwin, D., Feng, M., and Khajehdehi, R. (2017). "Compatibility of Shrinkage-Reducing and Air-Entraining Admixtures," *ACI Materials Journal*, Vol. 114, No. 5, pp 809- 818.

Pigeon M., Plante P., and Plante M., (1989). "Air-Void Stability, Part I: Influence of Silica Fume and Other Parameters," *ACI Material Journal,* Vol. 86, No. 5, September, pp 482-490.

Popovic, P., Rewerts, T. L., and Sheahen, D. J. (1988). "Deck Cracking Investigation of the Hope Memorial Bridge," *Report,* Ohio Department of Transportation, January.

Powers, T. C., and Helmuth, R. A. (1953). "Theory of Volume Changes in Hardened Portland-Cement Paste during Freezing," *Proceedings*, *Highway Research Board Annual Meeting*, National Academy of Science, pp. 285-297.

Powers, T. C. (1968). *The Properties of Fresh Concrete*, John Wiley and Sons, Inc. NY, 664 pp.

Price, W. H. (1982). "Control of Cracking during Construction," *Concrete International: Design and Construction*, Vol. 4, No. 1, January, pp. 40-43.

Qi, C., Weiss, J., and Olek, J. (2003). "Characterization of Plastic Shrinkage Cracking in Fiber Reinforced Concrete Using Image Analysis and a Modified Weibull Approach," *Materials & Structures*, Vol. 36, No. 6, January, pp. 386-395.

Qi, C., Weiss, J., and Olek, J. (2004). "Assessing the Settlement of Fresh Concrete Using a Non-Contact Laser Profiling Approach," *In International Conference on Construction Materials: ConMat'05*. Vancouver, Canada, December, 18 pp.

Ramachandran, V. S. (1995). *Concrete Admixtures Handbook,* second edition, Noyes Publications, Park Ridge, New Jersey, 1183 pp.

Ramey, G. E., Wolff, A. R., and Wright, R. L. (1997). "Structural Design Actions to Mitigate Bridge Deck Cracking," *Practice Periodical on Structural Design and Construction*, ASCE, Vol. 2, No. 3, July, pp. 118-124.

Rangaraju, P., Balitsaris, M., and Kizhakommudom, H. (2013). "Impact of Aggregate Gradation on Properties of Portland Cement," *Final Report*, Federal Highway Administration, Clemson University, South Carolina USA, October, 102 pp.

Reynolds, D., Browning, D., and Darwin, D. (2009). "Lightweight Aggregates as an Internal Curing Agent for Low-Cracking High-Performance Concrete," *SM Report* No. 97, University of Kansas Center for Research, Inc. Lawrence, KS, December, 151 pp.

Rose, J. H. (1987). "The Effects of Cementitious Blast-Furnace Slag on Chloride Permeability of Concrete," *Corrosion, Concrete, and Chlorides*, ACI SP-102, American Concrete Institute, Detroit, September, pp. 107-125.

Roy, D. M., and Idorn, G. M. (1983). "Hydration, Structure, and Properties of Blast Furnace Slag Cements, Mortars, and Concrete," *ACI Journal,* Vol. 79, No. 6, November, pp. 444-457.

Russell, H. G. (2004). "Concrete Bridge Deck Performance," *National Cooperative Highway Research Program (NCHRP) Synthesis* 333, Transportation Research Board, Washington, DC, 32 pp.

Sant, G., Eberhardt, A., Bentz, D., and Weiss, J. (2010). "Influence of Shrinkage-Reducing Admixtures on Moisture Absorption in Cementitious Materials at Early Ages," *Journal of Materials in Civil Engineering*, ASCE, Vol. 22, No. 3, March, pp. 277-286.

Sant, G., Lothenbach, B., Juilland, P., Le Saout, G., Weiss, J., and Scrivener, K. (2011). "The Origin of Early Age Expansions Induced in Cementitious Materials Containing Shrinkage Reducing Admixtures," *Cement and Concrete Research*, Vol. 41, No. 3, March, PP. 218-229.

Sayahi, F. (2016). "Plastic Shrinkage Cracking in Concrete," *Licentiate Thesis*, Lulea University of Technology, SE- 97187 Lulea, Sweden, September, 146 pp.

Scholer, C.F., and Baker, S. D. (1973). "Effect of variations in coarse aggregate gradation on properties of portland cement concrete," *Joint Highway Research Project*, West Lafayette, Purdue University, FHWA/IN/JHRP-73/12, Project C-36-42J, 1973, File No. 5-9-10, June, 55 pp.

Schemmel, J. J., Ray, J. C., and Kuss, M.L. (1999). "Impact of Shrinkage Reducing Admixture on Properties and Performance of Bridge Deck Concrete," *High-Performance Concrete: Research to practice, ACI SP – 189,* American Concrete Institute, Farmington Hills, Mich., January, pp. 367-386.

Schmeckpeper, E. R., and Lecoultre, S. T. (2008). "Synthesis into the Causes of Concrete Bridge Deck Cracking and Observation on the Initial Use of the High-Performance Concrete in the US 95 Bridge over the South Fork of the Palouse River," *Final Report* KLK491, National Institute for Advanced Transportation Technology, University of Idaho prepared for the Idaho Department of Transportation, June, 143 pp.

Schmitt, T. R., and Darwin, D. (1995). "Cracking in Concrete Bridge Decks," *SM Report* No. 39, University of Kansas Center for Research, Inc. Lawrence, KS, April, 164 pp.

Schmitt, T. R., and Darwin, D. (1999). "Effect of Material Properties on Cracking in Bridge Decks," *Journal of Bridge Engineering*, ASCE, Vol. 4, No. 1, February, pp. 8-13.

Sommer, H. (1979). "The Precision of the Microscopical Determination of the Air-Void System in Hardened Concrete," *Cement, Concrete, and Aggregates*, ASTM, Vol. 1, No. 2, January, pp. 49-55.

Stewart, C. F., and Gunderson, B. J. (1969). "Factors Affecting the Durability of Concrete Bridge Decks," *Interim Report* No. 2, Research and Development Section of Bridge Department, Sacramento, CA: California Department of Transportation, 36 pp.

Transportation Research Board. (2006). "Control of Cracking in Concrete," Transportation Research Circular E-C 107, Washington, DC, 56 pp.

U.S. Government Accountability Office. (2016). Report to Congressional Committees: Highway Bridge-Linking Funding to Condition May Help Demonstrate Impact of Federal Investment, 43 pp.

Verbeck, G. J and Klieger, P. (1956). "Studies of 'Salt' Scaling of Concrete," *Highway Research Board Bulletin 150*, December, pp. 1-13.

Wang J., Liu B., Xie S., and Wu Z. (1986). "Improvement of Paste-Aggregate Interface by Adding Silica Fume," *Proceedings of the 8th International Congress on the Chemistry of Cement*, Rio de Janeiro, V. 3, pp. 460-465.

Weyers, R. E., Conway Jr., J. C., and Cady, P. D. (1982). "Photoelastic Analysis of Rigid Inclusions in Fresh Concrete," *Cement and Concrete Research*, Vol. 12, No. 4, July, pp. 475-484.

Yoon, D. J., Weiss, W. J., and Shah, S. P. (2000). "Assessing Damage in Corroded Reinforced Concrete Using Acoustic Emission," *Journal of Engineering Mechanics,* Vol. 126, No. 3, March, pp. 273–283.

Yuan, J., Darwin, D., and Browning, J. (2011). "Development and Construction of Low-Cracking High-Performance Concrete Bridge Decks: Free Shrinkage Tests, Restrained Shrinkage Tests, Construction Experience, and Crack Survey Results," *SM Report* No. 103, University of Kansas Center for Research, Inc. Lawrence, KS, September, 505 pp.

APPENDIX A: MATERIAL PROPERTIES AND CONCRETE MIXTURE PROPORTIONS

Table A.1 - Cement and supplementary cementitious materials chemical composition

Type	Portland Cement			Grade 100 Slag Cement	Silica Fume	Fly Ash	
Sample No.	I/II					Class F	Class C
	C1	C2	C3				
Manufacturer	La Farge	Ash Grove	Ash Grove	Ash Grove	Ash Grove	Headwaters	Ash Grove
Specific Gravity	3.15	3.15	3.12	2.86	2.2	2.55	2.87
Blaine Fineness (m^2/kg)	365	--	399	584	---	---	---
Oxides	**Percentage by Weight**						
Bogue Analysis							
C_3S	55	53	60	55.3	---	---	---
C_2S	17	19	14	16.6	---	---	---
C_3A	7	7	5	7.9	---	---	---
C_4AF	10	11	9	8.8	---	---	---
XRF							
SiO_2	20.4	20.05	20.7	34.92	94.49	55.67	34.99
Al_2O_3	4.70	4.46	3.97	7.64	0.07	15.42	17.06
Fe_2O_3	3.10	3.33	3.05	0.69	0.10	5.20	5.33
CaO	64.00	62.87	64.56	40.94	0.53	12.79	30.41
MgO	1.20	2.10	1.99	10.25	0.62	4.22	4.54
SO_3	2.90	2.68	2.97	2.72	0.11	0.66	1.87
Na_2O	0.27	0.22	0.20	0.3	0.09	1.99	1.47
K_2O	0.41	0.52	0.52	0.55	0.54	2.08	0.55
TiO_2	0.37	0.27	0.33	0.37	0.01	0.50	1.33
P_2O_5	1.60	0.16	1.50	0.01	0.08	0.12	0.79
Mn_2O_3	0.08	0.1	0.09	0.53	0.02	0.04	0.04
SrO	0.10	0.11	0.10	0.05	0.01	0.26	0.31
LOI	2.40	3.43	2.29	0.97	3.21	0.43	0.65
Total	100.13	100.3	100.16	100.01	99.9	99.83	99.68
Alkali Equivalent (EQV)	0.53	0.56	0.55	0.66	---	1.70	1.83

Table A.2 - Coarse aggregate properties and gradations

Granite-A					
Max. Aggregate Size	1-in. (25-mm)	3/4-in. (19-mm)	3/4-in. (19-mm)	3/4-in. (19-mm)	1-in. (25-mm)
Sample No.	G-1	G-2	G-3	G-4	G-5
Source	MCM				
Specific Gravity (SSD)	2.61	2.64	2.64	2.6	2.61
Absorption (%)	0.64	0.55	0.44	0.55	0.5
Sieve Size	**Percent Retained on Each Sieve**				
1-1/2-in. (37.5-mm)	0	0	0	0	0
1-in. (25-mm)	19.2	0	0	0	0.4
3/4-in. (19-mm)	25.1	5.7	25.1	16.5	15.9
1/2-in. (12.5-mm)	28.7	55.4	66.8	54.6	78.9
3/8-in. (9.5-mm)	12.2	36.6	7.4	24.7	4.1
No. 4 (4.75-mm)	10.7	2	0	1.5	0.1
No. 8 (2.36-mm)	2.1	0	0	2.7	0
No. 16 (1.18-mm)	0	0	0	0	0
No. 30 (0.60-mm)	0	0	0	0	0
No. 50 (0.30-mm)	0	0	0	0	0
No. 100 (0.15-mm)	0	0	0	0	0
Pan	1.90	0.30	0.70	0.00	0.70

Table A.2 - (Cont'd) Coarse aggregate properties and gradations

Granite-A						
Max. Aggregate Size	3/4-in. (19-mm)	1-in. (25-mm)	1-in. (25-mm)	3/4-in. (19-mm)	3/4-in. (19--mm)	3/4-in. (19-mm)
Sample No.	G-6	G-7	G-8	G-9	G-10	G-11
Source	MCM					
Specific Gravity (SSD)	2.61	2.64	2.64	2.62	2.62	2.61
Absorption (%)	0.5	0.5	0.5	0.58	0.58	---
Sieve Size	**Percentage Retained on Each Sieve**					
1-1/2-in. (37.5-mm)	0	0	0	0	0	0
1-in. (25-mm)	0	0.8	2.1	0	0	0
3/4-in. (19-mm)	15.6	29	26.9	16.7	16.7	6.9
1/2-in. (12.5-mm)	81.6	63.7	67	79.9	79.7	89.2
3/8-in. (9.5-mm)	1.2	5.5	3.8	3.0	2.9	3.8
No. 4 (4.75-mm)	0.1	0.35	0.1	0.1	0.1	0
No. 8 (2.36-mm)	0	0	0	0	0	0
No. 16 (1.18-mm)	0	0	0	0	0	0
No. 30 (0.60-mm)	0	0	0	0	0	0
No. 50 (0.30-mm)	0	0	0	0	0	0
No. 100 (0.15-mm)	0	0	0	0	0	0
Pan	1.50	1.00	0.30	0.40	0.35	0.00

Table A.2 - (Cont'd) Coarse aggregate properties and gradations

Granite-B						
Max. Aggregate Size	No. 4 (4.75-mm)	3/8-in. (9-mm)	3/8-in. (9-mm)	3/8-in. (9-mm)	1/2-in. (12.5-mm)	1/2-in. (12.5-mm)
Sample No.	G-1	G-2	G-3	G-4	G-5	G-6
Source	MCM					
Specific Gravity (SSD)	2.61	2.64	2.64	2.6	2.6	2.6
Absorption (%)	0.7	0.75	0.76	0.7	0.58	0.58
Sieve Size	**Percent Retained on Each Sieve**					
3/8-in. (9.5-mm)	0	1.9	62	0.7	38.2	52.1
No. 4 (4.75-mm)	85.9	84.9	34.9	90.5	57.4	43.0
No. 8 (2.36-mm)	11.7	12.1	1.6	3.7	2.8	2.1
No. 16 (1.18-mm)	0	0	0	0	0	0
No. 30 (0.60-mm)	0	0	0	0	0	0
No. 50 (0.30-mm)	0	0	0	0	0	0
No. 100 (0.15-mm)	0	0	0	0	0	0
Pan	2.30	1.10	1.60	5.10	1.10	2.10

Table A.2 - (Cont'd) Coarse aggregate properties and gradations

Granite-B						
Max. Aggregate Size	1/2-in. (12.5-mm)	3/4-in. (19-mm)	1-in. (25-mm)	3/4-in. (19-mm)	1/2-in. (12.5-mm)	1/2-in. (12.5-mm)
Sample No.	G-7	G-8	G-9	G-10	G-11	G-12
Source	MCM					
Specific Gravity (SSD)	2.64	2.64	2.62	2.62	2.62	2.6
Absorption (%)	0.58	0.58	0.58		0.58	---
Sieve Size	**Percent Retained on Each Sieve**					
1-in. (25-mm)	0	0	0	0	0	0
3/4-in. (19-mm)	0	2.1	0	0.2	0	0
1/2-in. (12.5-mm)	0.3	26.9	0.7	0.2	1.4	1.1
3/8-in. (9.5-mm)	20.3	67.0	44.5	44.9	52.2	26.5
No. 4 (4.75-mm)	72.6	3.8	52.3	44.6	43.4	65.8
No. 8 (2.36-mm)	5.6	0.1	2.1	3.8	2.7	3.9
No. 16 (1.18-mm)	0	0	0	0	0	0
No. 30 (0.60-mm)	0	0	0	0	0	0
No. 50 (0.30-mm)	0	0	0	0	0	0
No. 100 (0.15-mm)	0	0	0	0	0	0
Pan	1.20	0.20	0.30	6.50	0.35	2.56

Table A.3 – Fine aggregate properties and gradations

Sample No.	Sand					
	S-1	S-2	S-3	S-4	S-5	S-6
Source	MCM					
Specific Gravity (SSD)	2.59	2.63	2.62	2.62	2.62	2.62
Absorption (%)	0.64	0.42	0.69	0.69	----	0.56
Sieve Size	**Percent Retained on Each Sieve**					
3/8-in. (9.5-mm)	0	0	0	0	0	0
No. 4 (4.75-mm)	1.1	1.7	2.4	2.6	3.7	3.2
No. 8 (2.36-mm)	8.9	10.5	13.1	10.5	12.5	13.8
No. 16 (1.18-mm)	19.2	23.7	23.3	18.8	21.3	17.7
No. 30 (0.60-mm)	27.8	28.6	29.0	24.3	26.9	21.1
No. 50 (0.30-mm)	34.1	29.6	27.6	31.7	28.5	26.3
No. 100 (0.15-mm)	8.1	5.2	4.3	11.2	6.7	14.2
No. 200 (0.075-mm)	0.8	0.3	0.3	0.8	0.4	2.5
Pan	0.2	0.6	0.1	0.2	0	1.2

Table A.3 – (Cont'd) Fine aggregate properties and gradations

Sample No.	Sand						
	S-7	S-8	S-9	S-10	S-11	S-12	S-13
Source	MCM						
Specific Gravity (SSD)	2.62	2.62	2.62	2.62	2.62	2.62	2.62
Absorption (%)	0.42	0.41	0.47	0.49	0.47	0.47	0.47
Sieve Size	**Percentage Retained on Each Sieve**						
3/8-in. (9.5-mm)	0	0	0	0	0	0	0
No. 4 (4.75-mm)	3.0	0.9	2.2	1.1	1.2	2.5	2.1
No. 8 (2.36-mm)	12.5	11.7	11.4	6.7	11.0	14.4	11.0
No. 16 (1.18-mm)	16.8	18.2	16.5	15.9	20.3	22.4	22.7
No. 30 (0.60-mm)	17.4	20.9	19.4	21.6	21.8	23.0	25.8
No. 50 (0.30-mm)	32.5	30.8	31.3	26.6	26.1	23.2	26.4
No. 100 (0.15-mm)	14.6	13.8	15.2	19.5	15.2	10.5	9.6
No. 200 (0.075-mm)	2.2	1.5	1.1	0.1	0.1	3.1	1.6
Pan	1.1	2	2.9	8.5	4.4	0.9	0.9

Table A.3 – (Cont'd) Fine aggregate properties and gradations

Sample No.	Pea Gravel							
	PG-1	PG-2	PG-3	PG-4	PG-5	PG-6	PG-7	PG-8
Source	MCM							
Specific Gravity (SSD)	2.61	2.62	2.61	2.61	2.61	2.61	2.63	2.61
Absorption (%)	0.47	0.84	1.42	--	--	0.8	1.42	--
Sieve Size	**Percent Retained on Each Sieve**							
3/8-in. (9.5-mm)	0	0	0	0	0	0	0	0
No. 4 (4.75-mm)	11.5	14	15.1	13.3	11.4	14.4	14.4	19.1
No. 8 (2.36-mm)	50.2	59.1	49.7	51.3	58.2	53.1	53.1	69
No. 16 (1.18-mm)	31.5	24.4	29.9	30	26.3	28.5	28.5	9.8
No. 30 (0.60-mm)	5.1	2.1	4.4	4.3	3	3.1	3.1	0.9
No. 50 (0.30-mm)	1.2	0.3	0.6	0.9	0.7	0.6	0.6	0.6
No. 100 (0.15-mm)	0.3	0	0.1	0.2	0.2	0.2	0.2	0.3
No. 200 (0.075-mm)	0.1	0	0	0	0.1	0	0	0.1
Pan	0.2	0	0	0	0.2	0.1	0.2	0.3

Table A.4 – Lightweight aggregate properties and gradations

Sample No.	LWA	
	LWA-1	LWA-2
Source	Marquette, KS	
Specific Gravity (PSD)	1.6	1.72
Absorption (%)	26.24	23.99
Sieve Size	**Percentage Retained on Each Sieve**	
3/8-in. (9.5-mm)	0	0
No. 4 (4.75-mm)	7.1	8
No. 8 (2.36-mm)	80.7	59.2
No. 16 (1.18-mm)	10.6	21
No. 30 (0.60-mm)	0.8	5.6
No. 50 (0.30-mm)	0.5	1.8
No. 100 (0.15-mm)	0.3	0.8
No. 200 (0.075-mm)	0	0.9
Pan	0	2.8

Table A.5 - Mixture proportions of Control-1 concrete

Batch Number	C01	C02	C03	C04	C05	C06	C07	C08	C09
Cement lb/yd³	593[C2]	593[C2]	593[C2]	593[C2]	593[C2]	593[C2]	593[C2]	593[C2]	593[C2]
kg/m³	352	352	352	352	352	352	352	352	352
Water lb/yd³	267	267	267	267	267	267	267	267	267
kg/m³	158	158	158	158	158	158	158	158	158
Sand (SSD) lb/yd³	905[S12]	905[S12]	905[S12]	905[S12]	905[S12]	905[S12]	905[S12]	905[S12]	905[S12]
kg/m³	537	537	537	537	537	537	537	537	537
Pea Gravel (SSD) lb/yd³	534[PG7]	534[PG7]	534[PG7]	534[PG7]	534[PG7]	534[PG7]	534[PG7]	534[PG7]	534[PG7]
kg/m³	317	317	317	317	317	317	317	317	317
Granite A (SSD) lb/yd³	929[G10]	929[G10]	929[G10]	929[G10]	929[G10]	929[G10]	929[G10]	929[G10]	929[G10]
kg/m³	551	551	551	551	551	551	551	551	551
Granite B (SSD) lb/yd³	496[G11]	496[G11]	496[G11]	496[G11]	496[G11]	496[G11]	496[G11]	496[G11]	496[G11]
kg/m³	294	294	294	294	294	294	294	294	294
Superplasticizer fl oz/yd³	4.1	1.9	0.0	0.0	3.7	0.0	5.6	0.0	0.0
kg/m³	159	74	0	0	143	0	217	0	0
AEA fl oz/yd³	2.3	2.4	2.4	2.4	2.6	2.6	2.6	2.6	2.4
kg/m³	89	93	93	93	101	101	101	101	93

Note:
Cement – C2, see Table A.1,
Sand – S12, see Table A.3,
Pea Gravel – PG7, see Table A.3,
Granite A – G10, see Table A.2,
Granite B – G11, see Table A.2.

Table A.6 - Mixture proportions of Control-2 concrete

Batch Number	C10	C11	C12	C13	C14	C15	C16	C17	C18
Cement lb/yd³	593[C3]	593[C3]	593[C3]	593[C3]	593[C3]	593[C3]	593[C3]	593[C3]	593[C3]
kg/m³	352	352	352	352	352	352	352	352	352
Water lb/yd³	267	267	267	267	267	267	267	267	267
kg/m³	158	158	158	158	158	158	158	158	158
Sand (SSD) lb/yd³	1064[S13]	1064[S13]	1064[S13]	1064[S13]	1064[S13]	1064[S13]	1064[S13]	1064[S13]	1064[S13]
kg/m³	631	631	631	631	631	631	631	631	631
Pea Gravel (SSD) lb/yd³	371[PG8]	371[PG8]	371[PG8]	371[PG8]	371[PG8]	371[PG8]	371[PG8]	371[PG8]	371[PG8]
kg/m³	220	220	220	220	220	220	220	220	220
Granite A (SSD) lb/yd³	728[G11]	728[G11]	728[G11]	728[G11]	728[G11]	728[G11]	728[G11]	728[G11]	728[G11]
kg/m³	432	432	432	432	432	432	432	432	432
Granite B (SSD) lb/yd³	695[G12]	695[G12]	695[G12]	695[G12]	695[G12]	695[G12]	695[G12]	695[G12]	695[G12]
kg/m³	412	412	412	412	412	412	412	412	412
Superplasticizer fl oz/yd³	7.4	14.9	18.6	0.0	11.2	0.0	13.0	19.7	19.7
mL/m³	287	577	720	0	432	0	503	763	763
AEA fl oz/yd³	4.1	5.6	5.6	6.9	8.9	8.9	8.9	3.7	5.6
mL/m³	159	217	217	267	345	345	345	143	217

Note:
Cement – C3, see Table A.1,
Sand – S13, see Table A.3,
Pea Gravel – PG8, see Table A.3,
Granite A – G11, see Table A.2,
Granite B – G12, see Table A.2.

Table A.7 - Mixture proportions of Control-3 concrete

Batch Number	GA01	GA02	GA03	GA04	GA05	GA06
Cement lb/yd³	593[C3]	593[C3]	593[C3]	593[C3]	593[C3]	593[C3]
kg/m³	352	352	352	352	352	352
Water lb/yd³	267	267	267	267	267	267
kg/m³	158	158	158	158	158	158
Sand (SSD) lb/yd³	1101[S13]	1101[S13]	1101[S13]	1101[S13]	1101[S13]	1101[S13]
kg/m³	653	653	653	653	653	653
Pea Gravel (SSD) lb/yd³	0	0	0	0	0	0
kg/m³	0	0	0	0	0	0
Granite* (SSD) lb/yd³	1718	1718	1718	1718	1718	1718
kg/m³	1019	1019	1019	1019	1019	1019
Superplasticizer fl oz/yd³	7.4	0.0	14.9	14.9	0.0	11.1
mL/m³	287	0	575	575	0	431
AEA fl oz/yd³	8.2	8.9	8.2	8.2	8.9	8.2
mL/m³	316	345	316	316	345	316

Note:
Cement – C3, see Table A.1,
Sand – S13, see Table A.3.
* Granite – No gradation available.

Table A.8 - Mixture proportions of 5.9 lb-IC concrete

Batch Number	IC01	IC02	IC03	IC04	IC05	IC06	IC07	IC08
Cement lb/yd^3	593^{C1}	593^{C1}	593^{C1}	593^{C1}	593^{C1}	593^{C1}	593^{C1}	593^{C1}
kg/m^3	352	352	352	352	352	352	352	352
Water lb/yd^3	267	267	267	267	267	267	267	267
kg/m^3	158	158	158	158	158	158	158	158
LWA (WSD) lb/yd^3	180^{LWA1}	180^{LWA1}	180^{LWA1}	180^{LWA1}	180^{LWA1}	180^{LWA1}	180^{LWA1}	180^{LWA1}
kg/m^3	107	107	107	107	107	107	107	107
Sand (SSD) lb/yd^3	1081^{S12}	1081^{S12}	1081^{S12}	1081^{S12}	1081^{S12}	1081^{S12}	1081^{S12}	1081^{S12}
kg/m^3	641	641	641	641	641	641	641	641
Pea Gravel (SSD) lb/yd^3	172^{PG7}	172^{PG7}	172^{PG7}	172^{PG7}	172^{PG7}	172^{PG7}	172^{PG7}	172^{PG7}
kg/m^3	102	102	102	102	102	102	102	102
Granite A (SSD) lb/yd^3	535^{G10}	535^{G10}	535^{G10}	535^{G10}	535^{G10}	535^{G10}	535^{G10}	535^{G10}
kg/m^3	317	317	317	317	317	317	317	317
Granite B (SSD) lb/yd^3	812^{G11}	812^{G11}	812^{G11}	812^{G11}	812^{G11}	812^{G11}	812^{G11}	812^{G11}
kg/m^3	482	482	482	482	482	482	482	482
Superplasticizer fl oz/yd^3	0.0	0.0	0.0	3.7	0.0	3.7	7.4	7.4
mL/m^3	0	0	0	143	0	143	287	287
AEA fl oz/yd^3	2.4	1.9	1.9	1.9	1.9	1.9	2.6	2.7
mL/m^3	93	74	74	74	74	74	101	105

Note:
Cement – C2, see Table A.1,
LWA – LWA1, see Table A.4
Sand – S12, see Table A.3,
Pea Gravel – PG7, see Table A.3,
Granite A – G10, see Table A.2,
Granite B – G11, see Table A.2.

Table A.9 - Mixture proportions of 7 lb-IC concrete

Batch Number	IC09	IC10	IC11	IC12	IC13	IC14	IC15	IC16
Cement lb/yd^3	593^{C3}	593^{C3}	593^{C3}	593^{C3}	593^{C3}	593^{C3}	593^{C3}	593^{C3}
kg/m^3	352	352	352	352	352	352	352	352
Water lb/yd^3	267	267	267	267	267	267	267	267
kg/m^3	158	158	158	158	158	158	158	158
LWA (WSD) lb/yd^3	215^{LWA2}	215^{LWA2}	215^{LWA2}	215^{LWA2}	215^{LWA2}	215^{LWA2}	215^{LWA2}	215^{LWA2}
kg/m^3	128	128	128	128	128	128	128	128
Sand (SSD) lb/yd^3	907^{S13}	907^{S13}	907^{S13}	907^{S13}	907^{S13}	907^{S13}	907^{S13}	907^{S13}
kg/m^3	538	538	538	538	538	538	538	538
Pea Gravel (SSD) lb/yd^3	172^{PG8}	172^{PG8}	172^{PG8}	172^{PG8}	172^{PG8}	172^{PG8}	172^{PG8}	172^{PG8}
kg/m^3	102	102	102	102	102	102	102	102
Granite A (SSD) lb/yd^3	685^{G11}	685^{G11}	685^{G11}	685^{G11}	685^{G11}	685^{G11}	685^{G11}	685^{G11}
kg/m^3	406	406	406	406	406	406	406	406
Granite B (SSD) lb/yd^3	765^{G12}	765^{G12}	765^{G12}	765^{G12}	765^{G12}	765^{G12}	765^{G12}	765^{G12}
kg/m^3	454	454	454	454	454	454	454	454
Superplasticizer fl oz/yd^3	11.2	0.0	0.0	0.0	0.0	0.0	27.9	27.9
mL/m^3	434	0	0	0	0	0	1080	1080
AEA fl oz/yd^3	2.8	3.0	3.7	7.4	5.2	4.5	4.5	3.7
mL/m^3	108	116	143	287	201	174	174	143

Note:
Cement – C3, see Table A.1,
LWA – LWA2, see Table A.4,
Sand – S13, see Table A.3,
Pea Gravel – PG8, see Table A.3,
Granite A – G11, see Table A.2,
Granite B – G12, see Table A.2.

Table A.10 - Mixture proportions of 30% Slag concrete

Batch Number	S01	S02	S03	S04	S05	S06	S07	S08	S09	S10	S11
Cement lb/yd³	426[C3]	426[C3]	426[C3]	426[C3]	426[C3]	426[C3]	426[C3]	426[C3]	426[C3]	426[C3]	426[C3]
kg/m³	253	253	253	253	253	253	253	253	253	253	253
Water lb/yd³	264	264	264	264	264	264	264	264	264	264	264
kg/m³	157	157	157	157	157	157	157	157	157	157	157
Slag Cement lb/yd³	160	160	160	160	160	160	160	160	160	160	160
kg/m³	95	95	95	95	95	95	95	95	95	95	95
Sand (SSD) lb/yd³	1057[S13]	1057[S13]	1057[S13]	1057[S13]	1057[S13]	1057[S13]	1057[S13]	1057[S13]	1057[S13]	1057[S13]	1057[S13]
kg/m³	627	627	627	627	627	627	627	627	627	627	627
Pea Gravel (SSD) lb/yd³	373[PG8]	373[PG8]	373[PG8]	373[PG8]	373[PG8]	373[PG8]	373[PG8]	373[PG8]	373[PG8]	373[PG8]	373[PG8]
kg/m³	221	221	221	221	221	221	221	221	221	221	221
Granite A (SSD) lb/yd³	697[G11]	697[G11]	697[G11]	697[G11]	697[G11]	697[G11]	697[G11]	697[G11]	697[G11]	697[G11]	697[G11]
kg/m³	414	414	414	414	414	414	414	414	414	414	414
Granite B (SSD) lb/yd³	731[G12]	731[G12]	731[G12]	731[G12]	731[G12]	731[G12]	731[G12]	731[G12]	731[G12]	731[G12]	731[G12]
kg/m³	434	434	434	434	434	434	434	434	434	434	434
Superplasticizer fl oz/yd³	7.4	18.6	0.0	0.0	0.0	18.6	0.0	11.2	0.0	22.3	27.9
mL/m³	287	720	0	0	0	720	0	434	0	863	1080
AEA fl oz/yd³	2.71	2.23	2.68	2.67	4.46	4.09	4.83	5.57	5.2	5.57	5.76
mL/m³	105	86	104	103	173	158	187	216	201	216	223

Note:
Cement – C3, see Table A.1,
Sand – S13, see Table A.3,
Pea Gravel – PG8, see Table A.3,
Granite A – G11, see Table A.2,
Granite B – G12, see Table A.2.

Table A.11 - Mixture proportions of 30% Slag - 3% SF concrete

Batch Number	SSF01	SSF02	SSF03	SSF04	SSF05	SSF06	SSF07	SSF08	SSF09	SSF10
Cement lb/yd³	411[C3]	411[C3]	411[C3]	411[C3]	411[C3]	411[C3]	411[C3]	411[C3]	411[C3]	411[C3]
kg/m³	244	244	244	244	244	244	244	244	244	244
Water lb/yd³	263	263	263	263	263	263	263	263	263	263
kg/m³	156	156	156	156	156	156	156	156	156	156
Slag Cement lb/yd³	160	160	160	160	160	160	160	160	160	160
kg/m³	95	95	95	95	95	95	95	95	95	95
Silica Fume lb/yd³	13	13	13	13	13	13	13	13	13	13
kg/m³	8	8	8	8	8	8	8	8	8	8
Sand (SSD) lb/yd³	1056[S13]	1056[S13]	1056[S13]	1056[S13]	1056[S13]	1056[S13]	1056[S13]	1056[S13]	1056[S13]	1056[S13]
kg/m³	626	626	626	626	626	626	626	626	626	626
Pea Gravel (SSD) lb/yd³	375[PG8]	375[PG8]	375[PG8]	375[PG8]	375[PG8]	375[PG8]	375[PG8]	375[PG8]	375[PG8]	375[PG8]
kg/m³	222	222	222	222	222	222	222	222	222	222
Granite A (SSD) lb/yd³	698[G11]	698[G11]	698[G11]	698[G11]	698[G11]	698[G11]	698[G11]	698[G11]	698[G11]	698[G11]
kg/m³	414	414	414	414	414	414	414	414	414	414
Granite B (SSD) lb/yd³	731[G12]	731[G12]	731[G12]	731[G12]	731[G12]	731[G12]	731[G12]	731[G12]	731[G12]	731[G12]
kg/m³	434	434	434	434	434	434	434	434	434	434
Superplasticizer fl oz/yd³	0.0	7.40	14.9	27.9	22.3	14.9	11.2	24.2	3.7	0.0
mL/m³	0	287	575	1079	863	575	432	935	144	0
AEA fl oz/yd³	4.5	7.4	10.0	10.0	9.3	8.6	8.2	8.9	9.7	9.7
mL/m³	173	288	388	388	360	331	316	345	374	374

Note:
Cement – C3, see Table A.1,
Sand – S13, see Table A.3,
Pea Gravel – PG8, see Table A.3,
Granite A – G11, see Table A.2,
Granite B – G12, see Table A.2.

Table A.12 - Mixture proportions of 30% slag - 7 lb-IC concrete

Batch Number	SIC01	SIC02	SIC03	SIC04	SIC05	SIC06	SIC07	SIC08	SIC09
Cement lb/yd^3	426^{C3}	426^{C3}	426^{C3}	426^{C3}	426^{C3}	426^{C3}	426^{C3}	426^{C3}	426^{C3}
kg/m^3	253	253	253	253	253	253	253	253	253
Water lb/yd^3	264	264	264	264	264	264	264	264	264
kg/m^3	157	157	157	157	157	157	157	157	157
Slag Cement lb/yd^3	160	160	160	160	160	160	160	160	160
kg/m^3	95	95	95	95	95	95	95	95	95
LWA (WSD) lb/yd^3	212^{LWA2}	212^{LWA2}	212^{LWA2}	212^{LWA2}	212^{LWA2}	212^{LWA2}	212^{LWA2}	212^{LWA2}	212^{LWA2}
(kg/m^3	126	126	126	126	126	126	126	126	126
Sand (SSD) lb/yd^3	884^{S13}	884^{S13}	884^{S13}	884^{S13}	884^{S13}	884^{S13}	884^{S13}	884^{S13}	884^{S13}
kg/m^3	524	524	524	524	524	524	524	524	524
Pea Gravel (SSD) lb/yd^3	198^{PG8}	198^{PG8}	198^{PG8}	198^{PG8}	198^{PG8}	198^{PG8}	198^{PG8}	198^{PG8}	198^{PG8}
kg/m^3	117	117	117	117	117	117	117	117	117
Granite A (SSD) lb/yd^3	764^{G11}	764^{G11}	764^{G11}	764^{G11}	764^{G11}	764^{G11}	764^{G11}	764^{G11}	764^{G11}
kg/m^3	453	453	453	453	453	453	453	453	453
Granite B (SSD) lb/yd^3	686^{G12}	686^{G12}	686^{G12}	686^{G12}	686^{G12}	686^{G12}	686^{G12}	686^{G12}	686^{G12}
kg/m^3	407	407	407	407	407	407	407	407	407
Superplasticizer fl oz/yd^3	0.0	9.3	18.6	11.2	13.0	18.6	24.2	27.1	22.3
mL/m^3	0	360	720	434	503	720	937	1049	863
AEA fl oz/yd^3	5.2	5.6	5.8	5.9	5.6	5.6	5.9	5.8	5.6
mL/m^3	202	217	225	228	217	217	228	225	217

Note:
Cement – C3, see Table A.1,
LWA – LWA2, see Table A.4,
Sand – S13, see Table A.3,
Pea Gravel – PG8, see Table A.3,
Granite A – G11, see Table A.2,
Granite B – G12, see Table A.2.

Table A.13 - Mixture proportions of 30% Slag - 3% SF - 7 lb-IC concrete

Batch Number	SSFIC01	SSFIC02	SSFIC03	SSFIC04	SSFIC05	SSFIC06	SSFIC07	SSFIC08
Cement lb/yd³	411[C3]	411[C3]	411[C3]	411[C3]	411[C3]	411[C3]	411[C3]	411[C3]
kg/m³	244	244	244	244	244	244	244	244
Water lb/yd³	263	263	263	263	263	263	263	263
kg/m³	156	156	156	156	156	156	156	156
Slag Cement lb/yd³	160	160	160	160	160	160	160	160
kg/m³	95	95	95	95	95	95	95	95
Silica Fume lb/yd³	13	13	13	13	13	13	13	13
kg/m³	8	8	8	8	8	8	8	8
LWA (WSD) lb/yd³	212[LWA2]	212[LWA2]	212[LWA2]	212[LWA2]	212[LWA2]	212[LWA2]	212[LWA2]	212[LWA2]
kg/m³	126	126	126	126	126	126	126	126
Sand (SSD) lb/yd³	1056[S13]	1056[S13]	1056[S13]	1056[S13]	1056[S13]	1056[S13]	1056[S13]	1056[S13]
kg/m³	626	626	626	626	626	626	626	626
Pea Gravel (SSD) lb/yd³	375[PG8]	375[PG8]	375[PG8]	375[PG8]	375[PG8]	375[PG8]	375[PG8]	375[PG8]
kg/m³	222	222	222	222	222	222	222	222
Granite A (SSD) lb/yd³	698[G11]	698[G11]	698[G11]	698[G11]	698[G11]	698[G11]	698[G11]	698[G11]
kg/m³	414	414	414	414	414	414	414	414
Granite B (SSD) lb/yd³	731[G12]	731[G12]	731[G12]	731[G12]	731[G12]	731[G12]	731[G12]	731[G12]
kg/m³	434	434	434	434	434	434	434	434
Superplasticizer fl oz/yd³	0.0	7.4	14.9	22.3	26.0	0.0	37.2	24.2
mL/m³	0	287	577	863	1007	0	1440	937
AEA fl oz/yd³	8.9	10.0	11.2	11.2	9.7	11.3	9.3	9.7
mL/m³	345	387	434	434	376	437	360	376

Note:
Cement – C3, see Table A.1,
LWA – LWA2, see Table A.4,
Sand – S13, see Table A.3,
Pea Gravel – PG8, see Table A.3,
Granite A – G11, see Table A.2,
Granite B – G12, see Table A.2.

Table A.14 - Mixture proportions of 2% SRA concrete

Batch Number	SRA01	SRA02	SRA03	SRA04	SRA05	SRA06	SRA07	SRA08
Cement lb/yd^3	593^{C3}	593^{C3}	593^{C3}	593^{C3}	593^{C3}	593^{C3}	593^{C3}	593^{C3}
kg/m^3	352	352	352	352	352	352	352	352
Water lb/yd^3	255	255	255	255	255	255	255	255
kg/m^3	151	151	151	151	151	151	151	151
Sand (SSD) lb/yd^3	1064^{S13}	1064^{S13}	1064^{S13}	1064^{S13}	1064^{S13}	1064^{S13}	1064^{S13}	1064^{S13}
kg/m^3	631	631	631	631	631	631	631	631
Pea Gravel (SSD) lb/yd^3	371^{PG8}	371^{PG8}	371^{PG8}	371^{PG8}	371^{PG8}	371^{PG8}	371^{PG8}	371^{PG8}
kg/m^3	220	220	220	220	220	220	220	220
Granite A (SSD) lb/yd^3	695^{G11}	695^{G11}	695^{G11}	695^{G11}	695^{G11}	695^{G11}	695^{G11}	695^{G11}
kg/m^3	412	412	412	412	412	412	412	412
Granite B (SSD) lb/yd^3	728^{G12}	728^{G12}	728^{G12}	728^{G12}	728^{G12}	728^{G12}	728^{G12}	728^{G12}
kg/m^3	432	432	432	432	432	432	432	432
SRA fl oz/yd^3	182	182	182	182	182	182	182	182
mL/m^3	7036	7036	7036	7036	7036	7036	7036	7036
Superplasticizer fl oz/yd^3	1.86	0.0	3.7	7.43	14.9	0.0	29.7	24.2
mL/m^3	55	0	143	288	575	0	1150	934
AEA fl oz/yd^3	7.06	4.83	4.46	3.71	2.97	4.1	3.7	3.7
mL/m^3	273	187	173	144	115	159	143	143

Note:
Cement – C3, see Table A.1,
Sand – S13, see Table A.3,
Pea Gravel – PG8, see Table A.3,
Granite A – G11, see Table A.2,
Granite B – G12, see Table A.2.

Table A.15 - Mixture proportions of concrete, containing shrinkage-reducing admixtures, evaluated for durability performance

Batch Number	**926**	**927**	**976**	**894**	**896**	**887**	**960**	**886**	**897**	**928**	**963**
Batch Designation	**Control # 1**	**Control # 2**	**Control # 3**	**0.5% SRA-2**	**1% SRA-2 # 1**	**1% SRA-2 # 2**	**1% SRA-2 # 3**	**2% SRA-2 # 1**	**2% SRA-2 # 2**	**0.75% SRA-3**	**2.25% SRA-3**
Cement lb/yd³	520[C1]	520[C1]	520[C1]	520[C1]	520[C1]	520[C1]	520[C1]	520[C1]	520[C1]	520[C1]	520[C1]
kg/m³	309	309	309	309	309	309	309	309	309	309	309
Water lb/yd³	234	234	218	231	228	228	228	223	223	230	222
kg/m³	139	139	129	137	135	135	135	132	132	136	132
Sand (SSD) lb/yd³	1031[S10]	1079[S11]	1035[S11]	1053[S7]	1053[S7]	983[S6]	1053[S7]	930[S5]	1086[S8]	1073[S10]	1103[S11]
kg/m³	612	640	614	625	625	583	625	552	644	637	654
Pea Gravel (SSD) lb/yd³	602[PG6]	605[PG6]	540[PG6]	561[PG5]	561[PG5]	739[PG4]	561[PG5]	806[PG3]	562[PG5]	565[PG6]	493[PG6]
kg/m³	357	359	320	333	333	438	333	478	333	335	292
Granite A (SSD) lb/yd³	854[G7]	802[G8]	477[G9]	1043[G4]	1043[G4]	505[G3]	1043[G4]	508[G3]	671[G5]	559[G7]	579[G9]
kg/m³	507	476	283	619	619	300	619	301	398	332	344
Granite B (SSD) lb/yd³	541[G8]	541[G9]	964[G10]	347[G5]	347[G5]	796[G4]	347[G5]	779[G4]	685[G6]	829[G8]	841[G10]
kg/m³	321	321	572	206	206	472	206	462	406	492	499
SRA fl oz/yd³	0.0	0.0	0.0	40	80	80	80	160	160	60	180
mL/m³	0	0	0	1547	3095	3095	3095	6189	6189	2321	6963
Superplasticizer fl oz/yd³	0.0	0.68	6.76	2.3	4.0	2.3	4.0	4.5	4.5	2.25	2.25
mL/m³	0	27	262	89	155	89	155	174	174	87	87
AEA fl oz/yd³	2.03	3.0	7.4	1.7	1.65	1.7	1.65	1.8	1.8	3.0	3.0
mL/m³	79	116	288	66	64	66	64	70	70	116	116

Note:
Cement – C1, see Table A.1,
Sand – S5, S6, S7, S8, S10, and S11, see Table A.3,
Pea Gravel – PG3, PG4, PG5, PG6, PG8, PG9, and PG10, see Table A.3,
Granite A – G3, G4, G5, G7, G8, and G9, see Table A.2,
Granite B – G4, G5, G6, G8, G9, and G10, see Table A.2.

Table A.16 - Mixture proportions of concrete, containing fly ash and a rheology modifying admixture, evaluated for durability performance

Batch Number	**879**	**890**	**913**	**889**	**880**	**905**	**909**	**899**	**967**	**911**	**912**
Batch Designation	**20% FA-F # 1**	**20% FA-F # 2**	**20% FA-C**	**40% FA-F # 1**	**40% FA-F # 2**	**0.05% RMA**	**0.075% RMA**	**0.05% RMA - 40% FA-C**	**0.075% RMA - 40% FA-C**	**0.15% RMA - 40% FA-C**	**0.15% RMA - 20% FA-C**
Cement lb/yd^3	427[C1]	427[C1]	424[C1]	337[C1]	337[C1]	520[C1]	520[C1]	322[C1]	324[C1]	324[C1]	424[C1]
kg/m^3	253	253	252	200	200	309	309	191	192	192	252
Water lb/yd^3	231	231	232	228	228	233	229	229	229	229	232
kg/m^3	137	137	138	135	135	138	136	136	136	136	138
Fly Ash lb/yd^3	87	87	92	171	171	0	0	187	187	187	92
kg/m^3	52	52	55	101	101	0	0	111	111	111	55
Sand (SSD) (lb/yd^3	1035[S4]	1057[S6]	1036[S11]	1002[S6]	1126[S4]	1161[S9]	1159[S9]	1093[S8]	1159[S9]	1035[S10]	1030[S10]
kg/m^3	614	627	615	594	668	689	688	648	688	614	611
Pea Gravel (SSD) lb/yd^3	606[PG2]	738[PG5]	565[PG6]	738[PG4]	283[PG2]	539[PG5]	540[PG5]	502[PG5]	540[PG5]	565[PG6]	565[PG6]
kg/m^3	360	438	335	438	168	320	320	298	320	335	335
Granite A (SSD) lb/yd^3	956[G2]	574[G3]	585[G6]	546[G3]	983[G2]	558[G5]	558[G5]	644[G5]	558[G5]	585[G6]	585[G6]
kg/m^3	567	341	347	324	583	331	331	382	331	347	347
Granite B (SSD) lb/yd^3	425[G3]	731[G4]	819[G7]	731[G4]	631[G3]	742[G6]	741[G6]	764[G6]	741[G6]	818[G7]	818[G7]
kg/m^3	252	434	486	434	374	440	440	453	440	485	485
RMA lb/yd^3	0	0	0	0	0	2	3	1.65	3	5	5.25
kg/m^3	0	0	0	0	0	1	2	1	2	3	3
Superplasticizer fl oz/yd^3	5.0	0.0	2.25	0.0	5.0	18.03	1.9	1.9	1.9	4.5	2.7
mL/m^3	193	0	87	0	193	697	38	38	38	174	104
AEA fl oz/yd^3	3.04	2.03	3.25	2.03	3.04	6.22	7.9	5.0	7.9	6.2	6.2
mL/m^3	118	79	123	79	118	241	306	193	306	241	241

Note:
Cement – C1, see Table A.1,
Sand – S4, S6, S8, S9, S10, and S11, see Table A.3,
Pea Gravel – PG2, PG4, PG5, and PG6, see Table A.3,
Granite A – G2, G3, G5, and G6, see Table A.2,
Granite B – G3, G4, G6, and G7, see Table A.2.

Table A.17 - Mixture proportions of concrete, containing shrinkage compensating admixtures, evaluated for durability performance

Batch Number	855	861	857	862	860	955
Batch Designation	2.5% SCA-1 # 1	2.5% SCA-1 # 2	5% SCA-1	7.5% SCA-1 # 1	7.5% SCA-1 # 2	6% SCA-2
Cement lb/yd^3	520[C1]	520[C1]	520[C1]	520[C1]	520[C1]	520[C1]
kg/m^3	309	309	309	309	309	309
Water lb/yd^3	234	234	235	234	234	218
kg/m^3	139	139	139	139	139	139
Sand (SSD) lb/yd^3	980[S2]	743[S2]	974[S2]	943[S3]	918[S1]	1035[S11]
kg/m^3	581	441	574	559	545	614
Pea Gravel (SSD) lb/yd^3	413[PG1]	748[PG1]	413[PG1]	617[PG1]	390[PG1]	540[PG6]
kg/m^3	245	444	245	366	231	320
Granite A (SSD) lb/yd^3	703[G1]	748[G1]	767[G1]	791[G1]	723[G1]	477[G9]
kg/m^3	417	444	455	469	429	283
Granite B (SSD) lb/yd^3	899[G1]	737[G2]	1002[G1]	794[G2]	922[G2]	964[G10]
kg/m^3	533	437	594	471	547	572
SCA lb/yd^3	13	13	26	39	39	31
kg/m^3	8	8	15	23	23	18
Superplasticizer fl oz/yd^3	2.0	5.0	2.0	5.0	5.0	6.8
mL/m^3	77	193	77	193	193	262
AEA fl oz/yd^3	2.7	1.0	1.0	1.0	4.1	10.4
mL/m^3	105	39	39	39	157	133

Note:
Cement – C1, see Table A.1,
Sand – S1, S2, S3, and S11, see Table A.3,
Pea Gravel – PG1 and PG6, see Table A.3,
Granite A – G1 and G9, see Table A.2,
Granite B – G1, G2, and G10, see Table A.2.

APPENDIX B: PROPERTIES AND SETTLEMENT CRACKING RESULTS OF CONCRETE MIXTURES

Table B.1 – Slump, air content, concrete temperature, unit weight, compressive strength, and settlement cracking results of the Control-1 mixtures

Batch No.	Slump		Air Content, %	Concrete Temperature		Unit Weight		28-Day Compressive Strength		Crack Length		Crack Length/ Bar Length	Crack Width (10^{-3})		Crack Width (10^{-3})	
	in.	mm		°F	°C	lb/ft^3	kg/m^3	psi	MPa	in.	mm	in./in.	in.	mm	in.	mm
										6.50	165		4	100		
C01	8	205	7.5	70	21	138.6	82.2	3930	27.1	10.00	255	0.67	4	100	4	100
										7.50	190		4	100		
										6.50	165		4	100		
C02	7 3/4	195	7.75	72	22	140.3	83.2	4010	27.7	7.75	195	0.63	5	125	4.7	120
										8.50	215		5	125		
										10.00	255		5	125		
C03	6 1/2	165	--	69	21	137.4	81.5	4060	28.9	10.50	265	0.81	4	100	4	100
										8.75	220		3	75		
										7.25	185		3	75		
C04	3 1/2	90	--	74	23	135.7	80.5	4750	32.8	6.25	160	0.58	3	75	3	75
										7.25	185		3	75		
										6.50	165		3	75		
C05	5 1/4	135	8.25	70	21	137.7	81.7	4170	28.8	7.50	190	0.60	3	75	3	75
										7.50	190		3	75		
										3.25	85		1	25		
C06	2 1/2	65	6.5	75	24	139.2	82.6	4330	29.9	2.50	65	0.28	2	50	1.3	35
										4.25	110		1	25		
										7.75	195		4	100		
C07	6	150	7.25	73	23	138.8	82.3	4200	28.9	6.75	170	0.58	2	50	2.7	70
										6.25	160		2	50		
										6.75	170		2	50		
C08	4 1/4	110	7.25	75	24	138	81.9	4310	29.7	5.00	127	0.49	2	50	2.3	60
										5.75	145		3	75		
										7.25	185		3	75		
CS09	3 1/2	90	8.50	74	23	137.5	81.6	4630	31.9	3.25	85	0.37	1	25	1.7	45
										2.75	70		1	25		

Note:
All mixtures represent concrete containing a 100% portland cement, referred to as "Control-1."

Table B.2 – Slump, air content, concrete temperature, unit weight, compressive strength, and settlement cracking results of the Control-2 mixtures

Batch No.	Slump		Air Content, %	Concrete Temperature		Unit Weight		28-Day Compressive Strength		Crack Length		Crack Length/ Bar Length	Crack Width		Crack Width	
	in.	mm		°F	°C	lb/ft³	kg/m³	psi	MPa	in.	mm	in./in.	(10^{-3}) in.	mm	(10^{-3}) in.	mm
										6.00	150		2	50		
C10	5 1/4	135	6.5	69	21	140	83	3710	25.6	4.00	100	0.42	1	25	1.3	35
										5.25	135		1	25		
										5.75	145		1	25		
C11	7	180	7.75	70	21	138	82	3210	22.1	4.75	120	0.47	2	50	1.7	45
										6.25	160		2	50		
										5.00	125		2	50		
C12	7 3/4	195	7.25	72	22	139	82	3590	24.8	7.50	190	0.51	3	75	2.7	70
										6.00	150		3	75		
										4.75	120		1	25		
C13	4 1/2	115	6.5	70	21	140	83	3790	26.1	4.75	120	0.37	1	25	1	25
										3.75	95		1	25		
										4.25	110		1	25		
C14	6	150	8	73	23	138	82	2990	20.6	5.00	125	0.43	1	25	1.7	45
										6.25	160		3	75		
										4.00	100		1	25		
C15	3 1/4	80	7.25	74	23	139	82	3230	22.3	4.50	115	0.34	1	25	1	25
										3.75	95		1	25		
										6.25	160		2	50		
C16	8	205	7.75	70	21	139	82	3370	23.2	6.00	150	0.54	2	50	1.7	45
										7.25	185		1	25		
										7.50	190		2	50		
C17	8 1/2	215	7.25	71	22	138	82	3180	21.9	7.00	180	0.6	3	75	2.3	60
										7.00	180		2	50		
										6.75	170		2	50		
C18	8 1/2	215	7.5	71	22	139	82	----	----	6.50	165	0.53	1	25	2	50
										5.75	145		3	75		

Note:
All mixtures represent concrete containing a 100% portland cement, referred to as "Control-2." Concrete of these mixtures contained a finer aggregate gradation than the Control-1 mixtures.

Table B.3 – Slump, air content, concrete temperature, unit weight, compressive strength, and settlement cracking results of the Control-3 mixtures

Batch No.	Slump		Air Content, %	Concrete Temperature		Unit Weight		28-Day Compressive Strength		Crack Length		Crack Length/ Bar Length	Crack Width		Crack Width	
	in.	mm		°F	°C	lb/ft³	kg/m³	psi	MPa	in.	mm	in./in.	(10^{-3}) in.	(10^{-3}) mm	(10^{-3}) in.	(10^{-3}) mm
										5.25	135		2	50		
GA01	5 1/2	140	8	72	22	138.4	82	3750	25.9	5.75	145	0.49	3	75	2.7	70
										6.75	170		3	75		
										5.25	135		2	50		
GA02	4 1/2	115	7.25	72	22	138.1	82	3050	21.0	4.50	115	0.46	2	50	2	50
										6.75	170		2	50		
										8.00	205		2	50		
GA03	7 1/4	185	8.25	70	21	138.0	82	3500	24.1	7.75	195	0.65	2	50	2.3	60
										7.75	195		3	75		
										8.00	205		2	50		
GA04	8 1/4	210	9.25	70	21	134.2	80	2800	19.3	8.00	205	0.67	3	75	2.7	70
										8.25	210		3	75		
										6.00	150		2	50		
GA05	3 1/2	90	7.5	71	22	137.3	81	3150	21.7	5.00	125	0.44	1	25	1.7	45
										5.00	125		2	50		
										7.25	185		2	50		
GA06	6	150	7.25	71	22	137.8	82	3300	22.8	6.75	170	0.62	1	25	2.3	60
										8.25	210		4	100		

Note:
All mixtures represent concrete containing a 100% portland cement with non-optimized aggregate gradation, referred to as "Control-3."

Table B.4 – Slump, air content, concrete temperature, unit weight, compressive strength, and settlement cracking results of the 5.9 lb-IC mixtures

Batch No.	Slump		Air Content, %	Concrete Temperature		Unit Weight		28-Day Compressive Strength		Crack Length		Crack Length/ Bar Length	Crack Width		Crack Width	
	in.	mm		°F	°C	lb/ft³	kg/m³	psi	MPa	in.	mm	in./in.	(10^{-3}) in.	(10^{-3}) mm	(10^{-3}) in.	(10^{-3}) mm
										2.00	50		2	50		
IC01	6	150	8	70	21	134	79	3780	26.1	3.25	85	0.26	1	25	1.7	45
										4.00	100		2	50		
										4.75	120		2	50		
IC02	6½	165	--	70	21	137	81	4140	28.5	4.25	110	0.38	3	75	3	75
										4.50	115		4	100		
										2.00	50		2	50		
IC03	3¾	95	--	71	22	136	81	4450	30.7	3.25	85	0.24	3	75	2.7	70
										3.50	90		3	75		
										3.75	95		2	50		
IC04	5	125	--	71	22	138	82	4490	31.0	4.25	110	0.36	3	75	2.3	60
										5.00	125		2	50		
										3.50	90		1	25		
IC05	4¼	110	--	74	23	137	81	3800	26.2	3.75	95	0.36	1	25	1.3	35
										5.75	145		2	50		
										0.00	0		0	0		
IC06	2½	65	--	75	24	137	81	4860	33.5	6.00	150	0.24	2	50	1.7	45
										2.75	70		3	75		
										7.50	190		3	75		
IC07	7	180	8.5	71	22	134	79	5000	34.5	5.75	145	0.58	2	50	2.7	70
										7.75	195		3	75		
										3.75	95		2	50		
IC08	5½	140	7.75	70	21	137	81	4170	28.8	3.75	95	0.33	1	25	1.3	35
										4.50	115		1	50		

Note:
All mixtures represent concrete containing a 100% portland cement with 5.9 lb internal curing water per 100 lb of cementitious materials, referred to as "5.9 lb-IC."

Table B.5 – Slump, air content, concrete temperature, unit weight, compressive strength, and settlement cracking results of the 7 lb-IC mixture

Batch No.	Slump		Air Content, %	Concrete Temperature		Unit Weight		28-Day Compressive Strength		Crack Length		Crack Length/ Bar Length	Crack Width		Crack Width	
	in.	mm		°F	°C	lb/ft^3	kg/m^3	psi	MPa	in.	mm	in./in.	(10^{-3}) in.	(10^{-3}) mm	(10^{-3}) in.	(10^{-3}) mm
										3.00	75		1	25		
IC09	7 1/4	185	6.5	70	21	135.7	81	3530	24.3	2.75	70	0.34	1	25	1.3	35
										6.50	165		2	50		
										3.00	75		3	75		
IC10	5 1/2	140	7	69	21	138.9	82	3770	26.0	4.00	100	0.33	1	25	2	50
										5.00	125		2	50		
										5.00	125		2	50		
IC11	6 1/2	165	6.5	70	21	136.0	81	3040	21.0	3.50	90	0.35	2	50	2	50
										4.25	110		2	50		
										2.00	50		1	25		
IC12	4	100	9.5	70	21	131.4	78	2990	20.6	1.75	45	0.19	1	25	1	25
										3.00	75		1	25		
										2.00	50		1	25		
IC13	5	125	9	70	21	132.0	78	3000	20.7	3.00	75	0.21	1	25	1	25
										2.50	65		1	25		
										1.75	45		1	25		
IC14	3	75	7.25	71	22	137.4	82	3850	26.5	1.50	40	0.15	1	25	1	25
										2.25	55		1	25		
										5.00	125		2	50		
IC15	8 1/4	210	9	70	21	130.7	78	3850	26.5	2.00	50	0.26	1	25	1.3	35
										2.25	55		1	25		
										5.00	125		2	50		
IC16	8 1/2	215	8.25	70	21	133.2	79	3390	23.4	4.50	115	0.38	2	50	2	50
										4.00	100		2	50		

Note:
All mixtures represent concrete containing a 100% portland cement with 7 lb internal curing water per 100 lb of cementitious materials, referred to as "7 lb-IC."

Table B.6 – Slump, air content, concrete temperature, unit weight, compressive strength, and settlement cracking results of 30 % Slag mixture

Batch No.	Slump in.	Slump mm	Air Content, %	Concrete Temperature °F	Concrete Temperature °C	Unit Weight lb/ft³	Unit Weight kg/m³	28-Day Compressive Strength psi	28-Day Compressive Strength MPa	Crack Length in.	Crack Length mm	Crack Length/ Bar Length in./in.	Crack Width (10^{-3}) in.	Crack Width (10^{-3}) mm	Crack Width (10^{-3}) in.	Crack Width (10^{-3}) mm
										1.50	40		1	25		
S01	$5^3/_4$	145	7.5	68	20	138.6	82	4290	29.6	3.25	80	0.25	2	50	1.7	45
										4.25	110		2	50		
										3.00	75		1	25		
S02	$6^1/_4$	160	6.75	70	21	140.5	83	4300	29.7	4.25	110	0.3	2	50	1.7	45
										3.50	90		2	50		
										4.25	110		2	50		
S03	6	150	6.5	73	23	141.4	84	4790	33.0	2.25	55	0.29	1	25	1.7	45
										4.00	100		2	50		
										4.25	110		2	50		
S04	3	75	6.5	70	21	141.2	84	5100	35.1	2.00	50	0.25	1	25	1.3	35
										2.75	70		1	25		
										1.25	30		1	25		
S05	4	100	7.75	69	21	137.8	82	4370	30.1	1.25	30	0.16	1	25	1.7	45
										3.25	85		3	75		
										7.50	190		3	75		
S06	$7^1/_4$	185	6.5	70	21	139.6	83	4000	27.6	5.00	125	0.56	2	50	2.7	70
										7.75	195		3	75		
										2.00	50		1	25		
S07	5	125	6.5	70	21	139.3	83	3950	27.2	4.00	100	0.28	3	75	2.3	60
										4.00	100		3	75		
										0.50	15		1	25		
S08	8	205	8.25	71	22	137.5	82	3470	23.9	1.25	30	0.13	1	25	1	25
										2.75	70		1	25		
										1.00	25		1	25		
S09	3	75	6.5	74	23	140.8	84	3890	26.8	1.00	25	0.1	1	25	1	25
										1.50	40		1	25		
										4.75	120		2	50		
S10	7	180	7.5	70	21	138.5	82	3400	23.4	3.50	90	0.33	1	25	1.7	45
										3.50	90		2	50		
										5.00	125		2	50		
S11	$7^3/_4$	195	9.5	70	21	136.1	81	3060	21.1	1.25	30	0.31	1	25	1.3	35
										4.75	120		1	25		

Note:
All mixtures represent concrete containing a 30% Slag cement replacement of cement with volume without internal curing, referred to as “30% Slag.”

Table B.7 – Slump, air content, concrete temperature, unit weight, compressive strength, and settlement cracking results of 30% slag - 3% SF mixture

Batch No.	Slump		Air Content, %	Concrete Temperature		Unit Weight		28-Day Compressive Strength		Crack Length		Crack Length/Bar Length	Crack Width		Crack Width	
	in.	mm		°F	°C	lb/ft³	kg/m³	psi	MPa	in.	mm	in./in.	(10^{-3}) in.	(10^{-3}) mm	(10^{-3}) in.	(10^{-3}) mm
										1.25	30		1	25		
SSF01	1 3/4	45	6.5	70	21	143.3	85	4540	31.3	0.00	0	0.04	0	0	0.3	10
										0.00	0		0	0		
										1.50	40		1	25		
SSF02	3 1/2	90	6.5	69	21	139.9	83	3970	27.3	0.75	20	0.08	1	25	1	25
										0.75	20		1	25		
										0.50	15		1	25		
SSF03	4	100	7.0	69	21	134.8	80	3300	22.8	0.75	20	0.07	1	25	1	25
										1.25	30		1	25		
										1.50	40		1	25		
SSF04	8 1/2	215	8.5	72	22	135.7	81	3050	21	1.25	30	0.1	1	25	1	25
										0.75	20		1	25		
										1.50	40		1	25		
SSF05	6 1/2	165	8.25	69	21	134.5	80	3260	22.5	0.50	15	0.08	1	25	1	25
										1.00	25		1	25		
										1.25	30		1	25		
SSF06	5	125	8.25	70	21	138.1	82	4150	28.6	1.25	30	0.09	1	25	1	25
										0.75	20		1	25		
										0.50	15		2	50		
SSF07	4 3/4	120	7.75	70	21	138.9	82	3860	26.6	0.75	20	0.06	1	25	1.3	35
										0.75	20		1	25		
										1.00	25		1	25		
SSF08	7	180	8.0	71	22	135.7	81	3440	23.7	1.00	25	0.07	1	25	1	25
										0.50	15		1	25		
										0.50	15		1	25		
SSF09	4 1/2	115	6.5	72	22	138.7	82	3490	24.1	0.50	15	0.04	1	25	1	25
										0.50	15		1	25		
										0.50	15		1	25		
SSF10	2 3/4	70	6.75	69	21	138.4	82	4070	28.1	0.25	5	0.04	1	25	1	25
										0.75	20		1	25		

Note:
All mixtures represent concrete containing a 30% slag cement and 3% silica fume replacement of cement with volume without internal curing, referred to as "30% Slag - 3% SF."

Table B.8 – Slump, air content, concrete temperature, unit weight, compressive strength, and settlement cracking results of 30% slag – 7 lb-IC mixture

Batch No.	Slump in.	Slump mm	Air Content, %	Concrete Temperature °F	Concrete Temperature °C	Unit Weight lb/ft^3	Unit Weight kg/m^3	28-Day Compressive Strength psi	28-Day Compressive Strength MPa	Crack Length in.	Crack Length mm	Crack Length/Bar Length in./in.	Crack Width (10^{-3}) in.	Crack Width (10^{-3}) mm	Crack Width (10^{-3}) in.	Crack Width (10^{-3}) mm
										1.50	40		1	25		
SIC01	4 1/4	110	8	70	21	132.9	79	3730	25.7	3.00	75	0.2	2	50	1.3	35
										2.75	70		1	25		
										1.50	40		1	25		
SIC02	4	100	7	69	21	135.2	80	3780	26.1	2.75	70	0.13	1	25	1	25
										0.50	15		1	25		
										1.25	30		1	25		
SIC03	8 1/4	210	7.5	70	21	134.3	80	4100	28.3	4.50	115	0.27	1	25	1	25
										4.00	100		1	25		
										3.50	90		1	25		
SIC04	5 3/4	145	7.5	70	21	134.5	80	3960	27.3	2.00	50	0.17	1	25	1	25
										0.75	20		1	25		
										0.50	15		1	25		
SIC05	3 1/2	90	6.5	70	21	136.0	81	4180	28.8	2.25	55	0.1	1	25	1	25
										2.75	70		1	25		
										2.75	70		1	25		
SIC06	5 1/4	135	7.5	71	22	132.5	79	3200	22.1	2.25	55	0.21	1	25	1	25
										2.50	65		1	25		
										1.50	40		1	25		
SIC07	4 3/4	120	9.5	69	21	129.9	77	2290	15.8	0.25	5	0.08	1	25	1	25
										1.00	25		1	25		
										2.75	70		1	25		
SIC08	7 1/2	190	8.25	70	21	132.8	79	3630	25.0	3.00	75	0.23	1	25	1	25
										2.50	65		1	25		
										1.00	25		1	25		
SIC09	4	100	9.5	70	21	131.2	78	3470	23.9	2.25	55	0.15	1	25	1.3	35
										2.00	50		2	50		

Note:
All mixtures represent concrete containing a 30% slag cement replacement of cement with volume and 7 lb internal curing water per 100 lb of cementitious materials, referred to as "30% Slag – 7 lb-IC."

Table B.9 – Slump, air content, concrete temperature, unit weight, compressive strength, and settlement cracking results of 30% slag - 3% SF – 7 lb-IC mixture

Batch No.	Slump in.	Slump mm	Air Content, %	Concrete Temperature °F	Concrete Temperature °C	Unit Weight lb/ft³	Unit Weight kg/m³	28-Day Compressive Strength psi	28-Day Compressive Strength MPa	Crack Length in.	Crack Length mm	Crack Length/ Bar Length in./in.	Crack Width (10^{-3}) in.	Crack Width (10^{-3}) mm	Crack Width (10^{-3}) in.	Crack Width (10^{-3}) mm
										0.75	20		1	25		
SSFIC01	3 1/4	85	8.0	73	23	133.0	79	4080	28.1	0.25	5	0.03	1	25	1	25
										0.25	5		1	25		
										0.75	20		1	25		
SSFIC02	4 1/4	110	7.0	72	22	134.0	79	4310	29.7	1.00	25	0.08	1	25	1	25
										1.00	25		1	25		
										0.25	5		1	25		
SSFIC03	5	125	7.5	72	22	134.4	80	4120	28.4	0.50	5	0.05	1	25	1.3	35
										1.00	25		2	50		
										0.50	15		1	25		
SSFIC04	6 1/4	160	8.5	73	23	132.3	80	3710	25.6	0.75	20	0.06	1	25	1	25
										0.75	20		1	25		
										0.50	15		1	25		
SSFIC05	7 3/4	195	8.25	73	23	132.1	80	3730	25.7	1.00	25	0.08	1	25	1	25
										1.25	30		1	25		
										0.25	5		1	25		
SSFIC06	2 3/4	70	8.0	74	23	132.9	79	3640	25.1	0.25	5	0.03	1	25	1	25
										0.50	15		1	25		
										0.50	15		1	25		
SSFIC07	8 1/4	210	9.5	72	22	130.1	77	3550	24.5	1.00	25	0.08	1	25	1	25
										1.25	30		1	25		
										0.75	20		1	25		
SSFIC08	7	180	9.0	69	21	130.1	77	3610	24.9	0.50	15	0.06	1	25	1	25
										1.00	25		1	25		

Note:
All mixtures represent concrete containing a 30% slag cement and 3% silica fume replacement of cement with volume and 7 lb internal curing water per 100 lb of cementitious materials, referred to as "30% Slag - 3% SF – 7 lb-IC."

Table B. 10 – Slump, air content, concrete temperature, unit weight, compressive strength, and settlement cracking results of 2% SRA mixture

Batch No.	Slump		Air Content, %	Concrete Temperature		Unit Weight		28-Day Compressive Strength		Crack Length		Crack Length/ Bar Length	Crack Width		Crack Width	
	in.	mm		°F	°C	lb/ft^3	kg/m^3	psi	Mpa	in.	mm	in./in.	(10^{-3}) in.	(10^{-3}) mm	(10^{-3}) in.	(10^{-3}) mm
										1.75	45		1	25		
SRA01	3 3/4	95	9.0	71	22	133.5	79	2570	17.7	3.00	75	0.21	1	25	1	25
										2.75	70		1	25		
										1.75	45		1	25		
SRA02	4	100	8.5	71	22	135.9	81	2440	16.8	1.75	45	0.16	1	25	1	25
										2.25	55		1	25		
										3.50	90		1	25		
SRA03	5 1/2	140	8.5	72	22	136.0	81	2470	17.0	3.25	85	0.29	1	25	1	25
										3.50	90		1	25		
										5.00	125		1	25		
SRA04	6 1/4	160	8.5	72	22	136.9	81	2310	15.9	4.50	115	0.39	1	25	1	25
										4.50	115		1	25		
										2.25	55		1	25		
SRA05	4 3/4	120	7.0	73	23	138.2	82	2930	20.2	3.00	75	0.23	1	25	1	25
										3.00	75		1	25		
										1.75	45		1	25		
SRA06	2 3/4	70	7.5	74	23	136.9	81	2710	18.7	2.00	50	0.16	1	25	1	25
										2.00	50		1	25		
										5.25	135		1	25		
SRA07	8 1/4	210	8.5	71	22	136.0	81	2750	19.0	5.00	125	0.44	1	25	1	25
										5.50	140		1	25		
										4.25	110		1	25		
SRA08	7 1/4	185	8.0	71	22	136.7	81	2760	19.0	4.25	110	0.38	1	25	1	25
										5.00	125		1	25		

Note:
All mixtures represent concrete containing 2% shrinkage-reducing admixture by weight of cement without internal curing, referred to as “2% SRA.”

APPENDIX C: STUDENT'S T-TEST RESULTS

Table C.1 – Student's t-test results for the Control-1 and 5.9 lb-IC mixtures

Slump (in.)	Average Control-1	Average 5.9 lb-IC	SD* Control-1	SD 5.9 lb-IC	n** Control-1	n 5.9 lb-IC	*p****	t†	Difference
1	0.283	0.140	0.099	0.082	9	8	5.74E-03	3.22	Statistically Significant
2	0.347	0.190					3.08E-03	3.52	Statistically Significant
3	0.411	0.241					1.65E-03	3.83	Statistically Significant
4	0.475	0.291					8.90E-04	4.13	Statistically Significant
5	0.539	0.342					4.83E-04	4.43	Statistically Significant
6	0.603	0.392					2.64E-04	4.74	Statistically Significant
7	0.666	0.442					1.46E-04	5.04	Statistically Significant
8	0.730	0.493					8.17E-05	5.35	Statistically Significant

* Standard Deviation.
** Number of samples.
*** Level of significance, which represents the probability that any apparent differences in the data sets are due to random variation and not statistically meaningful differences.
† The t- *value* for each interval of the slump is calculated using the equation for independent sets of unequal sample sizes.

Table C.2 – Student's t-test results for the Control-2 and Control-3 mixtures

Slump (in.)	Average Control-2	Average Control-3	SD Control-2	SD Control-3	n Control-2	n Control-3	*p*	t	Difference
1	0.228	0.289	0.022	0.032	9	6	7.24E-04	4.40	Statistically Significant
2	0.271	0.344					1.55E-04	5.26	Statistically Significant
3	0.314	0.400					3.65E-05	6.12	Statistically Significant
4	0.358	0.455					9.56E-06	6.98	Statistically Significant
5	0.401	0.510					2.76E-06	7.85	Statistically Significant
6	0.445	0.566					8.70E-07	8.71	Statistically Significant
7	0.488	0.621					2.97E-07	9.57	Statistically Significant
8	0.531	0.677					1.09E-07	10.44	Statistically Significant

* See footnotes for Table C.1.

Table C.3 – Student's t-test results for the Control-2 and 7 lb-IC mixtures

Slump (in.)	Average Control-2	Average 7 lb-IC	SD Control-2	SD 7 lb-IC	n Control-2	n 7 lb-IC	*p*	t	Difference
1	0.228	0.110	0.022	0.055	9	8	2.68E-05	5.95	Statistically Significant
2	0.271	0.143					1.07E-05	6.46	Statistically Significant
3	0.314	0.176					4.45E-06	6.98	Statistically Significant
4	0.358	0.210					1.92E-06	7.49	Statistically Significant
5	0.401	0.243					8.52E-07	8.01	Statistically Significant
6	0.445	0.276					3.92E-07	8.52	Statistically Significant
7	0.488	0.309					1.86E-07	9.04	Statistically Significant
8	0.531	0.342					9.01E-08	9.55	Statistically Significant

* See footnotes for Table C.1.

Table C.4 – Student's t-test results for the Control-2 and 30% Slag mixtures

Slump (in.)	Average Control-2	Average 30% Slag	SD Control-2	SD 30% Slag	n Control-2	n 30% Slag	*p*	t	Difference
1	0.228	0.121	0.022	0.112	9	11	1.16E-02	2.81	Statistically Significant
2	0.271	0.152					5.70E-03	3.14	Statistically Significant
3	0.314	0.183					2.77E-03	3.46	Statistically Significant
4	0.358	0.214					1.34E-03	3.79	Statistically Significant
5	0.401	0.245					6.47E-04	4.12	Statistically Significant
6	0.445	0.276					3.13E-04	4.44	Statistically Significant
7	0.488	0.307					1.53E-04	4.77	Statistically Significant
8	0.531	0.338					7.52E-05	5.10	Statistically Significant

* See footnotes for Table C.1.

Table C.5 – Student's t-test results for the Control-2 and 30% Slag-3% SF mixtures

Slump (in.)	Average Control-2	Average 30% Slag-3% SF	SD Control-2	SD 30% Slag-3% SF	n Control-2	n 30% Slag-3% SF	*p*	t	Difference
1	0.228	0.038	0.022	0.016	9	10	7.27E-14	21.80	Statistically Significant
2	0.271	0.045					4.20E-15	25.91	Statistically Significant
3	0.314	0.053					3.63E-16	30.01	Statistically Significant
4	0.358	0.060					4.24E-17	34.12	Statistically Significant
5	0.401	0.068					6.29E-18	38.23	Statistically Significant
6	0.445	0.076					1.13E-18	42.33	Statistically Significant
7	0.488	0.083					2.37E-19	46.44	Statistically Significant
8	0.531	0.091					5.67E-20	50.54	Statistically Significant

* See footnotes for Table C.1.

Table C.6 – Student's t-test results for the Control-2 and 30% Slag- 7 lb-IC mixtures

Slump (in.)	Average Control-2	Average 30% Slag- 7 lb-IC	SD Control-2	SD 30% Slag- 7 lb-IC	n Control-2	n 30% Slag- 7 lb-IC	*p*	t	Difference
1	0.228	0.042	0.022	0.039	9	8	3.23E-09	12.23	Statistically Significant
2	0.271	0.072					1.29E-09	13.10	Statistically Significant
3	0.314	0.103					5.32E-10	13.96	Statistically Significant
4	0.358	0.133					2.29E-10	14.83	Statistically Significant
5	0.401	0.163					1.03E-10	15.69	Statistically Significant
6	0.445	0.194					4.80E-11	16.55	Statistically Significant
7	0.488	0.224					2.32E-11	17.42	Statistically Significant
8	0.531	0.254					1.16E-11	18.28	Statistically Significant

* See footnotes for Table C.1.

Table C.7 – Student's t-test results for the Control-2 and 30% Slag-3% SF-7 lb-IC mixtures

Slump (in.)	Average Control-2	Average 30% Slag-3% SF-7 lb-IC	SD Control-2	SD 30% Slag-3% SF-7 lb-IC	n Control-2	n 30% Slag-3% SF-7 lb-IC	*p*	t	Difference
1	0.228	0.025	0.022	0.012	9	8	3.70E-13	23.17	Statistically Significant
2	0.271	0.032					3.33E-14	27.3	Statistically Significant
3	0.314	0.039					4.17E-15	31.44	Statistically Significant
4	0.358	0.046					6.69E-16	35.57	Statistically Significant
5	0.401	0.053					1.31E-16	39.7	Statistically Significant
6	0.445	0.061					3.00E-17	43.83	Statistically Significant
7	0.488	0.068					7.85E-18	47.96	Statistically Significant
8	0.531	0.075					2.29E-18	52.09	Statistically Significant

* See footnotes for Table C.1.

Table C.8 – Student's t-test results for Control-2 and 2% SRA mixtures

Slump (in.)	Average Control-2	Average 2% SRA	SD Control-2	SD 2% SRA	n Control-2	n 2% SRA	*p*	t	Difference
1	0.228	0.040	0.022	0.031	9	8	3.15E-10	14.49	Statistically Significant
2	0.271	0.096					8.15E-10	13.54	Statistically Significant
3	0.314	0.152					2.23E-09	12.59	Statistically Significant
4	0.358	0.207					6.54E-09	11.64	Statistically Significant
5	0.401	0.263					2.06E-08	10.69	Statistically Significant
6	0.445	0.319					7.07E-08	9.74	Statistically Significant
7	0.488	0.374					2.66E-07	8.79	Statistically Significant
8	0.531	0.430					1.11E-06	7.84	Statistically Significant

* See footnotes for Table C.1.

APPENDIX D: DATA MEASURED FROM FREEZE-THAW AND SCALING TESTS FOR SPECIMENS IN PROGRAMS 1, 2, AND 3

Table D.1 Program 1 – Fundamental transverse frequency and mass data (ASTM C666 and C215)

Mixture: Control # 1*

Cycles	0			23			50		
Specimen Number	926A	926B	926C	926A	926B	926C	926A	926B	926C
Frequency n [Hz]	2204	2026	2152	2206	2024	2150	2208	2028	2154
Mass M [g]	7568.1	7053.7	7542.6	7568.5	7053.9	7543	7568.9	7054.9	7543.9
Dynamic Modulus (Pa)	3.98E+10	3.14E+10	3.79E+10	3.99E+10	3.13E+10	3.78E+10	4.00E+10	3.14E+10	3.79E+10
Avg. Dy. Modulus (Pa)	3.64E+10			3.63E+10			3.65E+10		

Cycles	78			107			127		
Specimen Number	926A	926B	926C	926A	926B	926C	926A	926B	926C
Frequency n [Hz]	2208	2026	2152	2210	2024	2150	2208	2020	2148
Mass M [g]	7569.5	7055.8	7543.8	7569.7	7055.3	7543.8	7569.8	7055.2	7543.8
Dynamic Modulus (Pa)	4.00E+10	3.14E+10	3.79E+10	4.01E+10	3.13E+10	3.78E+10	4.00E+10	3.12E+10	3.77E+10
Avg. Dy. Modulus (Pa)	3.64E+10			3.64E+10			3.63E+10		

Cycles	141			173			202		
Specimen Number	926A	926B	926C	926A	926B	926C	926A	926B	926C
Frequency n [Hz]	2204	2022	2146	2202	2024	2144	2200	2024	2144
Mass M [g]	7569.1	7055	7543	7568.5	7054.5	7543.2	7567.9	7054.1	7543
Dynamic Modulus (Pa)	3.98E+10	3.13E+10	3.76E+10	3.98E+10	3.13E+10	3.76E+10	3.97E+10	3.13E+10	3.76E+10
Avg. Dy. Modulus (Pa)	3.62E+10			3.62E+10			3.62E+10		

Cycles	231			260			289		
Specimen Number	926A	926B	926C	926A	926B	926C	926A	926B	926C
Frequency n [Hz]	2202	2024	2142	2200	2022	2150	2202	2030	2156
Mass M [g]	7567.3	7053.8	7542.8	7568.2	7054.2	7543.4	7569.5	7055.2	7544
Dynamic Modulus (Pa)	3.98E+10	3.13E+10	3.75E+10	3.97E+10	3.13E+10	3.78E+10	3.98E+10	3.15E+10	3.80E+10
Avg. Dy. Modulus (Pa)	3.62E+10			3.62E+10			3.64E+10		

Cycles	317		
Specimen Number	926A	926B	926C
Frequency n [Hz]	2206	2036	2154
Mass M [g]	7568.8	7054.8	7544.2
Dynamic Modulus (Pa)	3.99E+10	3.17E+10	3.79E+10
Avg. Dy. Modulus (Pa)	3.65E+10		

*Batch is designated as “Control #1” in Program 1, 2, and 3.

Table D.1 (Cont'd) Program 1 – Fundamental transverse frequency and mass data (ASTM C666 and C215)

Mixture: Control # 2*

Cycles	0			23			50		
Specimen Number	927A	927B	927C	927A	927B	927C	927A	927B	927C
Frequency n [Hz]	2204	2314	2186	2206	2318	2190	2206	2316	2192
Mass M [g]	7451.2	7365	7369.9	7452	7364.2	7370.5	7452.9	7364.5	7371.1
Dynamic Modulus (Pa)	3.92E+10	4.27E+10	3.82E+10	3.93E+10	4.29E+10	3.83E+10	3.93E+10	4.28E+10	3.84E+10
Avg. Dy. Modulus (Pa)	4.00E+10			4.02E+10			4.02E+10		

Cycles	107			127			141		
Specimen Number	927A	927B	927C	927A	927B	927C	927A	927B	927C
Frequency n [Hz]	2210	2316	2196	2212	2314	2194	2208	2310	2194
Mass M [g]	7452.7	7364.5	7371.4	7452.5	7364.9	7371.6	7452.8	7365.2	7371.9
Dynamic Modulus (Pa)	3.94E+10	4.28E+10	3.85E+10	3.95E+10	4.27E+10	3.85E+10	3.94E+10	4.26E+10	3.85E+10
Avg. Dy. Modulus (Pa)	4.03E+10			4.02E+10			4.01E+10		

Cycles	173			202			231		
Specimen Number	927A	927B	927C	927A	927B	927C	927A	927B	927C
Frequency n [Hz]	2208	2310	2192	2204	2308	2190	2200	2306	2190
Mass M [g]	7453	7365.5	7372.1	7453.5	7366.1	7371.7	7452.2	7365.2	7371.9
Dynamic Modulus (Pa)	3.94E+10	4.26E+10	3.84E+10	3.92E+10	4.25E+10	3.83E+10	3.91E+10	4.24E+10	3.83E+10
Avg. Dy. Modulus (Pa)	4.01E+10			4.00E+10			3.99E+10		

Cycles	260			289			317		
Specimen Number	927A	927B	927C	927A	927B	927C	927A	927B	927C
Frequency n [Hz]	2204	2310	2192	2208	2316	2192	2208	2314	2190
Mass M [g]	7451.3	7365	7372.1	7450.8	7364.6	7372.2	7451.2	7365.2	7372.3
Dynamic Modulus (Pa)	3.92E+10	4.26E+10	3.84E+10	3.94E+10	4.28E+10	3.84E+10	3.94E+10	4.27E+10	3.83E+10
Avg. Dy. Modulus (Pa)	4.01E+10			4.02E+10			4.01E+10		

*Batch is designated as "Control #2" in Program 1, 2, and 3.

Table D.1 (Cont'd) Program 1 – Fundamental transverse frequency and mass data (ASTM C666 and C215)

Mixture: Control # 3*

Cycles	0			28			54		
Specimen Number	976A	976B	976C	976A	976B	976C	976A	976B	976C
Frequency n [Hz]	2180	2142	2118	2180	2140	2116	2180	2146	2120
Mass M [g]	7604.4	7296.9	7235.7	7608	7305.4	7242.1	7611.5	7308.6	7245.7
Dynamic Modulus (Pa)	3.92E+10	3.63E+10	3.52E+10	3.92E+10	3.63E+10	3.51E+10	3.92E+10	3.65E+10	3.53E+10
Avg. Dy. Modulus (Pa)	3.69E+10			3.69E+10			3.70E+10		

Cycles	80			110			131		
Specimen Number	976A	976B	976C	976A	976B	976C	976A	976B	976C
Frequency n [Hz]	2176	2142	2116	2188	2148	2126	2188	2150	2126
Mass M [g]	7618.5	7311.9	7249.5	7621.6	7316	7252.7	7623.1	7318.9	7253.4
Dynamic Modulus (Pa)	3.91E+10	3.64E+10	3.52E+10	3.95E+10	3.66E+10	3.55E+10	3.95E+10	3.67E+10	3.55E+10
Avg. Dy. Modulus (Pa)	3.69E+10			3.72E+10			3.72E+10		

Cycles	157			190			218		
Specimen Number	976A	976B	976C	976A	976B	976C	976A	976B	976C
Frequency n [Hz]	2190	2152	2126	2192	2156	2130	2192	2158	2134
Mass M [g]	7624.8	7321.5	7257	7625.8	7322.3	7255.6	7626.5	7322.3	7255.8
Dynamic Modulus (Pa)	3.96E+10	3.67E+10	3.55E+10	3.97E+10	3.69E+10	3.57E+10	3.97E+10	3.70E+10	3.58E+10
Avg. Dy. Modulus (Pa)	3.73E+10			3.74E+10			3.75E+10		

Cycles	247			273			288		
Specimen Number	976A	976B	976C	976A	976B	976C	976A	976B	976C
Frequency n [Hz]	2194	2156	2132	2196	2160	2136	2194	2160	2134
Mass M [g]	7626.9	7328.4	7261.5	7627.1	7324	7256.8	7627.6	7328.6	7256.9
Dynamic Modulus (Pa)	3.98E+10	3.69E+10	3.58E+10	3.99E+10	3.70E+10	3.59E+10	3.98E+10	3.71E+10	3.58E+10
Avg. Dy. Modulus (Pa)	3.75E+10			3.76E+10			3.76E+10		

Cycles	317		
Specimen Number	976A	976B	976C
Frequency n [Hz]	2196	2158	2138
Mass M [g]	7626.5	7323.6	7257
Dynamic Modulus (Pa)	3.99E+10	3.70E+10	3.59E+10
Avg. Dy. Modulus (Pa)	3.76E+10		

*Batch is designated as "Control #3" in Program 1, 2, and 3.

Table D.1 (Cont'd) Program 1 – Fundamental transverse frequency and mass data (ASTM C666 and C215)

Mixture: 0.5% SRA-2*

Cycles	0			38			70		
Specimen Number	894A	894B	894C	894A	894B	894C	894A	894B	894C
Frequency n [Hz]	2218	2230	2256	2230	2244	2264	2230	2244	2264
Mass M [g]	7523.3	7624.5	7645.5	7531.4	7632.8	7653.2	7533.9	7634.8	7654.5
Dynamic Modulus (Pa)	4.01E+10	4.11E+10	4.22E+10	4.06E+10	4.16E+10	4.25E+10	4.06E+10	4.17E+10	4.25E+10
Avg. Dy. Modulus (Pa)	4.11E+10			4.16E+10			4.16E+10		

Cycles	85			110			125		
Specimen Number	894A	894B	894C	894A	894B	894C	894A	894B	894C
Frequency n [Hz]	2234	2248	2268	2238	2248	2270	2234	2246	2268
Mass M [g]	7534.2	7634.8	7655.1	7534.5	7635.9	7655.9	7536	7637.2	7657
Dynamic Modulus (Pa)	4.07E+10	4.18E+10	4.27E+10	4.09E+10	4.18E+10	4.27E+10	4.08E+10	4.17E+10	4.27E+10
Avg. Dy. Modulus (Pa)	4.17E+10			4.18E+10			4.17E+10		

Cycles	151			187			205		
Specimen Number	894A	894B	894C	894A	894B	894C	894A	894B	894C
Frequency n [Hz]	2238	2250	2272	2240	2254	2274	2242	2248	2278
Mass M [g]	7536.1	7636.8	7656.6	7537.9	7638.5	7658.3	7537.9	7638.5	7658.1
Dynamic Modulus (Pa)	4.09E+10	4.19E+10	4.28E+10	4.10E+10	4.21E+10	4.29E+10	4.11E+10	4.18E+10	4.31E+10
Avg. Dy. Modulus (Pa)	4.19E+10			4.20E+10			4.20E+10		

Cycles	230			246			275		
Specimen Number	894A	894B	894C	894A	894B	894C	894A	894B	894C
Frequency n [Hz]	2234	2244	2274	2238	2254	2276	2244	2254	2280
Mass M [g]	7537.8	7638.4	7658.1	7538.6	7639.2	7659.3	7538.9	7639.7	7659.1
Dynamic Modulus (Pa)	4.08E+10	4.17E+10	4.29E+10	4.09E+10	4.21E+10	4.30E+10	4.11E+10	4.21E+10	4.31E+10
Avg. Dy. Modulus (Pa)	4.18E+10			4.20E+10			4.21E+10		

Cycles	321		
Specimen Number	894A	894B	894C
Frequency n [Hz]	2244	2252	2276
Mass M [g]	7538.8	7639.6	7659.3
Dynamic Modulus (Pa)	4.11E+10	4.20E+10	4.30E+10
Avg. Dy. Modulus (Pa)	4.20E+10		

*Batch is designated as "0.5% SRA-2" in Program 1.

Table D.1 (Cont'd) Program 1 – Fundamental transverse frequency and mass data (ASTM C666 and C215)

Mixture: 1% SRA-2 # 1*

Cycles	0			38			70		
Specimen Number	896A	896B	896C	896A	896B	896C	896A	896B	896C
Frequency n [Hz]	2216	2174	2208	2226	2182	2214	2228	2186	2218
Mass M [g]	7450	7381.1	7494.4	7458.3	7388.4	7502.2	7461	7391.3	7504.9
Dynamic Modulus (Pa)	3.96E+10	3.78E+10	3.96E+10	4.00E+10	3.81E+10	3.98E+10	4.01E+10	3.83E+10	4.00E+10
Avg. Dy. Modulus (Pa)	3.90E+10			3.93E+10			3.95E+10		

Cycles	85			110			125		
Specimen Number	896A	896B	896C	896A	896B	896C	896A	896B	896C
Frequency n [Hz]	2232	2184	2220	2232	2186	2222	2236	2186	2220
Mass M [g]	7461.6	7392	7506.1	7462.8	7392.8	7506.9	7464.4	7394.4	7508.5
Dynamic Modulus (Pa)	4.03E+10	3.82E+10	4.01E+10	4.03E+10	3.83E+10	4.02E+10	4.04E+10	3.83E+10	4.01E+10
Avg. Dy. Modulus (Pa)	3.95E+10			3.96E+10			3.96E+10		

Cycles	151			187			205		
Specimen Number	896A	896B	896C	896A	896B	896C	896A	896B	896C
Frequency n [Hz]	2234	2190	2224	2236	2190	2224	2238	2194	2226
Mass M [g]	7464.8	7394.7	7508.4	7467	7396.7	7509.5	7466.9	7393.4	7509.7
Dynamic Modulus (Pa)	4.04E+10	3.84E+10	4.02E+10	4.05E+10	3.84E+10	4.02E+10	4.05E+10	3.86E+10	4.03E+10
Avg. Dy. Modulus (Pa)	3.97E+10			3.97E+10			3.98E+10		

Cycles	230			246			275		
Specimen Number	896A	896B	896C	896A	896B	896C	896A	896B	896C
Frequency n [Hz]	2232	2194	2226	2246	2194	2222	2240	2200	2226
Mass M [g]	7466.5	7391	7508.3	7465.6	7390.6	7508.8	7465.7	7388.6	7509.1
Dynamic Modulus (Pa)	4.03E+10	3.86E+10	4.03E+10	4.08E+10	3.86E+10	4.02E+10	4.06E+10	3.88E+10	4.03E+10
Avg. Dy. Modulus (Pa)	3.97E+10			3.98E+10			3.99E+10		

Cycles	321		
Specimen Number	896A	896B	896C
Frequency n [Hz]	2238	2200	2228
Mass M [g]	7458.2	7388.1	7504.7
Dynamic Modulus (Pa)	4.05E+10	3.87E+10	4.04E+10
Avg. Dy. Modulus (Pa)	3.99E+10		

*Batch is designated as "1% SRA-2 # 1" in Program 1.

Table D.1 (Cont'd) Program 1 – Fundamental transverse frequency and mass data (ASTM C666 and C215)

Mixture: 1% SRA-2 # 3*

Cycles	0			27			55		
Specimen Number	960A	960B	960C	960A	960B	960C	960A	960B	960C
Frequency n [Hz]	2176	2198	2204	2186	2210	2220	2190	2208	2218
Mass M [g]	7410.4	7477.8	7595	7419.2	7486	7604.5	7421.6	7488.6	7606.2
Dynamic Modulus (Pa)	3.80E+10	3.91E+10	4.00E+10	3.84E+10	3.96E+10	4.06E+10	3.86E+10	3.96E+10	4.05E+10
Avg. Dy. Modulus (Pa)	3.90E+10			3.96E+10			3.96E+10		

Cycles	79			108			136		
Specimen Number	960A	960B	960C	960A	960B	960C	960A	960B	960C
Frequency n [Hz]	2190	2214	2224	2194	2216	2226	2190	2216	2226
Mass M [g]	7422.2	7489.5	7606.8	7423.1	7490	7607.4	7424.1	7491.1	7608.6
Dynamic Modulus (Pa)	3.86E+10	3.98E+10	4.08E+10	3.87E+10	3.99E+10	4.08E+10	3.86E+10	3.99E+10	4.09E+10
Avg. Dy. Modulus (Pa)	3.97E+10			3.98E+10			3.98E+10		

Cycles	162			188			213		
Specimen Number	960A	960B	960C	960A	960B	960C	960A	960B	960C
Frequency n [Hz]	2194	2218	2228	2198	2218	2230	2194	2220	2230
Mass M [g]	7424.2	7491.5	7608.8	7426.1	7493.7	7611.2	7426.4	7494.1	7611.3
Dynamic Modulus (Pa)	3.87E+10	3.99E+10	4.09E+10	3.89E+10	3.99E+10	4.10E+10	3.87E+10	4.00E+10	4.10E+10
Avg. Dy. Modulus (Pa)	3.99E+10			3.99E+10			3.99E+10		

Cycles	240			268			294		
Specimen Number	960A	960B	960C	960A	960B	960C	960A	960B	960C
Frequency n [Hz]	2194	2218	2230	2198	2222	2228	2198	2224	2234
Mass M [g]	7426.5	7494.2	7611.1	7427.2	7495.2	7611.8	7428.1	7496	7612.6
Dynamic Modulus (Pa)	3.87E+10	4.00E+10	4.10E+10	3.89E+10	4.01E+10	4.09E+10	3.89E+10	4.02E+10	4.12E+10
Avg. Dy. Modulus (Pa)	3.99E+10			4.00E+10			4.01E+10		

Cycles	302		
Specimen Number	960A	960B	960C
Frequency n [Hz]	2192	2218	2230
Mass M [g]	7420.1	7483.1	7605.3
Dynamic Modulus (Pa)	3.86E+10	3.99E+10	4.10E+10
Avg. Dy. Modulus (Pa)	3.98E+10		

*Batch is designated as "1% SRA-2 # 3" in Program 1.

Table D.1 (Cont'd) Program 1 – Fundamental transverse frequency and mass data (ASTM C666 and C215)

Mixture: 2% SRA-2 # 1*

Cycles	0			35			51		
Specimen Number	886A	886B	886C	886A	886B	886C	886A	886B	886C
Frequency n [Hz]	2178	2176	2190	2172	2172	2180	2175	2170	2185
Mass M [g]	7328.2	7417.5	7426.3	7331.4	7422.7	7425.1	7332.3	7423.8	7425.7
Dynamic Modulus (Pa)	3.77E+10	3.81E+10	3.86E+10	3.75E+10	3.79E+10	3.82E+10	3.76E+10	3.79E+10	3.84E+10
Avg. Dy. Modulus (Pa)	3.81E+10			3.79E+10			3.80E+10		

Cycles	73			120			136		
Specimen Number	886A	886B	886C	886A	886B	886C	886A	886B	886C
Frequency n [Hz]	2174	2165	2180	2178	2164	2182	2175	2168	2180
Mass M [g]	7333.3	7425.4	7426.5	7333	7425.8	7426.4	7335.6	7427.8	7429.2
Dynamic Modulus (Pa)	3.76E+10	3.77E+10	3.82E+10	3.77E+10	3.77E+10	3.83E+10	3.76E+10	3.78E+10	3.83E+10
Avg. Dy. Modulus (Pa)	3.78E+10			3.79E+10			3.79E+10		

Cycles	160			206			269		
Specimen Number	886A	886B	886C	886A	886B	886C	886A	886B	886C
Frequency n [Hz]	2175	2162	2180	2175	2160	2190	2182	2126	2192
Mass M [g]	7335.6	7427.9	7429	7336.4	7438.7	7429.7	7340.6	7429.2	7433.5
Dynamic Modulus (Pa)	3.76E+10	3.76E+10	3.83E+10	3.76E+10	3.76E+10	3.86E+10	3.79E+10	3.64E+10	3.87E+10
Avg. Dy. Modulus (Pa)	3.78E+10			3.79E+10			3.77E+10		

Cycles	315		
Specimen Number	886A	886B	886C
Frequency n [Hz]	2184	2094	2192
Mass M [g]	7341.3	7436.9	7434.8
Dynamic Modulus (Pa)	3.79E+10	3.53E+10	3.87E+10
Avg. Dy. Modulus (Pa)	3.73E+10		

*Batch is designated as "2% SRA-2 # 1" in Program 1.

Table D.1 (Cont'd) Program 1 – Fundamental transverse frequency and mass data (ASTM C666 and C215)

Mixture: 2% SRA-2 # 2*

Cycles	0			38			70		
Specimen Number	897A	897B	897C	897A	897B	897C	897A	897B	897C
Frequency n [Hz]	2182	2212	2194	2204	2232	2216	2204	2234	2218
Mass M [g]	7518	7599.6	7508.8	7527	7608.1	7517.8	7530.3	7610.8	7520.9
Dynamic Modulus (Pa)	3.88E+10	4.03E+10	3.92E+10	3.96E+10	4.11E+10	4.00E+10	3.96E+10	4.12E+10	4.01E+10
Avg. Dy. Modulus (Pa)	3.94E+10			4.02E+10			4.03E+10		

Cycles	85			110			125		
Specimen Number	897A	897B	897C	897A	897B	897C	897A	897B	897C
Frequency n [Hz]	2208	2238	2222	2208	2240	2222	2212	2242	2226
Mass M [g]	7531.3	7612	7522.5	7532.6	7612.6	7523.3	7534.4	7614.2	7525.2
Dynamic Modulus (Pa)	3.98E+10	4.13E+10	4.02E+10	3.98E+10	4.14E+10	4.03E+10	3.99E+10	4.15E+10	4.04E+10
Avg. Dy. Modulus (Pa)	4.04E+10			4.05E+10			4.06E+10		

Cycles	151			187			205		
Specimen Number	897A	897B	897C	897A	897B	897C	897A	897B	897C
Frequency n [Hz]	2212	2244	2226	2218	2248	2230	2212	2250	2228
Mass M [g]	7533.9	7613.5	7524.1	7535.8	7615.6	7526.5	7533.9	7615.5	7526.3
Dynamic Modulus (Pa)	3.99E+10	4.15E+10	4.04E+10	4.02E+10	4.17E+10	4.06E+10	3.99E+10	4.18E+10	4.05E+10
Avg. Dy. Modulus (Pa)	4.06E+10			4.08E+10			4.07E+10		

Cycles	230			246			275		
Specimen Number	897A	897B	897C	897A	897B	897C	897A	897B	897C
Frequency n [Hz]	2216	2246	2232	2212	2250	2232	2218	2252	2234
Mass M [g]	7535.2	7614.8	7526.3	7535.9	7615.8	7526.7	7535.7	7616.1	7527.4
Dynamic Modulus (Pa)	4.01E+10	4.16E+10	4.06E+10	4.00E+10	4.18E+10	4.06E+10	4.02E+10	4.19E+10	4.07E+10
Avg. Dy. Modulus (Pa)	4.08E+10			4.08E+10			4.09E+10		

Cycles	321		
Specimen Number	897A	897B	897C
Frequency n [Hz]	2222	2246	2236
Mass M [g]	7536.1	7617.1	7527.3
Dynamic Modulus (Pa)	4.03E+10	4.16E+10	4.08E+10
Avg. Dy. Modulus (Pa)	4.09E+10		

*Batch is designated as "2% SRA-2 #2" in Program 1.

Table D.1 (Cont'd) Program 1 – Fundamental transverse frequency and mass data (ASTM C666 and C215)

Mixture: 0.75% SRA-3*

Cycles	0			23			50		
Specimen Number	928A	928B	928C	928A	928B	928C	928A	928B	928C
Frequency n [Hz]	2148	2256	2204	2146	2254	2206	2146	2254	2208
Mass M [g]	7586.4	7628.1	7645.9	7587.1	7628.9	7646.5	7587.5	7629.1	7647.1
Dynamic Modulus (Pa)	3.79E+10	4.21E+10	4.02E+10	3.79E+10	4.20E+10	4.03E+10	3.79E+10	4.20E+10	4.04E+10
Avg. Dy. Modulus (Pa)	4.01E+10			4.01E+10			4.01E+10		

Cycles	78			107			127		
Specimen Number	928A	928B	928C	928A	928B	928C	928A	928B	928C
Frequency n [Hz]	2148	2252	2210	2146	2250	2208	2144	2252	2204
Mass M [g]	7587.7	7629.5	7647.2	7587.5	7629.3	7647.4	7587.3	7629.5	7647.5
Dynamic Modulus (Pa)	3.79E+10	4.19E+10	4.05E+10	3.79E+10	4.19E+10	4.04E+10	3.78E+10	4.19E+10	4.03E+10
Avg. Dy. Modulus (Pa)	4.01E+10			4.00E+10			4.00E+10		

Cycles	141			173			202		
Specimen Number	928A	928B	928C	928A	928B	928C	928A	928B	928C
Frequency n [Hz]	2136	2250	2200	2130	2248	2194	2130	2248	2194
Mass M [g]	7589.9	7632.1	7648.8	7591.3	7634.5	7650.2	7590.1	7627.1	7680.5
Dynamic Modulus (Pa)	3.75E+10	4.19E+10	4.01E+10	3.73E+10	4.18E+10	3.99E+10	3.73E+10	4.18E+10	4.01E+10
Avg. Dy. Modulus (Pa)	3.98E+10			3.97E+10			3.97E+10		

Cycles	231			260			289		
Specimen Number	928A	928B	928C	928A	928B	928C	928A	928B	928C
Frequency n [Hz]	2130	2248	2194	2132	2250	2194	2134	2246	2196
Mass M [g]	7589.4	7626.8	7680.6	7587.2	7625.9	7680.8	7587.7	7626.6	7680.6
Dynamic Modulus (Pa)	3.73E+10	4.18E+10	4.01E+10	3.74E+10	4.18E+10	4.01E+10	3.74E+10	4.17E+10	4.01E+10
Avg. Dy. Modulus (Pa)	3.97E+10			3.98E+10			3.98E+10		

Cycles	317		
Specimen Number	928A	928B	928C
Frequency n [Hz]	2132	2244	2194
Mass M [g]	7588	7627.4	7680.5
Dynamic Modulus (Pa)	3.74E+10	4.16E+10	4.01E+10
Avg. Dy. Modulus (Pa)	3.97E+10		

*Batch is designated as "0.75% SRA-3" in Program 1.

Table D.1 (Cont'd) Program 1 – Fundamental transverse frequency and mass data (ASTM C666 and C215)

Mixture: 2.25% SRA-3*

Cycles	0			27			55		
Specimen Number	963A	963B	963C	963A	963B	963C	963A	963B	963C
Frequency n [Hz]	2.33E+03	2.24E+03	2.21E+03	2.31E+03	2.21E+03	2.18E+03	2.31E+03	2.21E+03	2.19E+03
Mass M [g]	7.53E+03	7.59E+03	7.43E+03	7.54E+03	7.59E+03	7.44E+03	7.54E+03	7.60E+03	7.44E+03
Dynamic Modulus (Pa)	4.42E+10	4.14E+10	3.92E+10	4.35E+10	4.03E+10	3.83E+10	4.37E+10	4.00E+10	3.86E+10
Avg. Dy. Modulus (Pa)	4.16E+10			4.07E+10			4.08E+10		

Cycles	79			108			136		
Specimen Number	963A	963B	963C	963A	963B	963C	963A	963B	963C
Frequency n [Hz]	2.32E+03	2.21E+03	2.19E+03	2.31E+03	2.20E+03	2.19E+03	2.29E+03	2.20E+03	2.19E+03
Mass M [g]	7.54E+03	7.60E+03	7.44E+03	7.54E+03	7.60E+03	7.44E+03	7.54E+03	7.60E+03	7.44E+03
Dynamic Modulus (Pa)	4.39E+10	4.00E+10	3.86E+10	4.34E+10	4.00E+10	3.87E+10	4.29E+10	3.99E+10	3.86E+10
Avg. Dy. Modulus (Pa)	4.09E+10			4.07E+10			4.05E+10		

Cycles	162			188			213		
Specimen Number	963A	963B	963C	963A	963B	963C	963A	963B	963C
Frequency n [Hz]	2.29E+03	2.20E+03	2.19E+03	2.29E+03	2.20E+03	2.19E+03	2.27E+03	2.19E+03	2.18E+03
Mass M [g]	7.54E+03	7.60E+03	7.45E+03	7.55E+03	7.61E+03	7.45E+03	7.55E+03	7.60E+03	7.45E+03
Dynamic Modulus (Pa)	4.28E+10	4.00E+10	3.87E+10	4.28E+10	4.00E+10	3.87E+10	4.20E+10	3.97E+10	3.84E+10
Avg. Dy. Modulus (Pa)	4.05E+10			4.05E+10			4.00E+10		

Cycles	240			268		
Specimen Number	963A	963B	963C	963A	963B	963C
Frequency n [Hz]	2.25E+03	2.19E+03	2.17E+03	2.23E+03	2.17E+03	2.16E+03
Mass M [g]	7.55E+03	7.60E+03	7.45E+03	7.55E+03	7.60E+03	7.45E+03
Dynamic Modulus (Pa)	4.13E+10	3.93E+10	3.81E+10	4.07E+10	3.88E+10	3.77E+10
Avg. Dy. Modulus (Pa)	3.96E+10			3.91E+10		

*Batch is designated as "2.25% SRA-3" in Program 1.

Table D.2 Program 2 – Fundamental transverse frequency and mass data (ASTM C666 and C215)

Mixture: 20% FA-F # 2*

Cycles	0			38			70		
Specimen Number	890A	890B	890C	890A	890B	890C	890A	890B	890C
Frequency n [Hz]	2174	2146	2184	2190	2162	2194	2194	2168	2204
Mass M [g]	7454.9	7373.6	7447.8	7468.1	7386.3	7459.5	7471.3	7390	7462.6
Dynamic Modulus (Pa)	3.82E+10	3.68E+10	3.85E+10	3.88E+10	3.74E+10	3.89E+10	3.90E+10	3.76E+10	3.93E+10
Avg. Dy. Modulus (Pa)	3.78E+10			3.84E+10			3.86E+10		

Cycles	85			110			125		
Specimen Number	890A	890B	890C	890A	890B	890C	890A	890B	890C
Frequency n [Hz]	2198	2168	2206	2200	2170	2210	2202	2176	2210
Mass M [g]	7472.7	7391.5	7463.5	7473.7	7392.4	7464.4	7474.4	7393.8	7465.1
Dynamic Modulus (Pa)	3.91E+10	3.76E+10	3.94E+10	3.92E+10	3.77E+10	3.95E+10	3.93E+10	3.79E+10	3.95E+10
Avg. Dy. Modulus (Pa)	3.87E+10			3.88E+10			3.89E+10		

Cycles	151			187			205		
Specimen Number	890A	890B	890C	890A	890B	890C	890A	890B	890C
Frequency n [Hz]	2204	2174	2210	2208	2174	2208	2210	2176	2210
Mass M [g]	7475.3	7394.7	7466	7478	7396.7	7468.1	7477.6	7397.1	7468.3
Dynamic Modulus (Pa)	3.93E+10	3.79E+10	3.95E+10	3.95E+10	3.79E+10	3.95E+10	3.96E+10	3.80E+10	3.95E+10
Avg. Dy. Modulus (Pa)	3.89E+10			3.89E+10			3.90E+10		

Cycles	230			246			275		
Specimen Number	890A	890B	890C	890A	890B	890C	890A	890B	890C
Frequency n [Hz]	2208	2182	2212	2208	2178	2220	2212	2182	2222
Mass M [g]	7478.1	7397.4	7468.7	7479.1	7398.1	7468.9	7479.4	7398.5	7469.6
Dynamic Modulus (Pa)	3.95E+10	3.82E+10	3.96E+10	3.95E+10	3.80E+10	3.99E+10	3.97E+10	3.82E+10	4.00E+10
Avg. Dy. Modulus (Pa)	3.91E+10			3.91E+10			3.93E+10		

Cycles	321		
Specimen Number	890A	890B	890C
Frequency n [Hz]	2212	2178	2222
Mass M [g]	7480.1	7399.6	7470.0
Dynamic Modulus (Pa)	3.97E+10	3.80E+10	4.00E+10
Avg. Dy. Modulus (Pa)	3.92E+10		

*Batch is designated as “20% FA-F # 2” in Program 2.

Table D.2 (Cont'd) Program 2 – Fundamental transverse frequency and mass data (ASTM C666 and C215)

Mixture: 20% FA-C *

Cycles	0			38			70		
Specimen Number	913A	913B	913C	913A	913B	913C	913A	913B	913C
Frequency n [Hz]	2215	2182	2220	2190	2164	2200	2192	2157	2198
Mass M [g]	7558.9	7626.8	7392.2	7559.2	7627.1	7392.5	7559.2	7627.2	7392.6
Dynamic Modulus (Pa)	4.02E+10	3.93E+10	3.95E+10	3.93E+10	3.87E+10	3.88E+10	3.94E+10	3.85E+10	3.87E+10
Avg. Dy. Modulus (Pa)	3.97E+10			3.89E+10			3.88E+10		

Cycles	85			110			125		
Specimen Number	913A	913B	913C	913A	913B	913C	913A	913B	913C
Frequency n [Hz]	2190	2160	2192	2175	2155	2185	2145	2142	2185
Mass M [g]	7559.3	7627.5	7392.4	7559.5	7627.6	7392.4	7559.6	7627.5	7392.6
Dynamic Modulus (Pa)	3.93E+10	3.86E+10	3.85E+10	3.88E+10	3.84E+10	3.82E+10	3.77E+10	3.79E+10	3.82E+10
Avg. Dy. Modulus (Pa)	3.88E+10			3.85E+10			3.80E+10		

Cycles	151			187			205		
Specimen Number	913A	913B	913C	913A	913B	913C	913A	913B	913C
Frequency n [Hz]	2120	2135	2185	2110	2140	2180	2072	2132	2170
Mass M [g]	7559.9	7627.4	7392.5	7559.8	7627.6	7392.6	7560.2	7628.1	7392.8
Dynamic Modulus (Pa)	3.68E+10	3.77E+10	3.82E+10	3.65E+10	3.79E+10	3.81E+10	3.52E+10	3.76E+10	3.77E+10
Avg. Dy. Modulus (Pa)	3.76E+10			3.75E+10			3.68E+10		

Cycles	230			276			295		
Specimen Number	913A	913B	913C	913A	913B	913C	913A	913B	913C
Frequency n [Hz]	2060	2132	2168	2058	2118	2160	2050	2120	2160
Mass M [g]	7560.1	7628.6	7392.4	7560.2	7628.7	7392.5	7560.2	7628.6	7392.1
Dynamic Modulus (Pa)	3.48E+10	3.76E+10	3.77E+10	3.47E+10	3.71E+10	3.74E+10	3.44E+10	3.72E+10	3.74E+10
Avg. Dy. Modulus (Pa)	3.67E+10			3.64E+10			3.63E+10		

Cycles	324		
Specimen Number	913A	913B	913C
Frequency n [Hz]	2060	2116	2164
Mass M [g]	7561.2	7629.1	7391.8
Dynamic Modulus (Pa)	3.48E+10	3.70E+10	3.75E+10
Avg. Dy. Modulus (Pa)	3.64E+10		

*Batch is designated as "20% FA-C" in Program 2.

Table D.2 (Cont'd) Program 2 – Fundamental transverse frequency and mass data (ASTM C666 and C215)

Mixture: 40% FA-F # 1 *

Cycles	0			35			51		
Specimen Number	889A	889B	889C	889A	889B	889C	889A	889B	889C
Frequency n [Hz]	2130	2132	2124	2120	2120	2110	2132	2120	2118
Mass M [g]	7322.9	7422.2	7317.4	7328.3	7427.8	7323.2	7329.9	7429.1	7324.5
Dynamic Modulus (Pa)	3.60E+10	3.66E+10	3.58E+10	3.57E+10	3.62E+10	3.53E+10	3.61E+10	3.62E+10	3.56E+10
Avg. Dy. Modulus (Pa)	3.61E+10			3.57E+10			3.60E+10		

Cycles	73			120			136		
Specimen Number	889A	889B	889C	889A	889B	889C	889A	889B	889C
Frequency n [Hz]	2134	2120	2115	2142	2138	2128	2142	2140	2125
Mass M [g]	7331.1	7430.3	7326.2	7332.6	7432.3	7328.1	7332.9	7433	7328.6
Dynamic Modulus (Pa)	3.62E+10	3.62E+10	3.55E+10	3.65E+10	3.68E+10	3.60E+10	3.65E+10	3.69E+10	3.59E+10
Avg. Dy. Modulus (Pa)	3.60E+10			3.64E+10			3.64E+10		

Cycles	160			206			269		
Specimen Number	889A	889B	889C	889A	889B	889C	889A	889B	889C
Frequency n [Hz]	2140	2140	2136	2160	2158	2150	2164	2162	2152
Mass M [g]	7333.6	7433	7328.1	7333.5	7432.8	7327.4	7335.7	7435.1	7330.8
Dynamic Modulus (Pa)	3.64E+10	3.69E+10	3.62E+10	3.71E+10	3.75E+10	3.67E+10	3.72E+10	3.77E+10	3.68E+10
Avg. Dy. Modulus (Pa)	3.65E+10			3.71E+10			3.72E+10		

Cycles	315		
Specimen Number	889A	889B	889C
Frequency n [Hz]	2168	2164	2152
Mass M [g]	7337	7436.4	7331.3
Dynamic Modulus (Pa)	3.74E+10	3.77E+10	3.68E+10
Avg. Dy. Modulus (Pa)	3.73E+10		

*Batch is designated as "40% FA-F # 1" in Program 2.

Table D.2 (Cont'd) Program 2 – Fundamental transverse frequency and mass data (ASTM C666 and C215)

Mixture: 40% FA-F # 2 *

Cycles	0			35			51		
Specimen Number	**889A**	**889B**	**889C**	**889A**	**889B**	**889C**	**889A**	**889B**	**889C**
Frequency n [Hz]	2140	2140	2136	2160	2158	2150	2164	2162	2152
Mass M [g]	7333.6	7433	7328.1	7333.5	7432.8	7327.4	7335.7	7435.1	7330.8
Dynamic Modulus (Pa)	3.64E+10	3.69E+10	3.62E+10	3.71E+10	3.75E+10	3.67E+10	3.72E+10	3.77E+10	3.68E+10
Avg. Dy. Modulus (Pa)	3.67E+10			3.63E+10			3.63E+10		

Cycles	73			120			136		
Specimen Number	**880A**	**880B**	**880C**	**880A**	**880B**	**880C**	**880A**	**880B**	**880C**
Frequency n [Hz]	2140	2110	2100	2148	2126	2104	2140	2126	2110
Mass M [g]	7474.1	7491.9	7496.4	7473.6	7492.4	7497.3	7473.7	7491.5	7498.2
Dynamic Modulus (Pa)	3.71E+10	3.61E+10	3.58E+10	3.74E+10	3.67E+10	3.60E+10	3.71E+10	3.67E+10	3.62E+10
Avg. Dy. Modulus (Pa)	3.64E+10			3.67E+10			3.67E+10		

Cycles	160			206			269		
Specimen Number	**880A**	**880B**	**880C**	**880A**	**880B**	**880C**	**880A**	**880B**	**880C**
Frequency n [Hz]	2150	2132	2112	2184	2144	2128	2170	2144	2126
Mass M [g]	7475	7493.8	7498	7472.2	7491.9	7498.4	7474.8	7494	7500.7
Dynamic Modulus (Pa)	3.74E+10	3.69E+10	3.62E+10	3.86E+10	3.73E+10	3.68E+10	3.81E+10	3.73E+10	3.67E+10
Avg. Dy. Modulus (Pa)	3.69E+10			3.76E+10			3.74E+10		

Cycles	315		
Specimen Number	**880A**	**880B**	**880C**
Frequency n [Hz]	2170	2146	2120
Mass M [g]	7475.5	7494.6	7501.3
Dynamic Modulus (Pa)	3.81E+10	3.74E+10	3.65E+10
Avg. Dy. Modulus (Pa)	3.74E+10		

*Batch is designated as "40% FA-F # 2" in Program 2.

Table D.2 (Cont'd) Program 2 – Fundamental transverse frequency and mass data (ASTM C666 and C215)

Mixture: 0.05% RMA *

Cycles	0			22			37		
Specimen Number	905A	905B	905C	905A	905B	905C	905A	905B	905C
Frequency n [Hz]	2164	2126	2128	2172	2126	2136	2176	2138	2144
Mass M [g]	7368.1	7332.2	7301.7	7378.5	7341.5	7311.1	7382.5	7345.1	7314.6
Dynamic Modulus (Pa)	3.74E+10	3.59E+10	3.58E+10	3.77E+10	3.60E+10	3.61E+10	3.79E+10	3.64E+10	3.64E+10
Avg. Dy. Modulus (Pa)	3.64E+10			3.66E+10			3.69E+10		

Cycles	75			110			134		
Specimen Number	905A	905B	905C	905A	905B	905C	905A	905B	905C
Frequency n [Hz]	2188	2150	2154	2180	2134	2144	2185	2142	2120
Mass M [g]	7391.5	7354.6	7323.8	7391.3	7353.6	7323.5	7392.5	7355.7	7325.2
Dynamic Modulus (Pa)	3.83E+10	3.68E+10	3.68E+10	3.81E+10	3.63E+10	3.65E+10	3.82E+10	3.66E+10	3.57E+10
Avg. Dy. Modulus (Pa)	3.73E+10			3.69E+10			3.68E+10		

Cycles	149			164			187		
Specimen Number	905A	905B	905C	905A	905B	905C	905A	905B	905C
Frequency n [Hz]	2190	2150	2156	2196	2152	2162	2194	2150	2160
Mass M [g]	7394.7	7357.9	7327.1	7397.3	7359.4	7328.3	7395.1	7359.1	7328.3
Dynamic Modulus (Pa)	3.84E+10	3.69E+10	3.69E+10	3.87E+10	3.69E+10	3.71E+10	3.86E+10	3.69E+10	3.71E+10
Avg. Dy. Modulus (Pa)	3.74E+10			3.76E+10			3.75E+10		

Cycles	216			246			269		
Specimen Number	905A	905B	905C	905A	905B	905C	905A	905B	905C
Frequency n [Hz]	2190	2150	2156	2194	2152	2154	2198	2154	2158
Mass M [g]	7394.3	7357.6	7327.6	7395.4	7360.6	7330.2	7393.8	7358.5	7328.3
Dynamic Modulus (Pa)	3.84E+10	3.69E+10	3.69E+10	3.86E+10	3.69E+10	3.69E+10	3.87E+10	3.70E+10	3.70E+10
Avg. Dy. Modulus (Pa)	3.74E+10			3.75E+10			3.76E+10		

Cycles	313		
Specimen Number	905A	905B	905C
Frequency n [Hz]	2196	2156	2156
Mass M [g]	7388.7	7363.5	7321.2
Dynamic Modulus (Pa)	3.86E+10	3.71E+10	3.69E+10
Avg. Dy. Modulus (Pa)	3.75E+10		

*Batch is designated as "0.05% RMA" in Program 2.

Table D.2 (Cont'd) Program 2 – Fundamental transverse frequency and mass data (ASTM C666 and C215)

Mixture: 0.075% RMA *

Cycles	0			29			57		
Specimen Number	909A	909B	909C	909A	909B	909C	909A	909B	909C
Frequency n [Hz]	2158	2124	2146	2158	2126	2144	2154	2126	2148
Mass M [g]	7205.6	7221.8	7193.9	7208.1	7223.5	7194.2	7207.9	7223.4	7196
Dynamic Modulus (Pa)	3.64E+10	3.53E+10	3.59E+10	3.64E+10	3.54E+10	3.58E+10	3.62E+10	3.54E+10	3.60E+10
Avg. Dy. Modulus (Pa)	3.59E+10			3.59E+10			3.59E+10		

Cycles	84			114			136		
Specimen Number	909A	909B	909C	909A	909B	909C	909A	909B	909C
Frequency n [Hz]	2156	2128	2146	2152	2130	2148	2152	2132	2150
Mass M [g]	7207.5	7223.1	7193.8	7207.4	7223.5	7194	7207.1	7223.6	7193.5
Dynamic Modulus (Pa)	3.63E+10	3.54E+10	3.59E+10	3.62E+10	3.55E+10	3.60E+10	3.62E+10	3.56E+10	3.60E+10
Avg. Dy. Modulus (Pa)	3.59E+10			3.59E+10			3.59E+10		

Cycles	164			190			218		
Specimen Number	909A	909B	909C	909A	909B	909C	909A	909B	909C
Frequency n [Hz]	2156	2134	2154	2158	2132	2152	2160	2130	2150
Mass M [g]	7207.5	7224	7193.8	7207.4	7223.4	7193.6	7207	7223	7194
Dynamic Modulus (Pa)	3.63E+10	3.56E+10	3.62E+10	3.64E+10	3.56E+10	3.61E+10	3.64E+10	3.55E+10	3.60E+10
Avg. Dy. Modulus (Pa)	3.60E+10			3.60E+10			3.60E+10		

Cycles	247			276			295		
Specimen Number	909A	909B	909C	909A	909B	909C	909A	909B	909C
Frequency n [Hz]	2162	2134	2152	2158	2132	2150	2160	2132	2152
Mass M [g]	7206.5	7224	7193.8	7207	7223.8	7194	7206.8	7223.6	7192
Dynamic Modulus (Pa)	3.65E+10	3.56E+10	3.61E+10	3.86E+10	3.69E+10	3.69E+10	3.87E+10	3.70E+10	3.70E+10
Avg. Dy. Modulus (Pa)	3.61E+10			3.60E+10			3.60E+10		

Cycles	324		
Specimen Number	909A	909B	909C
Frequency n [Hz]	2160	2130	2150
Mass M [g]	7206.7	7223.5	7192.8
Dynamic Modulus (Pa)	3.64E+10	3.55E+10	3.60E+10
Avg. Dy. Modulus (Pa)	3.60E+10		

*Batch is designated as "0.075% RMA" in Program 2.

Table D.2 (Cont'd) Program 2 – Fundamental transverse frequency and mass data (ASTM C666 and C215)

Mixture: 0.05% RMA - 40 % FA-C *

Cycles	0			22			37		
Specimen Number	899A	899B	899C	899A	899B	899C	899A	899B	899C
Frequency n [Hz]	2228	2206	2196	2228	2204	2190	2228	2204	2192
Mass M [g]	7606	7488.4	7551.7	7608.9	7493.7	7556.1	7612	7497	7559.3
Dynamic Modulus (Pa)	4.09E+10	3.95E+10	3.95E+10	4.09E+10	3.94E+10	3.93E+10	4.09E+10	3.95E+10	3.94E+10
Avg. Dy. Modulus (Pa)	4.00E+10			3.99E+10			3.99E+10		

Cycles	75			110			134		
Specimen Number	899A	899B	899C	899A	899B	899C	899A	899B	899C
Frequency n [Hz]	2238	2212	2204	2234	2208	2198	2239	2214	2203
Mass M [g]	7617.5	7502.4	7563.7	7617.1	7499.5	7562.5	7618.3	7501.7	7564.5
Dynamic Modulus (Pa)	4.13E+10	3.98E+10	3.98E+10	4.12E+10	3.96E+10	3.96E+10	4.14E+10	3.98E+10	3.98E+10
Avg. Dy. Modulus (Pa)	4.03E+10			4.01E+10			4.03E+10		

Cycles	149			164			187		
Specimen Number	899A	899B	899C	899A	899B	899C	899A	899B	899C
Frequency n [Hz]	2244	2220	2208	2248	2222	2212	2250	2218	2212
Mass M [g]	7619.5	7503.9	7566	7620.8	7505.3	7566.9	7619.3	7504.5	7566
Dynamic Modulus (Pa)	4.16E+10	4.01E+10	4.00E+10	4.17E+10	4.02E+10	4.01E+10	4.18E+10	4.00E+10	4.01E+10
Avg. Dy. Modulus (Pa)	4.05E+10			4.07E+10			4.06E+10		

Cycles	216			246			269		
Specimen Number	899A	899B	899C	899A	899B	899C	899A	899B	899C
Frequency n [Hz]	2248	2228	2216	2250	2232	2220	2250	2228	2214
Mass M [g]	7616.2	7502	7561.9	7620.7	7505.3	7566.2	7620.5	7505.7	7566.8
Dynamic Modulus (Pa)	4.17E+10	4.04E+10	4.02E+10	4.18E+10	4.05E+10	4.04E+10	4.18E+10	4.04E+10	4.02E+10
Avg. Dy. Modulus (Pa)	4.08E+10			4.09E+10			4.08E+10		

Cycles	313		
Specimen Number	899A	899B	899C
Frequency n [Hz]	2248	2230	2210
Mass M [g]	7625	7497.7	7570.5
Dynamic Modulus (Pa)	4.18E+10	4.04E+10	4.01E+10
Avg. Dy. Modulus (Pa)	4.07E+10		

*Batch is designated as "0.05% RMA - 40% FA-C" in Program 2.

Table D.2 (Cont'd) Program 2 – Fundamental transverse frequency and mass data (ASTM C666 and C215)

Mixture: 0.075% RMA - 40 % FA-C *

Cycles	0			27			55		
Specimen Number	967A	967B	967C	967A	967B	967C	967A	967B	967C
Frequency n [Hz]	2174	2136	2159	2152	2115	2140	2150	2120	2139
Mass M [g]	7418.5	7373.1	7417.2	7421.6	7376.9	7418.9	7422.4	7378.3	7419.2
Dynamic Modulus (Pa)	3.80E+10	3.65E+10	3.75E+10	3.72E+10	3.58E+10	3.68E+10	3.72E+10	3.59E+10	3.68E+10
Avg. Dy. Modulus (Pa)	3.73E+10			3.66E+10			3.66E+10		

Cycles	79			108			136		
Specimen Number	967A	967B	967C	967A	967B	967C	967A	967B	967C
Frequency n [Hz]	2154	2122	2140	2155	2122	2142	2154	2120	2138
Mass M [g]	7421.8	7378.9	7419.9	7421.5	7378.2	7421.8	7420.8	7377.9	7423
Dynamic Modulus (Pa)	3.73E+10	3.60E+10	3.69E+10	3.72E+10	3.58E+10	3.66E+10	3.71E+10	3.59E+10	3.67E+10
Avg. Dy. Modulus (Pa)	3.67E+10			3.65E+10			3.66E+10		

Cycles	162			186			213		
Specimen Number	967A	967B	967C	967A	967B	967C	967A	967B	967C
Frequency n [Hz]	2152	2117	2132	2150	2122	2134	2148	2120	2135
Mass M [g]	7419.1	7376.7	7421	7419.6	7377.9	7422.9	7419.8	7378.3	7423.6
Dynamic Modulus (Pa)	3.72E+10	3.59E+10	3.68E+10	3.73E+10	3.59E+10	3.68E+10	3.71E+10	3.59E+10	3.67E+10
Avg. Dy. Modulus (Pa)	3.66E+10			3.67E+10			3.66E+10		

Cycles	240			268			294		
Specimen Number	967A	967B	967C	967A	967B	967C	967A	967B	967C
Frequency n [Hz]	2150	2120	2136	2152	2120	2138	2154	2122	2136
Mass M [g]	7419	7378.6	7424.6	7418.3	7377.6	7423.4	7418.6	7379.1	7424.6
Dynamic Modulus (Pa)	3.72E+10	3.59E+10	3.67E+10	3.72E+10	3.59E+10	3.68E+10	3.73E+10	3.60E+10	3.67E+10
Avg. Dy. Modulus (Pa)	3.66E+10			3.66E+10			3.67E+10		

Cycles	321		
Specimen Number	967A	967B	967C
Frequency n [Hz]	2155	2120	2138
Mass M [g]	7419.3	7377.2	7424.9
Dynamic Modulus (Pa)	3.73E+10	3.59E+10	3.68E+10
Avg. Dy. Modulus (Pa)	3.67E+10		

*Batch is designated as "0.075% RMA- 40% FA-C" in Program 2.

Table D.2 (Cont'd) Program 2 – Fundamental transverse frequency and mass data (ASTM C666 and C215)

Mixture: 0.15% RMA - 40 % FA-C *

Cycles	0			29			57		
Specimen Number	911A	911B	911C	911A	911B	911C	911A	911B	911C
Frequency n [Hz]	2218	2230	2256	2230	2244	2264	2230	2244	2264
Mass M [g]	7270.1	7221.8	7193.9	7271.2	7222.3	7194	7271.5	7222.1	7194.2
Dynamic Modulus (Pa)	3.88E+10	3.89E+10	3.97E+10	3.92E+10	3.94E+10	4.00E+10	3.92E+10	3.94E+10	4.00E+10
Avg. Dy. Modulus (Pa)	3.91E+10			3.95E+10			3.95E+10		

Cycles	84			114			136		
Specimen Number	911A	911B	911C	911A	911B	911C	911A	911B	911C
Frequency n [Hz]	2234	2248	2268	2238	2248	2270	2234	2246	2268
Mass M [g]	7271.3	7222.5	7194.4	7271.6	7222.6	7195.1	7273	7223.1	7195.8
Dynamic Modulus (Pa)	3.93E+10	3.96E+10	4.01E+10	3.95E+10	3.96E+10	4.02E+10	3.93E+10	3.95E+10	4.01E+10
Avg. Dy. Modulus (Pa)	3.97E+10			3.97E+10			3.96E+10		

Cycles	164			190			218		
Specimen Number	911A	911B	911C	911A	911B	911C	911A	911B	911C
Frequency n [Hz]	2238	2250	2272	2240	2254	2274	2242	2248	2278
Mass M [g]	7272.4	7223	7195.6	7272.6	7271.9	7196.2	7273.5	7271.8	7196.2
Dynamic Modulus (Pa)	3.95E+10	3.96E+10	4.02E+10	3.95E+10	4.00E+10	4.03E+10	3.96E+10	3.98E+10	4.05E+10
Avg. Dy. Modulus (Pa)	3.98E+10			4.00E+10			4.00E+10		

Cycles	247			276			295		
Specimen Number	911A	911B	911C	911A	911B	911C	911A	911B	911C
Frequency n [Hz]	2234	2244	2274	2238	2254	2276	2244	2254	2280
Mass M [g]	7273	7271.6	7195.8	7273.2	7271.9	7196.5	7273.6	7271.6	7196.5
Dynamic Modulus (Pa)	3.93E+10	3.97E+10	4.03E+10	3.95E+10	4.00E+10	4.04E+10	3.97E+10	4.00E+10	4.05E+10
Avg. Dy. Modulus (Pa)	3.98E+10			4.00E+10			4.01E+10		

Cycles	321		
Specimen Number	911A	911B	911C
Frequency n [Hz]	2244	2252	2276
Mass M [g]	7274.1	7272.3	7197.2
Dynamic Modulus (Pa)	3.97E+10	4.00E+10	4.04E+10
Avg. Dy. Modulus (Pa)	4.00E+10		

*Batch is designated as "0.15% RMA-1 - 40% FA-C" in Program 2.

Table D.2 (Cont'd) Program 2 – Fundamental transverse frequency and mass data (ASTM C666 and C215)

Mixture: 0.15% RMA - 20 % FA-C *

Cycles	0			29			57		
Specimen Number	912A	912B	912C	912A	912B	912C	912A	912B	912C
Frequency n [Hz]	2211	2270	2298	2205	2261	2290	2204	2268	2295
Mass M [g]	7332.3	7346.8	7348.4	7332.4	7347	7349.5	7333.1	7247.6	7348.3
Dynamic Modulus (Pa)	3.88E+10	4.10E+10	4.21E+10	3.86E+10	4.07E+10	4.18E+10	3.86E+10	4.04E+10	4.19E+10
Avg. Dy. Modulus (Pa)	4.06E+10			4.04E+10			4.03E+10		

Cycles	84			114			136		
Specimen Number	912A	912B	912C	912A	912B	912C	912A	912B	912C
Frequency n [Hz]	2202	2277	2306	2207	2274	2303	2212	2270	2300
Mass M [g]	7333.5	7248.6	7349.1	7333.5	7248.4	7349.6	7333.9	7248.9	7349.8
Dynamic Modulus (Pa)	3.85E+10	4.07E+10	4.23E+10	3.87E+10	4.06E+10	4.22E+10	3.89E+10	4.05E+10	4.21E+10
Avg. Dy. Modulus (Pa)	4.05E+10			4.05E+10			4.05E+10		

Cycles	164			190			218		
Specimen Number	912A	912B	912C	912A	912B	912C	912A	912B	912C
Frequency n [Hz]	2208	2268	2302	2205	2270	2302	2209	2276	2298
Mass M [g]	7333.6	7248.7	7349.2	7334.5	7247.9	7349.4	7334.6	7248.2	7349.6
Dynamic Modulus (Pa)	3.87E+10	4.04E+10	4.22E+10	3.86E+10	4.05E+10	4.22E+10	3.88E+10	4.07E+10	4.21E+10
Avg. Dy. Modulus (Pa)	4.04E+10			4.04E+10			4.05E+10		

Cycles	247			276			295		
Specimen Number	912A	912B	912C	912A	912B	912C	912A	912B	912C
Frequency n [Hz]	2208	2274	2298	2206	2276	2296	2208	2278	2300
Mass M [g]	7334.4	7248.1	7349.6	7334.5	7249.1	7349.1	7335	7249.3	7349.2
Dynamic Modulus (Pa)	3.87E+10	4.06E+10	4.21E+10	3.87E+10	4.07E+10	4.20E+10	3.88E+10	4.08E+10	4.21E+10
Avg. Dy. Modulus (Pa)	4.05E+10			4.05E+10			4.05E+10		

Cycles	324		
Specimen Number	912A	912B	912C
Frequency n [Hz]	2204	2276	2300
Mass M [g]	7334.4	7248.6	7348.9
Dynamic Modulus (Pa)	3.86E+10	4.07E+10	4.21E+10
Avg. Dy. Modulus (Pa)	4.05E+10		

*Batch is designated as "0.15% RMA - 20% FA-C" in Program 2.

Table D.3 Program 3 – Fundamental transverse frequency and mass data (ASTM C666 and C215)

Mixture: 2.5% SCA-1 # 1 *

Cycles	0			22			83		
Specimen Number	**855A**	**855B**	**855C**	**855A**	**855B**	**855C**	**855A**	**855B**	**855C**
Frequency n [Hz]	2097	2138	2123	2089	2131	2120	2069	2125	2118
Mass M [g]	7252	7328.1	7255.9	7265.4	7337.3	7265.9	7274.8	7348	7276.1
Dynamic Modulus (Pa)	3.46E+10	3.63E+10	3.54E+10	3.44E+10	3.61E+10	3.54E+10	3.37E+10	3.60E+10	3.54E+10
Avg. Dy. Modulus (Pa)	3.54E+10			3.53E+10			3.50E+10		

Cycles	128			173			272		
Specimen Number	**855A**	**855B**	**855C**	**855A**	**855B**	**855C**	**855A**	**855B**	**855C**
Frequency n [Hz]	2074	2131	2116	2073	2130	2118	2078	2130	2125
Mass M [g]	7278.8	7349	7280.3	7273.7	7347.7	7279.4	7278.5	7350.1	7285.8
Dynamic Modulus (Pa)	3.39E+10	3.62E+10	3.53E+10	3.39E+10	3.61E+10	3.54E+10	3.41E+10	3.61E+10	3.57E+10
Avg. Dy. Modulus (Pa)	3.51E+10			3.51E+10			3.53E+10		

Cycles	289			353		
Specimen Number	**855A**	**855B**	**855C**	**855A**	**855B**	**855C**
Frequency n [Hz]	2079	2135	2128	2082	2138	2135
Mass M [g]	7279.1	7352.2	7284.4	7280	7353.2	7285.6
Dynamic Modulus (Pa)	3.41E+10	3.63E+10	3.57E+10	3.42E+10	3.64E+10	3.60E+10
Avg. Dy. Modulus (Pa)	3.54E+10			3.55E+10		

*Batch is designated as “2.5% SCA-1 # 1” in Program 3.

Table D.3 (Cont'd) Program 3 – Fundamental transverse frequency and mass data (ASTM C666 and C215)

Mixture: 2.5% SCA-1 # 2 *

Cycles	0			31			40		
Specimen Number	861A	861B	861C	861A	861B	861C	861A	861B	861C
Frequency n [Hz]	2215	2182	2220	2190	2164	2200	2192	2157	2198
Mass M [g]	7512.3	7398.9	7519	7523.8	7405.5	7527.7	7526.4	7410	7529.9
Dynamic Modulus (Pa)	3.99E+10	3.82E+10	4.02E+10	3.91E+10	3.76E+10	3.95E+10	3.912E+10	3.74E+10	3.94E+10
Avg. Dy. Modulus (Pa)	3.94E+10			3.87E+10			3.87E+10		

Cycles	71			108			146		
Specimen Number	861A	861B	861C	861A	861B	861C	861A	861B	861C
Frequency n [Hz]	2190	2160	2192	2175	2155	2185	2145	2142	2185
Mass M [g]	7527.1	7412.2	7533.8	7532.8	7417.5	7537.4	7534.8	7419.2	7540.2
Dynamic Modulus (Pa)	3.91E+10	3.75E+10	3.92E+10	3.86E+10	3.73E+10	3.90E+10	3.76E+10	3.69E+10	3.90E+10
Avg. Dy. Modulus (Pa)	3.86E+10			3.83E+10			3.78E+10		

Cycles	164			197			215		
Specimen Number	861A	861B	861C	861A	861B	861C	861A	861B	861C
Frequency n [Hz]	2120	2135	2185	2110	2140	2180	2072	2132	2170
Mass M [g]	7535.2	7419.8	7540.2	7535.7	7420.5	7541.5	7535.8	7419.8	7541.1
Dynamic Modulus (Pa)	3.67E+10	3.67E+10	3.90E+10	3.64E+10	3.68E+10	3.89E+10	3.51E+10	3.66E+10	3.85E+10
Avg. Dy. Modulus (Pa)	3.75E+10			3.73E+10			3.67E+10		

Cycles	246			289			326		
Specimen Number	861A	861B	861C	861A	861B	861C	861A	861B	861C
Frequency n [Hz]	2060	2132	2168	1980	2115	2140	1970	2130	2160
Mass M [g]	7536.1	7420.2	7541.8	7534	7415.9	7539.9	7537.2	7420.6	7542.9
Dynamic Modulus (Pa)	3.47E+10	3.66E+10	3.84E+10	3.20E+10	3.60E+10	3.74E+10	3.17E+10	3.65E+10	3.81E+10
Avg. Dy. Modulus (Pa)	3.65E+10			3.51E+10			3.54E+10		

*Batch is designated as "2.5% SCA-1 # 2" in Program 3.

Table D.3 (Cont'd) Program 3 – Fundamental transverse frequency and mass data (ASTM C666 and C215)

Mixture: 5% SCA-1 *

Cycles	0			99			116		
Specimen Number	**857A**	**857B**	**857C**	**857A**	**857B**	**857C**	**857A**	**857B**	**857C**
Frequency n [Hz]	2348	2313	2318	2321	2269	2279	2320	2273	2285
Mass M [g]	7878.9	7797.6	7849.5	7886.1	7801.7	7857.7	7886.4	7803.4	7858.8
Dynamic Modulus (Pa)	4.71E+10	4.52E+10	4.57E+10	4.60E+10	4.35E+10	4.42E+10	4.60E+10	4.37E+10	4.45E+10
Avg. Dy. Modulus (Pa)	4.60E+10			4.46E+10			4.47E+10		

Cycles	180			225			263		
Specimen Number	**857A**	**857B**	**857C**	**857A**	**857B**	**857C**	**857A**	**857B**	**857C**
Frequency n [Hz]	2322	2270	2282	2320	2255	2270	2310	2200	2248
Mass M [g]	7889.3	7804.7	7862.9	7889.6	7806.6	7865.5	7889.6	7810.7	7867.3
Dynamic Modulus (Pa)	4.61E+10	4.36E+10	4.44E+10	4.60E+10	4.30E+10	4.39E+10	4.56E+10	4.10E+10	4.31E+10
Avg. Dy. Modulus (Pa)	4.47E+10			4.43E+10			4.32E+10		

Cycles	277			315		
Specimen Number	**857A**	**857B**	**857C**	**857A**	**857B**	**857C**
Frequency n [Hz]	2308	2185	2235	2298	2130	2182
Mass M [g]	7888.8	7810.3	7866.2	7890.6	7814.7	7868.6
Dynamic Modulus (Pa)	4.55E+10	4.04E+10	4.26E+10	4.52E+10	3.84E+10	4.06E+10
Avg. Dy. Modulus (Pa)	4.28E+10			4.14E+10		

*Batch is designated as "5% SCA-1" in Program 3.

Table D.3 (Cont'd) Program 3 – Fundamental transverse frequency and mass data (ASTM C666 and C215)

Mixture: 7.5% SCA-1 # 1 *

Cycles	0			9			40		
Specimen Number	**862A**	**862B**	**862C**	**862A**	**862B**	**862C**	**862A**	**862B**	**862C**
Frequency n [Hz]	2355	2375	2310	2320	2340	2280	2260	2268	2205
Mass M [g]	7886.3	7954.4	7734	7898.5	7955.3	7745.3	7910.4	7975.5	7758.8
Dynamic Modulus (Pa)	4.74E+10	4.86E+10	4.47E+10	4.61E+10	4.72E+10	4.36E+10	4.38E+10	4.45E+10	4.09E+10
Avg. Dy. Modulus (Pa)	4.69E+10			4.56E+10			4.30E+10		

Cycles	77			115			133		
Specimen Number	**862A**	**862B**	**862C**	**862A**	**862B**	**862C**	**862A**	**862B**	**862C**
Frequency n [Hz]	1890	1820	1850	1560	1520	1550	1420	1395	1460
Mass M [g]	7925.4	7991.3	7775.1	7931.7	7997.5	7781.4	7934.8	8000.9	7785.1
Dynamic Modulus (Pa)	3.07E+10	2.87E+10	2.88E+10	2.09E+10	2.00E+10	2.03E+10	1.73E+10	1.69E+10	1.80E+10
Avg. Dy. Modulus (Pa)	2.94E+10			2.04E+10			1.74E+10		

*Batch is designated as "7.5% SCA-1 # 1" in Program 3.

Table D.3 (Cont'd) Program 3 – Fundamental transverse frequency and mass data (ASTM C666 and C215)

Mixture: 7.5% SCA-1 # 2 *

Cycles	0			38			52		
Specimen Number	**860A**	**860B**	**860C**	**860A**	**860B**	**860C**	**860A**	**860B**	**860C**
Frequency n [Hz]	2130	2123	2108	2118	2110	2095	2115	2108	2095
Mass M [g]	7310.8	7305.2	7304.4	7321.3	7313.8	7312.4	7322.6	7316.6	7315.1
Dynamic Modulus (Pa)	3.59E+10	3.57E+10	3.52E+10	3.56E+10	3.53E+10	3.48E+10	3.55E+10	3.52E+10	3.48E+10
Avg. Dy. Modulus (Pa)	3.56E+10			3.52E+10			3.52E+10		

Cycles	90			121			136		
Specimen Number	**860A**	**860B**	**860C**	**860A**	**860B**	**860C**	**860A**	**860B**	**860C**
Frequency n [Hz]	2116	2112	2098	2112	2108	2095	2112	2105	2095
Mass M [g]	7329	7320.9	7320.7	7332	7323.6	7323.1	7332.6	7325.4	7324.1
Dynamic Modulus (Pa)	3.56E+10	3.54E+10	3.49E+10	3.54E+10	3.53E+10	3.48E+10	3.54E+10	3.52E+10	3.48E+10
Avg. Dy. Modulus (Pa)	3.53E+10			3.52E+10			3.52E+10		

Cycles	167			176			207		
Specimen Number	**860A**	**860B**	**860C**	**860A**	**860B**	**860C**	**860A**	**860B**	**860C**
Frequency n [Hz]	2112	2109	2091	2112	2108	2098	2110	2105	2095
Mass M [g]	7332.5	7323.4	7323.1	7333.4	7324.4	7324.5	7334.9	7326	7325.7
Dynamic Modulus (Pa)	3.54E+10	3.53E+10	3.47E+10	3.54E+10	3.53E+10	3.49E+10	3.54E+10	3.52E+10	3.48E+10
Avg. Dy. Modulus (Pa)	3.51E+10			3.52E+10			3.51E+10		

Cycles	244			282			300		
Specimen Number	**860A**	**860B**	**860C**	**860A**	**860B**	**860C**	**860A**	**860B**	**860C**
Frequency n [Hz]	2110	2108	2090	2110	2105	2090	2105	2105	2092
Mass M [g]	7337.5	7328.9	7325.4	7339	7329.8	7326	7339.6	7329.9	7326.3
Dynamic Modulus (Pa)	3.54E+10	3.53E+10	3.47E+10	3.54E+10	3.52E+10	3.47E+10	3.52E+10	3.52E+10	3.47E+10
Avg. Dy. Modulus (Pa)	3.51E+10			3.51E+10			3.51E+10		

*Batch is designated as "7.5% SCA-1 # 2" in Program 3.

Table D.3 (Cont'd) Program 3 – Fundamental transverse frequency and mass data (ASTM C666 and C215)

Mixture: 6% SCA-2 *

Cycles	0			27			56		
Specimen Number	955A	955B	955C	955A	955B	955C	955A	955B	955C
Frequency n [Hz]	2354	2374	2310	2358	2380	2320	2358	2380	2318
Mass M [g]	7886.8	7956.8	7735.8	7891.5	7959.8	7741.8	7891.5	7961.5	7745.9
Dynamic Modulus (Pa)	4.74E+10	4.86E+10	4.47E+10	4.75E+10	4.89E+10	4.52E+10	4.75E+10	4.89E+10	4.51E+10
Avg. Dy. Modulus (Pa)	4.69E+10			4.72E+10			4.72E+10		

Cycles	83			112			140		
Specimen Number	955A	955B	955C	955A	955B	955C	955A	955B	955C
Frequency n [Hz]	2360	2382	2320	2362	2384	2322	2362	2386	2324
Mass M [g]	7895.6	7965.5	7749.8	7899.8	7968.2	7753.9	7901.3	7969.8	7754.2
Dynamic Modulus (Pa)	4.77E+10	4.90E+10	4.52E+10	4.78E+10	4.91E+10	4.53E+10	4.78E+10	4.92E+10	4.54E+10
Avg. Dy. Modulus (Pa)	4.73E+10			4.74E+10			4.74E+10		

Cycles	165			192			222		
Specimen Number	955A	955B	955C	955A	955B	955C	955A	955B	955C
Frequency n [Hz]	2360	2386	2322	2360	2386	2320	2362	2382	2318
Mass M [g]	7900.5	7968.3	7755.6	7899.5	7964.2	7754.5	7898.6	7965.2	7756.3
Dynamic Modulus (Pa)	4.77E+10	4.92E+10	4.53E+10	4.77E+10	4.91E+10	4.52E+10	4.78E+10	4.90E+10	4.52E+10
Avg. Dy. Modulus (Pa)	4.74E+10			4.73E+10			4.73E+10		

Cycles	248			274			303		
Specimen Number	955A	955B	955C	955A	955B	955C	955A	955B	955C
Frequency n [Hz]	2360	2378	2314	2360	2376	2312	2360	2378	2312
Mass M [g]	7897.3	7965.8	7756.3	7896.8	7964.3	7756.9	7898	7965.8	7757.3
Dynamic Modulus (Pa)	4.77E+10	4.88E+10	4.50E+10	4.77E+10	4.87E+10	4.49E+10	4.77E+10	4.88E+10	4.49E+10
Avg. Dy. Modulus (Pa)	4.72E+10			4.71E+10			4.71E+10		

*Batch is designated as "6% SCA-2" in Program 3.

Table D.4 Program 1 – Scaling mass loss data (BNQ NQ 2621-900 Annex B)

Mixture: Control #1

Specimen Number	Effective Area in^2	Mass at 7 days		Mass at 21 days		Mass at 35 days		Mass at 56 days	
		g	lb/in^2	g	lb/in^2	g	lb/in^2	g	lb/in^2
926A	58.1	7.2	2.84E-04	4.2	1.66E-04	2.8	1.11E-04	5.7	2.25E-04
926B	63.7	6.8	2.45E-04	5.4	1.94E-04	4.7	1.69E-04	3.9	1.40E-04
926C	60.7	5.9	2.23E-04	5.1	1.93E-04	3.7	1.40E-04	9.3	3.52E-04
Average	60.8		2.51E-04		1.84E-04		1.40E-04		2.39E-04
Cumulative mass loss (lb/ft^2)			3.61E-02		6.27E-02		8.29E-02		1.17E-01

Mixture: Control #2

Specimen Number	Effective Area in^2	Mass at 7 days		Mass at 21 days		Mass at 35 days		Mass at 56 days	
		g	lb/in^2	g	lb/in^2	g	lb/in^2	g	lb/in^2
927A	76.3	2.6	7.82E-05	0.7	2.11E-05	2.1	6.32E-05	0.8	2.41E-05
927B	78.5	3.7	1.08E-04	1.3	3.80E-05	3.9	1.14E-04	0.9	2.63E-05
927C	77.2	2.5	7.44E-05	1.4	4.16E-05	4.5	1.34E-04	1	2.97E-05
Average	77.3		8.69E-05		3.36E-05		1.04E-04		2.67E-05
Cumulative mass loss (lb/ft^2)			1.25E-02		1.74E-02		3.23E-02		3.61E-02

Mixture: Control #3

Specimen Number	Effective Area in^2	Mass at 7 days		Mass at 21 days		Mass at 35 days		Mass at 56 days	
		g	lb/in^2	g	lb/in^2	g	lb/in^2	g	lb/in^2
976A	74.4	2.3	7.10E-05	2.5	7.71E-05	0.5	1.54E-05	0.4	1.23E-05
976B	71.4	2.6	8.36E-05	1.8	5.79E-05	0.7	2.25E-05	2	6.43E-05
976C	72.7	3.1	9.78E-05	2.4	7.57E-05	0.3	9.47E-06	2.8	8.84E-05
Average	72.8		8.41E-05		7.03E-05		1.58E-05		5.50E-05
Cumulative mass loss (lb/ft^2)			1.21E-02		2.22E-02		2.45E-02		3.24E-02

Table D.4 (Cont'd) Program 1 – Scaling mass loss data (BNQ NQ 2621-900 Annex B)

Mixture: 0.5% SRA-2

Specimen Number	Effective Area in^2	Mass at 7 days		Mass at 21 days		Mass at 35 days		Mass at 56 days	
		g	lb/in^2	g	lb/in^2	g	lb/in^2	g	lb/in^2
894A	65.8	2.7	9.41E-05	2.6	9.07E-05	1.4	4.88E-05	20.4	7.11E-04
894B	65.0	3.3	1.17E-04	2.9	1.02E-04	1.6	5.65E-05	17.4	6.15E-04
894C	63.9	3.6	1.29E-04	3.9	1.40E-04	2	7.18E-05	24.7	8.87E-04
Average	64.9		1.13E-04		1.11E-04		5.91E-05		7.38E-04
Cumulative mass loss (lb/ft^2)			1.63E-02		3.23E-02		4.08E-02		1.47E-01

Mixture: 1% SRA-2 # 1

Specimen Number	Effective Area in^2	Mass at 7 days		Mass at 21 days		Mass at 35 days		Mass at 56 days	
		g	lb/in^2	g	lb/in^2	g	lb/in^2	g	lb/in^2
896A	66.1	1.1	3.82E-05	4.4	1.53E-04	9.9	3.44E-04	16.4	5.70E-04
896B	67.9	2.6	8.79E-05	6.5	2.20E-04	13.6	4.60E-04	15.6	5.28E-04
896C	64.2	1.2	4.29E-05	4.7	1.68E-04	6.7	2.40E-04	8.9	3.18E-04
Average	66.0		5.64E-05		1.80E-04		3.48E-04		4.72E-04
Cumulative mass loss (lb/ft^2)			8.12E-03		3.41E-02		8.42E-02		1.52E-01

Mixture: 1% SRA-2 # 2

Specimen Number	Effective Area in^2	Mass at 7 days		Mass at 21 days		Mass at 35 days		Mass at 56 days	
		g	lb/in^2	g	lb/in^2	g	lb/in2	g	lb/in^2
887A	67.3	2.3	7.84E-05	1.7	5.80E-05	0.9	3.07E-05	5.6	1.91E-04
887B	64.6	3.2	1.14E-04	1.1	3.91E-05	0.7	2.49E-05	6.2	2.20E-04
887C	65.7	4.2	1.47E-04	2.7	9.44E-05	1.1	3.84E-05	0	0.00E+00
Average	65.9		1.13E-04		6.38E-05		3.13E-05		2.06E-04
Cumulative mass loss (lb/ft^2)			1.63E-02		2.55E-02		3.00E-02		5.96E-02

Table D.4 (Cont'd) Program 1 – Scaling mass loss data (BNQ NQ 2621-900 Annex B)

Mixture: 1% SRA-2 # 3

Specimen Number	Effective Area in^2	Mass at 7 days		Mass at 21 days		Mass at 35 days		Mass at 56 days	
		g	lb/in^2	g	lb/in^2	g	lb/in^2	g	lb/in^2
960A	72.4	4.6	1.46E-04	12.2	3.87E-04	4.2	1.33E-04	7	2.22E-04
960B	72.7	7.2	2.27E-04	8.8	2.78E-04	10.8	3.41E-04	48	1.52E-03
960C	47.0	4.7	2.30E-04	6.6	3.23E-04	5.6	2.74E-04	12.9	6.31E-04
Average	64.0		2.01E-04		3.29E-04		2.49E-04		7.90E-04
Cumulative mass loss (lb/ft^2)			2.89E-02		7.63E-02		1.12E-01		2.26E-01

Mixture: 2% SRA-2 # 1

Specimen Number	Effective Area in^2	Mass at 7 days		Mass at 21 days		Mass at 35 days		Mass at 56 days	
		g	lb/in^2	g	lb/in^2	g	lb/in^2	g	lb/in^2
886A	68.7	5.9	1.97E-04	3.4	1.14E-04	2.1	7.02E-05	0	0.00E+00
886B	64.5	12.2	4.34E-04	13.5	4.80E-04	10.1	3.59E-04	26.8	9.53E-04
886C	65.9	7.4	2.58E-04	7.6	2.65E-04	5.2	1.81E-04	9.9	3.45E-04
Average	66.4		2.96E-04		2.86E-04		2.04E-04		6.49E-04
Cumulative mass loss (lb/ft^2)			4.27E-02		8.39E-02		1.13E-01		2.07E-01

Mixture: 2% SRA-2 # 2

Specimen Number	Effective Area in^2	Mass at 7 days		Mass at 21 days		Mass at 35 days		Mass at 56 days	
		g	lb/in^2	g	lb/in^2	g	lb/in2	g	lb/in^2
897A	66.4	2.5	8.64E-05	5.5	1.90E-04	22.8	7.88E-04	57.6	1.99E-03
897B	64.7	2.1	7.46E-05	4.9	1.74E-04	22.3	7.92E-04	51.7	1.84E-03
897C	63.8	3.1	1.12E-04	5.8	2.09E-04	30.8	1.11E-03	64.2	2.31E-03
Average	65.0		9.08E-05		1.91E-04		8.96E-04		2.05E-03
Cumulative mass loss (lb/ft^2)			1.31E-02		4.06E-02		1.70E-01		4.64E-01

Table D.4 (Cont'd) Program 1 – Scaling mass loss data (BNQ NQ 2621-900 Annex B)

Mixture: 0.75% SRA-3

Specimen Number	Effective Area in^2	Mass at 7 days		Mass at 21 days		Mass at 35 days		Mass at 56 days	
		g	lb/in^2	g	lb/in^2	g	lb/in^2	g	lb/in^2
928A	76.2	7.4	2.23E-04	7.4	2.23E-04	0.9	2.71E-05	6.5	1.96E-04
928B	63.0	5.9	2.15E-04	4.9	1.79E-04	2	7.29E-05	5.4	1.97E-04
928C	70.9	8.8	2.85E-04	6.6	2.14E-04	2.3	7.45E-05	6.9	2.23E-04
Average	70.0		2.41E-04		2.05E-04		5.82E-05		2.05E-04
Cumulative mass loss (lb/ft^2)			3.47E-02		6.43E-02		7.26E-02		1.02E-01

Mixture: 2.25% SRA-3

Specimen Number	Effective Area in^2	Mass at 7 days		Mass at 21 days		Mass at 35 days		Mass at 56 days	
		g	lb/in^2	g	lb/in^2	g	lb/in^2	g	lb/in^2
963A	72.3	6.6	2.09E-04	83.9	2.66E-03	74.8	2.37E-03	115.5	3.67E-03
963B	71.9	8.6	2.75E-04	92.1	2.94E-03	79.9	2.55E-03	108.4	3.46E-03
963C	70.7	28.1	9.12E-04	81.3	2.64E-03	83.2	2.70E-03	97	3.15E-03
Average	71.6		4.65E-04		2.80E-03		2.46E-03		3.56E-03
Cumulative mass loss (lb/ft^2)			6.70E-02		4.71E-01		8.25E-01		1.34E+00

Table D.5 Program 2 – Scaling mass loss data (BNQ NQ 2621-900 Annex B)

Mixture: 20% FA-F # 1

Specimen Number	Effective Area in^2	Mass at 7 days		Mass at 21 days		Mass at 35 days		Mass at 56 days	
		g	lb/in^2	g	lb/in^2	g	lb/in^2	g	lb/in^2
879A	71.8	50.4	1.61E-03	0	0.00E+00	0	0.00E+00	0	0.00E+00
879B	68.5	38.7	1.30E-03	173.1	5.80E-03	0	0.00E+00	0	0.00E+00
879C	65.7	44.5	1.55E-03	190.3	6.65E-03	0	0.00E+00	0	0.00E+00
Average	68.7		1.49E-03		6.22E-03		0.00E+00		0.00E+00
Cumulative mass loss (lb/ft^2)			2.14E-01		1.11E+00		1.11E+00		1.11E+00

Mixture: 20% FA-F # 2

Specimen Number	Effective Area in^2	Mass at 7 days		Mass at 21 days		Mass at 35 days		Mass at 56 days	
		g	lb/in^2	g	lb/in^2	g	lb/in^2	g	lb/in^2
890A	65.6	4.8	1.68E-04	3.3	1.15E-04	0.8	2.80E-05	0.8	2.80E-05
890B	66.1	5.0	1.74E-04	3.2	1.11E-04	1.2	4.17E-05	0.4	1.39E-05
890C	66.9	5.8	1.99E-04	4.4	1.51E-04	1.3	4.46E-05	1.1	3.78E-05
Average	66.2		1.80E-04		1.26E-04		3.81E-05		2.65E-05
Cumulative mass loss (lb/ft^2)			2.60E-02		4.41E-02		4.96E-02		5.34E-02

Mixture: 20% FA-C

Specimen Number	Effective Area in^2	Mass at 7 days		Mass at 21 days		Mass at 35 days		Mass at 56 days	
		g	lb/in^2	g	lb/in^2	g	lb/in^2	g	lb/in^2
913A	63.9	3.5	1.26E-04	7.4	2.66E-04	5.1	1.83E-04	21.2	7.62E-04
913B	64.1	4.4	1.57E-04	7.7	2.76E-04	5.1	1.83E-04	19.7	7.05E-04
913C	67.9	3.8	1.29E-04	5.7	1.93E-04	5.5	1.86E-04	21	7.11E-04
Average	65.3		1.37E-04		2.45E-04		1.84E-04		7.26E-04
Cumulative mass loss (lb/ft^2)			1.98E-02		5.50E-02		8.15E-02		1.86E-01

Table D.5 (Cont'd) Program 2 – Scaling mass loss data (BNQ NQ 2621-900 Annex B)

Mixture: 40% FA-F # 1

Specimen Number	Effective Area in^2	Mass at 7 days		Mass at 21 days		Mass at 35 days		Mass at 56 days	
		g	lb/in^2	g	lb/in^2	g	lb/in^2	g	lb/in^2
889A	65.6	3.5	1.22E-04	8.5	2.97E-04	10.7	3.74E-04	2.7	9.45E-05
889B	65.7	3.6	1.26E-04	9.7	3.39E-04	11.3	3.95E-04	2.9	1.01E-04
889C	67.1	5.7	1.95E-04	8.7	2.98E-04	19.7	6.74E-04	5.6	1.92E-04
Average	66.2		1.48E-04		3.11E-04		4.81E-04		1.29E-04
Cumulative mass loss (lb/ft^2)			2.13E-02		6.61E-02		1.35E-01		1.54E-01

Mixture: 40% FA-F # 2

Specimen Number	Effective Area in^2	Mass at 7 days		Mass at 21 days		Mass at 35 days		Mass at 56 days	
		g	lb/in^2	g	lb/in^2	g	lb/in^2	g	lb/in^2
880A	70.6	1.9	6.18E-05	20.4	6.63E-04	2.3	7.48E-05	2.4	7.80E-05
880B	67.4	3.9	1.33E-04	16.2	5.52E-04	0	0.00E+00	0	0.00E+00
880C	69.1	1.8	5.98E-05	6.8	2.26E-04	13.2	4.39E-04	5.4	1.79E-04
Average	69.0		8.48E-05		4.80E-04		2.57E-04		1.29E-04
Cumulative mass loss (lb/ft^2)			1.22E-02		8.14E-02		1.18E-01		1.37E-01

Mixture: 0.05% RMA

Specimen Number	Effective Area in^2	Mass at 7 days		Mass at 21 days		Mass at 35 days		Mass at 56 days	
		g	lb/in^2	g	lb/in^2	g	lb/in^2	g	lb/in^2
905A	59.3	0.8	3.10E-05	2.9	1.12E-04	3.7	1.43E-04	5	1.94E-04
905B	65.5	1.1	3.85E-05	4.7	1.65E-04	4	1.40E-04	3.9	1.37E-04
905C	60.0	0.5	1.91E-05	3.2	1.22E-04	4.7	1.80E-04	5.2	1.99E-04
Average	61.6		2.96E-05		1.33E-04		1.54E-04		1.76E-04
Cumulative mass loss (lb/ft^2)			4.26E-03		2.34E-02		4.57E-02		7.11E-02

Table D.5 (Cont'd) Program 2 – Scaling mass loss data (BNQ NQ 2621-900 Annex B)

Mixture: 0.075% RMA

Specimen Number	Effective Area in^2	Mass at 7 days		Mass at 21 days		Mass at 35 days		Mass at 56 days	
		g	lb/in^2	g	lb/in^2	g	lb/in^2	g	lb/in^2
909A	65.1	13.6	4.79E-04	15.1	5.32E-04	15.2	5.36E-04	29.3	1.03E-03
909B	62.4	18.7	6.88E-04	18.8	6.92E-04	11.8	4.34E-04	30.1	1.11E-03
909C	64.5	17.4	6.20E-04	22.2	7.90E-04	13.8	4.91E-04	33.3	1.19E-03
Average	64.0		5.96E-04		6.71E-04		4.87E-04		1.11E-03
Cumulative mass loss (lb/ft^2)			8.58E-02		1.82E-01		2.53E-01		4.12E-01

Mixture: 0.05% RMA - 40% FA-C

Specimen Number	Effective Area in^2	Mass at 7 days		Mass at 21 days		Mass at 35 days		Mass at 56 days	
		g	lb/in^2	g	lb/in^2	g	lb/in^2	g	lb/in^2
899A	66.6	0.2	6.89E-06	21.2	7.30E-04	33.3	1.15E-03	19.1	6.58E-04
899B	66.3	0.9	3.12E-05	28.5	9.87E-04	25.7	8.90E-04	14.9	5.16E-04
899C	66.3	0.3	1.04E-05	0	0.00E+00	0	0.00E+00	0	0.00E+00
Average	66.4		1.61E-05		8.59E-04		1.02E-03		5.87E-04
Cumulative mass loss (lb/ft^2)			2.33E-03		1.26E-01		2.73E-01		3.57E-01

Mixture: 0.075% RMA - 40% FA-C

Specimen Number	Effective Area in^2	Mass at 7 days		Mass at 21 days		Mass at 35 days		Mass at 56 days	
		g	lb/in^2	g	lb/in^2	g	lb/in^2	g	lb/in^2
967A	71.2	20.8	6.71E-04	9.9	3.19E-04	9	2.90E-04	30.2	9.74E-04
967B	72.5	32.9	1.04E-03	34.9	1.11E-03	10.5	3.33E-04	3.4	1.08E-04
967C	71.1	32.1	1.04E-03	4.1	1.32E-04	26.3	8.50E-04	25	8.08E-04
Average	71.6		9.17E-04		7.12E-04		3.11E-04		5.41E-04
Cumulative mass loss, lb/ft^2			1.32E-01		2.35E-01		2.79E-01		3.57E-01

Table D.5 (Cont'd) Program 2 – Scaling mass loss data (BNQ NQ 2621-900 Annex B)

Mixture: 0.15% RMA - 40% FA-C

Specimen Number	Effective Area in^2	Mass at 7 days		Mass at 21 days		Mass at 35 days		Mass at 56 days	
		g	lb/in^2	g	lb/in^2	g	lb/in^2	g	lb/in^2
911A	62.3	21.4	7.89E-04	26.5	9.77E-04	10.9	4.02E-04	23.1	8.51E-04
911B	61.5	26	9.71E-04	19.4	7.24E-04	10.9	4.07E-04	24.1	9.00E-04
911C	63.1	21.5	7.82E-04	20.6	7.50E-04	10.9	3.97E-04	24.3	8.84E-04
Average	62.3		8.47E-04		8.17E-04		4.02E-04		8.78E-04
Cumulative mass loss (lb/ft^2)			1.22E-01		2.40E-01		2.97E-01		4.24E-01

Mixture: 0.15% RMA - 20% FA-C

Specimen Number	Effective Area in^2	Mass at 7 days		Mass at 21 days		Mass at 35 days		Mass at 56 days	
		g	lb/in^2	g	lb/in^2	g	lb/in^2	g	lb/in^2
912A	63.0	6.9	2.51E-04	7.9	2.88E-04	7.4	2.69E-04	19.8	7.21E-04
912B	62.3	6.6	2.43E-04	7.4	2.73E-04	4.1	1.51E-04	23.3	8.59E-04
912C	61.2	6.6	2.47E-04	8	3.00E-04	7.9	2.96E-04	19	7.12E-04
Average	62.2		2.47E-04		2.87E-04		2.39E-04		7.64E-04
Cumulative mass loss (lb/ft^2)			3.56E-02		7.69E-02		1.11E-01		2.21E-01

Table D.6 Program 3 – Scaling mass loss data (BNQ NQ 2621-900 Annex B)

Mixture: 2.5% SCA-1 #1

Specimen Number	Effective Area in^2	Mass at 7 days		Mass at 21 days		Mass at 35 days		Mass at 56 days	
		g	lb/in^2	g	lb/in^2	g	lb/in^2	g	lb/in^2
855A	74.9	0.3	9.20E-06	0.2	6.13E-06	0.1	3.07E-06	1.3	3.99E-05
855B	73.3	0.7	2.19E-05	0.8	2.51E-05	0.3	9.40E-06	2.9	9.08E-05
855C	70.6	0.1	3.25E-06	0.1	3.25E-06	0.8	2.60E-05	2.3	7.48E-05
Average	72.9		1.15E-05		1.15E-05		1.28E-05		6.85E-05
Cumulative mass loss (lb/ft^2)			1.65E-03		3.30E-03		5.15E-03		1.50E-02

Mixture: 2.5% SCA-1 #2

Specimen Number	Effective Area in^2	Mass at 7 days		Mass at 21 days		Mass at 35 days		Mass at 56 days	
		g	lb/in^2	g	lb/in^2	g	lb/in^2	g	lb/in^2
861A	68.0	2.6	8.77E-05	4.8	1.62E-04	1.6	5.40E-05	1.2	4.05E-05
861B	66.8	3.1	1.06E-04	2.1	6.87E-05	2.0	6.87E-05	0.6	2.06E-05
861C	70.9	7.2	2.33E-04	5.0	1.62E-04	1.8	5.83E-05	0.4	1.29E-05
Average	68.6		1.42E-04		1.31E-04		6.03E-05		2.47E-05
Cumulative mass loss (lb/ft^2)			2.05E-02		3.94E-02		4.80E-02		5.16E-02

Mixture: 5% SCA-1

Specimen Number	Effective Area in^2	Mass at 7 days		Mass at 21 days		Mass at 35 days		Mass at 56 days	
		g	lb/in^2	g	lb/in^2	g	lb/in^2	g	lb/in^2
857A	73.7	1.8	5.61E-05	0.6	1.87E-05	1.4	4.36E-05	5.4	1.68E-04
857B	72.8	0.3	9.46E-06	0.2	6.31E-06	1.8	5.68E-05	3.2	1.01E-04
857C	75.3	0.3	9.15E-06	0	0.00E+00	2.7	8.24E-05	5.4	1.65E-04
Average	73.9		2.49E-05		8.33E-06		6.09E-05		1.45E-04
Cumulative mass loss (lb/ft^2)			3.58E-03		4.78E-03		1.36E-02		3.44E-02

Table D.6 (Cont'd) Program 3 – Scaling mass loss data (BNQ NQ 2621-900 Annex B)

Mixture: 7.5% SCA-1 #1

Specimen Number	Effective Area in^2	Mass at 7 days		Mass at 21 days		Mass at 35 days		Mass at 56 days	
		g	lb/in^2	g	lb/in^2	g	lb/in^2	g	lb/in^2
862A	70.0	24.5	8.03E-04	34	1.11E-03	0	0.00E+00	0	0.00E+00
862B	71.2	14.5	4.68E-04	18.6	6.00E-04	10.7	3.45E-04	0	0.00E+00
862C	71.8	28.8	9.21E-04	59.0	1.89E-03	48.7	1.56E-03	0	0.00E+00
Average	71.0		7.31E-04		1.20E-03		9.51E-04		0.00E+00
Cumulative mass loss (lb/ft^2)			1.05E-01		2.78E-01		4.15E-01		4.15E-01

Mixture: 7.5% SCA-1 #2

Specimen Number	Effective Area in^2	Mass at 7 days		Mass at 21 days		Mass at 35 days		Mass at 56 days	
		g	lb/in^2	g	lb/in^2	g	lb/in^2	g	lb/in^2
860A	68.0	2.4	8.10E-05	6.4	2.16E-04	3	1.01E-04	2.9	9.79E-05
860B	64.6	1.2	4.26E-05	3.6	1.28E-04	1.6	5.69E-05	1.7	6.04E-05
860C	63.4	0.9	3.26E-05	3.1	1.12E-04	1.7	6.16E-05	3.6	1.30E-04
Average	65.3		5.21E-05		1.52E-04		7.32E-05		9.62E-05
Cumulative mass loss (lb/ft^2)			7.50E-03		2.94E-02		3.99E-02		5.38E-02

Mixture: 6% SCA-2

Specimen Number	Effective Area in^2	Mass at 7 days		Mass at 21 days		Mass at 35 days		Mass at 56 days	
		g	lb/in^2	g	lb/in^2	g	lb/in^2	g	lb/in^2
955A	73.4	0.8	2.50E-05	1.8	5.63E-05	0.5	1.56E-05	0.2	6.25E-06
955B	75.3	1.2	3.66E-05	1.8	5.49E-05	0.1	3.05E-06	0	0.00E+00
955C	72.9	0.8	2.52E-05	2.2	6.93E-05	0.3	9.45E-06	1.0	3.15E-05
Average	73.9		2.89E-05		6.02E-05		9.38E-06		1.26E-05
Cumulative mass loss (lb/ft^2)			4.17E-03		1.28E-02		1.42E-02		1.60E-02

APPENDIX E: MIXTURES PROPERTIES AND HARDENED AIR-VOID CHARACTERISTICS DATA FOR THE MIXTURES IN PROGRAM 1, 2, AND 3

Table E.1 – Slump, concrete temperature, plastic air content, unite weight, and compressive strength for the mixtures evaluated for freeze-thaw, scaling, and hardened air-void analysis

Batch Designation	Batch Number	Slump (in.)	Slump (mm)	Concrete Temperature (°F)	Concrete Temperature (°C)	Air Content-Plastic, %	Unit Weight (lb/ft^3)	Unit Weight (kg/m^3)	28-Day Compressive Strength (psi)	28-Day Compressive Strength (MPa)
Control #1	926	2 1/4	55	52	23	5.75	144.3	85.6	6790	46.8
Control #2	927	3 1/4	80	65	18	8.75	141.8	84.1	5330	36.8
Control #3	976	3/4	15	65	18	7.50	142.5	84.5	4860	33.5
0.5% SRA-2	894	1 1/4	30	76	22	6.00	146.4	86.9	4240	29.2
1% SRA-2 # 1	896	1 3/4	45	76	18	8.25	142.4	84.5	4160	28.7
1% SRA-2 # 2	887	1 3/4	45	68	22	9.25	142.9	84.8	4560	31.4
1% SRA-2 # 3	960	2 1/4	55	76	18	7.75	143.1	84.9	4000	27.6
2% SRA-2 # 1	886	2 1/2	65	81	18	9.25	139.2	82.6	3530	24.3
2% SRA-2 # 2	897	2	50	72	23	9.75	141.2	83.8	3840	26.5
0.75% SRA-3	928	2 3/4	70	40	18	8.00	142.8	84.7	5400	37.2
2.25% SRA-3	963	1 1/4	30	----	18	7.50	142.4	84.5	4370	30.1
20% FA-F # 1	879	2 1/2	65	70	18	2.75	151.2	89.7	5410	37.3
20% FA-F # 2	890	4 3/4	120	83	18	9.75	137.7	81.7	3590	24.8
20% FA-C	913	2 3/4	70	74	18	7.00	143.5	85.1	4720	32.5
40% FA-F #1	889	7 1/4	185	78	18	8.50	142.7	84.7	3260	22.5
40% FA-F #2	880	8	200	63	23	10.00	142.7	84.7	3450	23.8
0.05% RMA	905	1	25	71	18	8.75	----	-----	4040	27.9
0.075% RMA	909	1 1/2	40	73	23	7.75	140.7	83.5	3480	24.0
0.05% RMA - 40% FA-C	899	2	50	74	18	5.75	145.9	86.6	3920	27.0
0.075% RMA - 40% FA-C	967	4	100	60	18	8.25	---	----	3250	22.4
0.15% RMA - 40% FA-C	911	3 1/2	90	67	22	8.50	138.3	82.1	2890	19.9
0.15% RMA - 20% FA-C	912	1 1/4	30	74	18	6.50	143.5	85.1	2940	20.3
2.5% SCA-1 # 1	855	4 3/4	120	73	21	8.50	138.4	82.1	3700	25.5
2.5% SCA-1 # 2	861	3	75	74	18	7.50	141.2	83.8	4240	29.2
5% SCA-1	857	1 3/4	45	68	18	4.75	146.0	86.6	5250	36.2
7.5% SCA-1 # 1	862	2	51	72	18	5.00	147.5	87.5	4950	34.1
7.5% SCA-1 # 2	860	2 1/2	65	72	18	9.00	139.7	82.9	3020	20.8
6% SCA-2	955	2 1/4	55	71	18	8.50	142.4	84.5	4400	30.3

Table E.2 – Air-Voids characteristics of the hardened concrete of Control # 1 mixture

	Batch No. and Slab Designation	Orientation	Air Content, %	Spacing Factor, in	Specific Surface, in^{-1}	Void Frequency, in^{-1}	Average Chord Length, in
Control # 1, passed Freeze-Thaw and Scaling Tests	926D	0º	6.08	0.0055	705.9	10.73	0.0057
		90º	5.42	0.0055	789.7	10.70	0.0051
		180º	5.67	0.0055	758.1	10.75	0.0053
		270º	5.35	0.0057	767.8	10.26	0.0052
	Average		5.63	0.0056	755.4	10.61	0.0053
	926D	0º	5.60	0.0055	650.7	9.11	0.0057
		90º	5.89	0.0057	718.4	9.10	0.0056
		180º	5.73	0.0060	666.6	9.55	0.0060
		270º	5.64	0.0058	642.7	9.77	0.0063
	Average		5.72	0.0058	669.6	9.38	0.0058
	926E	0º	5.68	0.0050	685.8	13.17	0.0058
		90º	5.32	0.0053	775.5	13.90	0.0059
		180º	5.57	0.0056	667.5	12.80	0.0060
		270º	5.48	0.0056	689.4	12.89	0.0058
	Average		5.15	0.0054	704.6	13.19	0.0059
	926E	0º	5.42	0.0054	684.9	9.28	0.0058
		90º	5.39	0.0053	695.5	9.38	0.0058
		180º	5.18	0.0057	744.0	9.34	0.0062
		270º	5.48	0.0058	728.4	9.61	0.0059
	Average		5.37	0.0056	713.2	9.40	0.0059
	Air Content - Plastic, %		5.75				
	Average		5.56	0.0056	710.7	10.65	0.0057

Note:
Mixture containing 100 percent portland cement.
Test is subjected on four slabs, two slabs from each cylinder (D and E).
Each slab is measured four times, the slab is rotated 90° between measurements. The average of the four readings of the slab is reported as the air-void parameters of that slab.

Table E.3 – Air-Voids characteristics of the hardened concrete of Control # 2 mixture

	Batch No. and Slab Designation	Orientation	Air Content, %	Spacing Factor, in	Specific Surface, in^{-1}	Void Frequency, in^{-1}	Average Chord Length, in
Control # 2, passed Freeze-Thaw and Scaling Tests	927D	0º	8.27	0.0032	893.2	18.46	0.0045
		90º	8.32	0.0033	878.1	18.27	0.0046
		180º	8.07	0.0035	836.2	16.86	0.0048
		270º	8.12	0.0035	822.3	16.88	0.0049
	Average		8.20	0.0034	857.0	17.62	0.0047
	927D	0º	7.59	0.0043	725.6	13.78	0.0055
		90º	7.79	0.0044	697.1	13.58	0.0057
		180º	7.38	0.0043	748.3	13.81	0.0053
		270º	7.56	0.0042	743.3	14.05	0.0054
	Average		7.58	0.0043	729.0	13.81	0.0055
	927E	0º	8.06	0.0041	717.5	14.46	0.0056
		90º	7.66	0.0041	752.7	14.41	0.0053
		180º	7.94	0.0044	647.6	12.86	0.0062
		270º	8.04	0.0043	635.9	12.79	0.0063
	Average		7.93	0.0042	688.1	13.63	0.0059
	927E	0º	8.18	0.0037	785.3	16.05	0.0051
		90º	7.72	0.0039	800.6	15.42	0.0050
		180º	8.10	0.0036	815.4	16.51	0.0049
		270º	8.14	0.0037	792.2	16.11	0.0051
	Average		8.03	0.0037	798.1	16.02	0.0050
	Air Content - Plastic, %		8.75				
	Average		7.93	0.0039	768	15.27	0.0053

Note:
Mixture containing 100 percent portland cement.
Test is subjected on four slabs, two slabs from each cylinder (D and E).
Each slab is measured four times, the slab is rotated 90° between measurements. The average of the four readings of the slab is reported as the air-void parameters of that slab.

Table E.4 –Air-Voids characteristics of the hardened concrete of Control # 3 mixture

	Batch No. and Slab Designation	Orientation	Air Content, %	Spacing Factor, in	Specific Surface, in^{-1}	Void Frequency, in^{-1}	Average Chord Length, in
Control # 3, passed Freeze-Thaw and Scaling Tests	976D	0º	6.80	0.0047	733.9	8.55	0.0080
		90º	7.09	0.0051	694.9	8.38	0.0085
		180º	7.07	0.0050	726.1	8.54	0.0083
		270º	6.58	0.0049	699.8	9.44	0.0070
	Average		6.89	0.0049	713.7	8.73	0.0080
	976D	0º	6.58	0.0050	721.5	11.87	0.0055
		90º	6.23	0.0050	766.1	11.94	0.0052
		180º	6.27	0.0052	722.1	11.31	0.0055
		270º	6.37	0.0049	768.1	12.24	0.0052
	Average		6.36	0.0050	744.5	11.84	0.0050
	976E	0º	6.37	0.0059	632.1	10.07	0.0063
		90º	6.77	0.0056	631.5	10.96	0.0063
		180º	7.15	0.0054	629.8	10.21	0.0065
		270º	6.48	0.0058	618.4	11.05	0.0064
	Average		6.69	0.0057	628.0	10.57	0.0060
	976E	0º	7.11	0.0048	700.9	12.46	0.0057
		90º	6.48	0.0051	723.6	11.71	0.0055
		180º	6.73	0.0050	712.7	12.00	0.0056
		270º	7.24	0.0051	643.1	11.64	0.0062
	Average		6.89	0.0050	695.0	11.95	0.0060
	Air Content - Plastic, %		7.50				
	Average		6.71	0.0052	695.1	10.77	0.0063

Note:
Mixture containing 100 percent portland cement.
Test is subjected on four slabs, two slabs from each cylinder (D and E).
Each slab is measured four times, the slab is rotated 90° between measurements. The average of the four readings of the slab is reported as the air-void parameters of that slab.

Table E.5 – Air-Voids characteristics of the hardened concrete of 0.5% SRA-2 mixture

	Batch No. and Slab Designation	Orientation	Air Content, %	Spacing Factor, in	Specific Surface, in^{-1}	Void Frequency, in^{-1}	Average Chord Length, in
0.5% SRA-2, passed Freeze-Thaw and Scaling Tests	894D	0º	6.37	0.0062	604.5	9.62	0.0066
		90º	5.94	0.0062	642.3	9.55	0.0062
		180º	5.42	0.0067	648.4	8.79	0.0062
		270º	5.85	0.0062	653.8	9.56	0.0061
	Average		5.90	0.0063	637.3	9.38	0.0063
	894D	0º	5.79	0.0066	626.4	9.07	0.0064
		90º	5.87	0.0065	618.6	9.08	0.0065
		180º	5.91	0.0067	598.3	8.84	0.0067
		270º	5.75	0.0064	645.2	9.27	0.0062
	Average		5.83	0.0066	622.1	9.07	0.0065
	894E	0º	6.07	0.0066	594.1	9.02	0.0067
		90º	5.44	0.0067	652.6	8.88	0.0061
		180º	5.47	0.0070	623.9	8.53	0.0064
		270º	5.75	0.0069	601.4	8.65	0.0067
	Average		5.68	0.0068	618.0	8.77	0.0065
	894E	0º	5.61	0.0070	605.7	8.49	0.0066
		90º	5.53	0.0069	623.8	8.62	0.0064
		180º	6.21	0.0064	598.1	9.29	0.0067
		270º	5.53	0.0069	619.6	8.57	0.0065
	Average		5.72	0.0068	611.8	8.74	0.0066
	Air Content - Plastic, %		6.00				
	Average		5.78	0.0066	622.3	8.99	0.0064

Note:
Mixture containing 0.5 percent shrinkage-reducing admixtures (SRA-2) by weight of cement.
Test is subjected on four slabs, two slabs from each cylinder (D and E).
Each slab is measured four times, the slab is rotated 90° between measurements. The average of the four readings of the slab is reported as the air-void parameters of that slab.

Table E.6 – Air-Voids characteristics of the hardened concrete of 1% SRA-2 # 1 mixture

	Batch No. and Slab Designation	Orientation	Air Content, %	Spacing Factor, in	Specific Surface, in^{-1}	Void Frequency, in^{-1}	Average Chord Length, in
1% SRA-2 # 1, passed Freeze-Thaw and Scaling Tests	896D	0º	6.94	0.0052	664.2	11.53	0.0060
		90º	7.12	0.0048	701.1	12.48	0.0057
		180º	7.24	0.0048	686.1	12.42	0.0058
		270º	7.65	0.0046	668.2	12.78	0.0060
	Average		7.24	0.0049	679.9	12.30	0.0059
	896D	0º	6.67	0.0052	645.5	10.77	0.0062
		90º	6.79	0.0053	664.2	11.27	0.0060
		180º	7.14	0.0051	647.6	11.56	0.0062
		270º	7.90	0.0051	615.0	11.67	0.0065
	Average		7.13	0.0052	643.1	11.32	0.0062
	896E	0º	7.22	0.0050	652.0	11.77	0.0061
		90º	7.42	0.0049	659.8	12.24	0.0061
		180º	7.79	0.0051	595.9	11.61	0.0067
		270º	7.55	0.0049	637.7	12.03	0.0063
	Average		7.50	0.0050	636.4	11.91	0.0063
	896E	0º	7.21	0.0049	674.7	12.17	0.0059
		90º	7.40	0.0046	699.6	12.94	0.0057
		180º	7.37	0.0050	643.4	11.85	0.0062
		270º	6.99	0.0050	684.5	11.96	0.0058
	Average		7.21	0.0049	675.5	12.23	0.0059
	Air Content - Plastic, %		8.25				
	Average		7.28	0.0050	658.7	11.94	0.0061

Note:
Mixture containing 1 percent shrinkage-reducing admixtures (SRA-2) by weight of cement.
Test is subjected on four slabs, two slabs from each cylinder (D and E).
Each slab is measured four times, the slab is rotated 90° between measurements. The average of the four readings of the slab is reported as the air-void parameters of that slab.

Table E.7 – Air-Voids characteristics of the hardened concrete of 1% SRA-2 # 2 mixture

	Batch No. and Slab Designation	Orientation	Air Content, %	Spacing Factor, in	Specific Surface, in^{-1}	Void Frequency, in^{-1}	Average Chord Length, in
1% SRA-2 # 2, passed Scaling Tests	887D	0º	7.09	0.0047	708.6	12.57	0.0056
		90º	7.51	0.0047	675.2	12.68	0.0059
		180º	7.13	0.0046	725.3	12.92	0.0055
		270º	6.89	0.0049	706.6	12.17	0.0057
	Average		7.16	0.0047	703.9	12.59	0.0057
	887D	0º	7.15	0.0045	745.8	13.32	0.0054
		90º	7.04	0.0047	714.5	12.57	0.0056
		180º	7.15	0.0044	749.1	13.39	0.0053
		270º	6.67	0.0050	715.0	11.91	0.0056
	Average		7.00	0.0047	731.1	12.80	0.0055
	887E	0º	7.32	0.0043	759.3	13.89	0.0053
		90º	7.62	0.0043	724.0	13.80	0.0055
		180º	7.87	0.0041	738.7	14.54	0.0054
		270º	8.06	0.0040	745.7	15.03	0.0054
	Average		7.72	0.0042	741.9	14.32	0.0054
	887E	0º	7.48	0.0057	559.2	10.45	0.0072
		90º	7.56	0.0054	580.2	10.97	0.0069
		180º	8.00	0.0051	577.8	11.56	0.0069
		270º	7.96	0.0053	558.8	11.11	0.0072
	Average		7.75	0.0054	569.0	11.02	0.0071
	Air Content – Plastic, %		9.25				
	Average		7.41	0.0047	686.5	12.68	0.0059

Note:
Mixture containing 1 percent shrinkage-reducing admixtures (SRA-2) by weight of cement.
Test is subjected on four slabs, two slabs from each cylinder (D and E).
Each slab is measured four times, the slab is rotated 90° between measurements. The average of the four readings of the slab is reported as the air-void parameters of that slab.
This mixture was not tested for Freeze-Thaw Test.

Table E.8 – Air-Voids characteristics of the hardened concrete of 1% SRA-2 # 3 mixture

	Batch No. and Slab Designation	Orientation	Air Content, %	Spacing Factor, in	Specific Surface, in^{-1}	Void Frequency, in^{-1}	Average Chord Length, in
1% SRA-2 # 3, passed Freeze-Thaw Test and failed Scaling Test	960D	0°	6.00	0.0055	715.9	10.75	0.0056
		90°	5.74	0.0055	755.6	10.84	0.0053
		180°	5.78	0.0055	753.0	10.87	0.0053
		270°	5.58	0.0058	731.6	10.20	0.0055
	Average		5.78	0.0056	739.0	10.67	0.0054
	960D	0°	6.41	0.0057	653.0	10.47	0.0061
		90°	6.01	0.0058	677.7	10.19	0.0059
		180°	6.23	0.0052	740.5	11.54	0.0054
		270°	5.97	0.0055	727.1	10.85	0.0055
	Average		6.16	0.0056	699.6	10.76	0.0057
	960E	0°	6.66	0.0052	680.5	11.34	0.0059
		90°	6.38	0.0053	698.5	11.15	0.0057
		180°	6.66	0.0057	631.3	10.51	0.0063
		270°	6.59	0.0057	637.8	10.50	0.0063
	Average		6.57	0.0055	662.0	10.88	0.0061
	960E	0°	6.61	0.0063	568.1	9.39	0.0070
		90°	5.94	0.0064	628.5	9.34	0.0064
		180°	5.84	0.0072	567.8	8.29	0.0070
		270°	6.25	0.0068	562.6	8.79	0.0071
	Average		6.16	0.0067	581.8	8.95	0.0069
	Air Content – Plastic, %		7.75				
	Average		6.17	0.0059	670.6	10.31	0.0060

Note:
Mixture containing 1 percent shrinkage-reducing admixtures (SRA-2) by weight of cement.
Test is subjected on four slabs, two slabs from each cylinder (D and E).
Each slab is measured four times, the slab is rotated 90° between measurements. The average of the four readings of the slab is reported as the air-void parameters of that slab.

Table E.9 – Air-Voids characteristics of the hardened concrete of 2% SRA-2 # 1 mixture

	Batch No. and Slab Designation	Orientation	Air Content, %	Spacing Factor, in	Specific Surface, in^{-1}	Void Frequency, in^{-1}	Average Chord Length, in
2% SRA-2 # 1, passed Freeze-Thaw Test and failed Scaling Test	886D	0º	6.04	0.0061	650.1	9.82	0.0062
		90º	6.48	0.0058	627.7	10.17	0.0064
		180º	6.26	0.0057	667.5	10.44	0.0060
		270º	5.84	0.0061	664.0	9.69	0.0060
	Average		6.16	0.0059	652.3	10.03	0.0062
	886D	0º	6.14	0.0060	647.6	9.64	0.0062
		90º	5.93	0.0066	609.8	9.04	0.0066
		180º	5.84	0.0065	625.5	9.14	0.0064
		270º	5.38	0.0072	608.4	8.18	0.0066
	Average		5.82	0.0066	622.8	9.00	0.0065
	886E	0º	6.37	0.0061	611.8	9.75	0.0065
		90º	5.74	0.0066	623.2	8.94	0.0064
		180º	5.63	0.0072	584.7	8.23	0.0068
		270º	6.06	0.0063	623.6	9.44	0.0064
	Average		5.95	0.0066	610.8	9.09	0.0065
	886E	0º	6.36	0.0056	668.8	10.63	0.0060
		90º	6.83	0.0056	621.9	10.62	0.0064
		180º	5.95	0.0070	572.7	8.53	0.0042
		270º	6.25	0.0060	634.3	9.91	0.0033
	Average		6.35	0.0061	624.4	9.92	0.0050
	Air Content – Plastic, %		9.25				
	Average		6.07	0.0063	627.6	9.51	0.0060

Note:
Mixture containing 2 percent shrinkage-reducing admixtures (SRA-2) by weight of cement.
Test is subjected on four slabs, two slabs from each cylinder (D and E).
Each slab is measured four times, the slab is rotated 90° between measurements. The average of the four readings of the slab is reported as the air-void parameters of that slab.

Table E.10 – Air-Voids characteristics of the hardened concrete of 2% SRA-2 # 2 mixture

	Batch No. and Slab Designation	Orientation	Air Content, %	Spacing Factor, in	Specific Surface, in^{-1}	Void Frequency, in^{-1}	Average Chord Length, in
2% SRA-2 # 2, passed Freeze-Thaw Test and failed Scaling Test	897D	0º	7.17	0.0051	654.3	11.73	0.0061
		90º	6.61	0.0052	695.1	11.48	0.0058
		180º	6.60	0.0055	658.1	10.86	0.0061
		270º	6.72	0.0058	614.4	10.33	0.0065
	Average		6.78	0.0054	655.5	11.10	0.0061
	897D	0º	6.78	0.0049	717.5	12.16	0.0056
		90º	6.87	0.0052	665.9	11.44	0.0060
		180º	7.18	0.0051	656.3	11.78	0.0061
		270º	6.76	0.0050	709.5	12.00	0.0056
	Average		6.90	0.0051	687.3	11.85	0.0058
	897E	0º	6.03	0.0067	588.2	8.86	0.0068
		90º	6.34	0.0065	578.8	9.17	0.0069
		180º	6.32	0.0063	595.6	9.41	0.0067
		270º	5.75	0.0062	601.4	8.65	0.0067
	Average		6.06	0.0064	591.0	9.08	0.0068
	897E	0º	6.82	0.0052	672.6	11.47	0.0059
		90º	6.76	0.0052	674.6	11.40	0.0059
		180º	7.00	0.0053	643.8	11.27	0.0062
		270º	6.76	0.0055	634.3	10.73	0.0063
	Average		6.84	0.0053	656.3	11.22	0.0061
	Air Content – Plastic, %		9.75				
	Average		6.65	0.0055	6487.5	10.80	0.0062

Note:
Mixture containing 2 percent shrinkage-reducing admixtures (SRA-2) by weight of cement.
Test is subjected on four slabs, two slabs from each cylinder (D and E).
Each slab is measured four times, the slab is rotated 90° between measurements. The average of the four readings of the slab is reported as the air-void parameters of that slab.

Table E.11 – Air-Voids characteristics of the hardened concrete of 0.75% SRA-3 mixture

	Batch No. and Slab Designation	Orientation	Air Content, %	Spacing Factor, in	Specific Surface, in^{-1}	Void Frequency, in^{-1}	Average Chord Length, in
0.75% SRA-3, passed Freeze-Thaw and Scaling Tests	928D	0º	7.24	0.0046	715.7	12.96	0.0056
		90º	7.44	0.0045	703.5	13.09	0.0057
		180º	6.69	0.0044	714.8	14.30	0.0056
		270º	7.48	0.0044	713.9	13.36	0.0056
	Average		7.21	0.0045	712.0	13.43	0.0056
	928D	0º	7.28	0.0046	703.7	12.81	0.0057
		90º	7.63	0.0044	711.5	13.57	0.0056
		180º	7.65	0.0042	742.5	14.21	0.0054
		270º	7.41	0.0045	716.0	13.27	0.0056
	Average		7.49	0.0044	718.4	13.47	0.0056
	928E	0º	7.53	0.0053	590.7	11.13	0.0068
		90º	7.19	0.0055	598.1	10.75	0.0067
		180º	7.83	0.0051	593.8	11.62	0.0067
		270º	7.39	0.0053	609.4	11.25	0.0066
	Average		7.49	0.0053	598.0	11.19	0.0067
	928E	0º	7.79	0.0044	699.6	13.62	0.0057
		90º	7.58	0.0047	671.4	12.72	0.0060
		180º	7.54	0.0045	701.5	13.22	0.0057
		270º	7.29	0.0048	682.8	12.45	0.0059
	Average		7.55	0.0046	688.8	13.00	0.0058
	Air Content – Plastic, %		7.75				
	Average		7.49	0.0047	679.3	12.77	0.0059

Note:
Mixture containing 0.75 percent shrinkage-reducing admixtures (SRA-3) by weight of cement.
Test is subjected on four slabs, two slabs from each cylinder (D and E).
Each slab is measured four times, the slab is rotated 90° between measurements. The average of the four readings of the slab is reported as the air-void parameters of that slab.

Table E.12 – Air-Voids characteristics of the hardened concrete of 2.25% SRA-3 mixture

	Batch No. and Slab Designation	Orientation	Air Content, %	Spacing Factor, in	Specific Surface, in^{-1}	Void Frequency, in^{-1}	Average Chord Length, in
2.25% SRA-3, failed Freeze-Thaw and Scaling Tests	963D	0º	4.62	0.0076	675.6	7.81	0.0059
		90º	4.97	0.0073	637.6	7.93	0.0063
		180º	4.55	0.0078	660.2	7.50	0.0061
		270º	4.23	0.0072	714.4	7.57	0.0056
	Average		4.59	0.0075	672.0	7.70	0.0060
	963D	0º	4.66	0.0081	706.7	8.23	0.0057
		90º	4.80	0.0079	678.5	8.15	0.0059
		180º	4.87	0.0077	664.6	8.09	0.0060
		270º	4.85	0.0076	716.7	8.69	0.0056
	Average		4.80	0.0078	691.6	8.29	0.0058
	963E	0º	4.79	0.0080	544.5	6.52	0.0073
		90º	4.23	0.0085	565.3	5.98	0.0071
		180º	4.69	0.0081	485.2	5.69	0.0082
		270º	4.95	0.0078	521.3	6.45	0.0077
	Average		4.67	0.0081	529.1	6.16	0.0076
	963E	0º	4.66	0.0079	556.7	6.48	0.0072
		90º	4.42	0.0080	596.6	6.59	0.0067
		180º	4.83	0.0076	553.1	6.68	0.0072
		270º	4.30	0.0081	518.4	5.57	0.0077
	Average		4.55	0.0079	556.2	6.33	0.0072
	Air Content – Plastic, %		7.50				
	Average		4.65	0.0078	612.2	7.12	0.007

Note:
Mixture containing 2.25 percent shrinkage-reducing admixtures (SRA-3) by weight of cement.
Test is subjected on four slabs, two slabs from each cylinder (D and E).
Each slab is measured four times, the slab is rotated 90° between measurements. The average of the four readings of the slab is reported as the air-void parameters of that slab.

Table E.13 – Air-Voids characteristics of the hardened concrete of 20% FA-F # 1 mixture

	Batch No. and Slab Designation	Orientation	Air Content, %	Spacing Factor, in	Specific Surface, in^{-1}	Void Frequency, in^{-1}	Average Chord Length, in
20% FA-F # 1, failed Scaling Test	**879D**	**0º**	2.63	0.0113	534.8	3.52	0.0075
		90º	2.56	0.0095	645.4	4.14	0.0062
		180º	2.28	0.0115	496.8	2.83	0.0081
		270º	2.21	0.0109	603.2	3.34	0.0066
	Average		2.42	0.0108	570.1	3.46	0.0071
	879D	**0º**	2.29	0.0107	602.9	3.45	0.0066
		90º	2.51	0.0095	651.4	4.09	0.0061
		180º	2.49	0.0104	595.1	3.71	0.0067
		270º	2.24	0.0108	605.2	3.39	0.0066
	Average		2.38	0.0100	617.2	3.66	0.0065
	879E1	**0º**	2.51	0.0120	515.1	3.23	0.0078
		90º	2.71	0.0096	623.7	4.23	0.0064
		180º	2.42	0.0096	653.6	3.96	0.0061
		270º	2.65	0.0103	587.8	3.89	0.0068
	Average		2.57	0.0104	595.1	3.83	0.0068
	879E	**0º**	2.65	0.0120	493.1	3.26	0.0081
		90º	2.41	0.0121	519.8	3.13	0.0077
		180º	2.43	0.0121	501.1	2.74	0.0080
		270º	2.20	0.0119	471.0	2.59	0.0085
	Average		2.42	0.0120	496.3	2.93	0.0081
	Air Content – Plastic, %		2.75				
	Average		2.45	0.0109	56.5	3.47	0.0071

Note:
Mixture containing 20 percent volume replacement of cement with Class F Fly Ash.
Test is subjected on four slabs, two slabs from each cylinder (D and E).
Each slab is measured four times, the slab is rotated 90° between measurements. The average of the four readings of the slab is reported as the air-void parameters of that slab.
This mixture was not tested for Freeze-Thaw Test.

Table E.14 – Air-Voids characteristics of the hardened concrete of 20% FA-F # 2 mixture

	Batch No. and Slab Designation	Orientation	Air Content, %	Spacing Factor, in	Specific Surface, in^{-1}	Void Frequency, in^{-1}	Average Chord Length, in
20% FA-F # 2, passed Freeze-Thaw and Scaling Tests	890D	0º	8.84	0.0040	668.3	14.77	0.0060
		90º	8.75	0.0041	658.3	14.41	0.0061
		180º	9.20	0.0039	665.1	15.30	0.0060
		270º	8.46	0.0043	653.7	13.83	0.0061
	Average		8.81	0.0041	661.4	14.58	0.0061
	890D	0º	8.75	0.0039	692.7	15.16	0.0058
		90º	8.89	0.0040	665.1	14.79	0.0060
		180º	8.35	0.0042	681.5	14.23	0.0059
		270º	8.29	0.0043	664.0	13.77	0.0060
	Average		8.57	0.0041	675.8	14.49	0.0059
	890E	0º	8.61	0.0042	657.8	14.17	0.0061
		90º	8.76	0.0041	656.1	14.37	0.0061
		180º	9.09	0.0040	646.2	14.68	0.0062
		270º	8.79	0.0044	613.5	13.48	0.0065
	Average		8.81	0.0042	643.4	14.18	0.0062
	890E	0º	8.93	0.0043	622.1	13.88	0.0064
		90º	9.07	0.0039	676.2	15.39	0.0059
		180º	9.06	0.0041	644.2	14.59	0.0062
		270º	8.42	0.0044	647.2	13.63	0.0062
	Average		8.87	0.0042	647.4	14.37	0.0062
	Air Content – Plastic, %		9.75				
	Average		8.77	0.0041	657.0	14.40	0.0061

Note:
Mixture containing 20 percent volume replacement of cement with Class F Fly Ash.
Test is subjected on four slabs, two slabs from each cylinder (D and E).
Each slab is measured four times, the slab is rotated 90° between measurements. The average of the four readings of the slab is reported as the air-void parameters of that slab.

Table E.15 – Air-Voids characteristics of the hardened concrete of 20% FA-C mixture

	Batch No. and Slab Designation	Orientation	Air Content, %	Spacing Factor, in	Specific Surface, in^{-1}	Void Frequency, in^{-1}	Average Chord Length, in
20% FA-C, failed Freeze-Thaw test and passed Scaling Test	913D	0º	5.80	0.0065	627.4	9.10	0.0064
		90º	5.29	0.0069	636.5	8.42	0.0063
		180º	5.68	0.0070	599.3	8.50	0.0067
		270º	5.49	0.0068	638.2	8.76	0.0063
	Average		5.57	0.0068	625.4	8.70	0.0064
	913D	0º	5.53	0.0068	634.4	8.78	0.0063
		90º	6.32	0.0065	577.1	9.13	0.0069
		180º	5.94	0.0075	534.8	7.95	0.0075
		270º	5.92	0.0068	593.4	8.79	0.0067
	Average		5.93	0.0069	584.9	8.66	0.0069
	913E	0º	5.06	0.0073	612.8	7.76	0.0065
		90º	5.43	0.0077	563.4	7.65	0.0071
		180º	5.53	0.0074	582.2	8.05	0.0069
		270º	4.92	0.0071	638.7	7.86	0.0063
	Average		5.24	0.0074	599.3	7.83	0.0067
	913E	0º	5.20	0.0075	590.5	7.67	0.0068
		90º	5.52	0.0069	626.6	8.65	0.0064
		180º	5.40	0.0077	570.9	7.70	0.0070
		270º	5.16	0.0073	609.8	7.87	0.0066
	Average		5.32	0.0074	599.5	7.97	0.0067
	Air Content – Plastic, %		7.00				
	Average		5.51	0.0071	602.3	8.29	0.0067

Note:
Mixture containing 20 percent volume replacement of cement with Class C Fly Ash.
Test is subjected on four slabs, two slabs from each cylinder (D and E).
Each slab is measured four times, the slab is rotated 90° between measurements. The average of the four readings of the slab is reported as the air-void parameters of that slab.

Table E.16 – Air-Voids characteristics of the hardened concrete of 40% FA-F # 1 mixture

	Batch No. and Slab Designation	Orientation	Air Content, %	Spacing Factor, in	Specific Surface, in^{-1}	Void Frequency, in^{-1}	Average Chord Length, in
40% FA-F # 1, passed Freeze-Thaw and Scaling Tests	889D	0º	7.76	0.0046	670.4	13.01	0.0060
		90º	7.16	0.0046	716.0	12.81	0.0056
		180º	7.13	0.0051	651.3	11.61	0.0061
		270º	7.75	0.0048	645.1	12.49	0.0062
	Average		7.45	0.0048	670.7	12.48	0.0060
	889D	0º	7.17	0.0050	662.8	11.88	0.0060
		90º	7.48	0.0050	632.3	11.83	0.0063
		180º	7.57	0.0050	623.2	11.79	0.0064
		270º	7.13	0.0053	627.6	11.19	0.0064
	Average		7.34	0.0051	636.5	11.67	0.0063
	889E	0º	7.38	0.0048	676.8	12.49	0.0059
		90º	7.19	0.0052	638.1	11.47	0.0063
		180º	6.97	0.0054	634.0	11.04	0.0063
		270º	6.71	0.0055	645.5	10.83	0.0062
	Average		7.06	0.0052	648.6	11.46	0.0062
	889E	0º	6.29	0.0060	597.4	9.39	0.0067
		90º	6.79	0.0062	561.7	9.54	0.0071
		180º	6.28	0.0062	605.8	9.50	0.0066
		270º	6.96	0.0059	576.0	10.03	0.0069
	Average		6.58	0.0062	585.2	9.62	0.0068
	Air Content – Plastic, %		8.50				
	Average		7.11	0.0053	635.3	11.31	0.0063

Note:
Mixture containing 40 percent volume replacement of cement with Class F Fly Ash.
Test is subjected on four slabs, two slabs from each cylinder (D and E).
Each slab is measured four times, the slab is rotated 90° between measurements. The average of the four readings of the slab is reported as the air-void parameters of that slab.

Table E.17 – Air-Voids characteristics of the hardened concrete of 40% FA-F # 2 mixture

	Batch No. and Slab Designation	Orientation	Air Content, %	Spacing Factor, in	Specific Surface, in^{-1}	Void Frequency, in^{-1}	Average Chord Length, in
40% FA-F # 2, passed Freeze-Thaw and Scaling Tests	**880D**	**0º**	8.31	0.0044	649.6	13.50	0.0062
		90º	8.74	0.0042	654.5	14.30	0.0061
		180º	8.53	0.0044	649.6	13.50	0.0062
		270º	8.66	0.0041	674.4	14.60	0.0059
	Average		8.56	0.0043	657.0	13.98	0.0061
	880D	**0º**	8.94	0.0043	613.9	13.72	0.0065
		90º	9.19	0.0043	594.8	13.66	0.0067
		180º	9.13	0.0044	594.2	13.56	0.0067
		270º	9.13	0.0040	645.0	14.71	0.0062
	Average		9.10	0.0043	612.0	13.91	0.0065
	880E	**0º**	9.13	0.0041	641.9	14.65	0.0062
		90º	8.97	0.0042	632.2	14.18	0.0063
		180º	8.90	0.0044	612.7	13.64	0.0065
		270º	8.43	0.0044	614.4	13.52	0.0062
	Average		8.86	0.0043	625.3	14.00	0.0063
	880E	**0º**	9.35	0.0037	691.0	16.16	0.0058
		90º	9.25	0.0039	662.3	15.31	0.006
		180º	9.06	0.0038	689.2	16.61	0.0058
		270º	9.39	0.0037	686.3	16.11	0.0058
	Average		9.26	0.0038	682.2	16.05	0.0059
	Air Content – Plastic, %		10.00				
	Average		8.94	0.0042	644.1	14.48	0.006

Note:
Mixture containing 40 percent volume replacement of cement with Class F Fly Ash.
Test is subjected on four slabs, two slabs from each cylinder (D and E)
Each slab is measured four times, the slab is rotated 90° between measurements. The average of the four readings of the slab is reported as the air-void parameters of that slab.

Table E.18 – Air-Voids characteristics of the hardened concrete of 0.05% RMA mixture

	Batch No. and Slab Designation	Orientation	Air Content, %	Spacing Factor, in	Specific Surface, in^{-1}	Void Frequency, in^{-1}	Average Chord Length, in
0.05% RMA, passed Freeze-Thaw and Scaling Tests	905D	0º	6.78	0.0047	739.4	12.54	0.0054
		90º	6.59	0.0049	735.0	12.11	0.0054
		180º	6.23	0.0050	756.6	11.78	0.0053
		270º	6.47	0.0050	729.1	11.80	0.0055
	Average		6.52	0.0049	740.0	12.06	0.0054
	905D	0º	6.21	0.0050	810.0	11.50	0.0049
		90º	6.05	0.0052	811.4	11.18	0.0049
		180º	6.02	0.0052	780.9	10.76	0.0051
		270º	6.22	0.0052	756.2	10.66	0.0053
	Average		6.12	0.0052	745.2	11.03	0.0051
	905E	0º	6.89	0.0054	643.2	11.08	0.0062
		90º	6.65	0.0050	713.1	11.86	0.0056
		180º	6.27	0.0053	720.6	11.29	0.0056
		270º	6.75	0.0052	675.8	11.40	0.0059
	Average		6.64	0.0052	688.2	11.41	0.0058
	905E	0º	6.70	0.0056	635.9	10.65	0.0063
		90º	6.16	0.0057	674.8	10.40	0.0059
		180º	6.11	0.0057	640.7	9.79	0.0062
		270º	6.31	0.0056	673.6	10.63	0.0059
	Average		6.32	0.0057	656.3	10.37	0.0061
	Air Content – Plastic, %		8.75				
	Average		6.40	0.0052	718.5	11.21	0.0056

Note:
Mixture containing 0.05 percent a rheology modifier (RMA) by weight of dry materials.
Test is subjected on four slabs, two slabs from each cylinder (D and E)
Each slab is measured four times, the slab is rotated 90° between measurements. The average of the four readings of the slab is reported as the air-void parameters of that slab.

Table E.19 – Air-Voids characteristics of the hardened concrete of 0.075% RMA mixture

	Batch No. and Slab Designation	Orientation	Air Content, %	Spacing Factor, in	Specific Surface, in^{-1}	Void Frequency, in^{-1}	Average Chord Length, in
0.075% RMA, passed Freeze-Thaw Test and failed scaling test	**909D**	**0º**	5.10	0.0067	674.2	8.60	0.0059
		90º	4.77	0.0063	734.0	8.76	0.0054
		180º	4.81	0.0063	735.3	8.84	0.0054
		270º	4.97	0.0062	729.5	9.07	0.0055
	Average		4.90	0.0064	718.0	8.82	0.0056
	909D	**0º**	5.38	0.0061	717.1	9.65	0.0056
		90º	5.03	0.0067	673.8	8.47	0.0059
		180º	5.22	0.0063	704.9	9.20	0.0057
		270º	5.12	0.0067	670.6	8.58	0.0060
	Average		5.20	0.0065	692.0	8.98	0.0058
	909E	**0º**	4.93	0.0074	618.2	7.62	0.0065
		90º	4.68	0.0072	651.7	7.63	0.0061
		180º	4.40	0.0074	648.4	7.13	0.0062
		270º	4.77	0.0073	629.9	7.50	0.0064
	Average		4.70	0.0073	637.0	7.47	0.0063
	909E	**0º**	4.75	0.0061	754.5	8.97	0.0053
		90º	4.85	0.0059	774.0	9.38	0.0052
		180º	4.69	0.0063	736.6	8.63	0.0054
		270º	4.31	0.0063	771.2	8.30	0.0052
	Average		4.70	0.0062	759.0	8.82	0.0053
	Air Content – Plastic, %		7.75				
	Average		4.86	0.0066	701.0	8.52	0.0057

Note:
Mixture containing 0.075 percent a rheology modifier (RMA) by weight of dry materials.
Test is subjected on four slabs, two slabs from each cylinder (D and E).
Each slab is measured four times, the slab is rotated 90° between measurements. The average of the four readings of the slab is reported as the air-void parameters of that slab.

Table E.20 – Air-Voids characteristics of the hardened concrete of 0.05% RMA - 40% FA-C mixture

	Batch No. and Slab Designation	Orientation	Air Content, %	Spacing Factor, in	Specific Surface, in^{-1}	Void Frequency, in^{-1}	Average Chord Length, in
0.05% RMA - 40% FA-C, passed Freeze-Thaw Test and failed Scaling Test	899D	0º	5.92	0.0055	725.1	10.74	0.0055
		90º	5.64	0.0054	786.2	11.08	0.0051
		180º	5.93	0.0052	763.6	11.31	0.0052
		270º	5.50	0.0056	770.6	10.60	0.0052
	Average		5.75	0.0054	761.4	10.93	0.0053
	899D	0º	5.84	0.0057	710.3	10.37	0.0056
		90º	6.02	0.0056	704.7	10.60	0.0057
		180º	6.70	0.0051	712.1	11.94	0.0056
		270º	5.47	0.0058	745.2	10.20	0.0054
	Average		6.01	0.0055	745.2	10.97	0.0056
	899E	0º	5.65	0.0051	817.9	11.55	0.0049
		90º	5.62	0.0048	875.3	12.29	0.0046
		180º	5.65	0.0049	851.2	12.03	0.0047
		270º	5.59	0.0049	875.8	12.23	0.0046
	Average		5.63	0.0049	855.1	12.03	0.0047
	899E	0º	5.25	0.0061	724.2	9.50	0.0055
		90º	5.15	0.0063	705.8	9.08	0.0057
		180º	5.35	0.0059	741.9	9.93	0.0054
		270º	4.74	0.0060	771.6	9.14	0.0052
	Average		5.12	0.0061	735.9	9.41	0.0055
	Air Content – Plastic, %		5.75				
	Average		5.63	0.0055	767.6	10.79	0.0052

Note:
Mixture containing 0.05 percent a rheology modifier (RMA) with 40 percent volume replacement of cement with Class C Fly Ash.
Test is subjected on four slabs, two slabs from each cylinder (D and E).
Each slab is measured four times, the slab is rotated 90° between measurements. The average of the four readings of the slab is reported as the air-void parameters of that slab.

Table E.21 – Air-Voids characteristics of the hardened concrete of 0.075% RMA - 40% FA-C mixture

	Batch No. and Slab Designation	Orientation	Air Content, %	Spacing Factor, in	Specific Surface, in^{-1}	Void Frequency, in^{-1}	Average Chord Length, in
0.075% RMA - 40% FA-C, passed Freeze-Thaw Test and failed Scaling Test	967D	0º	8.29	0.0039	739.3	15.32	0.0054
		90º	8.65	0.0036	764.9	16.55	0.0052
		180º	8.32	0.0039	736.7	15.32	0.0054
		270º	8.12	0.0039	749.5	15.22	0.0053
	Average		8.35	0.0038	747.6	15.60	0.0053
	967D	0º	7.98	0.0040	751.4	14.99	0.0053
		90º	8.24	0.0037	769.0	15.84	0.0052
		180º	7.86	0.0040	758.5	14.91	0.0053
		270º	8.10	0.0040	740.9	15.01	0.0054
	Average		8.05	0.0039	745.2	15.60	0.0053
	967E	0º	8.20	0.0043	680.4	13.95	0.0059
		90º	8.39	0.0041	709.3	14.87	0.0056
		180º	8.69	0.0039	706.2	15.34	0.0057
		270º	8.00	0.0042	706.5	14.12	0.0057
	Average		8.32	0.0041	700.6	14.57	0.0057
	967E	0º	7.80	0.0041	737.9	14.40	0.0054
		90º	7.40	0.0043	750.3	13.87	0.0053
		180º	8.01	0.0042	699.6	14.01	0.0057
		270º	7.59	0.0041	757.4	14.37	0.0053
	Average		7.70	0.0042	736.3	14.16	0.0054
	Air Content – Plastic, %		8.25				
	Average		8.10	0.0040	734.9	14.88	0.0054

Note:
Mixture containing 0.075 percent a rheology modifier (RMA) with 40 percent volume replacement of cement with Class C Fly Ash.
Test is subjected on four slabs, two slabs from each cylinder (D and E).
Each slab is measured four times, the slab is rotated 90° between measurements. The average of the four readings of the slab is reported as the air-void parameters of that slab.

Table E.22 – Air-Voids characteristics of the hardened concrete of 0.15% RMA - 40% FA-C mixture

	Batch No. and Slab Designation	Orientation	Air Content, %	Spacing Factor, in	Specific Surface, in^{-1}	Void Frequency, in^{-1}	Average Chord Length, in
0.15% RMA - 40% FA-C, passed Freeze-Thaw Test and failed Scaling Test	911D	0º	7.60	0.0045	692.8	13.16	0.0058
		90º	7.58	0.0044	708.2	13.43	0.0056
		180º	7.74	0.0043	714.5	13.82	0.0056
		270º	7.00	0.0046	745.0	13.04	0.0054
	Average		7.50	0.0045	715.1	13.36	0.0056
	911D	0º	7.74	0.0040	767.3	14.8	0.0052
		90º	7.77	0.0041	752.2	14.61	0.0053
		180º	7.70	0.0041	744.7	14.34	0.0054
		270º	7.63	0.0042	734.8	14.02	0.0054
	Average		7.74	0.0041	749.8	14.44	0.0053
	911E	0º	7.78	0.0042	725.5	14.11	0.0055
		90º	8.02	0.0042	713.8	14.31	0.0056
		180º	8.12	0.0042	671.2	13.63	0.006
		270º	7.63	0.0044	709.4	13.52	0.0056
	Average		7.90	0.0043	705.0	13.89	0.0057
	911E	0º	7.61	0.0040	786.8	14.97	0.0051
		90º	7.19	0.0041	813.4	14.63	0.0049
		180º	7.84	0.0043	702.8	13.77	0.0057
		270º	6.94	0.0042	809.0	14.03	0.0049
	Average		7.40	0.0042	778.0	14.35	0.0052
	Air Content – Plastic, %		8.50				
	Average		7.62	0.0042	737.0	14.01	0.0054

Note:
Mixture containing 0.15 percent a rheology modifier (RMA) with 40 percent volume replacement of cement with Class C Fly Ash.
Test is subjected on four slabs, two slabs from each cylinder (D and E).
Each slab is measured four times, the slab is rotated 90° between measurements. The average of the four readings of the slab is reported as the air-void parameters of that slab.

Table E.23 – Air-Voids characteristics of the hardened concrete of 0.15% RMA - 20% FA-C mixture

	Batch No. and Slab Designation	Orientation	Air Content, %	Spacing Factor, in	Specific Surface, in^{-1}	Void Frequency, in^{-1}	Average Chord Length, in
0.15% RMA - 20% FA-C, passed Freeze-Thaw Test and failed Scaling Test	912D	0º	6.25	0.0046	820.1	12.82	0.0049
		90º	6.11	0.0050	784.1	11.98	0.0051
		180º	5.67	0.0052	809.1	11.46	0.0049
		270º	5.97	0.0054	743.2	11.09	0.0054
	Average		6.00	0.0051	789.1	11.84	0.0051
	912D	0º	6.28	0.0053	718.4	11.27	0.0056
		90º	6.44	0.0051	726.2	11.69	0.0055
		180º	6.20	0.0051	746.4	11.57	0.0054
		270º	5.86	0.0056	749.8	10.65	0.0053
	Average		6.20	0.0053	735.2	11.30	0.0055
	912E	0º	6.68	0.0045	785.8	13.17	0.0058
		90º	6.23	0.0043	775.5	13.90	0.0059
		180º	5.67	0.0046	767.5	13.80	0.0060
		270º	6.48	0.0046	789.4	13.89	0.0058
	Average		6.30	0.0045	779.6	13.69	0.0059
	912E	0º	6.22	0.0045	840.9	13.07	0.0048
		90º	6.05	0.0047	827.2	12.50	0.0048
		180º	6.22	0.0045	840.8	13.07	0.0048
		270º	6.26	0.0047	814.9	12.75	0.0049
	Average		6.22	0.0046	831.0	12.85	0.0048
	Air Content – Plastic, %		6.50				
	Average		6.16	0.0049	783.7	12.42	0.0053

Note:
Mixture containing 0.05 percent a rheology modifier (RMA) with 20 percent volume replacement of cement with Class C Fly Ash.
Test is subjected on four slabs, two slabs from each cylinder (D and E).
Each slab is measured four times, the slab is rotated 90° between measurements. The average of the four readings of the slab is reported as the air-void parameters of that slab.

Table E.24 – Air-Voids characteristics of the hardened concrete of 2.5% SCA-1 # 1 mixture

	Batch No. and Slab Designation	Orientation	Air Content, %	Spacing Factor, in	Specific Surface, in^{-1}	Void Frequency, in^{-1}	Average Chord Length, in
2.5% SCA-1 # 1, passed Freeze-Thaw Test and Scaling Test	855D	0º	7.47	0.0054	591.7	11.05	0.0068
		90º	7.60	0.0050	619.7	11.78	0.0065
		180º	8.26	0.0050	570.8	11.79	0.0070
		270º	8.15	0.0052	562.3	11.46	0.0071
	Average		7.87	0.0052	586.1	11.52	0.0069
	855D	0º	8.30	0.0044	655.0	13.59	0.0061
		90º	7.95	0.0043	697.7	13.87	0.0057
		180º	8.06	0.0045	658.2	13.26	0.0061
		270º	7.81	0.0048	638.3	12.46	0.0063
	Average		8.03	0.0045	662.3	13.30	0.0061
	855E	0º	7.99	0.0042	707.1	14.12	0.0057
		90º	7.85	0.0044	686.6	13.48	0.0058
		180º	7.44	0.0048	666.7	12.41	0.006
		270º	8.50	0.0042	671.1	14.26	0.0060
	Average		7.95	0.0044	682.9	13.57	0.0059
	855E	0º	7.95	0.0043	699.5	13.9	0.0057
		90º	7.42	0.0047	686.2	12.74	0.0058
		180º	7.85	0.0046	652.6	12.81	0.0061
		270º	7.60	0.0049	633.2	12.03	0.0063
	Average		7.71	0.0046	667.9	12.87	0.0060
	Air Content – Plastic, %		8.50				
	Average		7.89	0.0047	649.8	12.81	0.0062

Note:
Mixture containing 2.5 percent shrinkage compensating admixtures (SCA-1) by weight of cement.
Test is subjected on four slabs, two slabs from each cylinder (D and E).
Each slab is measured four times, the slab is rotated 90° between measurements. The average of the four readings of the slab is reported as the air-void parameters of that slab.

Table E.25 – Air-Voids characteristics of the hardened concrete of 2.5% SCA-1 # 2 mixture

	Batch No. and Slab Designation	Orientation	Air Content, %	Spacing Factor, in	Specific Surface, in^{-1}	Void Frequency, in^{-1}	Average Chord Length, in
2.5% SCA-1 # 2, failed Freeze-Thaw Test and passed Scaling Test	861D	0º	6.13	0.0073	566.5	8.68	0.0071
		90º	6.30	0.0072	524.5	8.26	0.0076
		180º	6.57	0.0070	532.1	8.74	0.0075
		270º	6.42	0.0072	524.6	8.42	0.0076
	Average		6.36	0.0072	536.9	8.53	0.0075
	861D	0º	6.92	0.0067	631.0	9.65	0.0065
		90º	6.30	0.0072	596.3	8.26	0.0071
		180º	6.76	0.0071	584.2	8.34	0.0066
		270º	6.83	0.0070	624.6	9.42	0.0072
	Average		6.70	0.0070	609.0	8.92	0.0069
	861E	0º	6.16	0.0084	460.7	7.09	0.0087
		90º	6.56	0.0079	460.3	7.55	0.0087
		180º	6.29	0.0080	475.0	7.47	0.0084
		270º	6.18	0.0079	486.0	7.50	0.0082
	Average		6.30	0.0081	470.5	7.40	0.0085
	Air Content – Plastic, %		8.50				
	Average		6.45	0.0074	538.8	8.28	0.0076

Note:
Mixture containing 2.5 percent shrinkage compensating admixtures (SCA-1) by weight of cement.
Test is subjected on three slabs, two slabs from cylinder D and one slab from cylinder E.
Each slab is measured four times, the slab is rotated 90° between measurements. The average of the four readings of the slab is reported as the air-void parameters of that slab.

Table E.26 – Air-Voids characteristics of the hardened concrete of 5% SCA-1 mixture

	Batch No. and Slab Designation	Orientation	Air Content, %	Spacing Factor, in	Specific Surface, in^{-1}	Void Frequency, in^{-1}	Average Chord Length, in
5% SCA-1 # 2, failed Freeze-Thaw Test and passed Scaling Test	**857D**	**0º**	4.02	0.0082	563.7	5.52	0.0060
		90º	4.03	0.0083	640.4	6.44	0.0054
		180º	4.46	0.0082	616.2	6.14	0.0065
		270º	4.04	0.0084	581.1	6.65	0.0059
	Average		4.14	0.0083	600.4	6.19	0.0060
	857D	**0º**	3.85	0.0090	558.0	5.61	0.0072
		90º	3.65	0.0094	577.8	6.01	0.0084
		180º	3.64	0.0090	462.6	5.60	0.0086
		270º	3.45	0.0091	546.7	5.52	0.0073
	Average		3.65	0.0091	536.3	5.69	0.0079
	857E	**0º**	3.82	0.0088	585.7	6.40	0.0075
		90º	3.48	0.0089	551.1	6.12	0.0069
		180º	3.98	0.0086	575.2	5.61	0.0074
		270º	3.91	0.0090	547.2	5.85	0.0069
	Average		3.80	0.0088	564.8	6.00	0.0072
	Air Content – Plastic, %		4.75				
	Average		3.86	0.0087	565.5	5.92	0.0070

Note:
Mixture containing 5 percent shrinkage compensating admixtures (SCA-1) by weight of cement.
Test is subjected on three slabs, two slabs from cylinder D and one slab from cylinder E.
Each slab is measured four times, the slab is rotated 90° between measurements. The average of the four readings of the slab is reported as the air-void parameters of that slab.

Table E.27 – Air-Voids characteristics of the hardened concrete of 7.5% SCA-1 # 1 mixture

	Batch No. and Slab Designation	Orientation	Air Content, %	Spacing Factor, in	Specific Surface, in^{-1}	Void Frequency, in^{-1}	Average Chord Length, in
7.5% SCA-1 # 1, failed Freeze-Thaw and Scaling Tests	**862D**	**0º**	4.41	0.0102	472.0	5.21	0.0085
		90º	4.43	0.0100	477.6	5.29	0.0084
		180º	4.46	0.0105	453.0	5.05	0.0088
		270º	4.45	0.0102	468.5	5.21	0.0085
	Average		4.44	0.0102	467.8	5.19	0.0086
	862D	**0º**	4.85	0.0094	485.7	5.89	0.0082
		90º	4.67	0.0096	486.9	5.68	0.0082
		180º	4.09	0.0091	546.2	5.59	0.0073
		270º	4.85	0.0089	513.3	6.22	0.0078
	Average		4.62	0.0093	508.0	5.85	0.0079
	862E	**0º**	4.44	0.0095	504.0	5.60	0.0079
		90º	4.80	0.0092	498.6	5.99	0.0080
		180º	4.44	0.0093	511.1	5.67	0.0078
		270º	4.39	0.0092	524.4	5.76	0.0076
	Average		4.52	0.0093	509.5	5.76	0.0078
	Air Content – Plastic, %		5.00				
	Average		4.52	0.0096	495.1	5.60	0.0081

Note:
Mixture containing 7.5 percent shrinkage compensating admixtures (SCA-1) by weight of cement.
Test is subjected on three slabs, two slabs from cylinder D and one slab from cylinder E.
Each slab is measured four times, the slab is rotated 90° between measurements. The average of the four readings of the slab is reported as the air-void parameters of that slab.

Table E.28 – Air-Voids characteristics of the hardened concrete of 7.5% SCA-1 # 2 mixture

	Batch No. and Slab Designation	Orientation	Air Content, %	Spacing Factor, in	Specific Surface, in^{-1}	Void Frequency, in^{-1}	Average Chord Length, in
7.5% SCA-1 # 2, Passed Freeze-Thaw and Scaling Tests	**860D**	**0º**	7.50	0.0054	591.2	11.08	0.0068
		90º	7.61	0.0054	576.1	10.97	0.0069
		180º	7.65	0.0052	595.0	11.38	0.0067
		270º	7.68	0.0053	587.8	11.29	0.0068
	Average		7.61	0.0053	587.5	11.18	0.0068
	860E	**0º**	8.02	0.0044	676.4	13.556	0.0059
		90º	7.64	0.0044	700.0	13.38	0.0057
		180º	8.09	0.0045	658.8	13.32	0.0061
		270º	7.42	0.0048	672.7	12.48	0.0059
	Average		7.79	0.0045	677.0	13.19	0.0059
	860E	**0º**	7.69	0.0045	687.0	13.21	0.0058
		90º	7.45	0.0047	672.8	12.52	0.0059
		180º	8.10	0.0046	644.6	13.06	0.0062
		270º	7.79	0.0046	667.8	13.01	0.0060
	Average		7.76	0.0046	668.1	12.95	0.0060
	Air Content – Plastic, %		9.00				
	Average		7.72	0.0048	644.2	12.44	0.0062

Note:
Mixture containing 7.5 percent shrinkage compensating admixtures (SCA-1) by weight of cement.
Test is subjected on three slabs, one slab from cylinder D and two slabs from cylinder E.
Each slab is measured four times, the slab is rotated 90° between measurements. The average of the four readings of the slab is reported as the air-void parameters of that slab.

Table E.29 – Air-Voids characteristics of the hardened concrete of 6% SCA-2 mixture

	Batch No. and Slab Designation	Orientation	Air Content, %	Spacing Factor, in	Specific Surface, in^{-1}	Void Frequency, in^{-1}	Average Chord Length, in
6% SCA-1 # 2, passed Freeze-Thaw and Scaling Tests	955D	0º	6.74	0.0045	796.1	13.20	0.0045
		90º	7.65	0.0048	783.2	15.78	0.0061
		180º	6.62	0.0048	795.0	11.38	0.0047
		270º	7.32	0.0051	707.8	11.29	0.0058
	Average		7.10	0.0048	770.5	12.66	0.0053
	955D	0º	6.92	0.0047	731.0	12.65	0.0055
		90º	7.67	0.0052	697.0	11.44	0.0067
		180º	7.76	0.0052	684.2	11.34	0.0060
		270º	6.38	0.0051	723.8	11.55	0.0055
	Average		7.18	0.0051	709.0	11.75	0.0059
	955E	0º	7.69	0.0048	787.0	13.71	0.0058
		90º	7.45	0.0047	772.5	12.52	0.0059
		180º	7.54	0.0046	744.6	13.15	0.0062
		270º	7.79	0.0045	767.8	12.86	0.0060
	Average		7.62	0.0047	768.1	12.81	0.0060
	Air Content – Plastic, %		8.50				
	Average		7.30	0.0048	749.2	12.41	0.0060

Note:
Mixture containing 6 percent shrinkage compensating admixtures (SCA-2) by weight of cement.
Test is subjected on three slabs, one slab from cylinder D and two slabs from cylinder E.
Each slab is measured four times, the slab is rotated 90° between measurements. The average of the four readings of the slab is reported as the air-void parameters of that slab.

Table E.30 – Average of air content in hardened concrete, maximum, minimum, standard deviation, and coefficient of variation of the readings for the four slabs from each mixture

Batch Designation	Batch No.	Specimen	Air Content – Hardened, %		Average	Maximum	Minimum	Standard Deviation	Coefficient of Variation
Control # 1	926	D	5.63	5.72	5.56	5.72	5.37	0.15	0.03
		E	5.51	5.37					
Control # 2	927	D	8.20	7.58	7.94	8.2	7.58	0.26	0.03
		E	7.93	8.03					
Control # 3	976	D	6.89	6.36	6.71	6.89	6.36	0.25	0.04
		E	6.69	6.89					
0.5% SRA-2	894	D	5.90	5.83	5.78	5.90	5.68	0.10	0.02
		E	5.68	5.72					
1% SRA-2 # 1	896	D	7.24	7.13	7.27	7.50	7.13	0.16	0.02
		E	7.50	7.21					
1% SRA-2 # 2	887	D	7.16	7.00	7.41	7.75	7.00	0.38	0.05
		E	7.72	7.75					
1% SRA-2 # 3	960	D	5.78	6.16	6.17	6.57	5.78	0.32	0.05
		E	6.57	6.16					
2% SRA-2 # 1	886	D	6.16	5.82	6.07	5.80	0.28	0.23	0.04
		E	5.95	6.35					
2% SRA-2 # 2	897	D	6.16	6.90	6.65	6.90	6.06	0.39	0.06
		E	6.06	6.84					
0.75% SRA-3	928	D	7.21	7.49	7.44	7.55	7.21	0.15	0.02
		E	7.49	7.55					
2.25% SRA-3	963	D	4.59	4.80	4.65	4.80	4.55	0.11	0.02
		E	4.67	4.55					
20% FA-F # 1	879	D	2.42	2.38	2.45	2.57	2.38	0.08	0.03
		E	2.57	2.42					
20% FA-F # 2	890	D	8.81	8.57	8.77	8.87	8.57	0.13	0.02
		E	8.81	8.87					
20% FA-C	913	D	5.57	5.93	5.52	5.93	5.24	0.31	0.06
		E	5.24	5.32					
40% FA-F # 1	889	D	7.45	7.34	7.11	7.45	6.58	0.39	0.05
		E	7.06	6.58					
40% FA-F # 2	880	D	8.56	9.10	8.95	9.26	8.56	0.30	0.03
		E	8.86	9.26					
0.05% RMA	905	D	6.52	6.12	6.40	6.64	6.12	0.23	0.04
		E	6.64	6.32					
0.075% RMA	909	D	4.90	5.20	4.88	5.20	4.70	0.24	0.05
		E	4.70	4.70					

Table E.30 (Cont'd) – Average of air content in hardened concrete, maximum, minimum, standard deviation, and coefficient of variation of the readings for the four slabs from each mixture

Batch Designation	Batch No.	Specimen	Air Contents – Hardened, %		Average	Maximum	Minimum	Standard Deviation	Coefficient of Variation
0.05% RMA - 40% FA-C	899	D	5.75	6.01	5.63	6.01	5.12	0.37	0.07
		E	5.63	5.12					
0.075%RMA - 40% FA-C	967	D	8.35	8.05	8.11	8.35	7.70	0.30	0.04
		E	8.32	7.70					
0.15%RMA -40% FA-C	911	D	7.50	7.74	7.64	7.90	7.40	0.23	0.03
		E	7.90	7.40					
0.15%RMA -20% FA-C	912	D	6.00	6.20	6.18	6.30	6.00	0.13	0.02
		E	6.30	6.22					
2.5% SCA-1 #1	855	D	7.90	8.00	7.88	8.00	7.70	0.13	0.02
		E	7.90	7.70					
2.5% SCA-1 #2*	861	D	6.36	6.70	6.45	6.70	6.30	0.22	0.03
		E	6.30	†					
5% SCA-1*	857	D	4.14	3.65	3.87	4.14	3.65	0.25	0.06
		E	3.82	†					
7.5% SCA-1 #1*	862	D	4.44	4.62	4.53	4.62	4.44	0.09	0.02
		E	4.52	†					
7.5% SCA-1 #2*	860	D	7.61	7.79	7.72	7.79	7.61	0.10	0.01
		E	7.76	†					
6% SCA-2*	955	D	7.10	7.18	7.30	7.62	7.10	0.28	0.04
		E	7.62	†					

* Mixtures have three slabs, instead of four, are evaluated based on hardened air-void analysis test
† Slabs are not subjected to the hardened air-void analysis test

Table E.31 – Air-void spacing factors, maximum, minimum, standard deviation, and coefficient of variation of the readings for the four slabs from each mixture

Batch Designation	Batch No.	Specimen	Average Air-Void Spacing Factor, in.		Average	Maximum	Minimum	Standard Deviation	Coefficient of Variation
Control # 1	926	D	0.0056	0.0058	0.0056	0.0058	0.0054	0.00016	0.03
		E	0.0054	0.0056					
Control # 2	927	D	0.0034	0.0043	0.0039	0.0043	0.0034	0.00040	0.10
		E	0.0042	0.0037					
Control # 3	976	D	0.0049	0.0050	0.0052	0.0057	0.0049	0.00037	0.07
		E	0.0057	0.0050					
0.5% SRA-2	894	D	0.0063	0.0066	0.0066	0.0068	0.0063	0.00024	0.04
		E	0.0068	0.0068					
1% SRA-2 # 1	896	D	0.0049	0.0052	0.0050	0.0052	0.0049	0.00014	0.03
		E	0.0050	0.0049					
1% SRA-2 # 2	887	D	0.0047	0.0047	0.0048	0.0054	0.0042	0.00049	0.10
		E	0.0042	0.0054					
1% SRA-2 # 3	960	D	0.0056	0.0056	0.0058	0.0067	0.0054	0.00059	0.10
		E	0.0054	0.0067					
2% SRA-2 # 1	886	D	0.0059	0.0066	0.0063	0.0066	0.0059	0.00036	0.06
		E	0.0066	0.0061					
2% SRA-2 # 2	897	D	0.0054	0.0050	0.0055	0.0062	0.0050	0.00051	0.09
		E	0.0062	0.0053					
0.75% SRA-3	928	D	0.0045	0.0044	0.0047	0.0053	0.0044	0.00041	0.09
		E	0.0053	0.0046					
2.25% SRA-3	963	D	0.0075	0.0078	0.0078	0.0081	0.0075	0.00025	0.03
		E	0.0081	0.0079					
20% FA-F # 1	879	D	0.0108	0.0104	0.0109	0.0120	0.0104	0.00076	0.07
		E	0.0104	0.0120					
20% FA-F # 2	890	D	0.0041	0.0041	0.0042	0.0042	0.0041	0.00006	0.01
		E	0.0042	0.0042					
20% FA-C	913	D	0.0068	0.0069	0.0071	0.0074	0.0068	0.00032	0.04
		E	0.0074	0.0074					
40% FA-F # 1	889	D	0.0048	0.0051	0.0053	0.0061	0.0048	0.00051	0.10
		E	0.0052	0.0060					
40% FA-F # 2	880	D	0.0043	0.0043	0.0042	0.0043	0.0038	0.00025	0.06
		E	0.0043	0.0038					
0.05% RMA	905	D	0.0049	0.0052	0.0053	0.0057	0.0049	0.00033	0.06
		E	0.0052	0.0057					
0.075% RMA	909	D	0.0064	0.0065	0.0066	0.0073	0.0062	0.00048	0.07
		E	0.0073	0.0062					

Table E.31 (Cont'd) – Air-void spacing factors, maximum, minimum, standard deviation, and coefficient of variation of the readings for the four slabs from each mixture

Batch Designation	Batch No.	Specimen	Average Air-Void Spacing Factor, in.		Average	Maximum	Minimum	standard Deviation	Coefficient of Variation
0.05% RMA - 40% FA-C	899	D	0.0054	0.0055	0.0055	0.0061	0.0049	0.00049	0.09
		E	0.0049	0.0061					
0.075% RMA - 40% FA-C	967	D	0.0038	0.0039	0.0040	0.0042	0.0038	0.00018	0.05
		E	0.0041	0.0042					
0.15% RMA -40% FA-C	911	D	0.0045	0.0041	0.0043	0.0045	0.0041	0.00017	0.04
		E	0.0043	0.0042					
0.15% RMA - 20% FA-C	912	D	0.0051	0.0053	0.0049	0.0053	0.0045	0.00039	0.08
		E	0.0045	0.0046					
2.5% SCA-1 # 1	855	D	0.0052	0.0045	0.0047	0.0052	0.0044	0.00036	0.08
		E	0.0044	0.0046					
2.5% SCA-1 # 2*	861	D	0.0072	0.0070	0.0074	0.0081	0.0070	0.00059	0.08
		E	0.0081	†					
5% SCA-1*	857	D	0.0083	0.0091	0.0087	0.0091	0.0083	0.00040	0.05
		E	0.0088	†					
7.5% SCA-1 # 1*	862	D	0.0102	0.0093	0.0096	0.0102	0.0093	0.00052	0.05
		E	0.0093	†					
7.5% SCA-1 # 2*	860	D	0.0053	0.0045	0.0048	0.0053	0.0045	0.00044	0.09
		E	0.0046	†					
6% SCA-2*	955	D	0.0048	0.0051	0.0049	0.0051	0.0046	0.00026	0.05
		E	0.0047	†					

* Mixtures have three slabs, instead of four, are evaluated based on hardened air-void analysis test
† Slabs are not subjected to the hardened air-void analysis test

Table E.33 – Repetition of measurements of the air-void parameters of 2% SRA-2 #1 mixture

Batch No. and Slab Designation	Orientation	Air Content, %	Air-Void Spacing Factor, in.	Specific Surface, in^{-1}	Void Frequency, in^{-1}	Average Chord Length, in.
886D / Test 1	**0º**	6.72	0.0029	1220.9	20.52	0.0033
886D / Test 2		6.66	0.0030	1190.0	19.82	0.0034
Difference, %		0.06	0.0001	30.9	0.7	0.0001
886D / Test 1	**90º**	6.33	0.0031	980.2	15.51	0.0041
886D / Test 2		6.26	0.0032	968.2	15.16	0.0041
Difference, %		0.07	0.0001	12	0.35	0
886D / Test 1	**180º**	6.39	0.0032	1154.0	18.43	0.0035
886D / Test 2		6.42	0.0033	1133.7	18.20	0.0035
Difference, %		0.03	0.0001	20.3	0.23	0.0000
886D / Test 1	**270º**	6.08	0.0029	1354.0	20.57	0.003
886D / Test 2		6.10	0.0030	1313.9	20.03	0.003
Difference, %		0.02	0.0001	40.1	0.54	0.0000

Batch No. and Slab Designation	Orientation	Air Content, %	Air-Void Spacing Factor, in.	Specific Surface, in^{-1}	Void Frequency, in^{-1}	Average Chord Length, in.
886E / Test 1	**0º**	7.81	0.0031	997.2	19.47	0.0040
886E / Test 2		7.85	0.0030	1043.5	19.77	0.0038
Difference, %		0.04	0.0001	46.3	0.3	0.0002
886E / Test 1	**90º**	7.88	0.0026	1144.3	22.54	0.0035
886E / Test 2		7.88	0.0027	1099.6	21.65	0.0036
Difference, %		0.00	0.0001	44.7	0.89	0.0001
886E / Test 1	**180º**	8.12	0.0024	1215.7	24.68	0.0033
886E / Test 2		8.12	0.0024	1212.4	24.81	0.0033
Difference, %		0.00	0.00	3.3	0.13	0.0000
886E / Test 1	**270º**	7.58	0.0028	1122.0	21.25	0.0036
886E / Test 2		7.58	0.0028	1131.9	21.46	0.0035
Difference, %		0.00	0.00	9.9	0.21	0.0001

Table E.34 – Repetition of measurements of the air-void parameters of 40% FA-F #1 mixture

Batch No. and Slab Designation	Orientation	Air Content, %	Air-Void Spacing Factor, in.	Specific Surface, in^{-1}	Void Frequency, in^{-1}	Average Chord Length, in.
889D / Test 1	**0º**	6.76	0.0034	1018.9	17.23	0.0039
889D / Test 2		6.78	0.0035	1014.5	17.2	0.0039
Difference, %		0.02	0.0001	4.4	0.03	0.0000
889D / Test 1	**90º**	7.29	0.0033	987.5	18.01	0.0041
889D / Test 2		7.30	0.0033	971.8	17.75	0.0041
Difference, %		0.01	0.0000	15.7	0.26	0.0000
889D / Test 1	**180º**	6.86	0.0030	1163.7	19.97	0.0034
889D / Test 2		6.95	0.0029	1180.5	20.51	0.0034
Difference, %		0.09	0.0001	16.8	0.54	0.0000
889D / Test 1	**270º**	7.43	0.0036	896.7	16.66	0.0045
889D / Test 2		7.44	0.0036	884.5	16.55	0.0045
Difference, %		0.01	0.0000	12.2	0.11	0.0000

Batch No. and Slab Designation	Orientation	Air Content, %	Air-Void Spacing Factor, in.	Specific Surface, in^{-1}	Void Frequency, in^{-1}	Average Chord Length, in.
889E / Test 1	**0º**	8.07	0.0025	1201.4	24.25	0.0033
889E / Test 2		7.95	0.0026	1102.1	23.81	0.0034
Difference, %		0.12	0.0001	99.3	0.44	0.0001
889E / Test 1	**90º**	7.82	0.0027	1129.1	22.08	0.0035
889E / Test 2		7.71	0.0028	1109.1	21.38	0.0036
Difference, %		0.11	0.0001	20.0	0.7	0.0001
889E / Test 1	**180º**	7.48	0.0031	1029.5	19.24	0.0039
889E / Test 2		7.56	0.0030	1036.1	19.59	0.0039
Difference, %		0.08	0.0001	6.6	0.35	0.0000
889E / Test 1	**270º**	7.25	0.0030	1091.9	19.80	0.0037
889E / Test 2		7.28	0.0030	1078.4	19.63	0.0037
Difference, %		0.03	0.0000	13.5	0.17	0.0000